VOLUME 37 SECOND SERIES NUMBER 5

THE PHYSICAL REVIEW

A JOURNAL OF EXPERIMENTAL AND THEORETICAL PHYSICS

CONDUCTED BY

THE AMERICAN PHYSICAL SOCIETY

BOARD OF EDITORS

Managing Editor, JOHN T. TATE, University of Minnesota, Minneapolis
Assistant Editor, J. W. BUCHTA, University of Minnesota, Minneapolis
E. U. CONDON, C. J. DAVISSON, F. K. RICHTMYER, K. F. HERZFELD, A. W. HULL,
F. W. LOOMIS, A. J. DEMPSTER, DAVID M. DENNISON, J. C. SLATER

MARCH 1, 1931

On Some Solar and Lunar Spectra Taken in Little America, Antarctica — MALCOLM P. HANSON AND E. O. HULBURT 477
Directed Valence in Polyatomic Molecules — J. C. SLATER 481
Rotational Analysis of the S_2 Bands — S. MROZOWSKI AND ANDREW CHRISTY 499
Orbital Valency — JAMES H. BARTLETT, JR. 507
Mass Absorption Coefficient of the *K* Shell According to the Dirac Relativistic Theory of the Electron — LOUIS C. ROSES 532
Interchange of Translational, Rotational, and Vibrational Energy in Molecular Collisions — CLARENCE ZENER 536
Absorption Coefficient for Slow Electrons in Thallium Vapor — ROBERT B. BROOKS 570
Oscillations and Travelling Striations in an Argon Discharge Tube — T. C. CHOW 574
Cold Emission from Unconditioned Surfaces — WILLARD H. BENNETT 582
Scattering of High Velocity Electrons in Hydrogen as a Test of the Interaction Energy of Two Electrons — HUGH C. WOLFE 594
On the Gravitational Field Produced by Light — RICHARD C. TOLMAN, PAUL EHRENFEST AND BORIS PODOLSKY 600
Raman Lines of Cyclopropane and Valence Properties of Some Organic Compounds — ROBERT C. YATES 606
Dust Figure in Liquid Insulator — Y. TORIYAMA 620
Resistance of Bismuth in Alternating Magnetic Fields — WILLIAM W. MACALPINE 624
Strain and Diamagnetic Susceptibility — H. E. BANTA 630
Some Physical Properties of Compressed Gases. I. Nitrogen — W. EDWARDS DEMING AND LOLA E. SHUPE 638
Letters to the Editor 669
The Thermodynamic Treatment of Chemical Equilibria in Systems Composed of Real Gases. II. A Relation for the Heat of Reaction Applied to the Ammonia Synthesis Reaction. The Energy and Entropy Constants of Ammonia. A Correction. *E. J. Gallegos and J. A. Beattie*—669; Reflection of High Velocity Electrons from Solid Surfaces. *H. Tetrode*—670; The Extrapolation of Atomic Structure Energy Curves, *Morris Muskat*—670; Rhodium Salts of Ammonium. *R. C. Gibbs and P. G. Kruger*—670; Which Requirements must the Schrödinger Perturbation Series? *R. H. Fowler and M. Born*—670
Book Reviews 669

PUBLISHED BY THE

THE AMERICAN PHYSICAL SOCIETY

OFFICERS OF THE SOCIETY

President:	W. F. G. Swann	Bartol Research Foundation, Philadelphia, Pa.
Vice-President:	Paul D. Foote	The Gulf Companies, Pittsburgh, Pa.
Secretary:	W. L. Severinghaus	Columbia University, New York City
Treasurer:	G. B. Pegram	Columbia University, New York City
Editor:	John T. Tate	University of Minnesota, Minneapolis, Minn.
Local Secretary for the Pacific Coast:	L. B. Loeb	University of California, Berkeley, Calif.

THE PHYSICAL REVIEW

Published by the American Physical Society. Executive office: University of Minnesota, Minneapolis, Minn. Two volumes annually, twelve issues per volume.

First series. From July 1, 1893, to January 1, 1913, the Review was conducted by Edward L. Nicholas, Ernest Merritt and Frederick Bedell, with the financial support of Cornell University. The first four volumes were issued annually; subsequent volumes, semi-annually; thirty-five volumes in all.

Second series. On January 1, 1913, the Review was transferred to the American Physical Society as announced on the first page of the new series which was then begun. Since then it has been conducted by a Board of Editors elected by the Society. Semi-annual volumes begin in January and July. Since July 1, 1929, the Review has been issued twice a month.

Contributors are referred to page 2 of the advertisements for further information.

Annual subscription, throughout the Postal Union, $12.00 in advance.

General index, 1893-1920, $4.00, in advance.

Back Volumes, $9.00 per volume; Back Numbers, $1.50 per copy for issues prior to July 1, 1929 (Vols. 1-33), $.75 per copy for issues subsequent thereto. Postage is free if remittance accompanies order; otherwise postage is extra. No bound volumes can be supplied. The Review offers to purchase a limited number of First Series, Vol. 1, No. 1 (at $2.00 each); Second Series, Vol. 7, No. 1, January 1916; Vol. 7, No. 2, February 1916; Vol. 7, No. 4, April 1916; and Vol. 7, No. 5, May 1916 (at $2.00 each).

Advertisements. Rates will be supplied by the Editor on request. Copy for each number must be received at Minneapolis two weeks prior to the dates of issue; old copy is used until new copy is received. Send electrotypes direct to the printers, George Banta Publishing Co., Menasha, Wis.

Discount of ten per cent is allowed to members of the American Physical Society on purchase of back numbers.

Changes of Address and Complaints of failure to receive the Review, in the case of members of the Physical Society, should be addressed to the Treasurer; in the case of other subscribers, to the Editor. New copies can be sent free in response to complaint of non-delivery only if notice of non-delivery is received within three months of date of issue.

Editorial Correspondence should be addressed to the Physical Review, University of Minnesota, Minneapolis, Minn.

Entered at the postoffice at Menasha, Wis., as second class matter.
Acceptance for mailing at special rate of postage provided for in section 1103, Act of October 3, 1917, authorized September 6, 1926.

Second Series *March 1, 1931* *Vol. 37, No. 5*

THE

PHYSICAL REVIEW

ON SOME SOLAR AND LUNAR SPECTRA TAKEN IN LITTLE AMERICA, ANTARCTICA*

By Malcolm P. Hanson** and E. O. Hulburt

Naval Research Laboratory

(Received January 26, 1931)

Abstract

Solar spectra were taken with a small quartz spectrograph at noon on November 13, 1929, and January 25, 1930, in Little America, Antarctica, by Malcolm P. Hanson of the Byrd Antarctic Expedition. The ultraviolet limit of these spectra was at about 304$\mu\mu$ which was the same as the ultraviolet limit of noon solar spectra taken at Washington, D.C., in December and January. Assuming that the ultraviolet limit of the solar spectra was due to ozone in the upper atmosphere and that the amount of ozone in Washington was the same as that measured by Dobson, Harrison, and Lawrence at Oxford, England, it came out that the effective thickness of the ozone at N.T.P. above Little America was about 0.28 cm on November 13, 1929, and January 25, 1930.

The ultraviolet limit of lunar spectra taken at Little America on April 24, 1929, two days after the Antarctic winter night set in, and on July 18, 1929, thirty-five days before the night ended, was at about 305$\mu\mu$.

AMID the stress of final preparations for the departure of the Byrd Antarctic Expedition it was decided to take along a small quartz spectrograph, Hilger, Type E3. An experiment was hurriedly planned which consisted simply in photographing spectra of the sun and the moon in Antarctica with exposures long enough to bring out the ultraviolet region around 300$\mu\mu$. Meanwhile similar spectra were made with a similar spectrograph at the Naval Research Laboratory, Washington, D.C. By a comparison of the two sets of spectra it was hoped to learn something about the ozone in the upper atmosphere of Antarctica. The dispersion of the spectrographs was about 4$\mu\mu$ per mm at wave-length 300$\mu\mu$.

November 13, 1929, was clear and solar spectra were obtained at Little America, latitude 78.6° south, with a slit width of about 0.02 mm, being purposely over-exposed in the visible part of the spectrum in order to bring out the ultraviolet end. The ultraviolet limit of spectra taken at noon, local time, was at about 304$\mu\mu$. The same limit was given by similar spectra at noon on January 25, 1930. The midnight sun spectrum of January 25, 1930, ended at about 320$\mu\mu$; the sun was about 9° above the horizon at that time.

* Published with the permission of the Navy Department.

** In charge of radio of the Byrd Antarctic Expedition.

The noon solar spectra at the Naval Research Laboratory for November and December, 1929, and January, 1930, ended at about 303, 304 and 304$\mu\mu$, respectively; the same values were found, respectively, for November and December, 1930, and January, 1931. The noon spectra for June, 1930, ended at about 299$\mu\mu$. It is seen that the solar ultraviolet limit was the same on November 13, 1929, and January 25, 1930, at Little America as it was in December or January at Washington. The altitude of the sun was approximately the same at the two places, being about 30° from the horizon at Little America and 27° to 30° at Washington. Therefore, since the ultraviolet end of the solar spectrum is limited by the ozone in the upper atmosphere the measurements indicated that the ozone in November, 1929, and January, 1930, was of about the same thickness in Little America as it was in Washington in December and January. It is due to the fortunate circumstance that both the elevations of the sun and the ultraviolet solar spectrum limits were about the same at Little America and at Washington that one can say that the ozone thicknesses were the same at the two places. If, for example, the spectrum limits had been the same and the solar elevations different, or vice versa, the program of observations could probably not have been used with safety to derive an exact conclusion about the relative amounts of ozone in the two regions.

We do not know what the thickness of the ozone was in Washington but we may assume it to be roughly the same as that in Oxford, England, observed by Dobson, Harrison, and Lawrence[1] in 1925 and 1926. The justification of this assumption is found in the fact that the seasonal variation, with the maximum in August, of the intensity of the therapeutic solar wave-lengths 290 to 310$\mu\mu$, observed by Clark,[2] in 1927 and 1928 in Baltimore, Md., U.S.A., agreed fairly well with the intensity calculated[2] from the ozone absorption coefficients of Fabry and Buisson,[3] the 1925 and 1926 ozone thickness[1] at Oxford and the solar zenith distance at Baltimore. Clark's[4] further observations showed that the curve of the seasonal variation of the solar radiations from 290 to 310$\mu\mu$ was approximately the same in the years 1929 and 1930 as it was in the years 1927 and 1928.

Interpolating among the Oxford measurements (ref. 1, Table 3) gives the values for December and January to be 0.27 and 0.29 cm of ozone, respectively. Accordingly, the average of these, or 0.28 cm was the value of the effective thickness of the ozone in Little America on November 13, 1929, and January 25, 1930. It need hardly be said that the present method of determining ozone by means of the ultraviolet limit of the solar spectrum can not be depended upon to give great accuracy. It is to be hoped that future polar expeditions may be equipped to carry out much better determinations of ozone.

The value 0.28 cm of ozone in midsummer at Little America is in keeping

[1] Dobson, Harrison and Lawrence, Proc. Roy. Soc. **A114,** 521 (1927).
[2] Clark, Amer. Jr. Hygiene **9,** 646 (1929).
[3] Fabry and Buisson, Journ. de Phys. **3,** 196 (1913).
[4] Clark, Amer. Jr. Hygiene **12,** 690 (1930).

with the probable average values in north polar regions in midsummer, namely, 0.290 cm for July and 0.265 for August, estimated by Dobson.[5] Dobson[1,5] concluded that the ozone values found by various stations scattered over the earth would be most simply accounted for by the hypothesis that corpuscular radiation from the sun is "the chief ozone forming agent at the poles and possibly for the rest of the world" (ref. 5, page 431). We do not think that the observations call for any such extreme hypothesis. Maris'[6] calculations of the temperatures of the high atmosphere indicate wind movements in the high atmosphere which, combined with the hypothesis that ozone is formed by certain wave-lengths of the ultraviolet portion of the solar spectrum and is decomposed by other wave-lengths, would lead, qualitatively at any rate, to an ozone distribution in agreement with observation. One cannot make an exact calculation of the matter for the photochemical quantum efficiencies of the formation and destruction of ozone by the various ultraviolet wave-lengths are not yet known.

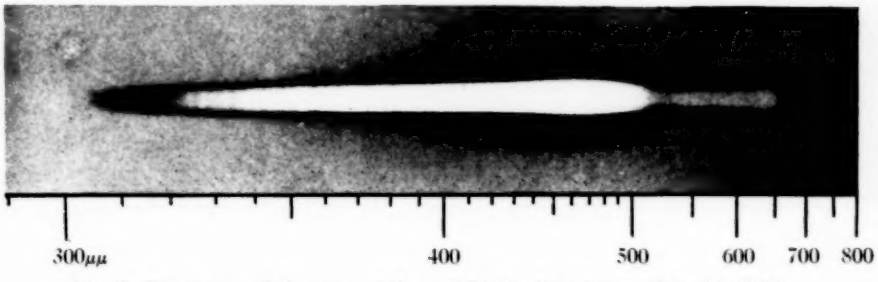

Fig. 1. Spectrum of the moon taken at Little America on July 18, 1929.

Spectra of the moon were taken at Little America on April 24, 1929, and on July 18, 1929. It will be remembered that the sun's last official appearance at Little America was on April 22 and his official reappearance was on August 22. Thus the moon spectrum of April 24 was obtained two days after the beginning of the Antarctic winter night and the one of July 18 was obtained thirty-five days before the end of the Antarctic night. The spectrograph was mounted outside on the snow, aimed at the moon and shifted by hand from time to time. The moon was focussed on the slit by a quartz lens 5 cm in diameter and 20 cm in focal length. The spectra of April 24 were taken with a slit width of 0.3 mm and exposures from 1 to 15 minutes. With such a wide slit the ultraviolet limit of the spectrum was not sharply defined, and the only safe conclusion that could be drawn was that the ultraviolet limit was between 310 and 300$\mu\mu$.

On July 18 the moon was about 40° from the horizon and the temperature was −50° Farenheit. A good spectrum, reproduced as a positive in Fig. 1, was obtained with an exposure of one hour at midnight, local time, and a slit width of 0.05 mm. Eastman Commercial Panchromatic cut film was

[5] Dobson, Proc. Roy. Soc. **A129,** 412 (1930).
[6] Maris, Terr. Mag. and Atmos. Elec. **33,** 233, (1928); **34,** 45 (1929).

used. The spectrum extended to about 305$\mu\mu$, the last solar absorption line being at this wave-length. It is doubtful whether the solar absorption lines, which are clear enough on the original negative, can be seen in the reproduction of Fig. 1.

The film was somewhat fogged throughout and the bright lunar spectrum of Fig. 1 is seen to be surrounded by a region relatively darker than the general fogged field. The dark halo around the spectrum is thought to be due to the Eberhard photographic effect. If a plate or film be uniformly exposed to light of moderate intensity and if a small area be then given an additional heavy exposure, on development a region of abnormally lowered density will be noted around the dense portion. This is caused by the large quantity of soluble bromide thrown off from the heavily exposed area of emulsion during the development which acts as a restrainer and slows up the development of the surrounding regions. It is not known whether the low temperature during the exposure had anything to do with the rather unusual appearance of the negative of Fig. 1. The development of the film, which was done about three days after the exposure, was effected under approximately normal conditions. The solar spectra and the moon spectra of April 22, as well as the Washington spectra, in general showed the Eberhard effect to a slight degree, but none to the extent of the negative of Fig. 1.

Since the lunar spectra ended at about 305$\mu\mu$ it is concluded that the ozone in the high atmosphere of Little America during the winter night was not greatly different from ozone in other parts of the world. Rosseland[7] also found that stellar spectra photographed in midwinter at 71° north latitude ended around 300$\mu\mu$.

In conclusion it is a pleasure to mention the assistance of Mr. R. B. Carleton in taking the long series of solar spectra at this laboratory.

[7] Rosseland, Nature **123,** 207 (1929), discussed by Wood on page 644 and by Dobson on page 712.

DIRECTED VALENCE IN POLYATOMIC MOLECULES

By J. C. Slater
Massachusetts Institute of Technology

(Received January 22, 1931)

Abstract

The interactions of atoms in polyatomic molecules are described qualitatively. Particular attention is paid to atoms of the types of F, O, N, C, where the valences come from p electrons. Directional effects are discussed, namely that the two valences of O, and the three of N, tend to be mutually at right angles, and the four of C have tetrahedral symmetry. Numerous examples are given, from the structure of metals and of organic and inorganic compounds. Mathematical treatment is postponed until a later paper.

IT HAS already been noticed by Born[1] that the method applied by the writer to the problem of complex atomic spectra is equally adaptable to molecular structure. The writer[2] has used the method in one problem of atomic interaction, the problem of cohesive forces in univalent metals. When applied to molecular problems in general, however, it yields not only the familiar results for diatomic molecules, but also information regarding valence in polyatomic molecules, particularly in the matter of directional properties, which seems to be new and which is capable of correlating a good deal of experimental material. In this paper, we give the results of the discussion in a qualitative way, postponing mathematical justification to a later paper.

The general ideas described in the paper were outlined in an informal talk at the Washington meeting of the American Physical Society last April, and I wish to thank several members of the society for valuable discussion at that time. I also wish to acknowledge valuable assistance and suggestions from several of my colleagues, particularly Dr. Warren, Dr. Ashdown, and Dr. Scatchard.

Two atoms containing all their electrons in closed shells repel each other. But if each atom has one wave function containing only one electron, rather than two of opposite spins, attraction is possible. This actually occurs if the spins of the electrons in question in the two atoms are oppositely directed. The attraction pulls the atoms together until the wave functions from which electrons are missing overlap as much as possible, when equilibrium occurs. In consequence of resonance, the charge concentrates at the place where the functions are overlapping, and in an approximate way we may consider that the two electrons, of opposite spin, spending their time in this region, form a closed shell. This is a homopolar valence bond, and two electrons forming such a bond are inactive in forming further bonds, just as if they were in closed shells within a single atom.

[1] M. Born, Zeits. f. Physik **64**, 729 (1930).
[2] J. C. Slater, Phys. Rev. **35**, 509 (1930).

The simplest and most familiar example of a single valence bond is found in H_2,[3] where each atom contains a single 1*s* electron, so that the 1*s* shell is not completed, and if the spins are oppositely directed, the electrons are shared and form a molecule. But almost equally simple is, for example, I_2. Here each atom lacks a single *p* electron from its outer shell. If the remaining electron in that particular *p* wave function in one atom has a spin opposite to that in the other, there will be attraction, which will proceed until the two wave functions overlap as much as possible. We meet at once the question, how does the degeneracy of the *p* shell affect the problem. And we can answer definitely from perfectly general considerations.

To get the lowest possible energy, we wish in a rough way the greatest possible overlapping of the *p* functions from the two atoms. This demands first that each of these functions be as concentrated as possible. Now the wave functions corresponding to the three *p* levels, in the ordinary axial system of coordinates, can be written

$$\begin{aligned} p^+ &: \quad (x + iy) \quad f(r) \\ p^0 &: \quad z \quad f(r) \\ p^- &: \quad (x - iy) \quad f(r). \end{aligned}$$

The charge densities corresponding to these are

$$\begin{aligned} p^+ &: \quad (x^2 + y^2) \quad f^2(r) \\ p^0 &: \quad z^2 \quad f^2(r) \\ p^- &: \quad (x^2 + y^2) \quad f^2(r). \end{aligned}$$

As shown in Fig 1, made by a very ingenious method by Dr. Langer, the first and third are great in the *x*-*y* plane, in a sort of ring-shaped region; the second

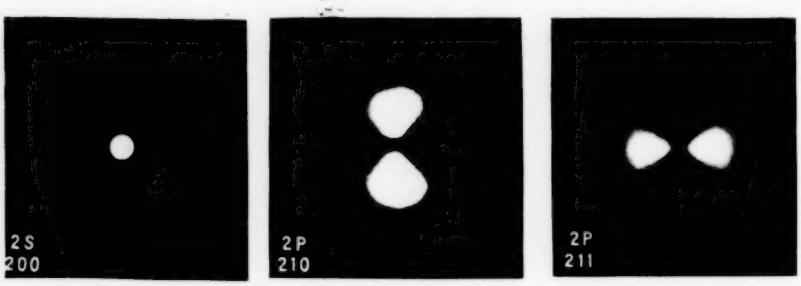

Fig. 1. Charge distribution of p^+ and p_0, with *s* for comparison.
I am indebted to Dr. Langer for this photograph.

is great along the *z* axis, and is more concentrated than the others. But we are allowed to use any three orthogonal linear combinations of these functions. If we take $(r \cdot u_1) f(r)$, $(r \cdot u_2) f(r)$, $(r \cdot u_3) f(r)$, when u_1, u_2, u_3 are three orthogonal unit vectors, these functions will be great, respectively, along the

[3] Heitler and London, Zeits. f. Physik **44**, 455 (1927).

axes of these three vectors, and each will be as concentrated as the p_0 before. These functions evidently give as concentrated a density as we can get, and hence are most suitable for use in discussing binding.

Let us now consider our I_2 molecule. We take the vector u_1 in each atom as the vector pointing toward the other atom. Then plainly the functions $(r \cdot u_1) f(r)$ for the two atoms, since they correspond to distributions pointing along the line of centers, and hence stretching out toward the other atom, can overlap. The other functions, on the other hand, are large in the planes normal to the line of centers, and do not overlap appreciably. We can visualize the atoms as the hubs of two wheels connected by an axle. The functions which overlap are extending along the axle, the others along the spokes of the two wheels. For binding, then, we assume an electron missing from this function $(r \cdot u_1) f(r)$ in each atom, and we can be confident that in this way we shall get the most stable molecule. In the usual description, if the z axis is taken as the axis of the molecule and at the same time the axis for axial wave functions for the electrons, an electron with function p_0 is missing from each atom. This coincides with the conventional description of this case.

Next let us consider an atom which lacks two electrons of having a complete shell, as for example O. Suppose we have another atom, as H, which can be bound to it. We choose our vectors u_1, u_2, u_3 so that one of them, say u_1, points along the line from O to H. Then by the previous argument we must have one electron missing from the state which we may symbolize by u_1, to form the bond with the H. The other missing electron must then be lacking from either the state u_2 or u_3, and hence must have its density along the direction at right angles to the line joining the O and H. A second hydrogen attempting to become bound to form a water molecule, would move so that its charge would overlap in place of this missing one. It would then take up a position so that the lines joining the centers of the oxygen and the two hydrogen atoms would form right angles. Of course, the interactions between the two hydrogen atoms would modify this; it is difficult to say in which direction. But in a general way we should expect a triangular model, as is shown in Fig. 2, and that of course is observed.

The same sort of argument would indicate that the two valences of a divalent atom like oxygen should always be at right angles, and we can obtain many actual examples of this. The atoms of this sort are O, S, Se, Te. In the elements Se and Te in the solid state the atoms form chains of an interesting helical form, as shown in Fig. 3, so that if we look along the axis of the helix every third atom lies in a corresponding position. But just such a spiral is formed if atoms are arranged in a chain with the lines joining successive atoms making right angles with each other, these lines pointing in succession along the $x, y, z, x, y, z, \cdots$, axes, which is the structure which our theory would suggest. Another illustration, less definite, is furnished by the crystal structure of the silicates. These are presumably in general ionic compounds. But some features of them resemble valence compounds: each silicon is surrounded by four oxygens, suggesting the valence of four and tetrahedral structure which we shall discuss in a later paragraph; and where an

oxygen is shared between tetrahedra, is shared by two only, as if it had just two valences for the two silicons. These features are both illustrated in Fig. 4. Now it is observed that in such a shared oxygen, the lines joining the oxygen to the silicons always form an angle with each other, as if there were

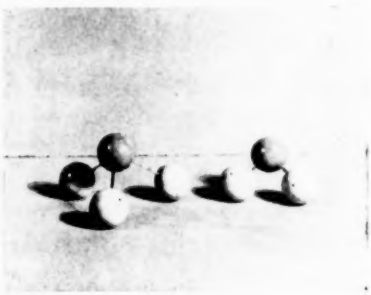

Fig. 2.

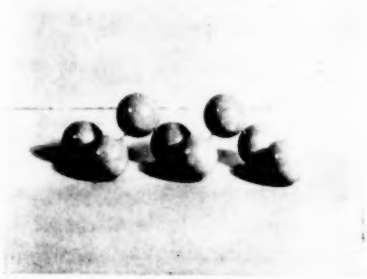

Fig. 3.

Fig. 2. NH_3 and H_2O. The angles here, and in the other figures, are taken to be just 90°, rather than adjusted to agree with experiment.

Fig. 3. Chain of atoms from Te. The actual chain continues indefinitely in both directions. The crystal is made of many chains packed together parallel to each other.

valences which tended to be at right angles to each other, rather than being parallel as one would otherwise expect.

The trivalent atoms, N, P, As, Sb, Bi, can be discussed by just the same principles: their three valences tend to be mutually at right angles, one elec-

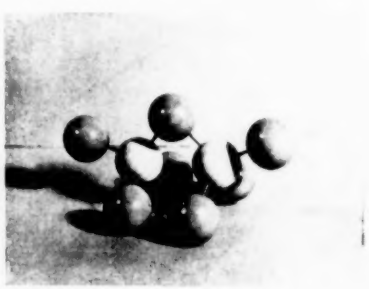

Fig. 4.

Fig. 5.

Fig. 4. $(Si_2O_7)^{-6}$ group from a silicate. The lighter atoms represent Si. Two tetrahedra are joined by sharing an O. In the actual case, the valences of this shared O are more nearly parallel than we have shown.

Fig. 5. Sheet of atoms from Bi. This consists of two layers of atoms, each atom being joined to three neighbors in the other sheet. The whole crystal consists of piles of these sheets.

tron being shared from each of the three functions with the factors $(r \cdot u_1)$, $(r \cdot u_2)$, $(r \cdot u_3)$. The most obvious example is ammonia, NH_3, which has the pyramidal structure which we should expect from this model, as is shown in Fig. 2. Then in the metals, As, Sb, Bi, we find good illustrations of the princi-

ple. The atoms in these metals form plates, which appear, when we look down on them, like hexagonal lattices, each atom being surrounded by three others symmetrically placed. But really alternate atoms are displaced above or below the plane, as shown in Fig. 5, so that each atom above the plane is at the apex of a pyramid whose base is formed by three atoms below the plane, and vice versa; and the three lines joining an atom with its neighbors are very nearly at right angles. The whole crystal is formed by piling these plates together in such a way as to approximate a simple cubic lattice.

Other examples can be found in organic compounds containing nitrogen, in which the nitrogen is connected to something else by a double bond. In the oximes, as shown in Fig. 6, it is connected in this way to a carbon atom; in the azo compounds as in Fig. 7, to another nitrogen. The double bond we visualize simply as the sharing of two electrons, so that the two bonds and the center of the atom determine a plane. The third valence of the nitrogen

Fig. 6.

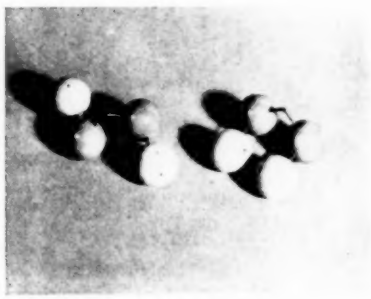

Fig. 7.

Fig. 6. Two isomeric forms of an oxime compound. A nitrogen and carbon are joined by a double bond. The two forms arise from the two possible orientations of the third valence of the nitrogen.

Fig. 7. Two isomeric forms of an azo compound. Two nitrogens are joined by a double bond.

should then, according to our picture, be at right angles to this plane, but it could point out in either of the two normal directions. If the rest of the molecule were not symmetrical about this plane, we should then expect two forms of the molecule, depending on which normal were chosen; and as a matter of fact, both these groups of compounds show isomerism which is attributed to just this sort of effect.

The tetravalent atoms, C, Si, Ge, Sn, Pb, demand a different treatment. If we assume that four electrons are removed from the group of six p's, this leaves none in one of the three wave functions, and one each in the remaining two. Thus there are two electrons to be shared, as in O, and we have divalent atoms as we observe for example in CO. But to obtain a valence of four, we must plainly have only three p's removed, leaving one electron each in these states; and the other missing electron must then be an s. This latter, having a spherical distribution of charge, has no directional properties. Thus in CH_4, for example, we should tentatively expect that the three hydrogens attached

to p valences would form a pyramid, as in NH_3, and the remaining hydrogen, bound to an s, and free to wander, would set itself opposite the apex of the pyramid to avoid the others, forming a rough tetrahedron. This would not be a symmetrical tetrahedron, however; and by a slight change in the conditions we can arrive at a really symmetrical one, which would undoubtedly have a lower energy, and which we consider to be the real form for a tetravalent compound.

To arrive at this symmetrical arrangement, we set up four linear combinations of the three p wave functions and the one s function, having a tetrahedral symmetry. We take four unit vectors, u_1, u_2, u_3, u_4, pointing to the four corners of a regular tetrahedron. Then the four functions $(r\cdot u_1)\,f(r)$, $\cdots$, $(r\cdot u_4)\,f(r)$ are, as we have seen, linear combinations of the three p functions, but of course they are not orthogonal. If however we take the s wave function, say $\phi(r)$, we can form combinations $(r\cdot u_1)\,f(r)+\alpha\phi(r)$, $\cdots$, $(r\cdot u_4)\,f(r)+\alpha\phi(r)$, where α is a parameter, and we can choose α to make the four

Fig. 8. Diamond lattice.

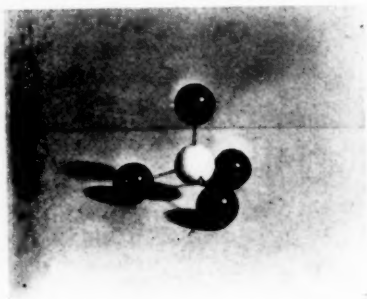

Fig. 9. CH_4.

functions orthogonal. These are then the required tetrahedral wave functions. The density of each one is great along one of the axes of a regular tetrahedron; the addition of the s function results in having the density much larger in one direction than in the opposite one. If now each of these wave functions lacks one electron, and other atoms share with the remaining ones, they will take up a tetrahedral arrangement about the central atom.

The tetrahedral structure for the valence of C and the other atoms of this group is too well known to require extensive comment; a very great number of observations of the organic chemists have led to it. But we may mention a few examples. The solids as diamond, forms of Pb and Si, form the diamond lattice shown in Fig. 8, in which each atom is surrounded by four others in tetrahedral arrangement. The gas CH_4, shown in Fig. 9, is undoubtedly tetrahedral, as shown by the absence of electric moment. The double carbon bond is explained very easily by the sharing of two electrons, meaning that two tetrahedra join by an edge. The remaining four valences then all lie in a plane, as shown in Fig. 10, and the isomerism of the derivatives of ethylene, $H_2C=CH_2$, is readily explained: given two unlike radicals attached to each atom, there will be two different compounds depending on the two possible

assignments of one pair to the two electrons of the corresponding atom. This explanation seems much more convincing than the ingenious theory of Hückel,[4] based wholly on *p* electron valence.

The weakness of Hückel's theory is that he does not consider carefully the nature of the other bonds than the double one, and hence does not notice the fact which we point out, that the *s* valence must be combined with the *p*'s to obtain a symmetrical arrangement. If one followed his argument through, each of the carbons in ethylene would have one *p* valence and one *s* free to join to hydrogens, and the latter would then hardly be equivalent.

Similarly the triple bond would correspond to the sharing of a whole face of two tetrahedra. The remaining valences would then point out along the line of centers, so that acetylene, HC≡CH, shown in Fig. 11, should be a linear molecule, as is observed from its lack of dipole moment.

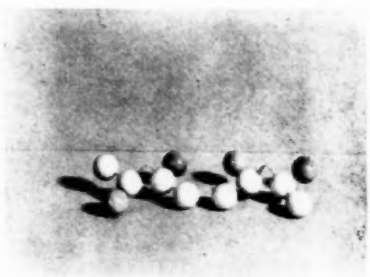

Fig. 10.

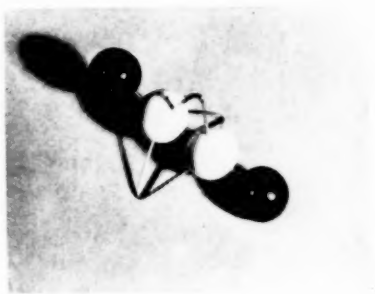

Fig. 11.

Fig. 10. Two isomeric forms of a substituted ethylene. Two carbons joined by a double bond. Two isomers if at least two sorts of radicals are attached to the carbon: trans form (at left) with like radicals opposite; cis form (right) with like radicals adjacent.

Fig. 11. C_2H_2. A linear molecule with a triple bond.

An ordinary chain compound is shown in Fig. 12. The zig-zag structure of the compound, observed for example by Müller,[5] is well shown in the figure.

The atoms beyond the tetravalent ones appear generally in ionic compounds rather than with valence bonds, and so do not concern us in this paper. But we should discuss one point: in a great many compounds there is ambiguity as to whether the bonds are homopolar or ionic. We have mentioned the silicates; other examples are H−Cl (which could be written also H^+Cl^-) and H–O–H (which could be written $H^+(OH)^-$ or $H^+O^-H^+$). Even such a compound as Al_2O_3 can be written in either way (Al—O—Al or $(Al^{+++})_2(O^=)_3$). Very general principles of wave mechanics tell us the outline of the treatment in these cases. The two explanations constitute two unperturbed states, from which the true one is to be found by linear combination, so that the real situation is intermediate between the two. If the energies of the two

[4] E. Hückel, Zeits. f. Physik **60,** 423 (1930).

[5] A. Müller, Proc. Roy. Soc. **A114,** 542 (1927).

models are approximately the same, the real state will lie roughly half way between, while if one has a much lower energy than the other, that will fairly accurately represent the real situation. Moreover, if the two are combined, there will be a resonance effect in the energy, which will generally bring the real energy lower than that computed from either model separately. This may well explain the unusual stability of the silicates, and of the other compounds we mentioned: their energy is lower on account of the two explanations of the binding.

It is important to consider the relation of our models, say for H_2O, to those of Debye,[6] based on the assumption of ionic compounds in which the polarizibility of the $O^=$ is considered. Debye has been able to give alternative explanations even of the triangular form of H_2O and the pyramidal form of NH_3. From the discussion of the last paragraphs, we see that both these explanations are to be regarded as legitimate starting points, with the true

Fig. 12.

Fig. 13.

Fig. 12. A chain compound, C_7H_{16}. The zig-zag arrangement of carbons, and the elongated cross-section of the chain, result from having the valences of carbon inclined at definite angles to each other.

Fig. 13. Benzene, C_6H_6. The Kekulé model.

state of affairs somewhere between them. The two descriptions, ionic and homopolar, are not as a matter of fact very different in fundamentals. Consider for example HCl. In the homopolar valence explanation, the electron from H, and one from Cl, are shared on the line joining the two atoms, and the net effect is that some of the hydrogen electron's charge has shifted toward the chlorine. In the ionic explanation, we start by assuming that the hydrogen electron is wholly transferred to the chlorine. But then we assume that polarization pulls some of it back again, and we are left in very much the same situation as before. The principal advantages of the homopolar method, with these ambiguous problems, are first that it seems rather nearer the real solution, as is shown, for example, by the small dipole moments of the hydrogen halides; and second that it is better able to deal in a general way with directional properties.

Another point connected with valence should be mentioned similar to the

[6] P. Debye, "Polar Molecules," Chemical Catalog Co.

ambiguity between the ionic and homopolar valence descriptions of a compound. In some cases there may be several ways of drawing valence bonds in a given compound. In such cases, the real situation is again a combination of the various possibilities, and on account of resonance the energy is lower than it would otherwise be. We can not then draw the valence bonds in an unambiguous way; we must rather imagine them shared between several atoms. Such cases of shared valence may well be commoner than is usually supposed. The writer has already explained the cohesion in monovalent metals as coming from this effect, and it probably persists through most of the metals other than those specifically discussed in this page; for in all of these, each atom has more neighbors than it has electrons to share, and hence than it has valence bonds in the ordinary sense. Another example is probably found in the benzene ring. Here the Kekulé model, shown in Fig. 13, allows either the structure

or

By wave mechanics we should have a combination of these two possible structures, resulting in a complete equivalence of the carbons of the ring, a shared valence (essentially 1–1/2 bonds between each pair), and an added stability for the structure on account of the resonance effect on the energy. Still another case presumably comes in the existence of shared valences where ordinarily we suppose no valence at all to act. In H_2O, there is probably a little valence attraction between the two H's, just as if they were forming a H_2 molecule, and as a consequence the angle between the lines to the two H's should be slightly acute. And even between molecules we may expect this shared valence to act. In crystals like Te and Sb we have spoken as if all valence forces acted within the chains or plates of which the crystals are formed, but this undoubtedly is not the case. In complicated organic compounds, probably the valence forces between one molecule and another are nearly as strong as within a molecule. Substances where this is true will hang together to form solids, and it will be nearly as difficult to separate the molecules as to break up the individual molecules, so that an attempt to vaporize them by heating will be very likely to disrupt the whole structure instead, a common phenomenon with these complicated compounds. Many examples of polymerization may well be cases where valences formerly operative within a molecule have partly changed over to the role of intermolecular forces. It seems, then, that this phenomenon of shared valence is of common occurrence, and that an understanding of it, as well as of the relation between ionic and homopolar binding, is essential.

THE ROTATIONAL ANALYSIS OF THE S_2 BANDS

By S. Meiring Naudé and Andrew Christy
Ryerson Physical Laboratory, University of Chicago

(Received January 23, 1931)

Abstract

The emission spectrum of S_2 has been obtained by means of a Geissler tube, the plates being taken in the third order of a 21 foot concave grating giving a dispersion of 0.878A per mm. The following bands have been studied; 9–1(λ2857.36), 7–0(λ2860.13), 8–1(λ2887.84), 9–2(λ2917.38) and 7–1(λ2920.28). Each band consists of three R and three P branches. For small values of K each band appears to have a weak and a strong R branch and a weak and a strong P branch. The lines of the strong branches separate into two components for $K \geqq 25$. This structure is similar to that of the Schumann-Runge bands of O_2. It is concluded that the S_2 bands investigated are due to a ${}^3\Sigma_u^- \rightarrow {}^3\Sigma_g^-$ transition (like O_2). The values of B_e'' and B_e' (by extrapolation) are 0.409 and 0.319 cm^{-1}, respectively, the nuclear separation of the lower state being $r_e'' = 1.603 \times 10^{-8}$ cm and of the upper state $r_e' = 1.814 \times 10^{-8}$ cm. It is shown that the rotational levels with *odd* K values are missing in the *upper state* and those with *even* K values in the *lower state*. The fact that alternate levels are missing shows that the internal angular momentum of the S^{32} nucleus is zero.

Introduction

THE band spectrum due to the S_2 molecule extends from about λ6000 to λ2300A. The spectrum consists of a large number of overlapping bands which degrade toward the red. These bands have been studied by various investigators. Henri[1] divides the spectrum into four regions according to the frequency equations which fit most accurately the heads obtained in absorption. Rosen[2] has shown, however, that all these bands belong to the same band system, and from the vibrational analysis obtained the following equation for the heads:

$$\nu = \nu_e + 427.1(v' + \tfrac{1}{2}) - 2.7(v' + \tfrac{1}{2})^2 - 727.4(v'' + \tfrac{1}{2}) + 2.91(v'' + \tfrac{1}{2})^2 \quad (1)$$

Henri[1] found the bands to become diffuse at λ2794.2, a phenomenon which he termed "predissociation."

Henri and Teves[3] using plates taken in absorption with relatively small dispersion, attempted a rotational analysis of the S_2 spectrum. They state that each band consists of P, Q, and R branches, giving the values of the nuclear separations for the upper and lower states as $r' = 0.70$A and $r'' = 0.73$A. Teves[4] continued this work in fluorescence obtaining results similar to those of Henri and Teves. Recently Swings[5] and Rompe[6] also working with the

[1] V. Henri, Structure des Molecules, Paris, p. 93 (1925).
[2] B. Rosen, Zeits. f. Physik **43**, 69 (1927).
[3] V. Henri and M. C. Teves, C. R. **179**, 1156 (1924).
[4] M. C. Teves, Dissertation, Zurich (1926).
[5] P. Swings, Zeits. f. Physik **61**, 681 (1930).
[6] R. Rompe, Zeits. f. Physik **65**, 404 (1930).

fluorescence spectrum of S_2, have tried to bring their results into agreement with those of Henri and Teves, but found it impossible to interpret completely the complex patterns obtained.

It has been shown that the molecules F_2, Cl_2, Br_2, and I_2 have similar electronic states. The same has also been found in the molecules Li_2, Na_2, and K_2.[7] One would therefore expect a corresponding similarity to hold for O_2 and S_2. In particular it seems probable that the S_2 bands mentioned above are analogous to the Schumann-Runge bands of O_2. Recently E. V. Martin and F. A. Jenkins[8] have also found the SO bands lying between λ2500 and λ3500 to correspond to the Schumann-Runge bands. The analysis of Henri and Teves, however, would indicate that S_2 differs fundamentally from O_2. Furthermore, the values of r_e'' and r_e' found for the O_2 Schumann-Runge bands[9,10] are 1.204 and 1.609A, respectively. Irrespective of the similarity of the S_2 and O_2 bands, the values of the nuclear separations for the two states obtained by Henri are too small, since the r_e values for S_2 are surely greater than those for O_2, whereas, according to Henri, the reverse is the case.

The purpose of the present work was to check Rosen's results by studying the spectrum of the S_2 bands photographed with greater dispersion than he used, and to obtain the rotational analysis. The work dealing with the vibrational analysis, perturbations, predissociation, etc., will be discussed in a later paper, and only that concerning the rotational structure will be given here. It will suffice to state that, except for the revision of the vibrational quantum numbers of a number of band heads and the discovery of numerous perturbations, mainly in the upper electronic state, our results agree with those of Rosen, so that his analysis with a few modifications can be made use of in the present paper.[11]

Experimental Procedure

The spectrum of S_2 was excited in a Geissler tube (see Fig. 1) of Pyrex, having large cylindrical aluminum electrodes, so that as much as 0.7 amps. could be passed through the tube. The current was supplied by a 5 KW transformer. The tube was provided with a quartz window *W* sealed on to one end of a quartz tube, the other end of which was ground flat. This end of the quartz tube was sealed onto the Pyrex tube with sealing wax. Considerable difficulty was experienced in keeping the quartz window from fogging due to sulphur condensing on it. The best results were obtained when the sulphur was introduced into the tube in the form of H_2S [12] which streamed continuously through the tube in the direction away from the window, thus opposing the diffusion of sulphur towards the window. In case the window did get fogged with sulphur, heating it gently with a bunsen burner restored

[7] R. S. Mulliken, Phys. Rev. **36,** 1440 (1930).

[8] E. V. Martin and F. A Jenkins, Phys Rev. **37,** 226 (1931).

[9] W. Ossenbrüggen, Zeits. f. Physik **49,** 167 (1928).

[10] W. Lochte-Holtgreven and G. H. Dieke, Ann. d. Physik (5) **3,** 937 (1929).

[11] P. Huber, Amer. Phys. Soc. Meeting, Paper No. 65, Cleveland. Dec. 30, 1930, has apparently also found that Rosen's vibrational analysis is fundamentally correct.

[12] H. H. Van Iddekinge (Nature **125,** 858 (1930)) has independently used the same method.

its transparency. The H_2S was dried over P_2O_5 before introduction into the tube. In the discharge tube the H_2S dissociated, giving sulphur and hydrogen.[13] The other end of the tube was connected to a liquid air trap in which the sulphur and H_2S were frozen out. This trap in turn was connected to a Megavac oil pump which was kept running while the discharge was going on. The pressure of the sulphur in the discharge tube could be regulated by controlling the flow of H_2S by means of a stopcock sealed on to a capillary tube.

Another method used for introducing the sulphur into the above discharge tube was by distilling the sulphur in vacuo into the side tube T (see Fig. 1). By heating T while the discharge was running pure sulphur could be introduced directly into the discharge tube. In this case a mercury diffusion pump was used to evacuate the discharge tube beforehand. More sulphur condensed on the window when this method was used and therefore the former method was preferred for long exposures. The spectrum obtained by

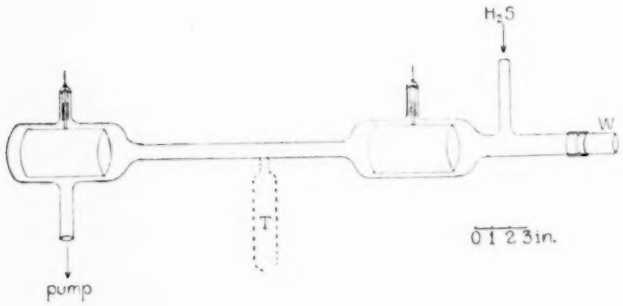

Fig. 1. Discharge tube used for obtaining the S_2 emission spectrum in the region $\lambda 2850 - \lambda 2950$ with great intensity. W is a quartz window sealed into a quartz tube which is in turn sealed on to the discharge tube with sealing wax. When sulphur is used instead of H_2S to obtain the spectrum the tube T with the dotted outline contains pure sulphur.

this method agreed with that obtained by introducing H_2S, as was determined by comparing plates taken in the second order of the 21 foot grating in both cases.

The photographs of the bands in the region $\lambda 2850$–$\lambda 2950$ used for the analysis were taken in the third order of the 21 foot Rowland grating giving a dispersion of 0.878A per mm. A red purple filter of the Corning Glass Company was used to cut out the second order between $\lambda 4250$ and $\lambda 4450$A which would otherwise overlap the spectrum obtained. Eastman 33 plates were used. The time of exposure was about 30 hours.

The plates were measured on a comparator with an accuracy of 0.003 mm. The iron arc was used as comparison spectrum, the wave-lengths of which were taken from Kayser's "Hauptlinien" (1926). The iron standards agreed to within 0.003A, so that the wave-lengths of the sulphur band lines

[13] In the region $\lambda 2850 - \lambda 2950$, which we studied for this work, the sulphur spectrum was very intense as compared with the weak continuous spectrum obtained from the hydrogen molecule.

may be assumed to be correct to 0.01A. The wave-lengths (in air) were converted to wave-numbers (in vacuo) by means of Kayser's "Schwingungszahlen."

Data and Rotational Analysis

The bands due to S_2 are very numerous so that there is practically no region of the emission spectrum in which overlapping does not occur. In the region between λ2828 and λ2950 the overlapping is the least. Therefore the bands: 9–1, with its head at λ2857.36; 7–0, λ2860.13; 8–1, λ2887.84; 9–2, λ2917.38 and 7–1, λ2920.28, have been chosen for the rotational analysis. Even with the large resolution used a large number of lines could not be separated, a few unresolved groups having a width as large as 1 cm^{-1}. The lines of the 9–1 and 9–2 bands could not be followed very far due to the overlapping of the 7–0 and 7–1 bands, the latter being considerably more intense than the former. Other weaker bands are partially superposed on the 8–1, the 7–1 and probably on the 7–0 band, making the assignment of the lines into series extremely difficult.

It was noticed that in the clear regions of the 9–1 and 9–2 bands the strong lines in each band could be assigned into two distinct series. For every strong line in the above bands there is a line of about half the intensity on the short wave-length side of the former, the interval between the strong and the weak lines remaining approximately constant. The same type of series, i.e. two strong and two weak series, has been found in each of the remaining bands. In the two bands, 7–0 and 7–1, in which the series could be followed to a considerable distance from the head, it was seen that each line of the strong series splits into two lines, the components of this doublet having equal intensity. The distance between each line of the weak series and the center of the corresponding doublet in the strong series, after its lines had split, is the same as before splitting occurred. In this region the three lines, i.e. the lines of the weak series and the two corresponding lines into which each line of the strong series splits, are approximately of the same intensity. It is evident, therefore, that each band consists of six series: A , A_y, A_z, B_x, B_y and B_z. In the 9–1 and 9–2 bands, where the overlapping by other bands is least, all lines but two have been assigned to the various branches.

The two sets of combinations which are given in Tables IV and V were obtained by performing the subtraction $A(\alpha)-B(\beta)$ and $A(\alpha)-B(\beta+1)$, where α and β are arbitrary numbers assigned to the series A and B respectively. Since the S_2 bands are those of a homopolar molecule $(S^{32})_2$, we may expect alternate band lines to be either missing or weak.[14] But if the latter were the case we would have noticed it. If, however, all lines are present in the series, the above combinations would correspond to $R(K)-Q(K)\approx\Delta_1F'(K)$ and $R(K)-Q(K+1)\approx\Delta_1F''(K)$, [or $Q(K)-P(K)\approx\Delta_1F'(K)$ and $Q(K)-$

[14] F. W. Aston (Proc. Roy. Soc. **A115,** 487 (1927)) has estimated that about 97 percent of the atomic weight of sulphur is due to the S^{32} isotope. Consequently these S_2 bands must be due to $(S^{32})_2$. The bands due to $S^{32}S^{34}$ and $S^{32}S^{33}$ have not been observed. These bands will be very much weaker and, furthermore their calculated positions lie within the bands investigated thus making their observation more difficult.

$P(K+1) \approx \Delta_1 F''(K)]$. The A_x, A_y, and A_z series would then be three R (or three Q) branches and the B_x, B_y and B_z series would be three Q (or three P)

TABLE I. *Wave-numbers of the lines in the 9–1 and 9–2 bands and the intervals between corresponding strong and weak lines*

	9-1 band				9–2 band			
K	R	P	$\delta\nu_R$	$\delta\nu_P$	R	P	$\delta\nu_R$	$\delta\nu_P$
3	—	34983.2* 82.3	—	−0.9	—	34263.4* 62.4	—	−1.0
5	34987.1* —	980.8* 79.7	—	−1.1	34267.4* 66.5	261.0* 60.0	−0.9	−1.0
7	986.3* 84.7	977.4* 76.4	−1.6	−1.0	266.5* 65.5	257.7* 56.6	−1.0	−1.1
9	985.2* 84.2	973.4* 72.1	−1.0	−1.3	265.2* 64.3	253.6* 52.6	−0.9	−1.0
11	983.2* 82.3	969.1* 68.0	−0.9	−1.1	263.4* 62.4	249.3* 48.3	−1.0	−1.0
13	980.8* 79.7	964.0*[1] 62.8	−1.1	−1.2	261.2* 60.0	244.7* 43.3	−1.2	−1.4
15	978.1* 76.4	958.2* 57.0	−1.7	−1.2	257.9* 56.7	238.7* 37.2	−1.2	−1.5
17	974.2* 72.7[1]	952.3* 50.7	−1.5	−1.6	254.4* 52.9	232.6* 31.1	−1.5	−1.5
19	970.0* 68.6	945.1* 43.6	−1.4	−1.5	250.4* 49.3	225.2* 24.0	−1.1	−1.2
21	965.3* 63.7[1]	937.4* 35.9	−1.6	−1.5	245.8* 44.7	218.0* 17.1	−1.1	−0.9
23	959.9* 58.2	929.6* 28.0	−1.7	−1.6	240.2* 38.7	210.0* 08.6	−1.5	−1.4
25	954.0* 52.7	921.9 21.4[1] 20.0[1]	−1.3	−1.6	234.5* 33.3	201.4* 00.0	−1.2	−1.4
27	947.2* 45.5[1]	— 911.6 09.9	−1.7	−1.7	228.1* 26.8	193.0 92.5 91.5	−1.3	−1.3
29	—	—	—	—	222.4 21.7 20.4	183.9 83.2 82.1	−1.6	−1.4
31	—	—	—	—	214.7 14.0 12.7	173.6 73.0 72.0	−1.6	−1.3
33	—	—	—	—	—	163.1 62.5 61.2	—	−1.6

* These lines are made up of two components which become resolvable at $K=25$. They are referred to in the text as R_{xy} and P_{xy}, and when they become resolvable R_x, R_y, P_x and P_y. The remaining values are then R_z and P_z. It will be shown later in the text that R_x, R_y and R_z correspond to R_1, R_3 and R_2, respectively, and similarly for the P branches.

[1] Smoothed values, the observed lines being composite.

branches. But if alternate lines are missing, the combinations correspond to $R(K)-P(K)=\Delta_2F'(K)$ and $R(K)-P(K+2)=\Delta_2F''(K+1)$. The equations for Δ_1F and Δ_2F are:

$$\Delta_1F = \text{constant} + 2(B+3D)K + 4DK^3 \quad (2)$$

$$\Delta_2F = \text{constant} + 4(B+3D)K + 8DK^3 \quad (3)$$

where $B=h/8\pi^2\mu cr^2$ and $D=-4\overline{B}^3/\omega_e^2$, μ being the reduced mass of the molecule. If we assume the first alternative, i.e. no lines missing, we obtain from our data $B''=0.818$ cm^{-1}, while the second gives $B''=0.409$ cm.$^{-1}$ From the empirical formula[15] $B=(27.7/\mu)\ (3000/\omega'')^{-2/3}$ which holds within a few percent for all known molecules composed of atoms of equal or nearly equal mass, we obtain $B''=0.404$ cm.$^{-1}$ Furthermore, if we assume that all lines are present, the value of D calculated from the theoretical relation $D_e=-4B_e^3/\omega_e^2$ is sixteen times as large as the value actually obtained from our data, whereas if we assume alternate lines missing, the value of D obtained from our data agrees within experimental error with the above theoretical value. These comparisons show that we must adopt Δ_2F and alternate missing lines. The series A and B therefore correspond to three R and three P branches.

In Tables I, II, and III, listed under their respective headings, R or P, are given the lines of the five bands investigated. The lines indicated by asterisks are the strong lines made up of two components which become resolvable at about $K=25$. The values with superscript (1) are assumed values, the observed lines being composite. $\delta\nu_R$ and $\delta\nu_P$ are the intervals between the weak and the strong lines in the R and P branches, except that where the strong lines are separated into two components, $\delta\nu$ is the interval between the weak line and the center of gravity of the doublet. It is seen that these intervals are the same within experimental error for all the bands investigated.

The values of $\Delta_2F''(K)=R(K-1)-P(K+1)$, which should agree for the $7-1$, $8-1$ and $9-1$ bands are given in Table IV B. In Tables IV A and IV C the corresponding Δ_2F'''s of 7–0 and 9–2 are tabulated. The values of $\Delta_2F'(K)$ which should agree for the 7–1 and 7–0, and for the 9–1 and 9–2 bands are given in Table VA and VC. The corresponding $\Delta_2F'(K)$'s for the 8–1 bands are given in Table VB. It will be seen that all the expected agreements are fulfilled within experimental error.

The absence of strong Q branches indicates that we are dealing with a transition for which $\Delta\Lambda=0$. Furthermore, the great intensity of the entire system makes it evident that the transition is between two states of equal multiplicity, i.e. $\Delta S=0$. From the structure of the band, three R and three P branches, we conclude that the electronic states involved are triplets. The possible transitions are $^3\Sigma\rightarrow{}^3\Sigma$, $^3\Pi\rightarrow{}^3\Pi$ and perhaps $^3\Delta\rightarrow{}^3\Delta$.[16] The fact that

[15] P. M. Morse, Phys. Rev. **34**, 57 (1929).

[16] In a $^3\Pi\rightarrow{}^3\Pi$ or $^3\Delta\rightarrow{}^3\Delta$ transition we would expect three strong R and three strong P branches present, spaced approximately as in a $^2\Sigma\rightarrow{}^2\Sigma$ transition, if we have case (b) for both upper and lower electronic states, or if we had case (a) in which A is approximately the same in both the upper and the lower states (cf. TiO bands: A. Christy, Phys. Rev. **33**, 701 (1929)). For these transitions, however, we would expect all lines to be present and also the so called staggering effect, the magnitude of which would depend on λ type doubling.

TABLE II. *Wave-numbers of the lines in the 7–0 and 7–1 bands and the intervals between corresponding strong and weak lines.*

	7–0 band				7–1 band			
K	R	P	$\delta\nu_R$	$\delta\nu_P$	R	P	$\delta\nu_R$	$\delta\nu_P$
3	—	34949.9*	—	−1.7	—	34230.0*	—	−1.0
		48.2				29.0		
5	34953.3*	947.2*	—	−1.7	34233.3*	227.6*	−1.4	−1.6
	—	45.5			31.9	26.0		
7	952.7*	944.2*	−1.7	−1.4	232.6*	224.2*	−1.5	−1.4
	51.0[1]	42.8			31.1	22.8		
9	951.6*	940.5*	−1.4	−1.3	231.9*	220.4*	−1.5	−1.4
	50.2	39.2			30.4	19.0		
11	949.9*	935.7*	−1.7	−1.6	230.0*	215.8*	−1.0	−1.4
	48.2	34.1			29.0	14.4		
13	947.2*	930.6*	−1.7	−1.4	227.6*	210.8*	−1.6	−1.6
	45.5	29.2			26.0	09.2		
15	943.6*	924.3*	−1.6	−1.6	223.6*	204.7*	−1.9	−1.5
	42.0[1]	22.7			21.7	03.2		
17	939.4*	917.7*	−1.6	−1.8	219.5*	197.8*	−1.5	−1.9
	37.8[1]	15.9			18.0	95.9		
19	934.1*	909.9*	−1.5	−1.7	214.4*	190.3*	−1.7	−1.8
	32.6	08.2			12.7	88.5		
21	928.7*	901.5*	−1.6	−1.0	208.6*	182.1*	−1.0	−1.8
	27.1	00.5			07.6	80.3		
23	921.9*	892.9*	−1.4	−1.4	201.4*	173.0*	−1.0	−1.1
	20.5	91.5			00.4	71.9		
	914.4	883.0						
25	14.0[1]	82.6	−1.4	−1.3	194.5*	163.1*	−1.1	−1.3
	12.8	81.5			93.4	61.8		
	906.4	872.6			186.2	153.0		
27	05.6	71.8	−1.7	−1.2	86.0	52.4	−1.4	−1.3
	04.3	71.0			84.7	51.4		
	34898.1	34862.4			34177.8	34141.5		
29	97.2	61.5	−1.4	−1.7	77.0	40.8	−1.9	−1.7
	96.2	60.2			75.5	39.4		
	888.7	849.8			167.8	128.8		
31	87.5	48.5	−1.3	−1.5	66.9	27.8	−1.8	−1.9
	86.8	47.6			65.5	26.4		
	877.6	836.6			157.0	116.2		
33	76.7	35.2	−1.4	−1.5	56.5	15.3	−1.7	−1.4
	75.7	34.4			55.0	14.3		
	865.9	822.5			145.7	102.2		
35	65.0	21.1	−1.2	−1.3	44.8	101.7	−1.3	−1.3
	64.3	20.5			44.0	00.4		
						088.2		
37	—	—	—	—	—	86.8	—	−1.4
						86.1		

* These lines are made up of two components which become resolvable at $K=25$. They are referred to in the text as R_{xy} and P_{xy}, and when they become resolvable R_x, R_y, P_x and P_y. The remaining values are then R_z and P_z. It will be shown later in the text that R_x, R_y and R_z correspond to R_1, R_3, and R_2, respectively, and similarly for the P branches.

[1] Smoothed values, the observed lines being composite.

alternate lines are missing instead of staggering and that only three R and three P branches are present[17] clearly indicates that the bands are due to a

TABLE III. *Wave-numbers of the lines in the 8–1 band and the intervals between corresponding strong and weak lines.*

K	8–1 band R	8–1 band P	$\delta\nu_R$	$\delta\nu_P$
3	—	34614.1*	—	−1.7
		12.4		
5	34617.7*	612.0*	−1.4	−1.1
	16.3	10.9[1]		
7	616.9*	608.9*	−1.3	−1.8
	15.6	07.1		
9	616.3*	604.4*	−1.4	−1.6
	14.9	02.8		
11	614.1*	599.7*	−1.7	−1.1
	12.4	98.6		
13	612.0*	594.8*	−1.4	−1.4
	10.6	93.4		
15	608.9*	589.6*	−1.8	−1.3
	07.1	88.3		
17	604.4*	583.0*	−1.6	−1.5
	02.8	81.5		
19	599.7*	575.4*	−1.1	—
	98.6	—		
21	594.0*	567.4*	−1.6	−1.4
	92.4	66.0		
23	588.3*	558.8*	−1.5	−1.2
	86.8	57.6		
25	581.5*	549.7*	−1.7	−1.2
	79.8	48.5		
27	573.5*	539.0*	−1.4	−1.4
	72.1	37.6		
	565.9	529.6		
29	65.2	28.5	−1.8	−1.8
	63.7	27.2		
	—	516.8		
31	555.1	16.1	−1.6	—
	53.5	—		

* These lines are made up of two components which become resolvable at $K=29$. They are referred to in the text as R_{xy} and P_{xy}, and when they become resolvable R_x, R_y, P_x, and P_y. The remaining values are then R_z and P_z. It will be shown later in the text that R_x, R_y and R_z correspond to R_1, R_3 and R_2, respectively, and similarly for the P branches.

[1] Smoothed values, the observed lines being composite.

$^3\Sigma \rightarrow {}^3\Sigma$ transition, presumably analogous to that of the Schumann-Runge bands of O_2. We also know that the final $^3\Sigma$ state is the normal state, because these bands are observed with great intensity in absorption.[18,1,2]

[17] ^RQ and ^PQ band lines would probably be too weak to detect.

[18] We have found that this system of S_2 appears with great intensity in absorption.

TABLE IV. *The values of Δ_2F'' for the levels in which $v''=0$, 1 and 2.*

	A		*B*		*C*
	$0''$ level		$1''$ level		$2''$ level
K	7–0	7–1	8–1	9–1	9–2
6	9.1*	9.1*	8.8*	9.7*	9.7*
	—	9.1	9.2	—	9.9
8	12.2*	12.2*	12.5*	12.9*	12.9*
	11.8	12.1	12.8	12.6	12.9
10	15.9*	16.1*	16.6*	16.1*	15.9*
	16.1	16.0	16.3	16.2	16.0
12	19.3*	19.2*	19.3*	19.2*	18.7*
	19.0	19.8	19.0	19.5	19.1
14	22.9*	22.9*	22.4*	22.6*	22.5*
	22.8	22.8	22.3	22.7	22.8
16	25.9*	25.8*	25.9*	25.8*	25.3*
	26.1	25.8	25.6	25.7	25.6
18	29.5*	29.2*	29.0*	29.1*	29.2*
	29.6	29.5	—	29.1	28.9
20	32.6*	32.3*	32.3*	32.6*	32.4*
	32.1	32.4	32.6	32.7	32.2
22	35.8*	35.6*	35.2*	35.7*	35.8*
	35.6	35.7	34.8	35.7	36.1
24	39.3*	38.3*	38.6*	38.5*	38.8*
	39.0	38.6	38.3	38.2	38.7
26	{41.8	—		—	
	{42.2	42.1	42.5*	42.4	42.0*
	41.8	42.0	42.2	42.8	41.8
28	{44.0	{44.7	—		—
	{44.1	{45.2	45.0		44.9
	44.1	45.3	44.9		44.7
30	{48.3	{49.0	{49.1		{48.8
	{48.7	{49.2	{49.1		{48.7
	48.6	49.1	—		48.4
32	{52.1	{51.6			{51.6
	{52.3	{51.6	—	—	{51.5
	52.4	51.2			51.5
34	{55.1	{54.8			
	{55.6	{54.8	—	—	—
	55.2	54.6			
36	—	{57.5			
		{58.0	—	—	—
		57.9			

* These values are obtained from the stronger R and P branches before the lines become resolvable, and are referred to in the text as Δ_2F_{xy}. The bracketed values are then Δ_2F_x and Δ_2F_y. The remaining values are Δ_2F_z. As will be shown later in the text Δ_2F_x, Δ_2F_y and Δ_2F_z correspond to Δ_2F_1, Δ_2F_3 and Δ_2F_2, respectively.

The rotational levels of a $^3\Sigma$ state are given by[19]

$$F_i = B_vK(K+1) + f_i(K, J-K) + D_vK^2(K+1)^2 + \qquad (4)$$

[19] For a detailed discussion cf. R. S. Mulliken, Rev. Modern Physics **2**, 105 (1931.) The factor G has been omitted in Eq. (4).

TABLE V. *The values of Δ_2F' for the levels in which $v'=7$, 8 and 9.*

	A 7′ level		*B* 8′ level	*C* 9′ level	
K	7–0	7–1	8–1	9–1	9–2
5	6.1*	5.7*	5.7*	6.3*	6.4*
	—	5.9	5.4	—	6.5
7	8.5*	8.4*	8.0*	8.9*	8.8*
	8.2	8.3	8.5	8.3	8.9
9	11.1*	11.5*	11.9*	11.8*	11.6*
	11.0	11.4	12.1	12.1	11.7
11	14.2*	14.2*	14.4*	14.1*	14.1*
	14.1	14.6	13.8	14.3	14.1
13	16.6*	16.8*	17.2*	16.8*	16.5*
	16.3	16.8	17.2	16.9	16.7
15	19.3*	18.9*	19.3*	19.9*	19.2*
	19.3	18.5	18.8	19.4	19.5
17	21.7*	21.7*	21.4*	21.9*	21.8*
	21.9	22.1	21.3	22.0	21.8
19	24.2*	24.1*	24.3*	24.9*	25.2*
	24.4	24.2	—	25.0	25.3
21	27.2*	26.5*	26.6*	27.8*	27.8*
	26.6	27.3	26.4	27.8	27.6
23	29.0*	28.4*	29.5*	30.3*	30.2*
	29.0	28.5	29.2	30.2	30.1
25	{31.4				
	{31.4	31.4*	31.8*	32.6*	33.1*
	31.3	31.6	31.3	32.7	33.3
27	{33.8	{33.2			
	{33.8	{33.6	34.5*	35.6	35.6
	33.3	33.3	34.5	35.6	35.3
29	{35.7	{36.3	{36.3		{38.5
	{35.7	{36.2	{36.7	—	{38.5
	36.0	36.1	36.5		38.3
31	{38.9	{39.0	—		{41.1
	{39.0	{39.1	39.0	—	{41.0
	39.2	39.1	—		40.7
33	{41.0	{40.8			
	{41.5	{41.2	—	—	—
	41.3	40.7			
35	{43.4	{43.5			
	{43.9	{43.1	—	—	—
	43.8	43.6			

* These values are obtained from the stronger R and P branches before the lines become resolvable, and are referred to in the text as Δ_2F_{xy}. The bracketed values are then Δ_2F_x and Δ_2F_y. The remaining values are Δ_2F_z. As will be shown later in the text Δ_2F_x, Δ_2F_y and Δ_2F_z correspond to Δ_2F_1, Δ_2F_3 and Δ_2F_2, respectively.

Where J is the total angular momentum of the molecule, its values being $J=K+S$, $K+S-1$, . . . , $K-S$. S is the resultant electronic spin. For a

triplet state $S=1$, hence $J=K+1$, K and $K-1$. Due to the three values of J, we shall have, in general, three closely spaced energy states for each value of K. These energy states are designated by F_1, F_2 and F_3, where F_1 corresponds to $J=K+1$, F_2 to $J=K$ and F_3 to $J=K-1$.

As has been shown by Kramers,[20] $f_i(K, J-K)$ for ${}^3\Sigma$ states is made up of two parts, one of which is due to the interaction of the resultant electronic spin $\mathbf{S}^*$ with the rotational angular momentum $\boldsymbol{K}^*$, and is equal to

$$(1/2)\gamma[J(J+1) - K(K+1) - S(S+1)] = (1/2)\gamma[(J(J+1) - K(K+1) - 2] \quad (5)$$

while the other part is due to the interaction between the individual spins of the electrons and is designated by $w_i(K, J-K)$. $f_i(K, J-K)$ then becomes

$$f_i(K, J-K) = (1/2)\gamma[J(J+1) - K(K+1) - 2] + w_i(K, J-K) \quad (6)$$

It has been shown [20] that $w_i(K, J-K)$ has the following form for the three values of J:

$$J = K+1, \quad w_1 = -\epsilon(1 - 3/2K + 3) \quad (7)$$

$$J = K-1, \quad w_3 = -\epsilon(1 + 3/2K - 1) \quad (8)$$

$$J = K, \quad w_2 = +2\epsilon. \quad (9)$$

We can neglect terms in ϵ/K for moderate and large values of K, since ϵ is usually small. $f_i(K, J-K)$ then is:

$$J = K+1, \quad f_1 = -\epsilon + \gamma K \quad (10)$$

$$J = K-1, \quad f_3 = -\epsilon - \gamma(K+1) \quad (11)$$

$$J = K, \quad f_2 = 2\epsilon - \gamma \quad (12)$$

The lines of the R and P branches are given by:

$$R_i(K) = \nu^0 + F_i'(K+1) - F_i''(K) \quad (13)$$

$$P_i(K) = \nu^0 + F_i'(K-1) - F_i''(K) \quad (14)$$

Hence, for the three components of the triplet,

$$\Delta_2 F_i'(K) = R_i(K) - P_i(K) = F_i'(K+1) - F_i'(K-1) \text{ is:}[21]$$

$$J = K+1, \quad \Delta_2 F_1'(K) = 2(B_v' + 2D_v' + \gamma') + 4(B_v' + 3D_v')K + 8D_v'K^3 \quad (15)$$

$$J = K-1, \quad \Delta_2 F_3'(K) = 2(B_v' + 2D_v' - \gamma') + 4(B_v' + 3D_v')K + 8D_v'K^3 \quad (16)$$

$$J = K, \quad \Delta_2 F_2'(K) = 2(B_v' + 2D_v') + 4(B_v' + 3D_v')K + 8D_v'K^3 \quad (17)$$

For the lower electronic state,

[20] H. A. Kramers, Zeits. f. Physik **53**, 422 (1929).

[21] We should include in these equations an additional term $+12\,D_v\,K^2$; but D_v is of the order of magnitude of 10^{-7}, so that, for values of K in which this term will become appreciable, the contribution of the cubic term will be much greater than that of the squared term, and hence the latter may be neglected.

$\Delta_2F_i''(K) = R_i(K+1) - P_i(K-1) = F_i''(K+1) - F_i''(K-1)$ has exactly the same form as in the above equations, except that the (′) is replaced by the (″).

In Tables IV and V the Δ_2F values with asterisks, Δ_2F_{xy}, are obtained from the lines of the strong R and P branches. When these lines are resolvable, the bracketed values, Δ_2F_x and Δ_2F_y, for any one K, are obtained from the corresponding components of the doublets. The remaining value Δ_2F_z for every K is obtained from the weak R and P branches. As will be shown later, Δ_2F_z corresponds to Δ_2F_2, cf. Eq. (17). The sets of values Δ_2F_{xy} correspond to the mean of Eqs. (15) and (16), i.e. $\overline{\Delta_2F_{13}(K)} = 2(B_v+2D_v)+4(B_v+3D_v)K+8D_vK^3$ which is the same as Eq. (17). If we assume γ negative (the justification will be discussed below) Δ_2F_1 and Δ_2F_3, cf. Eqs. (15) and (16), correspond to Δ_2F_x and Δ_2F_y, respectively.

The values of the molecular constants obtained from the data are listed in Table VI. The values of B were obtained from the slopes of our graphs corresponding to Eqs. (15), (16) and (17). The value of D_e was obtained from the equation $D_e = -4B_e^3/\omega_e^2$, which agrees within experimental error with the value obtained from Eqs. (15), (16), and (17).

$$B_e = B_0 + \tfrac{1}{2}\alpha_e \quad \text{and} \quad \alpha_e = \frac{B_0 - B_v}{v}$$

TABLE VI. *Values of molecular constants.*

		B (cm^{-1})	D_e (cm^{-1})	α_e, B_e and r_e[22]	ϵ and γ[23]
$^3\Sigma_g^-$	$v''=0$	0.408_3	$D_e''=$	$\alpha_e=0.000_7$	$\epsilon'-\epsilon''=0.47$
	$v''=1$	0.407_7	-5.2×10^{-7}	$B_e''=0.409\ cm^{-1}$	$\gamma'\approx\gamma''\approx-0.1$
	$v''=2$	0.407_0		$r_e''=1.603\times10^{-8}cm$	$\gamma-\gamma''=$
					$\pm0.014\pm0.003$
$^3\Sigma_u^-$	$v'=0$	0.318_5 (extrapolated)			
	$v'=7$	0.308	$D_e'=$	$\alpha_e=0.001_5$	
	$v'=8$	0.306	-7.2×10^{-7}	$B_e'=0.319\ cm^{-1}$	
	$v'=9$	{0.305 / 0.341		$r_e'=1.814\times10^{-8}cm$	

The experimental values of Δ_2F for $v'=9$ obtained from the $9-1$ and $9-2$ bands do not fall upon a straight line as one would expect. In order to represent these points we had to drawn two straight lines, one fitting the points for lower values of K giving $B_9'=0.305$ cm,$^{-1}$ and the other fitting the points for higher values of K giving $B_9'=0.341$ cm.$^{-1}$ It is thought that this effect is due to the perturbation of the rotational levels. This seems plausible, for

[22] In our letter, Phys. Rev. **36,** 1800 (1930), the values of r_e are incorrectly given due to an arithmetical error in obtaining the r_e values from the values of B_e.

[23] The constants ϵ and γ are discussed in the following section. From our data we are only able to determine the accuracy of $(\gamma'-\gamma'')$ and not of either γ' or γ'', so that the values given for these constants may be off by several percent.

it is known from our work to be published in a later paper that predissociation occurs at $v'=10$. All bands with $v'=10$ are diffuse in absorption and absent in emission.

The exact value of the quantum numbers K was obtained by extrapolating the Δ_2F_i curves given in Eqs. (15), (16), and (17) to $\Delta_2F_i=0$. It has thus been found that the levels with *even* K values are missing in the *lower state*, and those with *odd* K values are missing in the *upper state*.

Exactly the same results have been found in the Schumann-Runge bands of O_2 investigated by Ossenbrüggen[9] and Lochte-Holtgreven and Dieke.[10] As Mulliken[24] has shown, the normal state of the oxygen molecule is in all probability $^3\Sigma_g^-$, this being the lower state of the Schumann-Runge bands. According to the selection rules for $^3\Sigma\rightarrow{}^3\Sigma$, the upper state must then be $^3\Sigma_u^-$[19,24]. We conclude, therefore, that the S_2 here investigated are due to a $^3\Sigma_u^-\rightarrow{}^3\Sigma_g^-$ transition.

Since alternate levels are missing we conclude that the internal angular momentum of the S^{32} nucleus is zero.

Spin Fine Structure of Rotational Levels

As we have seen above, the splitting of the rotational levels of a $^3\Sigma$ state into three components is due firstly, to the interaction of the resultant electronic spin with the rotational angular momentum (see Eq. (5)), and secondly to the interaction of the individual spins of the electrons (see Eqs. (7), (8) and (9)). In the expression for the first interaction the constant γ enters and in that, for the second, the constant ϵ. As these constants have only been determined in a few band spectra, namely, O_2[20,10] and PH[25], it will be of value to determine them as accurately as possible from the data for S_2 given above.

In order to obtain the values of γ, we have to correlate Δ_2F_1, Δ_2F_2 and Δ_2F_3 given in Eqs. (15), (16) and (17) above with one of the three sets of Δ_2F values for $K\geqq 25$, Δ_2F_x, Δ_2F_y and Δ_2F_z given in Tables IV and V. By examining these Δ_2F values it is clear that γ must be small since the Δ_2F values for the same value of K are almost the same within experimental error. By averaging all the Δ_2F_x, Δ_2F_y and Δ_2F_z separately for the upper state, we find that these values can be represented by $(N-0.1)$, $(N+0.1)$ and N cm,$^{-1}$ respectively. The same result holds for the lower state. These results can now be explained by correlating the Δ_2F_z values with Δ_2F_2, and the Δ_2F_x and Δ_2F_y values with either Δ_2F_1 or Δ_2F_3 where $|\gamma'|\approx|\gamma''|\approx 0.1$. It is impossible, however, to determine definitely from our data alone whether Δ_2F_1 should be correlated with Δ_2F_x or Δ_2F_y, as we do not know whether γ is positive or negative.

It has been shown that the value of γ''[26] in the normal $^3\Sigma_g^-$ state of the O_2 molecule is negative $(=-0.025)$.[20] The value of γ'[26] for the excited $^3\Sigma_u^-$ state of the Schumann-Runge bands has also been found to be negative $(=-0.048)$.[10] We would, therefore, expect the value of γ for the normal $^3\Sigma_g^-$

[24] R. S. Mulliken, Phys. Rev. **32,** 880 (1928); **36,** 700 (1930).

[25] R. W. B. Pearse, Proc. Roy. Soc. **A129,** 328 (1930).

[26] The γ used here corresponds to $(-B)$ in Kramer's terminology (cf. ref. 20) and $(-D)$ in that of Lochte-Holtgreven and Dieke (cf. ref. 10).

and probably for the excited $^3\Sigma_u^-$ states of S_2 also to be negative.[27] Hence, if we assume γ negative Δ_2F_1 and Δ_2F_3 correspond to Δ_2F_x and Δ_2F_y, respectively, in Tables IV and V. Hence R_1(or P_1) R_3(or P_3) and R_2(or P_2) correspond to R_x (or P_x), R_y (or P_y) and R_z (or P_z), respectively, in Tables I, II and III.

A schematic drawing of the rotational levels of the S_2 molecule is given in Fig. 2, with the theoretical separation of each level from the dotted line

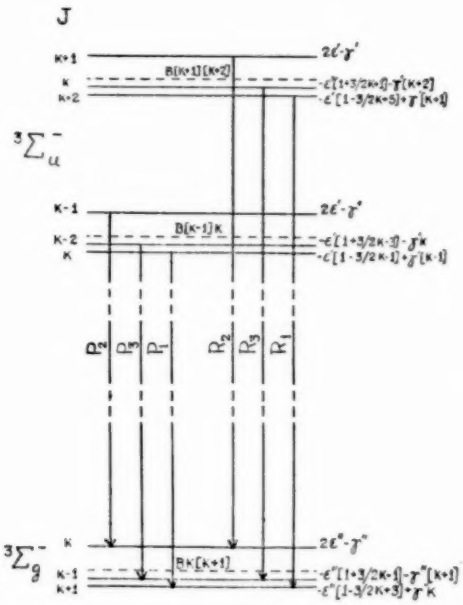

Fig. 2. A schematic representation of the structure of the rotational energy levels of S_2. The groups with rotational quantum numbers $K+1$ and $K-1$ refer to the upper $^3\Sigma_u^-$ state, and the group with quantum number K to the lower $^3\Sigma_g^-$ normal state. The dotted line represents the position of the rotational level if no interaction between K and S existed, its approximate energy value being given directly above it. The full lines represent the actual levels resulting from the interaction of the resultant electronic spin $\mathbf{S}^*$ with the rotational angular momentum $\mathbf{K}^*$ (see Eq. (5)) and the interaction between the individual spins of the electrons (see Eqs. (7), (8) and (9)). The calculated separation of these levels from the dotted line is given on the right. The lines joining the upper and the lower levels represent the observed transitions and are named accordingly. The K in the diagram is the value of K''.

for every K value given on the right. The equations for the separations of the three components in the triplet in the R and P branches, as may be seen with the help of Fig. 2, are[28]

[27] According to J. H. van Vleck (Phys. Rev. **33**, 467, 1929), $\gamma = \sum_K C_K A_K B_K / \nu_K$. The summation is to be taken over all the II states. It is likely, however, that there will be one II state whose influence is much greater than that of all others. ν_k then will be the interval between this II state and the Σ state in question. $C_K A_K$ is the coefficient at the magnetic interaction in this II state. B has the usual meaning. We would expect this II state to be similar in O_4 and S_2. Hence the sign at γ for both molecules would in all probability be the same.

[28] The values in ϵ/K have not been omitted in these equations.

$$R_1 - R_3 = -6\epsilon'(2K+3/4K^2+12K+5) + 6\epsilon''(2K-1/4K^2+4K-3) - (3\gamma' - \gamma'') - 2(\gamma' - \gamma'')K \quad (18a)$$

$$R_2 - R_1 = (3\epsilon' - 3\epsilon'') - (3\epsilon'/2K+5) + (3\epsilon''/2K+3) - 2\gamma' + \gamma'' - (\gamma' - \gamma'')K \quad (19a)$$

$$R_2 - R_3 = (3\epsilon' - 3\epsilon'') + (3\epsilon'/2K+1) - (3\epsilon''/2K-1) + \gamma' + (\gamma' - \gamma'')K \quad (20a)$$

$$P_1 - P_3 = -6\epsilon'(2K-2/4K^2-8K+3) + 6\epsilon''(2K-1/4K^2+4K-3) + \gamma' + \gamma'' - 2(\gamma' - \gamma'')K \quad (18b)$$

$$P_2 - P_1 = (3\epsilon' - 3\epsilon'') - (3\epsilon'/2K+1) + (3\epsilon''/2K+3) + \gamma'' - (\gamma' - \gamma'')K \quad (19b)$$

$$P_2 - P_3 = (3\epsilon' - 3\epsilon'') + (3\epsilon'/2K-3) - (3\epsilon''/2K-1) - \gamma' + (\gamma' - \gamma'')K. \quad (20b)$$

The average of Eqs. (19a) and (19b) is:

$$\approx (3\epsilon' - 3\epsilon'') - (3\epsilon' - 3\epsilon'')/(2K+3) - (\gamma' - \gamma'') - (\gamma' - \gamma'')K \quad (21)$$

and the average of Eqs. (20a) and 20b) for $K \geqq 5$:[29]

$$\approx (3\epsilon' - 3\epsilon'') + (3\epsilon' - 3\epsilon'')/(2K-1) + (\gamma' - \gamma'')K. \quad (22)$$

The interval between R_2 and the mean of R_1 and R_3 is for $K \geqq 3$ [29]

$$3(\epsilon' - \epsilon'') + \tfrac{1}{2}(\gamma' - \gamma''). \quad (23)$$

This interval is the same as that obtained from the P branches.

Eqs. (18a) to (23) may now be used to correlate definitely the branches designated by R_x, R_y and R_z (or P_x, P_y and P_z) with R_1, R_3 and R_2 (or P_1, P_3 and P_2). The average of the experimental values $\delta\nu_R$ and $\delta\nu_P$ given in Tables I, II, and III are plotted in Fig. 3, Graph A. It is recalled that $\delta\nu_R$ and $\delta\nu_P$ are the intervals between the weak R_z (or P_z) and the corresponding strong lines R_{xy} (or P_{xy}). When the components of the strong lines become resolvable, $\delta\nu_R$ ($\delta\nu_P$) are the intervals between R_z (or P_z) and the center of the resulting doublet. The values of the average intervals between the weak lines R_z (or P_z) and the corresponding short wave-length component of the doublet R_x (or P_x), i.e. the average of $(R_z - R_x)$ and $(P_z - P_x)$ are plotted below Graph A. The values of the average intervals between the weak line R_z (or P_z) and the long wave-length component of the doublet R_y (or P_y), i.e. the average of $(R_z - R_y)$ and $(P_z - P_y)$ are plotted above graph A.

We see that the plotted values of $\delta\nu_R$ and $\delta\nu_P$ (graph A) are approximately constant, and independent of K. Further, as can be seen from Fig. 3, the average of the intervals $\delta\nu_R - (R_z - R_x)$ and $\delta\nu_P - (P_z - P_x)$ is approximately equal but of opposite sign to the intervals $\delta\nu_R - (R_z - R_y)$ and $\delta\nu_P - (P_z - P_y)$.

[29] These equations contain approximations which hold only for the values of K as given.

Considering the results obtained above by comparing the experimental values of $\Delta_2 F$ and Eqs. (15), (16) and (17) and also Fig. 3, we see that the only possible correlation (assuming γ negative) is that R_x(or P_x) corresponds to R_1, (or P_1), R_y(or P_y), to R_3, (or P_3) and R_z (or P_z), to R_2, (or P_2).

From Eq. (23) and Graph A, $3\epsilon'-3\epsilon''+\frac{1}{2}(\gamma'-\gamma'')=-1.41$ from which we obtain $\epsilon'-\epsilon''=-0.47$[30] if we put $(\gamma'-\gamma'')=0.014$ (see below).

The points below and above graph A in Fig. 3, can now best be represented by graphs B and C, respectively, which are the graphs of Eqs. (21) and (22), if we take $(3\epsilon'-3\epsilon'')=-1.42$ and $(\gamma'-\gamma'')=0.014$. We have seen above that $\gamma'\approx\gamma''\approx-0.1$ and from $(\gamma-\gamma'')=0.014$, we conclude $|\gamma''|>|\gamma'|$.

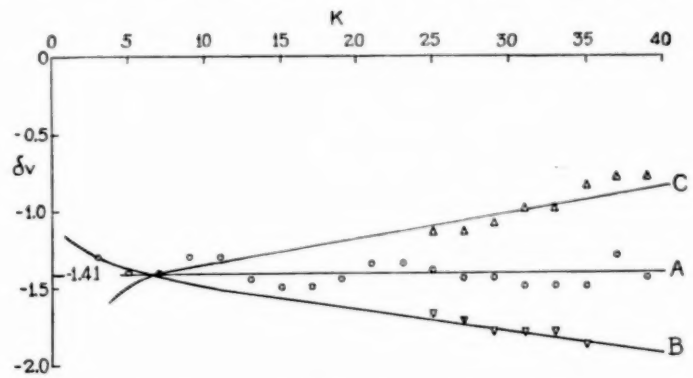

Fig. 3. Graphs showing the average observed separations of the triplets. The circular points represent the intervals between the weak R_z (or P_z) series and the strong R_{xy} (or P_{xy}) or the center of the doublets R_x and R_y (or P_x and P_y), when R_{xy} (or P_{xy}) become resolvable for $K\geqq 25$. These points are represented by Graph A. The triangles represent the intervals between the weak R_z (or P_z) series and the long wave-length component of the doublet R_y (or P_y) and the inverted triangles represents the intervals between the weak R_z (or P_z) series and the short wave-length component of the doublet R_x (or P_x). The triangles may best be represented by C which is the graph of Eq. (22), and the inverted triangles by B which is the graph of Eq. (21) where $3(\epsilon'-\epsilon'')=-1.42$ and $\gamma'-\gamma''=+0.014$. The plotted values are the averaged intervals for the R and P series.

From our data we are not able to determine the values of ϵ' and ϵ'' separately. This will be possible if the rotational structure of the S_2 bands similar to the O_2 atmospheric bands could be determined. These bands of S. which would lie in the infrared, have as yet not been discovered.

Discussion of Previous Work

With regard to previous work on the rotational analysis of S_2 there is every indication that the analysis of Henri and Teves[3] is probably incorrect, since the resolution used could not be sufficient to separate all the lines in the bands and thus to assign the lines correctly into series. The complexity of the patterns obtained in fluorescence by Teves[4], Swings,[5] and Rompe[6] are undoubtedly due to the following causes:

[30] In the O_2 Schumann-Runge bands ϵ' and ϵ'' were both found to be positive and also $\epsilon''>\epsilon'$. If we assume ϵ' and ϵ'' are also positive in the S_2 bands, then $\epsilon''>\epsilon'$.

(1) All the lines of the mercury arc have been used to excite fluorescence.

(2) As Rompe points out Swings' arc was not sufficiently cooled, giving him broad exciting lines, whereas Rompe states that he himself was unable to obtain step to step fluorescence in mercury vapour with his own source, indicating that his exciting lines were also too broad.

(3) The rotational lines of the S_2 bands lie close together.

Due to these facts and the small dispersion used by these investigators, it is extremely difficult, if not impossible, to interpret the results which have been obtained by them It will be interesting, however, if the fluorescence spectrum could be investigated using single line excitation and somewhat larger dispersion than that used by previous investigators.

Note added in proof: We have received a letter from Mons. P. Swings in which he states that according to results derived from an investigation of the fluorescence spectra of S_2 (obtained with a Crony spectrograph with 11 prisms giving a dispersion of 1A per mm at λ3000) he found $I'' = 70 \times 10^{-40}$ gm cm^2 corresponding to a value of $B'' = 0.396$ cm^{-1}. This value of B'' agrees within experimental error with our value $B_e'' = 0.409$ cm^{-1} given above. His results will be published in the Mém. Soc. royale Sciences, Liége.

The authors wish to express their appreciation to Professor R. S. Mulliken for his interest and advice in connection with this work.

ORBITAL VALENCY*

By James H. Bartlett, Jr.
Department of Physics, University of Illinois

(Received January 15, 1931)

Abstract

The interaction of two atoms, each with one $2p$ electron, is studied by a method similar to that used by Kemble and Zener. An atomic wave function whose radial part is of the form const. $re^{-kr/2}$ (that is, with no nodes) is used. Complete potential energy curves are obtained for the twelve possible states, which are $^1\Delta_g$, $^3\Delta_u$, $^1\Pi_g$, $^1\Pi_u$, $^3\Pi_g$, $^3\Pi_u$, $^1\Sigma_u^-$, $^3\Sigma_g^-$, two $^1\Sigma_g^+$, and two $^3\Sigma_u^+$. The most stable states are $^3\Sigma_u^+$ (lowest) and $^1\Sigma_g^+$, which arise from $m_{la}=0$ and $m_{lb}=0$, and in which there is the maximum overlapping of charge. The states with least overlapping of charge are those where $m_{la}=\pm 1$ and $m_{lb}=\pm 1$, resulting in $^1\Delta_g$, $^3\Delta_u$, $^1\Sigma_g^+$, $^1\Sigma_u^-$, $^3\Sigma_g^-$, $^3\Sigma_u^+$, which are all repulsive. The Π states lie in between, and are attractive. The present work gives precision to the ideas of Heitler on orbital valency, yields a positive exchange energy integral for the lowest states, and may be taken as supporting the conceptions of Slater about directed valency.

OUR knowledge of the rules underlying the formation of stable diatomic molecules from their constituent atoms is still very limited, in spite of the successes achieved by Heitler and London,[1] and by Kemble and Zener.[2] The idea of spin valency is quite useful, but its general inadequancy has been recognized by Heitler,[3] who has therefore proposed an "orbital" valency. Two atoms can exert on each other forces due not only to the coupling between the spins, but also to the coupling between the orbits, and the two types of interaction may give rise to effects of the same order of magnitude.[4] One must in general take the oribital valency into consideration, and it is highly desirable to formulate rules concerning the order of the resulting molecular states. This is the purpose of the present investigation.

The special problem here studied is that of the interaction of two similar atoms, each with one $2p$ valence electron. For simplicity, a hydrogenic wave function for the atom has been assumed, and the possible influence of internal s electrons has been neglected. Zener[5] has shown that it is legitimate, as an approximation, to assume such a wave function. The method is essentially the same as used by Kemble and Zener,[2] except that in the actual evaluation

* This work was done largely with the aid of a Parker Travelling Fellowship from Harvard University.

[1] W. Heitler u. F. London, Zeits. f. Physik **44**, 455 (1927).
[2] E. C. Kemble and C. Zener, Phys. Rev. **33**, 512 (1929).
[3] W. Heitler, Naturwiss. **17**, 546 (1929).
[4] This statement is rather inexact, but the precise formulation will be made later.
[5] C. Zener, Phys. Rev. **36**, 51 (1930).

of the integrals the procedure of Zener and Guillemin[6] has been followed. Without doubt, one could improve upon the energy values by using a variational method, but it will be assumed that their order would be the same, and it is primarily the order which is the object of this investigation.

We assume, therefore, the radial part of the atomic wave function to be of the form $R = \text{const}\ re^{-\kappa r/2}$, where κ is an arbitrary constant.

Notation. $a(nlm_l/1)$ = wave function for electron 1 on nucleus a, with quantum numbers m, l, m_l. (Similarly for nucleus b).

For one electron, a = distance from nucleus a
b = distance from nucleus b.

For two electrons a_1 = distance of electron one from nucleus a, etc.
R = internuclear distance
r = interelectronic distance
θ_{a1} = angle from internuclear axis to line joining a and 1.

In the case under consideration, it is unnecessary to write explicitly n and l, which are 2 and 1, respectively, for each electron. Accordingly, we shall abbreviate the notation to $a(m_l 1)$.

Thus

$$a(11) = c_1 a_1 e^{-\kappa a_1/2} \sin\theta_{a_1} e^{i\phi_1}$$

$$b(02) = c_2 b_2 e^{-\kappa b_2/2} \cos\theta_{b_2}.$$

Kemble and Zener show how one may set up a secular equation for the two-quantum excited states of H_2, and then separate it according to the constants of the motion, the spin-orbit interaction being supposed to be negligible. The same may be done in the present case, and one obtains a secular equation of the twelfth degree, which has eight linear factors, and two quadratic factors. The results are tabulated. The energy is measured from the "unperturbed" value, namely that for infinite separation. $^1\Sigma_g^+$ means that the electronic factor of the wave function is unchanged on reflection in a plane through the internuclear axis (+), and on reflection in the midpoint of this axis (g). The notation of Kemble and Zener is also given.

[6] C. Zener and V. Guillemin, Phys. Rev. **34**, 999 (1929).

WAVE FUNCTIONS AND ENERGY LEVELS

States m_{l_a}	States m_{l_b}	States Symmetry	Wave Function	"Diagonal" Energy
1	1	$^1\Delta_g(S^N)$	$a(11)b(12)+a(12)b(11)$	$\frac{1}{1+S_{11}}(I_1+I_2)$
1	1	$^3\Delta_u(A^N)$	$a(11)b(12)-a(12)b(11)$	$\frac{1}{1-S_{11}}(I_1-I_2)$
1	0	$^1\Pi_g(S^N)$	$a(11)b(02)+a(12)b(01)+a(01)b(12)+a(02)b(11)$	$\frac{1}{1+S_{10}}(I_3+I_4+I_5+I_6)$
1	0	$^1\Pi_u(A^N)$	$a(11)b(02)+a(12)b(01)-a(01)b(12)-a(02)b(11)$	$\frac{1}{1-S_{10}}(I_3-I_4-I_5+I_6)$
1	0	$^3\Pi_g(S^N)$	$a(11)b(02)-a(12)b(01)-a(01)b(12)+a(02)b(11)$	$\frac{1}{1+S_{10}}(I_3+I_4-I_5-I_6)$
1	0	$^3\Pi_u(A^N)$	$a(11)b(02)-a(12)b(01)+a(01)b(12)-a(02)b(11)$	$\frac{1}{1-S_{10}}(I_3-I_4+I_5-I_6)$
1	−1	$^1\Sigma_u^-(A^N)$	$a(11)b(-12)+a(12)b(-11)-a(-11)b(12)-a(-12)b(11)$	$\frac{1}{1-S_{11}}(I_1-I_2-I_7+I_8)$
1	−1	$^3\Sigma_g^-(S^N)$	$a(11)b(-12)-a(12)b(-11)-a(-11)b(12)+a(-12)b(11)$	$\frac{1}{1+S_{11}}(I_1+I_2-I_7-I_8)$
1	−1	$^1\Sigma_g^+(S^N)$	$a(11)b(-12)+a(12)b(-11)+a(-11)b(12)+a(-12)b(11)$	$\frac{1}{1+S_{11}}(I_1+I_2+I_7+I_8)$
0	0	$^1\Sigma_g^+(S^N)$	$a(01)b(02)+a(02)b(01)$	$\frac{1}{1+S_{00}}(I_9+I_{10})$
1	−1	$^3\Sigma_u^+(A^N)$	$a(11)b(-12)-a(12)b(-11)+a(-11)b(12)-a(-12)b(11)$	$\frac{1}{1-S_{11}}(I_1-I_2+I_7-I_8)$
0	0	$^3\Sigma_u^+(A^N)$	$a(01)b(02)-a(02)b(01)$	$\frac{1}{1-S_{00}}(I_9-I_{10})$

where

$$I_1 = \int H'[a(11)]^2[b(12)]^2 dv$$

$$I_2 = \int H' a(11)b(11)a(12)b(12)dv$$

$$I_3 = \int H'[a(11)]^2[b(02)]^2 dv$$

$$I_4 = \int H' a(11)b(11)a(02)b(02)dv$$

$$I_5 = \int H' a(01)a(11)b(02)b(12)\cos(\phi_1 - \phi_2)dv$$

$$I_6 = \int H' a(11)b(01)a(12)b(02)\cos(\phi_1 - \phi_2)dv$$

$$I_7 = \int H'[a(11)]^2[b(12)]^2 \cos 2(\phi_1 - \phi_2)dv$$

$$I_8 = \int H'a(11)b(11)a(12)b(12) \cos 2(\phi_1 - \phi_2)dv$$

$$I_9 = \int H'[a(01)]^2[b(02)]^2dv$$

$$I_{10} = \int H'a(01)b(01)a(02)b(02)dv$$

$$I_{11} = \int H'a(01)a(12)b(11)b(02) \cos (\phi_1 - \phi_2)dv$$

where H' is the "perturbative" part of the energy, e.g.,

$$H' = \frac{2}{R} + \frac{2}{r} - \frac{2}{a_2} - \frac{2}{b_1}, \text{ using atomic units.}$$

$$(S_{11})^{1/2} = \int a(11)b(11)dv_1, \quad (S_{00})^{1/2} = \int a(01)b(01)dv_1, \quad S_{10} = (S_{11}\, S_{00})^{1/2}.$$

There remain to be solved two two-degree secular equations, namely

$$(1) \qquad \begin{vmatrix} I_1 + I_2 + I_7 + I_8 - E(1 + S_{11}) & 2(I_5 + I_{11}) \\ -I_5 + I_{11} & I_9 + I_{10} - E(1 + S_{00}) \end{vmatrix} = 0$$

and

$$(2) \qquad \begin{vmatrix} I_1 - I_2 + I_7 - I_8 - E(1 - S_{11}) & 2(-I_5 + I_{11}) \\ +I_5 + I_{11} & I_9 - I_{10} - E(1 - S_{00}) \end{vmatrix} = 0$$

The solution of (1) gives us two states of the $^1\Sigma$, S^N type, and the solution of (2) two states of the $^3\Sigma$, A^N type. It turns out that the influence of the non-diagonal terms is negligible.

Evaluation of the Integrals

General formulae. One may classify the integrals according to whether it is necessary to use the Neumann expansion or not in their evaluation. One does not need to do so for the integrals I_1, I_3, I_9, I_5, and I_7. The only term in the Hamiltonian which offers difficulty is the $2/r$ term. The integrals involving the Neumann expansion are termed "exchange," and the others "Coulomb."

Before proceeding, the notation needs explanation. That used by Zener and Guillemin[6] will be adopted.

$$\Gamma_n = \int_0^\infty e^{-u}u^{n-1}du \quad \Gamma_n(\alpha) = \int_\alpha^\infty e^{-u}u^{n-1}du, \quad \gamma_n(\alpha) = \Gamma_n - \Gamma_n(\alpha)$$

$$A_n(\sigma, \alpha) = \int_\sigma^\infty e^{-\alpha x}x^n dx = \frac{1}{\alpha^{n+1}}\Gamma_{n+1}(\sigma\alpha)$$

$$B_n(\alpha) = \int_{-1}^{1} e^{-\alpha x} x^n dx = A_n(-1, \alpha) - A_n(1, \alpha)$$

$$f_r(m, \alpha) = \int_1^{\infty} e^{-\alpha x} x^m Q_r(x) dx$$

where

$$Q_0 = \frac{1}{2} \ln\left(\frac{x+1}{x-1}\right), \; x > 1, \quad \text{and} \quad Q_1 = xQ_0 - 1.$$

One may readily establish, by partial integration, the following recursion formulae:

$$A_{m+1}(1,\alpha) - A_m(1,\alpha) = \frac{1}{\alpha}\{(m+1)A_m(1,\alpha) - mA_{m-1}(1,\alpha)\}$$

$$A_{m+1}(1,\alpha) + A_m(1,\alpha) = \frac{1}{\alpha}\{2e^{-\alpha} + (m+1)A_m(1,\alpha) + mA_{m-1}(1,\alpha)\}$$

$$A_{m+2}(1,\alpha) - A_m(1,\alpha) = \frac{1}{\alpha}\{(m+2)A_{m+1}(1,\alpha) - mA_{m-1}(1,\alpha)\}$$

$$f_0(n+2,\alpha) - f_0(n,\alpha) = \frac{1}{\alpha}\{-A_n(1,\alpha) + 2f_0(n+1,\alpha) + n[f_0(n+1,\alpha) - f_0(n-1,\alpha)]\}$$

$$f_1(n+2,\alpha) - f_1(n,\alpha) = \frac{1}{\alpha}\{3f_1(n+1,\alpha) - f_0(n,\alpha) + n[f_1(n+1,\alpha) - f_1(n-1,\alpha)]\}$$

$$= \frac{1}{\alpha}\{2f_1(n+1,\alpha) - A_{n-1}(1,\alpha) + (n+1)[f_1(n+1,\alpha) - f_1(n-1,\alpha)]\}$$

We have here used the relations

$$(x^2 - 1)\frac{dQ_n}{dx} = nxQ_n - nQ_{n-1}, \quad n > 0$$

and

$$f_1(m, \alpha) = f_0(m+1, \alpha) - A_m(1, \alpha).$$

Now let

$$F(n, \lambda) = \int_{-1}^{1} \frac{e^{-\rho\mu} d\mu}{(\mu - \lambda)^n}$$

then $F(1) = e^{-\rho\lambda}[-E_i(\rho(1+\lambda)) + E_i(-\rho(1+\lambda))]$ where

$$-E_i(-x) = \int_x^{\infty} \frac{e^{-u}}{u} du.$$

In general,

$$F(n) = -\frac{1}{n-1}\left[\frac{e^{-\rho}}{(1-\lambda)^{n-1}} - \frac{e^{\rho}}{(-1-\lambda)^{n-1}}\right] - \frac{\rho}{n-1}F(n-1), n \neq 1$$

and

$$\frac{dF(n)}{d\lambda} = nF(n+1).$$

Abbreviating,

$$F_1(n) = -\frac{1}{n-1}\left[\frac{e^{-\rho}}{(1-\lambda)^{n-1}} - \frac{e^{\rho}}{(-1-\lambda)^{n-1}}\right]$$

and

$$F(n) = -\frac{\rho}{n-1}F(n-1) + F_1(n)$$

$$\int_1^\infty f(\lambda)F(n+1)e^{-\rho\lambda}d\lambda = \int_1^\infty f(\lambda)\,\frac{1}{n}\,\frac{dF(n)}{d\lambda}e^{-\rho\lambda}d\lambda = \frac{1}{2n}f(\lambda)F(n)e^{-\rho\lambda}\Big|_1^\infty \cdot$$

$$-\frac{1}{2n}\int_1^\infty e^{-\rho\lambda}\left\{F(n)\frac{df(\lambda)}{d\lambda} - f(\lambda)\frac{dF_1(n)}{d\lambda}\right\}d\lambda. \tag{3}$$

For the most part, two kinds of coordinate systems have been employed. One, with a, b, and ϕ as coordinates, and $(1/R)adabdbd\phi$ as volume element, is most convenient for integrals such as $\int e^{-\kappa a}f(a, b)dv$, since one can integrate over b first and avoid the occurrence of integral logarithms in the final integrand (using a wave function with radial part $R=cre^{-\kappa r/2}$). The other, with λ, μ, and ϕ as coordinates, where $a=(R/2)(\lambda+\mu)$ and $b=(R/2)(\lambda-\mu)$, and $(R/2)^3(\lambda^2-\mu^2)d\lambda d\mu d\phi$ is the volume element, is best for integrals such as $\int e^{-\kappa(a+b)}f(a, b)dv$, the integration over μ being performed first. The transformation is as follows:

$$\cos\theta_a = \frac{\lambda\mu+1}{\lambda+\mu} \quad \cos\theta_b = \frac{\lambda\mu-1}{\lambda-\mu} \quad \sin^2\theta_a = \frac{(\lambda^2-1)(1-\mu^2)}{(\lambda+\mu)^2},$$

$$\sin^2\theta_b = \frac{(\lambda^2-1)(1-\mu^2)}{(\lambda-\mu)^2}.$$

Normalization. The normalized atomic wave functions are $u=c_1e^{-\kappa r/2}r \sin\theta e^{\pm i\phi}$ and $u=c_2e^{-\kappa r/2}\, r\cos\theta$, where $2\pi c_1^2/\kappa^5=1/32$ and $2\pi c_2^2/\kappa^5=1/16$. Let $\alpha=\kappa R$.

$$(S_{11})^{1/2} = 2\pi c_1^2\int e^{-(\kappa/2)(a+b)}a\sin\theta_a\; b\sin\theta_b\; adabdb$$

$$= \frac{2\pi c_1^2}{\kappa^5}\left(\frac{\alpha}{2}\right)^5\int_1^\infty d\lambda\int_{-1}^1 d\mu e^{-\alpha\lambda/2}(\lambda^2-1)(\lambda^2-\mu^2)(1-\mu^2)$$

$$= 1/24\cdot(\alpha/2)^5\{A_4(1, \alpha/2) - (6/5)A_2(1, \alpha/2) + (1/5)A_0(1, \alpha/2)\}$$

$$(S_{00})^{1/2} = (2\pi c_2^2/\kappa^5)(\alpha/2)^5\int_1^\infty d\lambda\int_{-1}^1 d\mu e^{-\alpha\lambda/2}(\lambda^2\mu^2-1)(\lambda^2-\mu^2)$$

$$= 1/24\cdot(\alpha/2)^5\{A_4(1, \alpha/2) - (18/5)A_2(1, \alpha/2) + A_0(1, \alpha/2)$$

The integrals I_1, I_3, I_9, I_5, I_7.

Let

$$i_1 = \int \frac{2}{r}[a(11)]^2[b(12)]^2 dv = \int \frac{2}{r} c_1^4 a_1^2 b_2^2 \sin^2\theta_{a_1} \sin^2\theta_{b_2} e^{-\kappa(a_1+b_2)} dv$$

$$i_3 = \int \frac{2}{r}[a(11)]^2[b(02)]^2 dv = \int \frac{2}{r} c_1^2 c_2^2 a_1^2 b_2^2 \sin^2\theta_{a_1} \cos^2\theta_{b_2} e^{-\kappa(a_1+b_2)} dv$$

$$= \int \frac{2}{r}[a(01)]^2[b(12)]^2 dv = \int \frac{2}{r} c_1^2 c_2^2 a_1^2 b_2^2 \cos^2\theta_{a_1} \sin^2\theta_{b_2} e^{-\kappa(a_1+b_2)} dv$$

$$i_9 = \int \frac{2}{r}[a(01)]^2[b(02)]^2 dv = \int \frac{2}{r} c_2^4 a_1^2 b_2^2 \cos^2\theta_{a_1} \cos^2\theta_{b_2} e^{-\kappa(a_1+b_2)} dv$$

$$i_5 = \int \frac{2}{r} a(01)a(11)b(02)b(12) \cos(\phi_1 - \phi_2) dv$$

$$= \int \frac{2}{r} c_1^2 c_2^2 a_1^2 b_2^2 \sin\theta_{a_1} \cos\theta_{a_1} \sin\theta_{b_2} \cos\theta_{b_2} e^{-\kappa(a_1+b_2)} \cos(\phi_1 - \phi_2) dv$$

$$i_7 = \int \frac{2}{r}[a(11)]^2[b(12)]^2 \cos 2(\phi_1 - \phi_2) dv$$

$$= \int \frac{2}{r} c_1^4 a_1^2 b_2^2 \sin^2\theta_{a_1} \sin^2\theta_{b_2} e^{-\kappa(a_1+b_2)} \cos 2(\phi_1 - \phi_2) dv.$$

We can now expand $2/r$ as usual:—

$$\frac{2}{r} = \frac{2}{b_1}\left\{1 + \frac{b_2}{b_1}\cos\gamma + \left(\frac{b_2}{b_1}\right)^2 P_2(\cos\gamma) + \cdots\right\} \quad b_2 < b_1$$

$$= \frac{2}{b_2}\left\{1 + \frac{b_1}{b_2}\cos\gamma + \left(\frac{b_1}{b_2}\right)^2 P_2(\cos\gamma) + \cdots\right\} \quad b_2 > b_1$$

where γ is the angle between the lines b_1 and b_2, and

$$P_n(\cos\gamma) = P_n(\cos\theta_{b_1})P_n(\cos\theta_{b_2}) + 2\sum_{m=1}^{n}(-1)^m \frac{(n-m)!}{(n+m)!} P_n^m(\cos\theta_{b_1}) P_n^m(\cos\theta_{b_2}) \cos m(\phi_1 - \phi_2)$$

$$\int_0^{2\pi} P_n(\cos\gamma) \cos m(\phi_1 - \phi_2) d(\phi_1 - \phi_2) = 2\pi P_n(\cos\theta_{b_1}) P_n(\cos\theta_{b_2}), \quad m = 0$$

$$= 2\pi(-1)^m \frac{(n-m)!}{(n+m)!} P_n^m(\cos\theta_{b_1}) P_n^m(\cos\theta_{b_2}), \quad m \neq 0.$$

On performing the integrations, one obtains, letting

$$g_{5,1} = \frac{\gamma_5(\kappa b)}{\kappa b} + \Gamma_4(\kappa b)$$

$$g_{7,3} = \frac{\gamma_7(\kappa b)}{(\kappa b)^3} + (\kappa b)^2 \Gamma_2(\kappa b),$$

the following expressions:—

$$i_1 = (16\pi c_1^4/3\kappa^4)\int a^2 \sin^2\theta_a e^{-\kappa a}[g_{5,1} - (1/5)P_2(\cos\theta_b)g_{7,3}]dv$$

$$i_3 = (8\pi c_1^2 c_2^2/3\kappa^4)\int a^2 \sin^2\theta_a e^{-\kappa a}[g_{5,1} + (2/5)P_2(\cos\theta_b)g_{7,3}]dv$$

$$= (16\pi c_1^2 c_2^2/3\kappa^4)\int a^2 \cos^2\theta_a e^{-\kappa a}[g_{5,1} - (1/5)P_2(\cos\theta_b)g_{7,3}]dv$$

$$i_9 = (8\pi c_2^4/3\kappa^4)\int a^2 \cos^2\theta_a e^{-\kappa a}[g_{5,1} + (2/5)P_2(\cos\theta_b)g_{7,3}]dv$$

$$i_5 = -(8\pi c_1^2 c_2^2/5\kappa^4)\int a^2 \sin\theta_a \cos\theta_a \sin\theta_b \cos\theta_b e^{-\kappa a} g_{7,3}dv$$

$$i_7 = -(8\pi c_1^4/5\kappa^4)\int a^2 \sin^2\theta_a \sin^2\theta_b e^{-\kappa a} g_{7,3}dv$$

$$\int a^2 \sin^2\theta_a e^{-\kappa a}(\Gamma_5/\kappa b)dv = (8\pi\Gamma_5/3\kappa^5)[g_{5,1}(\alpha) - (1/5)g_{7,3}(\alpha)]$$

$$\int a^2 \cos^2\theta_a e^{-\kappa a}(\Gamma_5/\kappa b)dv = (4\pi\Gamma_5/3\kappa^5)[g_{5,1}(\alpha) + (2/5)g_{7,3}(\alpha)]$$

$$\int a^2 \sin^2\theta_a e^{-\kappa(a+b)}[(\kappa b)^3 + 6(\kappa b)^2 + 18\kappa b + 24](1/\kappa b)\cdot dv$$

$$= (2\pi/\kappa^5)(\alpha/2)^4\{(\alpha/2)^3[(4/3)(A_6 - A_4) - (4/35)(A_2 - A_0)]$$
$$+ 6(\alpha/2)^2[(4/3)(A_5 - A_3) - (4/15)(A_3 - A_1)] + 18(\alpha/2)[(4/3)(A_4 - A_2)$$
$$- (4/15)(A_2 - A_0)] + 24(4/3)(A_3 - A_1)\}$$

$$\int a^2 \cos^2\theta_a e^{-\kappa(a+b)}[(\kappa b)^3 + 6(\kappa b)^2 + 18\kappa b + 24](1/\kappa b)\cdot dv$$

$$= (2\pi/\kappa^5)(\alpha/2)^4\{(\alpha/2)^3[(2/3)(A_6 - A_4) + (46/35)A_2 - (2/5)A_0]$$
$$+ 6(\alpha/2)^2[(2/3)A_5 + (4/15)A_3 + (2/15)A_1] + 18(\alpha/2)[(2/3)A_4 + (8/5)A_2$$
$$- (2/3)A_0] + 24[(2/3)A_3 + (10/3)A_1]\}$$

$$\Gamma_7\int a^2 \sin^2\theta_a e^{-\kappa a}P_2(\cos\theta_b)(1/\kappa b)^3 dv$$

$$= (8\pi\Gamma_7/\kappa^5)[\gamma_5/3\alpha^3 - \Gamma_2/15 - 2\gamma_7/5\alpha^5]$$

$$\Gamma_7\int a^2 \cos^2\theta_a e^{-\kappa a}P_2(\cos\theta_b)(1/\kappa b)^3 dv$$

$$= (4\pi\Gamma_7/\kappa^5)[\gamma_5/3\alpha^3 + 2\Gamma_2/15 + 4\gamma_7/5\alpha^3 - \alpha^2 e^{-\alpha}/2]$$

$$\int a^2 \sin^2\theta_a e^{-\kappa a}(1/\kappa b)^3 P_2(\cos\theta_b)[\Gamma_7(\kappa b) - (\kappa b)^5\ \Gamma_2(\kappa b)]dv$$

$$= (2\pi\alpha^2/4\kappa^5)[(\alpha/2)^5\{-(4/3)(A_6 - A_4) + (64/7)(A_4 - A_2) - (12/7)(A_2 - A_0)\}$$
$$+ (\alpha/2)^4\{-8(A_5 - A_3) + 40(A_3 - A_1)\}$$
$$+ 15\alpha^3\{2(A_6 - A_4) - (76/15)(A_4 - A_2) + (62/15)(A_2 - A_0)\}$$
$$+ 90\alpha^2\{-8(A_5 - A_3) + (34/3)(A_3 - A_1)\}$$
$$+ 360\alpha\{(15/2)A_4 - (71/6)A_2 + (10/3)A_0\}]$$

$$\int a^2 \cos^2\theta_a e^{-\kappa a}(1/\kappa b)^3 P_2(\cos\theta_b)[\Gamma_7(\kappa b) - (\kappa b)^5\ \Gamma_2(\kappa b)]dv$$
$$= (2\pi\alpha^2/4\kappa^5)[(\alpha/2)^5\{(4/3)A_6 - (220/21)A_4 + (124/7)A_2 - 4A_0\}$$
$$+ (\alpha/2)^4\{8A_5 - 64A_3 + 88A_1\}$$
$$+ 15\alpha^3\{-2A_6 - (14/15)A_4 + (6/5)A_2 + (10/3)A_0\}$$
$$+ 90\alpha^2\{8A_5 + (14/3)A_3 - (26/3)A_1\}$$
$$+ 360\alpha\{-(23/2)A_4 - (25/6)A_2 + 2A_0\}$$
$$+ 720\{8A_3 + 2A_1\}]$$

$$\int a^2 \sin^2\theta_a e^{-\kappa a}(1/\kappa b)^3[\Gamma_7(\kappa b) - (\kappa b)^5\ \Gamma_2(\kappa b)]dv$$
$$= (2\pi\alpha^2/4\kappa^5)[5(\alpha/2)^5\{(4/3)(A_6 - A_4) - (4/35)(A_2 - A_0)\}$$
$$+ 30(\alpha/2)^4\{(4/3)(A_5 - A_3) - (4/15)(A_3 - A_1)\}$$
$$+ 15\alpha^3\{(4/3)(A_4 - A_2) - (4/15)(A_2 - A_0)\}$$
$$+ 120\alpha^2(A_3 - A_1) + 960(A_2 - A_0)]$$

$$\Gamma_7 \int a^2 \sin\theta_a \cos\theta_a \sin\theta_b \cos\theta_b e^{-\kappa a}(1/\kappa b)^3 dv$$
$$= (2\pi\Gamma_7/15\kappa^5\alpha^3)[-16\gamma_7(\alpha)/\alpha^2 + 4\alpha^3\Gamma_2(\alpha)]$$

$$\int a^2 \sin\theta_a \cos\theta_a \sin\theta_b \cos\theta_b e^{-\kappa a}(1/\kappa b)^3[\Gamma_7(\kappa b) - (\kappa b)^5\ \Gamma_2(\kappa b)]dv$$
$$= (2\pi\alpha^2/4\kappa^5)[(\alpha/2)^5\{(4/3)(A_6 - A_4) - (152/21)(A_4 - A_2) + (1/15)(A_2 - A_0)\}$$
$$+ (\alpha/2)^4\{8(A_5 - A_3) - 40(A_3 - A_1)\}$$
$$+ 20\alpha^3\{(A_6 - A_4) - (1/5)(A_4 - A_2) - 2(A_2 - A_0)\}$$
$$- 480\alpha^2(A_5 - A_3) + 360\alpha\{(23/3)A_4 - 5A_2 - 2A_0\} - 240\{16A_3 - 8A_1\}]$$

Evaluation of the integral

$$\int a^2 \cos^2\theta_a e^{-\kappa a} P_2(\cos\theta_b)(1/\kappa b)^3 dv = J$$

This is a conditionally convergent integral,[7] the value of which depends upon the particular coordinate system used. Since the companion integral has been evaluated in the λ, μ system (merely for convenience), this procedure must be followed here, even though much more laborious than the evaluation in the a, b, system. Setting $\rho = \alpha/2$,

$$J = \int\int e^{-\alpha(\lambda+\mu)/2}(2\pi/\kappa^5)(\alpha/2)^2(\lambda\mu+1)^2(1/(\lambda-\mu)^3)(\lambda^2-\mu^2)$$
$$\{1 - 3(\lambda^2-1)(1-\mu^2)/2(\lambda-\mu)^2\}\,d\lambda d\mu$$
$$= (2\pi\alpha^2/4\kappa^5)\Big[\int\int e^{-\rho(\lambda+\mu)}(\lambda\mu+1)^2(\lambda+\mu)/(\lambda-\mu)^2\cdot d\lambda d\mu$$
$$- (3/2)\int\int (\lambda^2-1)e^{-\rho(\lambda+\mu)}(\lambda\mu+1)^2\{(1-\lambda^2)(\lambda+\mu)/(\lambda-\mu)^4$$
$$+ (\lambda+\mu)^2/(\lambda-\mu)^3\}\,d\lambda d\mu\Big]$$
$$= (2\pi\alpha^2/4\kappa^5)\int_1^\infty e^{-\rho\lambda}d\lambda\,[I_0 - (3/2)(\lambda^2-1)\{(1-\lambda^2)I_1 + I_2\}]$$

where

$$I_0 = \int_{-1}^{1} d\mu e^{-\rho\mu}(\lambda\mu+1)^2(\lambda+\mu)/(\lambda-\mu)^2$$
$$I_1 = \int_{-1}^{1} d\mu e^{-\rho\mu}(\lambda\mu+1)^2(\lambda+\mu)/(\lambda-\mu)^4$$
$$I_2 = \int_{-1}^{1} d\mu e^{-\rho\mu}(\lambda\mu+1)^2(\lambda+\mu)^2/(\lambda-\mu)^3$$
$$I_0 = 2\lambda\{\lambda^2F(0) + 2\lambda(\lambda^2+1)F(1) + (\lambda^2+1)^2F(2)\} + \lambda^2F(-1)$$
$$+ 2\lambda(\lambda^2+1)F(0) + (\lambda^2+1)^2F(1)$$
$$I_1 = 2\lambda\{\lambda^2F(2) + 2\lambda(\lambda^2+1)F(3) + (\lambda^2+1)^2F(4)\} + \lambda^2F(1)$$
$$+ 2\lambda(\lambda^2+1)F(2) + (\lambda^2+1)^2F(3)$$
$$I_2 = -4\lambda^2\{\lambda^2F(1) + 2\lambda(\lambda^2+1)F(2) + (\lambda^2+1)^2F(3)\} - 4\lambda\{\lambda^2F(0)$$
$$+ 2\lambda(\lambda^2+1)F(1) + (\lambda^2+1)^2F(2)\} - \{\lambda^2F(-1) + 2\lambda(\lambda^2+1)F(0)$$
$$+ (\lambda^2+1)^2F(1)\}$$
$$J = (2\pi\alpha^2/4\kappa^5)\int_1^\infty e^{-\rho\lambda}d\lambda\{3\lambda(1-\lambda^4)^2F(4) + (3/2)(1-\lambda^4)(1-9\lambda^4)F(3)$$
$$+ (24\lambda^7 - \lambda^5 - 14\lambda^3 - \lambda)F(2) + (21\lambda^6 - 5\lambda^4/2 - 6\lambda^2 - 1/2)F(1)$$
$$+ (9\lambda^5 - 2\lambda^3 - \lambda)F(0) + (3\lambda^4/2 - \lambda^2/2)F(-1)\},$$

[7] This was not realized at first, and the a, b coordinate system was used. This gave a wrong result, and I wish to thank Mr. H. M. Mott-Smith, Jr. for his kindness in helping to locate the error.

Applying formula (3), one obtains

$$J = (4\pi/\kappa^5)(\gamma_5/3\alpha^3 + 2\Gamma_2/15 + 4\gamma_7/5\alpha^5 - \alpha^2 e^{-\alpha}/2).$$

This differs from the result using the a, b coordinate system in that the last term here does not occur in that result.

The integrals i_2, i_4, i_6, i_8, i_{10}, and i_{11}.

$$i_2 = c_1^4 \int dv_1 dv_2 a_1 \sin\theta_{a_1} b_1 \sin\theta_{b_1} a_2 \sin\theta_{a_2} b_2 \sin\theta_{b_2} e^{-(\kappa/2)(a_1+a_2+b_1+b_2)}(2/r)$$

$$i_4 = c_1^2 c_2^2 \int dv_1 dv_2 a_1 \sin\theta_{a_1} b_1 \sin\theta_{b_1} a_2 \cos\theta_{a_2} b_2 \cos\theta_{b_2} e^{-(\kappa/2)(a_1+a_2+b_1+b_2)}(2/r)$$

$$i_6 = c_1^2 c_2^2 \int dv_1 dv_2 a_1 \sin\theta_{a_1} b_1 \cos\theta_{b_1} a_2 \sin\theta_{a_2} b_2 \cos\theta_{b_2} \cos(\phi_1 - \phi_2) e^{-(\kappa/2)(a_1+a_2+b_1+b_2)}(2/r)$$

$$i_8 = c_1^4 \int dv_1 dv_2 a_1 \sin\theta_{a_1} b_1 \sin\theta_{b_1} a_2 \sin\theta_{a_2} b_2 \sin\theta_{b_2} \cos 2(\phi_1 - \phi_2) e^{-(\kappa/2)(a_1+a_2+b_1+b_2)}(2/r)$$

$$i_{10} = c_2^4 \int dv_1 dv_2 a_1 \cos\theta_{a_1} b_1 \cos\theta_{b_1} a_2 \cos\theta_{a_2} b_2 \cos\theta_{b_2} e^{-(\kappa/2)(a_1+a_2+b_1+b_2)}(2/r)$$

$$i_{11} = c_1^2 c_2^2 \int dv_1 dv_2 a_1 \cos\theta_{a_1} b_1 \sin\theta_{b_1} a_2 \sin\theta_{a_2} b_2 \cos\theta_{b_2} \cos(\phi_1 - \phi_2) e^{-(\kappa/2)(a_1+a_2+b_1+b_2)}(2/r).$$

We use Neumann's expansion:

$$\frac{1}{r} = \frac{2}{R} \sum_{\tau=0}^{\infty} \sum_{\nu=0}^{\tau} D_{\tau\nu} P_\tau^\nu \begin{pmatrix} \lambda_1 \\ \lambda_2 \end{pmatrix} Q_\tau^\nu \begin{pmatrix} \lambda_2 \\ \lambda_1 \end{pmatrix} P_\tau^\nu(\mu_1) P_\tau^\nu(\mu_2) \cos\nu(\phi_1 - \phi_2)$$

the upper arguments for $\lambda_2 > \lambda_1$, and the lower for $\lambda_2 < \lambda_1$

$$D_{\tau\nu} = (-1)^\nu \epsilon_\nu (2\tau + 1) \left[\frac{(\tau - \nu)!}{(\tau + \nu)!}\right]^2, \quad \epsilon_0 = 1, \ \epsilon_1 = \epsilon_2 = \cdots = 2.$$

One does not need to concern oneself as to whether the above series converges rapidly or not (for the integrals in question), for orthogonality relations reduce the number of terms to three or four. In general, but not always, the second term is so small compared with the first that its contribution may be neglected.

Let us denote the terms arising from $\tau = 0$ by $i_2^{(0)}$, $i_4^{(0)}$, etc. Also, let

$$\sigma_\tau(m, n, \alpha) = \int_1^\infty Q_\tau(\lambda) e^{-\alpha\lambda/2} \lambda^m . 1_n\left(\lambda, \frac{\alpha}{2}\right) d\lambda$$

$$= \sum_{\nu=0}^{n} (n!/\nu!) f_\tau(m + \nu, \alpha)(\alpha/2)^{\nu - n - 1}$$

$$s_\tau(m, n, \alpha) = \int_1^\infty Q_\tau(\lambda_1) e^{-\alpha\lambda_1/2} \lambda_1^m d\lambda_1 \int_1^{\lambda_1} e^{-\alpha\lambda_2/2} \lambda_2^n d\lambda_2$$

$$= f_\tau(m, \alpha/2)\, A_n(1, \alpha/2) - \sigma_\tau(m, n, \alpha)$$

Tables of σ_r, s_r, etc. are given later.

$$i_2^{(0)} = 2c_1^4(2\pi)^2(R/2)^9 \int (\lambda_1^2 - 1)(1 - \mu_1)^2(\lambda_2^2 - 1)(1 - \mu_2^2)(\lambda_1^2 - \mu_1^2)$$

$$(\lambda_2^2 - \mu_2^2)Q_0\binom{\lambda_2}{\lambda_1} e^{-\alpha R(\lambda_1+\lambda_2)/2} d\mu_1 d\mu_2 d\lambda_1 d\lambda_2$$

$$= (2\kappa/1024)(\alpha/2)^9 \int (\lambda_1^2 - 1)(\lambda_2^2 - 1)(4/3)^2(\lambda_1^2 - 1/5)$$

$$(\lambda_2^2 - 1/5)Q_0\binom{\lambda_2}{\lambda_1} e^{-\alpha R(\lambda_1+\lambda_2)/2} d\lambda_1 d\lambda_2$$

$$= (\kappa/144)(\alpha/2)^9\{s_0(00)/25 + 36s_0(22)/25 + s_0(44) - 6[s_0(02) + s_0(20)]/25$$
$$+ [s_0(04) + s_0(40)]/5 - 6[s_0(24) + s_0(42)]/5\}$$

$$i_4^{(0)} = (\kappa/144)(\alpha/2)^9\{s_0(00)/5 + 108s_0(22)/25 + s_0(44) - 24[s_0(02) + s_0(20)]/25$$
$$+ 3[s_0(04) + s_0(40)]/5 - 12[s_0(42) + s_0(24)]/5\}$$

$$i_{10}^{(0)} = (\kappa/16)(\alpha/2)^9[\{s_0(00) + s_0(04) + s_0(40) + s_0(44)\}/9 + 36s_0(22)/25$$
$$- 2\{s_0(02) + s_0(20) + s_0(42) + s_0(24)\}/5]$$

Let

$$t_2(2m, 2n, \alpha) = \int_1^\infty Q_2(\lambda_1)e^{-\alpha\lambda_1/2}\lambda_1^{2m} d\lambda_1 \int_1^{\lambda_1} P_2(\lambda_2)e^{-\alpha\lambda_2/2}\lambda_2^{2n} d\lambda_2$$
$$= (3/2)s_2(2m, 2n + 2) - (\tfrac{1}{2})s_2(2m, 2n).$$

Then

$$i_2^{(2)} = 10c_1^4(2\pi)^2(R/2)^9 \int (\lambda_1^2 - 1)(1 - \mu_1)^2(\lambda_2^2 - 1)(1 - \mu_2^2)(\lambda_1^2 - \mu_1^2)$$
$$(\lambda_2^2 - \mu_2^2)e^{-\alpha(\lambda_1+\lambda_2)/2} \cdot Q_2\binom{\lambda_2}{\lambda_1} P_2\binom{\lambda_1}{\lambda_2} P_2(\mu_1)P_2(\mu_2) d\mu_1 d\mu_2 d\lambda_1 d\lambda_2$$

$$= 10c_1^4(2\pi)^2(R/2)^9 \int (4/15)^2(\lambda_1^2 - 1)(\lambda_2^2 - 1)(\lambda_1^2 + 1/7)$$

$$(\lambda_2^2 + 1/7)Q_2\binom{\lambda_2}{\lambda_1} P_2\binom{\lambda_1}{\lambda_2} e^{-\alpha(\lambda_1+\lambda_2)/2} d\lambda_1 d\lambda_2$$

$$= (\kappa/720)(\alpha/2)^9[t_2(00)/49 + 36t_2(22)/49 + t_2(44) + 6\{t_2(02) + t_2(20)\}/49$$
$$- \{t_2(04) + t_2(40)\}/7 - 6\{t_2(24) + t_2(42)\}/7]$$

$$i_4^{(2)} = -(\kappa/120)(\alpha/2)^9[-t_2(00)/21 + 12t_2(22)/49 + t_2(44)/3$$
$$- 6\{t_2(02) + t_2(20)\}/49 + \{t_2(04) + t_2(40)\}/7 - 2\{t_2(24) + t_2(42)\}/7]$$

$$i_{10}^{(2)} = (\kappa/20)(\alpha/2)^9[\{t_2(00) + t_2(04) + t_2(40) + t_2(44)\}/9 + 4t_2(22)/49$$
$$- 2\{t_2(02) + t_2(20) + t_2(42) + t_2(24)\}/21]$$

Let

$$u_4(2m, 2n) = \int_1^{\infty} Q_4(\lambda_1) e^{-\alpha\lambda_1/2}\lambda_1^{2m} d\lambda_1 \int_1^{\lambda_1} P_4(\lambda_2) e^{-\alpha\lambda_2/2}\lambda_2^{2n} d\lambda_2$$

$$= (1/8)\left[35s_4(2m, 2n+4) - 30s_4(2m, 2n+2) + 3s_4(2m, 2n)\right]$$

Then

$$i_2^{(4)} = 18c_1^4(2\pi)^2(R/2)^9(16/315)^2 \int (\lambda_1^2-1)(\lambda_2^2-1)e^{-\alpha(\lambda_1+\lambda_2)/2} Q_4\binom{\lambda_2}{\lambda_1} P_4\binom{\lambda_1}{\lambda_2} d\lambda_1 d\lambda_2$$

$$= \kappa(1/105)^2(\alpha/2)^9\left[u_4(00) - u_4(02) - u_4(20) + u_4(22)\right].$$

The other integrals for $\tau = 4$ will be somewhat similar. Since the contributions from $\tau = 2$ are small with respect to those from $\tau = 0$, the influence of $\tau = 4$ has been neglected.

$$i_6^{(1)} = -c_1^2c_2^2(2\pi)^2D_{11}(R/2)^9 \int \frac{dP_1}{d\lambda}\binom{\lambda_1}{\lambda_2}\frac{dQ_1}{d\lambda}\binom{\lambda_2}{\lambda_1}(\lambda_1^2-1)(\lambda_2^2-1)(4/3)^2$$

$$(\lambda_1^2 - \tfrac{1}{5})(\lambda_2^2 - \tfrac{1}{5})e^{-\alpha(\lambda_1+\lambda_2)/2} d\lambda_1 d\lambda_2$$

$$= (\kappa/96)(\alpha/2)^9\left[\left\{s_1(12) - s_1(10) - s_0(02) + s_0(00)\right\}/25 + \left\{s_1(34) - s_1(32) - s_0(24) + s_0(22)\right\} - (\tfrac{1}{5})\left\{s_1(14) - s_1(12) + s_1(32) - s_1(30) - s_0(04) + s_0(02) - s_0(22) + s_0(20)\right\}\right]$$

$$i_6^{(2)} = (3\kappa/160)(\alpha/2)^9\left[\left\{s_2(24) - s_2(22) - s_1(14) + s_1(12)\right\}/49 + \left\{s_2(46) - s_2(44) - s_1(36) + s_1(34)\right\}/9 - (1/21)\left\{s_2(26) - s_2(24) - s_1(16) + s_1(14) + s_2(44) - s_2(42) - s_1(34) + s_1(32)\right\}\right]$$

$$i_{11}^{(1)} = -c_1^2c_2^2(2\pi)^2D_{11}(R/2)^9 \int (\lambda_1\mu_1 - 1)(\lambda_2\mu_2 - 1)(\lambda_1^2 - 1)(\lambda_2^2 - 1)$$

$$(\lambda_1^2 - \mu_1^2)(\lambda_2^2 - \mu_2^2)e^{-\alpha(\lambda_1+\lambda_2)/2}\frac{dP_1}{d\lambda}\binom{\lambda_1}{\lambda_2}\frac{dQ_1}{d\lambda}\binom{\lambda_2}{\lambda_1}$$

$$P_1'(\mu_1)P_1'(\mu_1)P_1'(\mu_2)P_1'(\mu_2)d\lambda_1 d\lambda_2 \cdot d\mu_1 d\mu_2$$

$$= -i_6^{(1)} \quad i_{11}^{(2)} = i_6^{(2)}, \text{ etc.}$$

For the evaluation of $i_8^{(2)}$, we use the formula

$$(\lambda^2 - 1)^2\frac{d^2Q_2}{d\lambda^2} = 2\left[(\lambda^2 - 1)Q_2 - \lambda Q_1 + Q_0\right]$$

$$i_8^{(2)} = 3c_1^4(2\pi)^2D_{22}(R/2)^9 \int (\lambda_1^2 - 1)^2(\lambda_2^2 - 1)^2\frac{d^2Q_2}{d\lambda^2}\binom{\lambda_2}{\lambda_1}(16/5)^2$$

$$(\lambda_1^2 - 1/7)(\lambda_2^2 - 1/7)e^{-\alpha(\lambda_1+\lambda_2)/2} d\lambda_1 d\lambda_2$$

$$= (\kappa/480)(\alpha/2)^9\left[s_2(44) + (1/7)\left\{s_2(04) + s_1(14)\right\} + s_0(24) - 8s_2(24)/7 - s_1(34) - s_0(04)/7 - (8/7)\left\{s_2(42) + (1/7)\left\{s_2(02) + s_1(12)\right\} + s_0(22) - 8s_2(22)/7 - s_1(32) - s_0(02)/7\right\} + (1/7)\left\{s_2(40) + (1/7)\left\{s_2(00) + s_1(10)\right\} + s_0(20) - 8s_2(20)/7 - s_1(30) - s_0(00)/7\right\}\right].$$

TABLE I. $A_m(1, \alpha)$.

α	$\alpha=1.5$	2.0	2.5	3.0	3.5	4.0	4.5	5.0	6.0	7.0	8.0	9.0	10.0
$A_0(1, \alpha)$	0.14875	0.06767	0.032834	0.01660	$0.0^2$8628	$0.0^3$4579	$0.0^3$24687	$0.0^4$13476	$0.0^5$4131	$0.0^5$1303	$0.0^4$193	$0.0^4$1371	$0.0^5$4540
$A_1(1, \alpha)$	.24792	.10151	.04597	.02213	.011093	$.0^2$5724	$.0^3$3017	$.0^3$1617	$.0^4$4820	$.0^4$1489	$.0^4$4717	$.0^4$1524	$.0^4$4994
$A_2(1, \alpha)$	.4793	.16917	.06961	.03135	.014967	**$.0^2$7441**	$.0^3$3810	$.0^3$1994	$.0^4$5738	$.0^4$1728	$.0^4$5373	$.0^4$1710	$.0^4$5539
$A_3(1, \alpha)$	1.1074	.32142	.11637	.04795	.02145	.010160	$.0^2$5008	$.0^3$2544	$.0^3$6999	$.0^3$2043	$.0^4$6209	$.0^4$1941	$.0^4$6202
$A_4(1, \alpha)$	3.1018	.7105	.21902	.08051	.03315	.01474	$.0^2$6920	$.0^3$3383	**$.0^3$8799**	**$.0^3$2470**	$.0^4$7300	$.0^4$2233	$.0^4$7021
$A_5(1, \alpha)$	10.488	1.844	.4709	.1508	.05598	.02300	.010158	$.0^2$4730	$.0^3$11464	$.0^3$3067	$.0^4$8755	$.0^4$2612	$.0^4$8050
$A_6(1, \alpha)$	42.10	5.599	1.1629	.3182	.10459	.03907	.016011	$.0^2$7024	$.0^2$15596	$.0^3$3931	$.0^3$10760	$.0^3$3110	$..0^4$9371
$A_7(1, \alpha)$				.7588		.07296		.01118	$.0^2$2232	$.0^2$5234	$.0^3$1361	$.0^3$3790	$.0^4$11100
$A_8(1, \alpha)$				2.0405		.1505		.01924	$.0^3$3389	$.0^3$7285	$.0^3$1780	$.0^4$4740	$.0^4$1342
$A_9(1, \alpha)$				6.138		.3432		.03598	$.0^2$5497	$.0^2$10669	$.0^2$2422	$.0^3$6111	$.0^4$16617
$A_{10}(1, \alpha)$				20.48		.8627		.07331	$.0^2$9575	$.0^2$16544	$.0^3$3447	$.0^3$8162	$.0^4$2116
$A_{11}(1, \alpha)$				75.10		2.377		.1625	.017969	$.0^2$2730	$.0^2$5159	$.0^3$11346	$.0^4$2781

TABLE II. $f_s(m, \alpha)$

α	$\alpha=1.5$	2.0	2.5	3.0	3.5	4.0	4.5	5.0	6.0	7.0	8.0	9.0	10.0
$f_0(0, \alpha)$	0.05250	0.02850	0.01575	$0.0^2$8810	$0.0^2$4977	$0.0^2$2831	$0.0^2$1620	$0.0^3$9315	$0.0^3$3115	$0.0^3$1054	$0.0^3$3600	$0.0^4$1238	$0.0^4$428
$f_1(1, \alpha)$	.06535	.03425	.01846	.010141	$.0^2$5647	$.0^3$3176	$.0^3$1800	$.0^2$10271	$.0^3$3392	$.0^3$1137	$.0^3$3854	$.0^4$1317	$.0^4$4536
$f_2(2, \alpha)$	.08714	.04316	.02242	.011997	$.0^2$6551	$.0^3$3628	$.0^3$2031	$.0^2$11473	$.0^3$3733	$.0^3$1236	$.0^4$4152	$.0^4$1409	$.0^4$482
$f_3(3, \alpha)$	.1285	.05823	.02861	.014732	$.0^2$7825	$.0^3$4244	$.0^3$2337	$.0^2$13028	$.0^3$4152	$.0^3$1356	$.0^4$4505	$.0^4$1516	$.0^4$515
$f_4(4, \alpha)$	.2194	.0866	.03909	.019034	$.0^2$9720	$.0^3$5120	$.0^3$2759	$.0^2$15105	$.0^3$4691	$.0^3$1504	$.0^4$4932	$.0^4$1643	$.0^4$554
$f_5(5, \alpha)$	.455	.1474	.0587	.02635	.012722	$.0^2$6436	$.0^3$3364	$.0^2$17986	$.0^3$5400	$.0^3$1693	$.0^4$5457	$.0^4$1795	$.0^4$599
$f_6(6, \alpha)$				.03999		$.0^2$8538		$.0^2$2217	$.0^3$6364	$.0^3$1936	$.0^4$6115	$.0^4$1981	$.0^4$653
$f_7(7, \alpha)$				.06808		.012147		$.0^2$2856	$.0^3$7727	$.0^3$2264	$.0^4$6960	$.0^4$2213	$.0^4$720
$f_8(8, \alpha)$				.13248		.018856		$.0^2$3894	$.0^3$9744	$.0^3$2715	$.0^4$8076	$.0^4$2507	$.0^4$800
$f_9(9, \alpha)$				.2970		.03243		$.0^2$5693	$.0^3$1288	$.0^3$3368	$.0^4$9595	$.0^4$2892	$.0^4$904
$f_{10}(10, \alpha)$				.7642		.06244		$.0^2$916	$.0^3$1805	$.0^3$4350	$.0^3$1174	$.0^3$3409	$.0^4$1036
$f_{11}(11, \alpha)$				2.231		.1351		.01602	$.0^2$2710	$.0^3$5906	$.0^3$1489	$.0^4$4124	$.0^4$1213

The integrals $i_6^{(3)}$, $i_6^{(4)}$, and $i_8^{(4)}$ have been assumed negligible, because of the smallness of the preceding terms.

TABLE III. $\sigma_0\ (m, n, \alpha)$

α	$\alpha=3$	4	5	6	7	8	9	10
$\sigma_0(0,0,\alpha)$	0.01391	$0.0^2$3170	$0.0^3$800	$0.0^3$2162	$0.0^4$611	$0.0^4$1787	$0.0^5$536	$0.0^5$1644
$\sigma_0(0,2,\alpha)$	.05647	$.0^2$9742	$.0^2$2043	$.0^3$4827	$.0^3$1235	$.0^4$3340	$.0^5$942	$.0^5$2743
$\sigma_0(0,4,\alpha)$	.4202	.04750	$.0^2$7474	$.0^2$1436	$.0^3$3149	$.0^4$7565	$.0^4$1942	$.0^5$5245
$\sigma_0(2,0,\alpha)$	.02152	$.0^2$445	$.0^2$1058	$.0^3$2737	$.0^4$7504	$.0^4$2143	$.0^5$6313	$.0^5$1906
$\sigma_0(2,2,\alpha)$	.09948	.01496	$.0^2$2884	$.0^3$6430	$.0^3$1577	$.0^4$4138	$.0^4$1138	$.0^5$3252
$\sigma_0(2,4,\alpha)$	.8257	.07945	.01128	$.0^2$2019	$.0^3$4203	$.0^4$9714	$.0^4$2419	$.0^5$6378
$\sigma_0(4,0,\alpha)$	.04180	$.0^2$720	$.0^2$1539	$.0^3$3717	$.0^4$9714	$.0^4$2679	$.0^5$768	$.0^5$2270
$\sigma_0(4,2,\alpha)$	.2438	.02824	$.0^2$4674	$.0^3$9446	$.0^3$2168	$.0^4$5417	$.0^4$1438	$.0^5$3995
$\sigma_0(4,4,\alpha)$	2.4886	.1748	.02051	$.0^2$3237	$.0^3$6183	$.0^3$13424	$.0^4$3192	$.0^5$8122

TABLE IV. $s_0(m,n,\alpha)$

α	$\alpha=3$	4	5	6	7	8	9	10
$S_0(0,0,\alpha)$	$0.0^2$753	$0.0^2$1798	$0.0^3$470	$0.0^3$1302	$0.0^4$375	$0.0^4$1117	$0.0^5$340	$0.0^5$1055
$S_0(0,2,\alpha)$	.01261	$.0^2$2678	$.0^3$650	$.0^3$1715	$.0^4$476	$.0^4$1378	$.0^5$410	$.0^5$1251
$S_0(0,4,\alpha)$	.0268	$.0^2$466	$.0^2$1000	$.0^3$243	$.0^4$640	$.0^4$1780	$.0^5$514	$.0^5$1528
$S_0(2,0,\alpha)$	.02508	$.0^2$474	$.0^2$1058	$.0^3$2620	$.0^4$694	$.0^4$1933	$.0^5$5580	$.0^5$1659
$S_0(2,2,\alpha)$	.05069	$.0^2$800	$.0^2$1601	$.0^3$370	$.0^4$928	$.0^4$2485	$.0^5$697	$.0^5$2023
$S_0(2,4,\alpha)$	.1460	.01700	$.0^2$283	$.0^3$580	$.0^3$1345	$.0^4$3405	$.0^5$914	$.0^5$2569
$S_0(4,0,\alpha)$	.1421	.01849	$.0^2$3221	$.0^3$669	$.0^3$1555	$.0^4$3917	$.0^4$1045	$.0^5$2916
$S_0(4,2,\alpha)$	.3485	.03599	$.0^2$5417	$.0^2$1022	$.0^3$2214	$.0^4$5301	$.0^4$1360	$.0^5$3681
$S_0(4,4,\alpha)$	1.345	.0949	.01124	$.0^2$1812	$.0^3$3520	$.0^4$7803	$.0^4$1891	$.0^4$490

TABLE V. $\sigma_1(m,n,\alpha)$

α	$\alpha=3$	4	5	6	7	8	9	10
$\sigma_1(1,0,\alpha)$	$0.0^2$6761	$0.0^2$1588	$0.0^3$41080	$.0^3$11307	$0.0^4$3249	$0.0^5$9636	$0.0^5$2927	$0.0^6$907
$\sigma_1(1,2,\alpha)$	.02649	$.0^2$4730	$.0^2$10197	$.0^3$2464	$.0^4$6422	$.0^4$1765	$.0^5$5049	$.0^5$1488
$\sigma_1(1,4,\alpha)$	.1927	.02253	$.0^2$3644	$.0^3$7171	$.0^3$1604	$.0^4$3921	$.0^4$10227	$.0^5$2799
$\sigma_1(1,6,\alpha)$	2.7214	.18784	.020763	$.0^2$3072	$.0^3$5523	$.0^3$11383	$.0^4$2594	$.0^5$6367
$\sigma_1(3,0,\alpha)$	$.0^2$9821	$.0^2$2122	$.0^3$5211	$.0^3$1384	$.0^4$3874	$.0^4$11264	$.0^5$3369	$.0^5$1030
$\sigma_1(3,2,\alpha)$	.04322	$.0^2$6839	$.0^2$13697	$.0^3$3150	$.0^4$7926	$.0^4$2121	$.0^5$5944	$.0^5$1722
$\sigma_1(3,4,\alpha)$	.3470	.03513	$.0^2$5194	$.0^3$9602	$.0^3$2055	$.0^4$4860	$.0^4$12354	$.0^5$3311
$\sigma_1(3,6,\alpha)$	5.177	.3079	.03096	$.0^2$4280	$.0^3$7327	$.0^3$1454	$.0^4$3217	$.0^5$7703

TABLE VI. $s_1\ (m, n, \alpha)$

α	$\alpha=3$	4	5	6	7	8	9	10
$S_1(1,0,\alpha)$	$0.0^2$2959	$0.0^3$730	$0.0^3$1953	$0.0^4$5525	$0.0^4$1623	$0.0^5$4907	$0.0^5$1518	$0.0^6$477
$S_1(1,2,\alpha)$	$.0^2$482	$.0^2$1064	$.0^3$2653	$.0^4$715	$.0^4$2030	$.0^5$599	$.0^5$1808	$.0^6$5607
$S_1(1,4,\alpha)$	$.0^2$998	$.0^2$1804	$.0^3$399	$.0^4$994	$.0^4$2678	$.0^5$760	$.0^5$2230	$.0^6$676
$S_1(1,6,\alpha)$	.0296	$.0^2$390	$.0^3$705	$.0^3$1544	$.0^4$383	$.0^4$103	$.0^5$2885	$.0^6$847
$S_1(3,0,\alpha)$	$.0^2$929	$.0^2$1818	$.0^3$4182	$.0^3$10612	$.0^4$2877	$.0^5$8169	$.0^5$2401	$.0^6$7253
$S_1(3,2,\alpha)$	.01837	$.0^2$300	$.0^3$6216	$.0^3$1468	$.0^3$3786	$.0^4$1037	$.0^5$2960	$.0^6$877
$S_1(3,4,\alpha)$	.0516	$.0^2$625	$.0^2$1070	$.0^3$2259	$.0^4$538	$.0^4$1395	$.0^5$3821	$.0^5$1096
$S_1(3,6,\alpha)$	.232	.0176	$.0^2$230	$.0^3$407	$.0^4$857	$.0^4$204	$.0^5$526	$.0^5$1448

RESULTS

The results have been tabulated in Tables I–XV. The values are based partly on integral logarithm tables given by Jahnke–Emde, and the accuracy

is limited thereby. The tables are, therefore, subject to revision on this account. Except for this, they are accurate up to a possible change of the last figure. In this connection, it is urged that the tabular method is the economical one, in that the calculations may be checked easily.

TABLE VII. $\sigma_2(m,n,\alpha)$

α	$\alpha=3$	4	5	6	7	8	9	10
$\sigma_2(0,0,\alpha)$	$0.0^{2}3185$	$0.0^{3}797$	$0.0^{3}2158$	$0.0^{4}6154$	$0.0^{4}1818$	$0.0^{5}552$	$0.0^{5}1709$	$0.0^{6}540$
$\sigma_2(0,2,\alpha)$	.011511	$.0^{2}2225$	$.0^{3}5079$	$.0^{3}12825$	$.0^{4}3459$	$.0^{5}979$	$.0^{5}2865$	$.0^{5}0861$
$\sigma_2(0,4,\alpha)$	.0792	.01004	$.0^{2}1729$	$.0^{3}3574$	$.0^{4}8318$	$.0^{4}2099$	$.0^{5}5628$	$.0^{5}1576$
$\sigma_2(0,6,\alpha)$	1.092	.0814	$.0^{2}955$	$.0^{2}1484$	$.0^{3}2777$	$.0^{4}5917$	$.0^{4}1388$	$.0^{5}3492$
$\sigma_2(2,0,\alpha)$	$.0^{3}3976$	$.0^{3}958$	$.0^{3}2528$	$.0^{4}708$	$.0^{4}2060$	$.0^{5}618$	$.0^{5}1897$	$.0^{6}593$
$\sigma_2(2,2,\alpha)$	.01511	$.0^{2}2775$	$.0^{3}6130$	$.0^{3}1510$	$.0^{4}4001$	$.0^{4}1113$	$.0^{5}3224$	$.0^{6}960$
$\sigma_2(2,4,\alpha)$	.10773	.01295	$.0^{2}2147$	$.0^{3}4311$	$.0^{4}981$	$.0^{4}2433$	$.0^{5}6432$	$.0^{5}1780$
$\sigma_2(2,6,\alpha)$	1.509	.1069	.01209	$.0^{2}1823$	$.0^{3}3335$	$.0^{4}6970$	$.0^{4}1609$	$.0^{5}3991$
$\sigma_2(4,0,\alpha)$	$.0^{2}545$	$.0^{2}1224$	$.0^{3}310$	$.0^{3}8415$	$.0^{4}2401$	$.0^{5}7066$	$.0^{5}2142$	$.0^{6}663$
$\sigma_2(4,2,\alpha)$	.02296	$.0^{2}3799$	$.0^{3}789$	$.0^{3}1862$	$.0^{4}4789$	$.0^{4}1305$	$.0^{5}3712$	$.0^{5}1090$
$\sigma_2(4,4,\alpha)$	.1787	.01892	$.0^{2}2904$	$.0^{3}5533$	$.0^{3}1214$	$.0^{4}2926$	$.0^{5}7566$	$.0^{5}2053$
$\sigma_2(4,6,\alpha)$	2.63	.1628	.01729	$.0^{2}2418$	$.0^{3}4247$	$.0^{3}8588$	$.0^{4}1937$	$.0^{5}4696$

TABLE VIII. $s_2(m,n,\alpha)$

α	$\alpha=3$	4	5	6	7	8	9	10
$S_2(0,0,\alpha)$	$0.0^{3}677$	$0.0^{3}195$	$0.0^{4}582$	$0.0^{4}1778$	$0.0^{5}558$	$0.0^{5}178$	$0.0^{6}577$	$0.0^{6}187$
$S_2(0,2,\alpha)$	$.0^{3}93$	$.0^{3}255$	$.0^{4}728$	$.0^{4}216$	$.0^{5}664$	$.0^{5}208$	$.0^{6}662$	$.0^{6}214$
$S_2(0,4,\alpha)$	$.0^{2}135$	$.0^{3}37$	$.0^{3}98$	$.0^{4}274$	$.0^{5}81$	$.0^{5}251$	$.0^{6}778$	$.0^{6}249$
$S_2(0,6,\alpha)$	$.0^{2}12$	$.0^{3}07$	$.0^{3}150$	$.0^{4}373$	$.0^{4}104$	$.0^{5}313$	$.0^{6}94$	$.0^{6}298$
$S_2(2,0,\alpha)$	$.0^{2}139$	$.0^{3}360$	$.0^{4}983$	$.0^{4}282$	$.0^{5}845$	$.0^{5}259$	$.0^{6}811$	$.0^{6}259$
$S_2(2,2,\alpha)$	$.0^{2}22$	$.0^{3}51$	$.0^{3}131$	$.0^{4}360$	$.0^{4}1037$	$.0^{5}313$	$.0^{6}957$	$.0^{6}300$
$S_2(2,4,\alpha)$	$.0^{2}43$	$.0^{3}88$	$.0^{3}195$	$.0^{4}491$	$.0^{4}1345$	$.0^{5}391$	$.0^{5}1162$	$.0^{6}359$
$S_2(2,6,\alpha)$	.011	$.0^{2}21$	$.0^{3}35$	$.0^{4}75$	$.0^{4}187$	$.0^{5}52$	$.0^{5}147$	$.0^{6}449$
$S_2(4,0,\alpha)$	$.0^{2}41$	$.0^{3}893$	$.0^{3}201$	$.0^{4}518$	$.0^{4}143$	$.0^{5}415$	$.0^{5}1247$	$.0^{6}381$
$S_2(4,2,\alpha)$	$.0^{2}79$	$.0^{3}1494$	$.0^{3}295$	$.0^{4}705$	$.0^{4}186$	$.0^{5}517$	$.0^{5}1517$	$.0^{6}455$
$S_2(4,4,\alpha)$	.021	$.0^{3}331$	$.0^{3}51$	$.0^{3}1061$	$.0^{4}260$	$.0^{5}683$	$.0^{5}1932$	$.0^{6}568$
$S_2(4,6,\alpha)$	.08	.0124	$.0^{3}81$	$.0^{3}188$	$.0^{4}41$	$.0^{5}98$	$.0^{5}261$	$.0^{6}745$

TABLE IX. $S_{mm}'(\alpha/2)$, *etc.*

α	$\alpha=3$	4	5	6	7	8	9	10
$(S_{00})^{1/2}$	0.4825	0.2256	$0.0^{2}5086$	−0.1597	−0.2649	−0.3187	−0.3326	−0.3190
S_{00}	.2328	.05088	$.0^{4}2587$	.02556	.07020	.10156	.11062	.10174
$(S_{11})^{1/2}$	.8089	.6947	.5778	.4679	.3702	.2871	.2185	.16405
S_{11}	.6542	.4826	.3339	.2189	.13695	.08241	.04774	.02692
S_{10}	.3903	.1567	$.0^{2}2939$	−.0747	−.09807	−.09147	−.07268	−.05233

In order not to make the labor prohibitive in other cases, some more straightforward method should be employed to obtain the entries for $s_2(m, n, \alpha)$ and similar quantities. As it is, the accuracy for small values of α is quite small. This is not serious, however, for the approximation method itself can be expected to give good results only for large values of the internuclear distance.

TABLE X. *List of Integrals*

	$\nu = 0$	$\nu = 1$	$\nu = 2$	$\nu = 3$	$\nu = 4$
$\int_{-1}^{1} (\lambda + \mu)^2(\lambda - \mu)^\nu d\mu$	$2\lambda(\lambda^2 + 1)$	$2\left(\lambda^4 - \frac{1}{5}\right)$	$2\lambda\left(\lambda^4 - \frac{2}{3}\lambda^2 + \frac{1}{5}\right)$	$2\left(\lambda^5 - \lambda^4 + \frac{3}{5}\lambda^2 - \frac{1}{7}\right)$	$2\lambda\left(\lambda^6 - \lambda^4 + \frac{3}{5}\lambda^2 - \frac{1}{7}\right)$
$\int (1-\mu^2)^2(\lambda+\mu)(\lambda-\mu)^\nu d\mu$	$\frac{16}{15}\lambda$	$\frac{16}{15}\left(\lambda^2 - \frac{1}{7}\right)$	$\frac{16}{15}\lambda\left(\lambda^2 - \frac{1}{7}\right)$		
$\int (\lambda\mu + 1)^2(\lambda + \mu)$ $\cdot(\lambda - \mu)^\nu d\mu$	$\frac{2}{3}\lambda(\lambda^2 + 5)$	$\frac{2}{3}\lambda^4 + \frac{8}{5}\lambda^2 - \frac{2}{3}$	$\frac{2}{3}\lambda^5 + \frac{4}{15}\lambda^3 + \frac{2}{15}\lambda$	$\frac{2}{3}\lambda^6 - \frac{2}{3}\lambda^4$ $+ \frac{46}{35}\lambda^2 - \frac{2}{5}$	$\frac{2}{3}\lambda^7 - \frac{6}{5}\lambda^5$ $+ \frac{218}{105}\lambda^3 - \frac{22}{35}\lambda$
$\int (\lambda\mu + 1)^2(\lambda + \mu)$ $(1 - \mu^2)(\lambda - \mu)^\nu d\mu$	$\frac{4}{15}\lambda^3 + \frac{28}{15}\lambda$	$\frac{4}{15}\lambda^4 + \frac{128}{105}\lambda^2 - \frac{4}{15}$	$\frac{4}{15}\lambda^5 + \frac{24}{35}\lambda^3 - \frac{4}{105}\lambda$		
$\int (1 - \mu^2)(\lambda + \mu)^2$ $\cdot(\lambda - \mu)^\nu d\mu$	$\frac{4}{3}\lambda^2 + \frac{12}{15}\lambda$	$\frac{4}{3}\lambda^4 - \frac{4}{35}$	$\frac{4}{3}\lambda^5 - \frac{8}{15}\lambda^3 + \frac{4}{35}\lambda$		
$\int (1-\mu^2)(\lambda+\mu)\cdot(\lambda-\mu)^\nu d\mu$	$\frac{4}{3}\lambda$	$\frac{4}{3}\lambda^2 - \frac{4}{15}$	$\frac{4}{3}\lambda^3 - \frac{4}{15}\lambda$	$\frac{4}{3}\lambda^4 - \frac{4}{35}$	$\frac{4}{3}\lambda^5 + \frac{8}{15}\lambda^3 - \frac{12}{35}\lambda$
$\int (1 - \mu^2)(\lambda^2\mu^2 - 1)$ $\cdot(\lambda + \mu)(\lambda - \mu)^\nu d\mu$	$\frac{4}{15}\lambda^2 - \frac{4}{3}\lambda$	$\frac{4}{15}\lambda^4 - \frac{152}{105}\lambda^2 + \frac{4}{15}$	$\frac{4}{15}\lambda^5 - \frac{152}{105}\lambda^3 + \frac{4}{15}\lambda$		
$\int (\lambda\mu - 1)(\lambda^2 - \mu^2)$ $\cdot(1 - \mu^2)d\mu$	$-\frac{4}{3}\left(\lambda^2 - \frac{1}{5}\right)$				
$\int (\lambda + \mu)^2(\lambda\mu - 1)^2$ $(\lambda - \mu)^\nu d\mu$	$\frac{2}{3}\lambda^5 - \frac{4}{5}\lambda^3 + \frac{6}{5}\lambda$	$\frac{2}{3}\lambda^6 - \frac{2}{3}\lambda^4 + \frac{46}{35}\lambda^2 - \frac{2}{5}$	$\frac{2}{3}\lambda^7 - \frac{2}{15}\lambda^5 + \frac{58}{105}\lambda^3$ $- \frac{6}{35}\lambda$		

List of Integrals (cont'd.)

	$\nu = 1$	$\nu = 2$	$\nu = 3$	$\nu = 4$
$\int_{-1}^{1} \frac{d\mu}{(\lambda-\mu)^\nu}$	$2Q_0$	$\frac{2}{\lambda^2-1} = -2Q_0'$	$\frac{2\lambda}{(\lambda^2-1)^2} = Q_0''$	$\frac{2}{3}\frac{3\lambda^2+1}{(\lambda^2-1)^3} = -\frac{1}{3}Q_0'''$
$\int \frac{\lambda+\mu}{(\lambda-\mu)^\nu}d\mu$	$4\lambda Q_0 - 2 = 4Q_1 + 2$	$\frac{4\lambda}{\lambda^2-1} - 2Q_0$ $= -2Q_0 - 4\lambda Q_0'$	$\frac{2(\lambda^2+1)}{(\lambda^2-1)^2} = 2(\lambda Q_0'' + Q_0')$ $= 2(Q_1'' - Q_0')$	$\frac{1}{3}\{-3Q_0'' - 2\lambda Q_0'''\}$ $= \frac{6\lambda^3+10\lambda}{3(\lambda^2-1)^3}$
$\int \frac{(\lambda+\mu)^2}{(\lambda-\mu)^\nu}d\mu$	$8\lambda Q_1 + 2\lambda$	$\frac{8}{\lambda^2-1} + 10 - 8\lambda Q_0$	$\frac{8\lambda}{(\lambda^2-1)^2} + 2Q_0$	$\frac{32}{3}\cdot\frac{1}{(\lambda^2-1)^3} + \frac{32}{3(\lambda^2-1)^2} + \frac{2}{\lambda^2-1}$
$\int \frac{(\lambda+\mu)^3}{(\lambda-\mu)^\nu}d\mu$	$16\lambda^3 Q_1 + 2\lambda^2 - \frac{2}{3}$	$10\lambda - 24\lambda^2 Q_0 + \frac{16\lambda^3}{\lambda^2-1}$ $= -24\lambda Q_1 + 2\lambda + \frac{16\lambda}{\lambda^2-1}$	$12\lambda Q_0 - 10 + \frac{8(\lambda^2+1)}{(\lambda^2-1)^2}$	$\frac{64\lambda}{3(\lambda^2-1)^3} + \frac{40\lambda}{3(\lambda^2-1)^2}$ $+ \frac{4\lambda}{\lambda^2-1} - 2Q_0$
$\int \frac{1-\mu^2}{(\lambda-\mu)^\nu}d\mu$	$2Q_0 - 2\lambda Q_1 = -2Q_1'(\lambda^2-1)$	$4Q_1$	$\frac{2\lambda}{\lambda^2-1} - 2Q_0 = \frac{2Q_0 - 2\lambda Q_1}{\lambda^2-1}$ $= -2Q_1'$	$\frac{4}{3(\lambda^2-1)^2} = \frac{2}{3}Q_1''$
$\int \frac{(1-\mu^2)^2}{(\lambda-\mu)^\nu}d\mu$	$(2\lambda^3 - 4\lambda)Q_1 + 2Q_0 - \frac{2}{3}\lambda$ $= (\lambda^2-1)^2 Q_0 - 4\lambda(\lambda^2-1)$ $+ 2\lambda\left(\lambda^2 - \frac{1}{3}\right)$	$8\left\{(1-\lambda^2)Q_1 + \frac{1}{3}\right\}$ $= -\frac{8}{3}Q_2'(\lambda^2-1)$	$8Q_2$	$-8Q_1 + \frac{8}{3(\lambda^2-1)} = -\frac{8}{3}Q_2'$
$\int \frac{(\lambda\mu+1)^2}{(\lambda-\mu)^\nu}d\mu$	$2\lambda^3 Q_1 + 4\lambda Q_1 + 2Q_0$	$-4\lambda^2 Q_1 - 4Q_1 - 6 + \frac{8\lambda^2}{\lambda^2-1}$	$2\lambda Q_1 + \frac{8\lambda}{(\lambda^2-1)^2}$	$\frac{32}{3(\lambda^2-1)^3} + \frac{32}{3(\lambda^2-1)^2} + \frac{2}{3(\lambda^2-1)}$
$\int \frac{(\lambda^2\mu^2-1)}{(\lambda-\mu)^\nu}d\mu$	$2\lambda^3 Q_1 - 2Q_0$	$-4\lambda^2 Q_1 + 2$	$2\lambda Q_1$	$\frac{2}{3}\frac{\lambda^2+1}{(\lambda^2-1)^2} = \frac{2}{3}\cdot\frac{1}{\lambda^2-1}$ $+ \frac{4}{3(\lambda^2-1)^2}$

List of Integrals (cont'd.)

	$\nu = 1$	$\nu = 2$	$\nu = 3$	$\nu = 4$
$\int \frac{\lambda\mu + 1}{(\lambda - \mu)^\nu} d\mu$	$2\lambda Q_1 + 2Q_0$	$-2Q_1 + \frac{4}{\lambda^2 - 1}$	$\frac{4\lambda}{(\lambda^2 - 1)^2}$	$\frac{14}{3(\lambda^2 - 1)^2} + \frac{16}{3(\lambda^2 - 1)^2}$
$\int \frac{(\lambda\mu + 1)^2(1 - \mu^2)}{(\lambda - \mu)^\nu} d\mu$	$(1-\lambda^2)(2\lambda^2 Q_1 + 4\lambda Q_1 + 2Q_0) + \frac{2}{3}\lambda^3 + \frac{10}{3}\lambda = (-2\lambda^5 - 2\lambda^3 + 2\lambda)Q_1 + 2Q_0 + \frac{2}{3}\lambda^3 + \frac{4}{3}\lambda$	$\frac{8}{3}(\lambda^2+1)(3\lambda^2 Q_1 - 1) - \frac{4}{3} = (8\lambda^4 + 8\lambda^2)Q_1 - \frac{8}{3}\lambda^2 - 4$	$-12\lambda^3 Q_1 - 10\lambda Q_1 + 4\lambda - 2Q_0 + \frac{8\lambda}{\lambda^2 - 1}$	$8\lambda^2 Q_1 + 4Q_1 - \frac{8}{3} - \frac{8}{3(\lambda^2 - 1)} + \frac{16}{3(\lambda^2 - 1)^2}$
$\int \frac{(1 - \mu^2)(\lambda + \mu)^2}{(\lambda - \mu)^\nu} d\mu$	$-8\lambda^3 Q_1 + 8\lambda Q_1 + 4\lambda$	$(24\lambda^2 - 8)Q_1 - \frac{20}{3}$	$-26\lambda Q_1 + 2Q_0 + \frac{8\lambda}{\lambda^2 - 1}$	$12Q_1 + \frac{16}{3(\lambda^2 - 1)^2} - \frac{8}{3(\lambda^2 - 1)}$
$\int \frac{(\lambda^2\mu^2 - 1)(1 - \mu^2)}{(\lambda - \mu)^\nu} d\mu$	$(-2\lambda^5 + 2\lambda^3 + 2\lambda)Q_1 - 2Q_0 + \frac{2}{3}\lambda^3$	$(8\lambda^4 - 4\lambda^2 - 4)Q_1 - \frac{8}{3}\lambda^2$	$-12\lambda^3 Q_1 + 2\lambda Q_1 + 4\lambda + 2Q_0$	$8\lambda^2 Q_1 - \frac{8}{3} - \frac{4}{3} \cdot \frac{1}{\lambda^2 - 1}$
$\int \frac{(\lambda\mu + 1)(1 - \mu^2)}{(\lambda - \mu)^\nu} d\mu$	$-2\lambda^2 Q_1 + 2Q_0 + \frac{2}{3}\lambda$	$6\lambda^2 Q_1 + 2Q_1 - 2$	$-6\lambda Q_1 - 2Q_0 + \frac{4\lambda}{\lambda^2 - 1}$	$2Q_1 - \frac{2}{3(\lambda^2 - 1)} + \frac{8}{3(\lambda^2 - 1)^2}$
$\int \frac{(\lambda\mu + 1)(\lambda + \mu)}{(\lambda - \mu)^\nu} d\mu$	$4\lambda^2 Q_1 + 4Q_1 + 2$	$-6\lambda Q_1 - 2Q_0 + \frac{8\lambda}{\lambda^2 - 1}$	$2Q_1 + \frac{4}{\lambda^2 - 1} + \frac{8}{(\lambda^2 - 1)^2}$	$\frac{32\lambda}{3(\lambda^2 - 1)^2} + \frac{16\lambda}{3(\lambda^2 - 1)^2}$
$\int \frac{(\lambda^2\mu^2 - 1)(\lambda + \mu)(1 - \mu^2)}{(\lambda - \mu)^\nu} d\mu$	$(-2\lambda^6 + 2\lambda^4 + 2\lambda^2 - 2) \cdot 2Q_1 + \frac{4}{3}\lambda^4 - \frac{4}{15}\lambda^2 - \frac{8}{3}$	$18\lambda^5 Q_1 - 10\lambda^3 Q_1 - 10\lambda Q_1 - 6\lambda^3 + 2Q_0$	$-32\lambda^4 Q_1 + 8\lambda^2 Q_1 + 8Q_1 + \frac{32}{3}\lambda^2 + 4$	$28\lambda^2 Q_1 - 2\lambda Q_1 - \frac{28}{3}\lambda - 2Q_0 - \frac{8}{3} \cdot \frac{\lambda}{\lambda^2 - 1}$
$\int \frac{(1 - \mu^2)^2(\lambda + \mu)}{(\lambda - \mu)^\nu} d\mu$	$4(\lambda^2-1)^2 Q_1 + \frac{8}{5} - \frac{4}{3}(\lambda^2-1)$	$-18\lambda^3 Q_1 + 20\lambda Q_1 + 6\lambda - 2Q_0$	$32\lambda^2 Q_1 - 16Q_1 - \frac{32}{3}$	$-28\lambda Q_1 + 4Q_0 + \frac{16}{3} \cdot \frac{\lambda}{\lambda^2 - 1}$

List of Integrals (cont'd.)

	$\nu = 1$	$\nu = 2$	$\nu = 3$	$\nu = 4$
$\int \frac{(\lambda\mu+1)^2(1-\mu^2)(\lambda+\mu)}{(\lambda-\mu)^\nu}d\mu$	$(-4\lambda^6-4\lambda^4+4\lambda^2+4)Q_1$	$(18\lambda^5+18\lambda^3-2\lambda)Q_1-6\lambda^3$	$(-32\lambda^4-28\lambda^2-4)Q_1$	$28\lambda^3Q_1+18\lambda Q_0-\frac{28}{3}\lambda+2Q_0$
	$+\frac{4}{3}\lambda^4+\frac{12}{5}\lambda^2-\frac{8}{3}$	$-\frac{28}{3}\lambda-2Q_0$	$+\frac{32}{3}\lambda^2+\frac{16\lambda^2}{\lambda^2-1}$	$-\frac{40}{3}\cdot\frac{\lambda}{\lambda^2-1}+\frac{32}{3}\cdot\frac{\lambda}{(\lambda^2-1)^2}$
$\int \frac{(\lambda\mu+1)^2(\lambda+\mu)}{(\lambda-\mu)^\nu}d\mu$	$(4\lambda^4+8\lambda^2+4)Q_1+2-\frac{2}{3}\lambda^2$	$-10\lambda^3Q_1-12\lambda Q_1+4\lambda$	$-8\lambda^2-6+\frac{8(\lambda^2+1)}{(\lambda^2-1)^2}$	
		$-2Q_0+\frac{16\lambda}{\lambda^2-1}$	$+8\lambda^3Q_0+4\lambda Q_0$	
$\int \frac{(\lambda+\mu)^3(1-\mu^2)}{(\lambda-\mu)^\nu}d\mu$	$-16\lambda^4Q_1+16\lambda^2Q_1+\frac{20}{3}\lambda^2-\frac{4}{15}$	$56\lambda^3Q_1-24\lambda Q_1-\frac{52}{3}\lambda$	$-76\lambda^2Q_1+12Q_1+\frac{32}{3}$	$50\lambda Q_1-2Q_0-\frac{40}{3}\cdot\frac{\lambda}{\lambda^2-1}$
			$+\frac{16\lambda^2}{\lambda^2-1}$	$+\frac{32}{3}\cdot\frac{\lambda}{(\lambda^2-1)^2}$
$\int \frac{(1-\mu^2)(\lambda+\mu)}{(\lambda-\mu)^\nu}d\mu$	$-4\lambda^2Q_1+4Q_1+\frac{8}{3}$	$10\lambda Q_1-2Q_0$	$-8Q_1+\frac{4}{\lambda^2-1}$	
$\int \frac{(1-\mu^2)(\lambda+\mu)^2}{(\lambda-\mu)^\nu}d\mu$	$-8\lambda^3Q_1+8\lambda Q_1+4\lambda$			
$\int \frac{(\lambda+\mu)^3(\lambda\mu-1)^2}{(\lambda-\mu)^\nu}d\mu$	$(1-\lambda^2)^2\cdot 16\lambda^2Q_1-\frac{14}{3}\lambda^4$	$(-56\lambda^5+80\lambda^3-24\lambda)Q_1$	$(76\lambda^4-72\lambda^2+12)Q_1$	$(-50\lambda^3+28\lambda)Q_1-2Q_0$
	$+\frac{104}{15}\lambda^2-\frac{2}{3}$	$+\frac{58}{3}\lambda^3-\frac{46}{3}\lambda$	$-\frac{74}{3}\lambda^2+10$	$+\frac{16\lambda}{3(\lambda^2-1)}+\frac{52\lambda}{3}.$

TABLE XI. *List of Integrals*

	$R > a^2$	$R < a$
$\int_{\lvert R-a \rvert}^{R+a} db$	$2a$	$2R$
$\int b^2 db$	$2a\left(R^2 + \frac{a^2}{3}\right)$	$2R\left(a^2 + \frac{R^2}{3}\right)$
$\int b^4 db$	$2a\left(R^4 + 2a^2R^2 + \frac{1}{5}a^4\right)$	$2R\left(a^4 + 2R^2a^2 + \frac{1}{5}R^4\right)$
$\int \frac{db}{b^2}$	$\frac{2a}{R^2 - a^2}$	$\frac{2R}{a^2 - R^2}$
$\int \frac{db}{b^4}$	$2a\frac{(R^2 + a^2/3)}{(R^2 - a^2)^3}$	$2R\frac{(a^2 + R^2/3)}{(a^2 - R^2)^3}$
$\int \sin^2\theta_b db$ $= \int a^2 \sin^2\theta_a \cdot db/b^2$	$\frac{4a^3}{3R^2}$	$\frac{4}{3}R$
$\int \sin^2\theta_b \cdot b^2 db$ $= \int a^2 \sin^2\theta_a db$	$\frac{4a^3}{3R^2}\left(R^2 - \frac{a^2}{5}\right)$	$\frac{4}{3}R\left(a^2 - \frac{R^2}{5}\right)$
$\int \sin^2\theta_b \cdot \frac{db}{b^2}$ $= \int a^2 \sin^2\theta_a \cdot \frac{db}{b^4}$	$\frac{4}{3}\frac{a^3}{R^2}\cdot\frac{1}{R^2 - a^2}$	$\frac{4}{3}R\cdot\frac{1}{a^2 - R^2}$
$\int \sin^4\theta_b db$ $= \int a^2 \sin^2\theta_a \sin^2\theta_b \cdot \frac{db}{b^2}$	$\frac{16}{15}\frac{a^5}{R^4}$	$\frac{16}{15}R$
$\int \frac{a^2\cos^2\theta_a}{b^2} db$	$\frac{2a}{R^2 - a^2}\cdot\frac{a^2}{3R^2}\cdot(2a^2 + R^2)$	$\frac{2R}{a^2 - R^2}\cdot\frac{1}{3}(a^2 + 2R^2) = \frac{2}{3}R + \frac{2R^3}{a^2 - R^2}$
$\int P_2(\cos\theta_a)\cdot\frac{db}{b^2}$	$\frac{2a}{R^2 - a^2}\cdot\frac{a^2}{R^2}$	$\frac{2R}{a^2 - R^2}\cdot\frac{R^2}{a^2}$
$\int \frac{a^2\cos^2\theta_a \sin^2\theta_b}{b^2} db$	$\frac{4a^5}{3R^4}\left(\frac{R^2 + 4a^2}{5(R^2 - a^2)}\right)$	$\frac{4}{3}R\cdot\frac{a^2 + 4R^2}{5(a^2 - R^2)} = \frac{4}{15}R + \frac{4}{3}\frac{R^3}{a^2 - R^2}$
$\int \cos^2\theta_b db$	$2a - \frac{4a^3}{3R^2}$	$2R - \frac{4}{3}R = \frac{2}{3}R$
$\int \cos^2\theta_a db$	$\frac{2a}{3R^2}\left(\frac{2}{5}a^2 + R^2\right)$	$\frac{2}{3}\cdot\frac{R}{a^2}\left(\frac{2}{5}R^2 + a^2\right)$
$\int P_2(\cos\theta_a) db$	$\frac{2}{5}\frac{a^3}{R^2}$	$\frac{2}{5}\frac{R^3}{a^2}$
$\int a^2 \sin\theta_a \sin\theta_b \cdot \cos\theta_a \cos\theta_b \cdot \frac{db}{b^2}$	$-\frac{16}{15}\frac{a^5}{R^4}$	$+\frac{4}{15}R$
$\int \frac{ab\cos\theta_a \cos\theta_b}{b^2} db$	$-\frac{4a^3}{3R^2}$	$+\frac{2}{3}R$
$\int \frac{a^2\cos^2\theta_a \cos^2\theta_b}{b^2} db$	$\frac{2}{3}\frac{a^3}{R^2 - a^2} + \frac{16}{15}\frac{a^5}{R^4}$	$\frac{2}{3}\frac{Ra^2}{a^2 - R^2} - \frac{4}{15}R$
$\int \frac{a^2 \sin^2\theta_a \cos^2\theta_b}{b^2} db$	$\frac{4}{3}\frac{a^3}{R^2} - \frac{16}{15}\frac{a^5}{R^4}$	$\frac{4}{15}R$
$\int \frac{a^2\cos^2\theta_b}{b^2} db$	$\frac{2}{3}\frac{a^3}{R^2 - a^2} + \frac{4}{3}\frac{a^3}{R^2}$	$\frac{2}{3}\frac{Ra^2}{a^2 - R^2}$

TABLE XII. *Numerical Results*

			3	4	5	6	7	8	9	10
I	(a)	$(\kappa^5/2\pi)\int a^2 \sin^2\theta_a e^{-\kappa a}(\Gamma_5/\kappa b)dv$	154.0	137.0	121.4	108.0	96.8	87.1	79.0	72.1
	(b)	$(\kappa^5/2\pi)\int a^2 \sin^2\theta_a e^{-\kappa a}[\Gamma_5(\kappa b)/\kappa b - \Gamma_4(\kappa b)]dv$	26.8	17.7	10.9	6.5	3.7	2.0	1.1	0.6
	(c)	$(\kappa^5/2\pi)\int a^2 \sin^2\theta_a e^{-\kappa a} g_{5,1}dv$	127.2	119.3	110.5	101.5	93.1	85.1	77.9	71.5
II	(a)	$(\kappa^5/2\pi)\int a^2 \cos^2\theta_a e^{-\kappa a}(\Gamma_5/\kappa b)dv$	103.1	94.6	83.6	72.6	62.9	54.6	48.0	42.6
	(b)	$(\kappa^5/2\pi)\int a^2 \cos^2\theta_a e^{-\kappa a}[\Gamma_5(\kappa b)/\kappa b - \Gamma_4(\kappa b)]dv$	36.7	31.0	23.3	16.1	10.4	6.4	3.8	2.1
	(c)	$(\kappa^5/2\pi)\int a^2 \cos^2\theta_a e^{-\kappa a} g_{5,1}dv$	66.4	63.6	60.3	56.5	52.5	48.8	44.2	40.5
III	(a)	$(\kappa^5/2\pi)\int a^2 \sin^2\theta_a e^{-\kappa a} P_2(\cos\theta_b)[\Gamma_7/(\kappa b)^3]dv$	4.9	26.3	32.2	31.1	27.0	22.6	18.4	15.0
	(b)	$(\kappa^5/2\pi)\int a^2 \sin^2\theta_a e^{-\kappa a} P_2(\cos\theta_b)[\Gamma_7(\kappa b)/(\kappa b)^2 - (\kappa b)^2\Gamma_2(\kappa b)]dv$	−0.8	13.6	15.6	12.1	8.2	5.0	2.7	1.7
	(c)	$(\kappa^5/2\pi)\int a^2 \sin^2\theta_a e^{-\kappa a} P_2(\cos\theta_b) g_{7,3}dv$	5.7	12.7	16.6	19.0	18.8	17.6	15.7	13.3
IV	(a)	$(\kappa^5/2\pi)\int a^2 \cos^2\theta_a e^{-\kappa a} P_2(\cos\theta_b)[\Gamma_7/(\kappa b)^2]dv$	−91.4	−37.0	1.3	19.1	24.2	22.8	19.1	15.3
	(b)	$(\kappa^5/2\pi)\int a^2 \cos^2\theta_a e^{-\kappa a} P_2(\cos\theta_b)[\Gamma_7(\kappa b)/(\kappa b)^3 - (\kappa b)^2\Gamma_2(\kappa b)]dv$	−97.5	−44.0	−7.0	9.6	13.5	11.8	8.6	5.6
	(c)	$(\kappa^5/2\pi)\int a^2 \cos^2\theta_a e^{-\kappa a} P_2(\cos\theta_b) g_{7,3}dv$	6.1	7.0	8.3	9.5	10.7	11.0	10.5	9.7
V	(a)	$-(\kappa^5/2\pi)\int a^2 \sin\theta_a\cos\theta_a\sin\theta_b\cos\theta_b e^{-\kappa a}[\Gamma_7/(\kappa b)^3]dv$	38.0	42.1	34.4	24.7	16.7	11.0	7.2	4.7
	(b)	$-(\kappa^5/2\pi)\int a^2 \sin\theta_a\cos\theta_a\sin\theta_b\cos\theta_b e^{-\kappa a}[\Gamma_7/(\kappa b)^3 - g_{7,3}]dv$	41.6	41.5	31.6	20.6	12.4	7.0	3.8	2.0
	(c)	$-(\kappa^5/2\pi)\int a^2 \sin\theta_a\cos\theta_a\sin\theta_b\cos\theta_b e^{-\kappa a} g_{7,5}dv$	−3.6	0.6	2.8	4.1	4.3	4.0	3.4	2.7
VI	(a)	$(\kappa^5/2\pi)\int a^2 \sin^2\theta_a \sin^2\theta_b e^{-\kappa a}[\Gamma_7/(\kappa b)^3]dv$	229.	131.0	73.1	41.3	23.7	13.9	8.4	5.2
	(b)	$(\kappa^5/2\pi)\int a^2 \sin^2\theta_a \sin^2\theta_b e^{-\kappa a}[\Gamma_7/(\kappa b)^3 - g_{7,3}]dv$	190.9	100.0	49.9	24.5	11.7	5.5	2.6	1.2
	(c)	$(\kappa^5/2\pi)\int a^2 \sin^2\theta_a \sin^2\theta_b e^{-\kappa a} g_{7,3}dv$	38.1	31.0	23.2	16.8	12.0	8.4	5.8	4.0

$$i_1 = (\kappa/384)[Ic - (\tfrac{1}{5})\mathrm{III}c]$$

$$i_3 = (\kappa/384)[Ic + (\tfrac{2}{5})\mathrm{III}c] = (\kappa/192)[\mathrm{II}c - (\tfrac{1}{5})\mathrm{IV}c]$$

$$i_9 = (\kappa/192)[IIc + (\tfrac{2}{5})\mathrm{IV}c]$$

$$i_5 = -\kappa \mathrm{V}c/640 \quad i_7 = -\kappa \mathrm{VI}c/1280$$

TABLE XIII

α	$\alpha=3$	4	5	6	7	8	9	10
i_1/κ	0.332	0.303	0.280	0.255	0.232	0.213	0.195	0.179
i_3/κ	.338	.324	.305	.285	.262	.241	.220	.200
i_9/κ	.359	.346	.332	.315	.296	.278	.252	.231
i_5/κ	−.0056	+.0009	+.0044	+.0064	+.0067	+.0062	+.0053	+.0042
i_7/κ	−.0312	−.0242	−.0181	−.0131	−.0094	−.0066	−.0045	−.0031

$$I_1 = 2\kappa/\alpha - 4c_1^2 \int e^{-\kappa a} a^2 \sin^2\theta_a (1/\kappa b)dv = \kappa[2/\alpha + i_1/\kappa - (\mathrm{I}a)/192]$$

$$I_3 = 2\kappa/\alpha - 2\int dv a_0^2/b - 2\int dv a_1^2/b + i_3 = \kappa[2/\alpha + i_3/\kappa - (\mathrm{II}a)/192 - (\mathrm{I}a)/384]$$

$$I_9 = 2\kappa/\alpha - 4\int dv a_0^2/b + i_9 = \kappa[2/\alpha + i_9/\kappa - (\mathrm{II}a)/96]$$

$$I_5 = i_5, \quad I_7 = i_7, \quad I_6 = i_6, \quad I_8 = i_8, \quad I_{11} = i_{11} \cong -i_6$$

$$I_2 = 2\kappa S_{11}/\alpha - 4(S_{11})^{1/2}\int dv a_1 b_1/b + i_2$$

$$I_4 = 2\kappa S_{10}/\alpha - 2(S_{00})^{1/2}\int dv a_1 b_1/b - 2(S_{11})^{1/2}\int dv a_0 b_0/b + i_4$$

$$I_{10} = 2\kappa S_{00}/\alpha - 4(S_{00})^{1/2}\int dv a_0 b_0/b + i_{10}$$

The resulting integrals, after the small quantities before mentioned have been neglected, are listed in Table XIV. The relative energies are given in Table XV, and plotted in Fig. 1.

TABLE XIV. *Integrals.*

α	$\alpha=3$	4	5	6	7	8	9	10
I_1/κ	0.196	0.088	0.047	0.025	0.013	0.009	0.005	0.003
I_3/κ	.068	−.026	−.046	−.042	−.032	−.021	−.014	−.010
I_9/κ	−.043	−.140	−.140	−.110	−.067	−.042	−.026	−.013
I_5/κ	−.006	+.0007	.0044	.0064	.0067	.0062	.0053	.0042
I_7/κ	−.031	−.0240	−.0181	−.0131	−.0094	−.0066	−.0045	−.0031
I_2/κ	.082	.005	−.0217	−.0183	−.0139	−.0086	−.006	−.0028
I_4/κ	.074	.009	.0198	.0173	.0161	.0126	.0103	.0060
I_{10}/κ	.096	.070	.035	.032	.017	.0081	.0035	.0021
I_6/κ	−.043	−.030	−.039	−.028	−.021	−.015	−.010	−.006
I_8/κ		.01	.01	.007	.005			

TABLE XV. *Relative energies.*

α	$\alpha=3$	4	5	6	7	8	9	10
$^3\Sigma_u^+/\kappa$		.100	.064	.032	.015			
$^3\Delta_u/\kappa$	.329	.162	.103	.056	.032	.019	.0118	.0062
$^1\Sigma_u^-/\kappa$		.225	.142	.081	.048			
$^3\Sigma_g^-/\kappa$		.074	.026	.012	.003			
$^1\Delta_g/\kappa$	.167	.063	.0188	.006	−.001	−.001	−.001	0
$^1\Sigma_g^+/\kappa$		.053	.011	−.0005	−.0042			
$^3\Pi_g/\kappa$	.137	.010	.009	−.003	−.002			
$^3\Pi_u/\kappa$	.05	−.002	−.027	−.024	−.018	−.012	−.009	−.006
$^1\Pi_g/\kappa$	.065	−.042	−.059	−.053	−.033	−.019	−.010	−.006
$^1\Pi_u/\kappa$	−.06	−.076	−.110	−.087	−.069	−.050	−.037	−.025
$^1\Sigma_g^+/\kappa$	.04	−.07	−.11	−.079	−.054	−.036	−.023	−.011
$^3\Sigma_u^+/\kappa$	−.18	−.22	−.177	−.146	−.102	−.057	−.033	−.017

DISCUSSION

Fig. 1 shows the relative energies plotted as a function of the internuclear distance. The lowest term,[8] for intermediate values of κR, is the $^3\Sigma_u^+$. For hydrogen, we may set $\kappa=1$, and the minimum of this curve lies at about 2.0A. The value of the heat of dissociation is 2.9 volts, approximately.

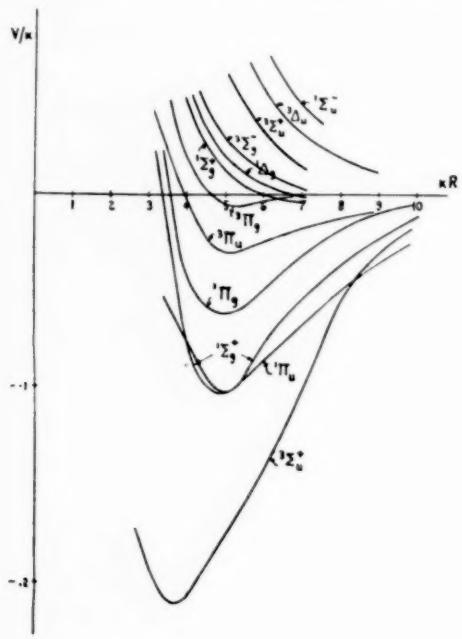

Fig. 1. Relative energies.

It is not possible to say, to the degree of approximation used here, whether the $^3\Pi_g$ state has a weak minimum or is repulsive. For the same reason, the relative positions of $^1\Sigma_g^+$ and $^1\Pi_u$ may actually be somewhat different. The

[8] This result has been predicted for B_2 by J. E. Lennard-Jones, Trans. Faraday Soc. **25**, 681 (1929).

reason for this uncertainty lies partly in the fact that we have neglected $i_6^{(3)}$ and $i_6^{(4)}$, and partly in the low degree of accuracy to which s_2 may be given.

Apart from these minor details, it is safe to assert that the curves do represent the interaction of two hydrogen-like atoms, each with one $2p$ electron, insofar as this interaction is to be found by a first order perturbation calculation of the Kemble and Zener type.

Heisenberg[9] has shown that there is reason to believe that the behavior of ferromagnetic substances may some day be understood, when it becomes possible to carry through detailed calculations. A necessary condition for ferromagnetism seems to be that the exchange integral for the lowest states be positive. This was found to be likely for $n \geqq 3$, where n is the principal quantum number. From our results, it is seen that a positive exchange energy integral is obtained for $n=2$, $l=1$, so that the possibility of ferromagnetism does not seem to be governed by the principal quantum number in so simple a fashion. The sufficient conditions for ferromagnetism have yet to be given.

One also sees from the curves in the figure that the "Coulomb" integrals are in general more important than the "exchange" integrals. The states arising from $m_{la}=0$, $m_{lb}=0$ lie the lowest, those from $m_{la}=0$, $m_{lb}=\pm 1$ are next higher, and those from $m_{la}=\pm 1$, $m_{lb}=\pm 1$ are highest. This means that the most stable configuration is that in which there is the maximum overlapping of charge, in accordance with the ideas of Slater[10] on directed valency. Orbital valency may be associated with the "Coulomb" integrals, and spin valency with the exchange integrals. The latter concept may, however, be misleading.

Though this analysis is strictly applicable only to the case where two excited hydrogen atoms interact (leaving out of account the influence of the s orbits) one might expect that similar conditions would obtain for boron, or excited lithium. Unfortunately, the band spectrum of B_2 has not been analyzed, so that a direct check of the theory is wanting. The inner s electrons would probably have some influence, but whether the order of the energy levels would be affected or not is open to question.

In conclusion, I wish to express may deep appreciation to the many people with whom the problem has been discussed. It was suggested by Professor Heisenberg, whom I also wish to thank for his help on previous problems. Acknowledgment must also be made to Dr. Dirac for discussion of allied problems. The work was continued at the Eigenössische Technische Hochschule, Zürich, and completed in Urbana. Thanks are due Mr. W. H. Furry for assistance in checking part of the calculations.

Note added to proof, Feb. 17, 1931: The influence of the inner $2s$ electrons is now being studied, and will be made the subject of a later paper.

[9] W. Heisenberg, Zeits. f. Physik **49**, 619 (1928).

[10] J. C. Slater, American Physical Society meeting, Dec. 29, 1930, paper 17.

THE MASS ABSORPTION COEFFICIENT OF THE *K* SHELL ACCORDING TO THE DIRAC RELATIVISTIC THEORY OF THE ELECTRON*

By Louis C. Roess
Cornell University

(Received January 19, 1931)

Abstract

Taking as model an atom containing two non-interacting electrons and a fixed nucleus with charge Ze, the mass absorption coefficient is calculated by use of the proper functions of the Dirac relativistic equation. Z is determined so as to make the lowest energy level agree with the experimental value determined from the K absorption edge. The numerical calculation presented difficulty because of lack of tables of complex gamma functions. The relativistic coefficient is found to be from 0 to 40 percent smaller than the non-relativistic coefficient calculated by Nishina and Rabi, the greatest difference occurring for the heavy elements and short wave-lengths; it agrees slightly worse with experiment than the non-relativistic coefficient. The difference between theory and experiment is least for the heavy atoms, as would be expected, since for the heavy atoms (large Z) the neglected electronic interaction-field is small in comparison with the nuclear field. The variation of the relativistic coefficient with wave-length is complicated, but in the range $\frac{1}{2}\lambda_k$ to λ_k (λ_k = wave-length of K absorption edge) it is more nearly linear with λ^3 than the non-relativistic coefficient. The importance of using the relativistic equation for heavy atoms and short x-ray wave-lengths is emphasized by these results, which also show that the model chosen is too approximate, even for the heavy elements.

The general normalizing factors for the discrete and continuous spectrum proper functions of a hydrogen-like atom are given.

Inroduction and Results

SEVERAL attempts[1] have been made, with classical or semi-classical theories, to calculate the atomic absorption coefficient for the K shell. More recently Wentzel[2] and Oppenheimer[3] obtained approximate formulae using non-relativistic quantum mechanics, while Nishina and Rabi[4] have given the explicit formula which follows from the Schrödinger theory. The comparison with experiment made by the latter authors shows fairly good agreement for the heavy elements and poor agreement for the light elements.

The purpose of the present paper is to calculate the mass absorption coefficient by use of the Dirac relativistic equation, and to compare the results

* Abridged Cornell Dissertation. Presented at the Cleveland Meeting of the American Physical Society, Dec. 30–31, 1930.

[1] J. J. Thomson, Conduction of Electricity. Through Gases, 2d Ed., p. 321; L. de Broglie, Journ. de Phys. et Rad. **3,** 33, (1922); A. H. Compton, Nat. Res. Council, Bul. **20,** 37, (1922); H. A. Kramers, Phil. Mag. **46,** 836, (1923).

[2] G. Wentzel, Zeits. f. Physik **40,** 574, (1926).

[3] J. R. Oppenheimer, Zeits. f. Physik **41,** 268, (1926).

[4] Y. Nishina and I. I. Rabi, Verh. d. deut. Phys. Ges. **9.** 6, (1928).

with experiment and with the non-relativistic theory. One can readily see from correspondence principle arguments that for the K electrons of the heavy atoms the relativity corrections should be important, and this is confirmed by the results.

The atom model used here as in the non-relativistic calculations consists of two non-interacting electrons in the field of a fixed nucleus with charge

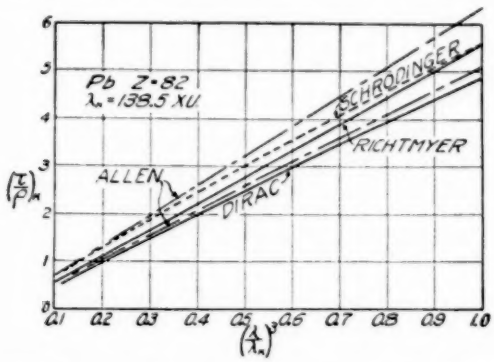

Fig. 1. The mass absorption coefficient for lead. The curves marked Allen and Richtmyer are plots of the experimental data.[7]

Z^*e, where Z^* is that charge (smaller than the true charge Z) which makes the lowest energy level of the atom model agree with the experimental value. It is obvious that this model will be most nearly correct when the interaction of the K electrons with the nucleus is large compared with their interaction with each other and with the outer electrons, i.e., for the heavy elements.

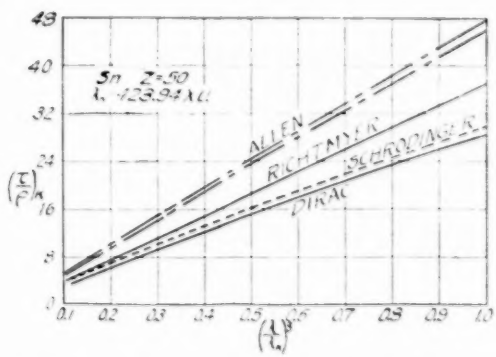

Fig. 2. The mass absorption coefficient for tin. The curves marked Allen and Richtmyer are plots of the experimental data.[7]

The calculation proceeds as follows: by use of the Dirac radiation theory[5] combined with the Dirac relativistic equation[6] the general formula for the absorption probability is derived. This formula contains a certain matrix element which is then evaluated for the case of the transition between the K

[5] P. A. M. Dirac, Roy. Soc. Proc. **A114,** 243 and 710, (1927).
[6] P. A. M. Dirac, Roy. Soc. Proc. **A117,** 610, (1928).

level and a state of the continuous spectrum corresponding to the removal of one of the K electrons. The resulting formula for the mass absorption coefficient of the K shell is then calculated numerically. The last two operations constitute what is new in the paper. The final formula is quite complicated so that the numerical calculation is very laborious, especially because of lack of tables of the gamma function of complex argument.

The results of the present calculation are collected in the Table I and Figs. 1–3. The relativistic theory gives values of the absorption coefficient which are consistently lower than those of the non-relativistic theory, the difference varying from about 40 percent for Pb at $\frac{1}{2}\lambda_k$ to less than 1 percent for Al at λ_k. The calculated absorption coefficients for Al cannot be compared with experiment because of lack of data for the long wave-lengths, but show how closely the two quantum-mechanical theories agree for the light elements.

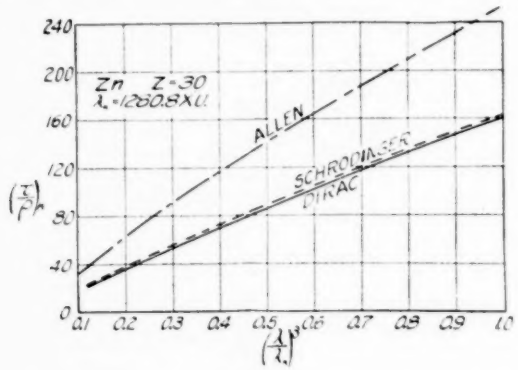

Fig. 3. The mass absorption coefficient for zinc. The curve marked Allen is a plot of the experimental data.[7]

It is found experimentally[7] that the mass absorption coefficient varies linearly with λ^n where n ranges from 2.9 to 3 and apparently changes in value with the wave-length. The classical and semi-classical theories referred to above all give a linear variation with λ^3. The quantum-mechanical theories predict a more complicated variation with λ, the non-relativistic theory indicating an exponent[8] 2.87 at $\lambda=\frac{1}{2}\lambda_k$ and 8/3 at $\lambda=\lambda_k$(λ_k=wave-length of K edge). The relativistic theory here developed gives an exponent which is somewhat closer to three for the heavy elements over the range $\frac{1}{2}\lambda_k$ to λ_k. For example, for Pb the exponent is 2.86 at $\lambda=\lambda_k$ and 3.13 at $\lambda=\frac{1}{2}\lambda_k$. For the light elements the two theories agree closely for wave-lengths which are not too short.

There are a number of reasons, aside from the inadequacy of the model, for the disagreement between theory and experiment.[9] In the first place, the

[7] F. K. Richtmyer, Phys. Rev. **27,** 1, (1926); **30,** 755, (1927). S. J. M. Allen, Phys. Rev. **28,** 907, (1926).

[8] As pointed out to me by Professor Kennard, the expression of the theoretical results in terms of these exponents is misleading, since the relation given by the quantum mechanics may be written $C(\lambda)\lambda^{n(\lambda)}$, not $K\lambda^{n(\lambda)}$ (K independent of λ).

[9] I wish to thank Professor F. K. Richtmyer for helpful discussions on these points.

TABLE I. *Mass absorption coefficient* $(\tau/\rho)_K$.

λ in X.U.†	λ_k/λ	Calculated Dirac	Calculated Schröd-inger	Percent Differ-ence††	Observed Richt-myer[7]	Observed Allen[7]	Expon-ent of λ (calc.)
			Pb $Z=82$				
138.5	1.0	4.86	5.58	14.6	5.56	5.10 to 6.35	2.86
125.9	1.1	3.70	4.32	16.9	4.18	3.76 to 4.79	
115.4	1.2	2.85	3.41	19.8	3.22	3.00 to 3.72	
106.5	1.3	2.24	2.75	22.6	2.53	2.35 to 2.95	
98.9	1.4	1.79	2.24	25.4	2.03	1.89 to 2.37	
92.3	1.5	1.44	1.85	28.1	1.65	1.53 to 1.93	
86.6	1.6	1.18	1.55	30.0	1.36	1.26 to 1.62	
81.5	1.7	0.97	1.30	33.9	1.13	1.06 to 1.36	
76.9	1.8	0.81	1.11	37.0	0.95	0.89 to 1.15	
72.9	1.9	0.68	0.95	40.1	0.81	0.77 to 0.98	
69.3	2.0	0.58	0.82	42.8	0.70	0.65 to 0.86	3.13
			Sn $Z=50$				
423.94	1.0	28.5	29.8	4.6	37.0	45.9 to 47.7	2.75
385.40	1.1	21.9	23.1	5.5	27.8	34.7 to 36.1	
353.28	1.2	17.2	18.2	6.3	21.4	26.9 to 28.0	
326.11	1.3	13.7	14.7	7.4	16.9	21.4 to 22.2	
302.81	1.4	11.0	12.0	8.4	13.5	17.2 to 17.9	
282.63	1.5	9.03	9.89	9.5	11.0	13.9 to 14.6	
264.96	1.6	7.48	8.26	10.4	9.02	11.5 to 12.1	
249.38	1.7	6.24	6.97	11.7	7.52	9.6 to 10.2	
235.52	1.8	5.26	5.93	12.8	6.34	8.0 to 8.5	
223.13	1.9	4.47	5.09	14.0	5.39	6.9 to 7.4	
211.97	2.0	3.82	4.40	15.2	4.62	5.9 to 6.3	2.96
			Zn $Z=30$				
1280.8	1.0	161	163	1.5	..	254	2.67
1164.4	1.1	125	127	1.3	..	199	
1067.3	1.2	98.2	100	1.9	..	181	
985.2	1.3	78.5	80.4	2.4	..	130	
914.9	1.4	63.9	65.6	2.7	..	107	
853.9	1.5	52.6	54.2	3.2	..	90	
800.5	1.6	43.8	45.3	3.5	..	76	
753.4	1.7	37.0	38.2	3.3	..	64	
711.6	1.8	31.2	32.6	4.4	..	54	
674.1	1.9	26.6	27.9	5.1	..	46	
640.4	2.0	22.9	24.2	5.4	..	40	2.87
			Al $Z=13$				
7947.0	1.0	2453	2459	0.3	..	..	2.67
7224.5	1.1	1905	1905	0.0	..	..	
6622.5	1.2	1493	1505	0.8	..	..	
6113.1	1.3	1205	1210	0.4	..	..	
5675.4	1.4	987	987	0.0	..	..	
5298.0	1.5	811	816	0.5	..	..	
4966.9	1.6	677	682	0.7	..	..	
4674.7	1.7	571	575	0.8	..	..	
4415.0	1.8	485	490	0.9	..	..	
4182.6	1.9	416	420	1.0	..	..	
3973.5	2.0	359	363	1.2	..	..	2.87

† The values of λ_K are taken from the article by Grebe in Geiger-Scheel's Handb. d. Phys, XXI, p. 336.

†† The percent difference is calculated from the Dirac value as base.

true absorption coefficient is not measured experimentally, since scattering is always present. The scattering coefficient, though small in comparison with the true absorption coefficient over the range $\frac{1}{2}\lambda_k$ to λ_k, varies in an un-

known[10] manner with the wave-length. In the second place, the experimenter measures the absorption coefficient for all the electrons in the atom, so that one must extrapolate the absorption curve for the $L+M+N+\cdots$ electrons down to wave-lengths below the K edge and then subtract this from the total absorption in this range to get the absorption coefficient for the K electrons. Such an extrapolation, while it may introduce only a small error in the magnitude of the absorption coefficient, can easily change its variation with wave-length. Finally, even an exact model of an *isolated* atom would be incorrect, since the experimental measurements are usually made upon atoms in crystals. In the writer's opinion the above effects are not large enough to account for the discrepancy which, as already suggested by Nishina and Rabi,[4] must be due to the inadequate model. The results obtained here show clearly that for the K shell of the heavy elements the relativistic theory must be used in conjunction with the correct model.

It should be possible to use a much better model for which the discrete proper functions are obtained by the variational method which has recently been used with such success, but how one can obtain more nearly correct proper functions for the continuous spectrum remains a difficult problem.

The Probability of Absorption

According to Dirac[6] the motion of an electron in an electromagnetic field with the vector potential $\boldsymbol{A}$ and scalar potential V is described by the wave-equation

$$\left[\frac{W+eV}{c}+\rho_1\boldsymbol{\sigma}\left(\boldsymbol{p}+\frac{e}{c}\boldsymbol{A}\right)+\rho_3 mc\right]\psi=0, \tag{1}$$

in which W is the energy parameter, $\boldsymbol{p}$ the momentum vector-operator with components $(h/2\pi i)(\partial/\partial x),\cdots$, and ρ_1, ρ_3, and $\boldsymbol{\sigma}$ are certain matrices having four rows and columns. The probability amplitude ψ is also a matrix having four rows and only one column. We shall let V represent the field of the fixed nucleus, and choose the vector potential $\boldsymbol{A}$ of the external field so that its scalar potential vanishes.

From Eq. (1) we obtain for the Hamiltonian function of the electron

$$H_e = H_0 - e\rho_1\boldsymbol{\sigma}\boldsymbol{A}$$

with

$$H_0 = -c\rho_1\boldsymbol{\sigma}\cdot\boldsymbol{p}-\rho_3 mc^2-eV. \tag{2}$$

H_0 is the Hamiltonian for the motion in the nuclear field alone. We now suppose the electromagnetic field to be quantized according to the Dirac[5] scheme, and obtain with Waller,[11] taking retardation into account, the following Hamiltonian for the system atom plus field:

$$H = H_0+\sum_r N_r h\nu_r - \sum_r \rho_1(\boldsymbol{\sigma}\mathfrak{u}_r)\left\{N_r^{1/2}e^{2\pi i/h[\Theta_r-(\mathfrak{K}_r\mathfrak{x}_s)]}+e^{-2\pi i/h[\Theta_r-(\mathfrak{K}_r\mathfrak{x})]}N_r^{1/2}\right\} \tag{3}$$

[10] This variation is very difficult to determine experimentally. For the most recent data see E. N. Coade, Phys. Rev. **36**, 1109, (1930).

[11] I. Waller, Zeits. f. Physik **58**, 75, (1929).

where N_r and Θ_r are operators which obey the relation

$$N_r e^{2\pi i\Theta_r/h} - e^{2\pi i\Theta_r/h} N_r = e^{2\pi i\Theta_r/h},$$

$\mathbf{x}$ is a vector with origin at the nucleus which gives the position in space, and

$$\mathfrak{y}_r = \left(\frac{e^2 h\nu_r}{2\pi c\sigma_r}\right)^{1/2} \mathbf{r}; \quad \kappa_r = \frac{h\nu_r}{c}\mathbf{n}_r, \tag{3'}$$

where $\sigma_r d\nu_r d\omega_r$ is the number of components r of the radiation field with given polarization $\mathbf{r}$ in the frequency interval $d\nu_r$ and with direction of motion in the element of solid angle $d\omega_r$ about $\mathbf{n}_r$.

If the stationary states of the atom are specified by the J''s, while N_r' is the number of photons in the component r, we obtain from the general transformation theory the Schrödinger equation corresponding to the Hamiltonian (3)[12]

$$\begin{aligned}\left[\frac{h}{2\pi i}\frac{\partial}{\partial t} + W(J'') + \sum_r N_r' h\nu_r\right]\Phi(J''; N_1', \cdots, N_r' \cdots) \\ = \sum_{J'} \sum_s \mathfrak{y}_s [N_s'^{1/2}\mathbf{A}^s(J''J')\Phi(J'; N_1' \cdots N_{s-1}', N_s' - 1, N_{s+1}' \cdots) \\ + (N_s' + 1)^{1/2}\mathbf{B}^s(J''J')\Phi(J'; N_1' \cdots N_{s-1}', N_s' + 1, N_{s+1}' \cdots)]\end{aligned} \tag{4}$$

with

$$\left.\begin{aligned}\mathbf{A}^s(J''J') &= \int \psi_{J''}^*(\mathbf{x})\rho_1 \boldsymbol{\sigma}\psi_{J'}(\mathbf{x})e^{-2\pi i(\kappa_s\cdot\mathbf{x})/h}d\mathbf{x} \\ \mathbf{B}^s(J''J') &= \int \psi_{J''}^*(\mathbf{x})\rho_1 \boldsymbol{\sigma}\psi_{J'}(\mathbf{x})e^{+2\pi i(\kappa_s\cdot\mathbf{x})/h}d\mathbf{x}\end{aligned}\right\} \tag{4'}$$

where $\psi_{J'}(\mathbf{x})$ and $W(J')$ are the characteristic function and characteristic value for the motion of the electron in the nuclear field. $|\Phi(J'; N')|^2$ gives the probability for the state $(J'; N')$ of the system, atom plus field.

In Eq. (4) the sum with respect to J' is to include an integral over the continuous spectrum if one is present. In this case the probability of finding the atom in the range $d\epsilon'$ about ϵ' is given by $|\Phi(\epsilon'; N')|^2 d\epsilon'$, where for the continuous spectrum ϵ' is used for J'.

It should be noted that the sum over J' in Eq. (4) includes the negative energy states of the atom. They do not cause difficulty in our application to absorption because here we can restrict ourselves to transitions between states having positive energy. Waller[12] has shown the importance of the negative energy states in calculating scattering and dispersion.

We want to calculate the transition probability $wd\epsilon''$ for an absorption process in which the atom jumps from an initial discrete state J' to a final state in the range $d\epsilon''$ about ϵ'' in the continuous spectrum, with absorption of a photon of definite direction (in $d\omega_s$) and definite polarization, regardless

[12] I. Waller, Zeits. f. Physik **61**, 837 (1930).

of what the final frequency state of the field may be. We suppose for the moment that the atomic states are non-degenerate.

The initial state of the field is to be taken as follows: only photons having a direction of motion within a solid angle $d\omega_s$ about n_s, a definite polarization $\mathbf{s}$, but arbitrary frequency ν_{sr}, where r expresses the variation in frequency of the component s, are to be present. For physically interesting results, the range of variation of ν_{sr} about the frequency corresponding to the atomic transition must be at least as great as the natural line breadth.

Following the well-known method,[5] we calculate the probability of the above-mentioned atomic transition with absorption of a photon of frequency ν_{sr}, and then sum over all such frequencies, obtaining finally for a time t which is large compared with the atomic period but small compared with the mean life time of the state under consideration

$$wd\epsilon'' = \frac{2\pi e^2 c^2 t}{h^2\nu^2} \left| \mathbf{s} \cdot \boldsymbol{B}^s(\epsilon''; J') \right|^2 \rho(\nu) d\omega_s d\epsilon'' \tag{5}$$

where

$$h\nu = W(\epsilon'') - W(J'), \tag{6}$$

and $\rho(\nu)$ is the spectral energy density per unit frequency range per unit solid angle for a definite polarization.

Our temporary assumption that the atomic states are non-degenerate is not true. According to the general theory of quantum mechanics, as presented by Born and Jordan,[13] when the assembly of atoms is in thermal equilibrium before the absorption process occurs, we merely add together those transition probabilities relating to transitions between the degenerate states. Therefore we obtain finally for the transition probability $wd\epsilon''$

$$wd\epsilon'' = d\omega_s \frac{2\pi e^2 c^2 t}{h^2\nu^2} \sum \left| \mathbf{s} \cdot \boldsymbol{B}^s(\epsilon''; J') \right|^2 \rho(\nu) d\epsilon'' \tag{7}$$

where the sum is to be taken over all initial states having the same energy and over all final states having the same energy.

In many practical applications we are interested in the absorption probability for arbitrary direction of motion and polarization of the absorbed photon. We can obtain this from Eq. (7) by summing over all directions of motion $d\omega_s$ and all polarizations $\mathbf{s}$. When the wave-length of the incident light is long compared with atomic dimensions, so that we can replace the exponential factor in the matrix element $\boldsymbol{B}^s$ in Eq. (4′) by unity, we can easily carry out this summation, obtaining for the absorption probability $w'd\epsilon''$ per unit time for arbitrary direction of motion and polarization of the absorbed photon

$$w'd\epsilon'' = \frac{16\pi^2 e^2 c^2}{3h^2\nu^2} \sum \left| P(\epsilon''; J') \right|^2 \rho(\nu) d\epsilon'' \tag{8}$$

[13] M. Born and P. Jordan, "Elementare Quantenmechanik," pp. 299, 321, and 329

where

$$|P|^2 = |B_x|^2 + |B_y|^2 + |B_z|^2. \tag{8'}$$

Solutions of the Dirac Equation

The solutions of Eq. (1) for the case when $\boldsymbol{A}=0$ and $V=Ze/r$ have been given by Darwin.[14] For given l and $u(=m-\frac{1}{2})$ there are two sets of solutions. We label these by introducing the quantum number j, which takes on the values $j=l\pm\frac{1}{2}$ to agree with spectroscopic notation. The two sets are:[15]

$$\begin{aligned}
j &= l+\tfrac{1}{2} & & j = l-\tfrac{1}{2} \\
\psi_1 &= -iM_\theta F_l P_{l+1}^u & & \psi_1 = -i(l+u)M_\theta F_{-l-1}P_{l-1}^u \\
\psi_2 &= -iM_\theta F_l P_{l+1}^{u+1} \quad (9a) & & \psi_2 = i(l-u-1)M_\theta F_{-l-1}P_{l-1}^{u+1} \quad (9b) \\
\psi_3 &= (l+u+1)M_\theta G_l P_l{}^u & & \psi_3 = M_\theta G_{-l-1}P_l{}^u \\
\psi_4 &= -(l-u)M_\theta G_l P_l{}^{u+1} & & \psi_4 = M_\theta G_{-l-1}P_l{}^{u+1},
\end{aligned}$$

in which M_θ is the part of the total normalizing factor associated with the angular coordinates. The radial functions F_l and G_l contain their own normalizing factor.

The function $P_l{}^u(\theta, \phi)$ is a spherical harmonic defined by Darwin as follows:

$$P_l{}^u = (l-u)!\sin^l\theta\left(\frac{d}{d\cos\theta}\right)^{l+u}\frac{(\cos^2\theta-1)^l}{2^l l!}e^{iu\phi}. \tag{10}$$

The radial functions F_l and G_l satisfy the equations

$$\begin{aligned}
\frac{2\pi}{h}\left(\frac{W+eV}{c}+mc\right)F_l + \frac{dG_l}{dr} - \frac{l}{r}G_l &= 0 \\
-\frac{2\pi}{h}\left(\frac{W+eV}{c}-mc\right)G_l + \frac{dF_l}{dr} + \frac{l+2}{r}F_l &= 0.
\end{aligned} \tag{11}$$

We shall use the solutions of Eq. (11) given by Gordon.[16] These are:

Discrete Spectrum: $W/mc^2<1$

$$\begin{aligned}
F_l &= \left(\frac{N_l-\rho_l-n_r}{N_l+\rho_l+n_r}\right)^{1/2} M_r(\sigma_1-\sigma_2) \\
G_l &= M_r(\sigma_1+\sigma_2)
\end{aligned} \tag{12}$$

$$\begin{aligned}
\sigma_1 &= (N_l+l+1)r^{\rho_l-1}e^{-k_0 r}{}_1F_1(-n_r;\ 2\rho_l+1;\ 2k_0 r) \\
\sigma_2 &= -n_r r^{\rho_l-1}e^{-k_0 r}{}_1F_1(-n_r+1;\ 2\rho_l+1;\ 2k_0 r)
\end{aligned} \tag{13}$$

[14] C. G. Darwin, Roy. Soc. Proc. **A118**, 654 (1928).

[15] In interpreting Eq. (9) it should be noted that in certain cases meaningless spherical harmonics are cancelled by a zero factor. Thus when $l=0$, and $u=-1$, ψ_3 in (9a) is to be taken to be zero.

[16] W. Gordon, Zeits. f. Physik **48**, 11 (1928).

where

$$
\begin{aligned}
{}_1F_1(\alpha;\beta;x) &= \sum_{n=0}^{\infty} \frac{(\alpha, n)}{(\beta, n)} x^n \\
(\alpha, n) &= \alpha(\alpha+1)\cdots(\alpha+n-1).
\end{aligned} \tag{14}
$$

M_r = radial normalizing factor.
n_r = radial quantum number.

$$\rho_l = ((l+1)^2 - \alpha^2)^{1/2}. \tag{15}$$

$$k_0 = \frac{2\pi mc}{h}\left(1 - \left(\frac{W}{mc^2}\right)^2\right)^{1/2} = \frac{1}{a_s N_l}. \tag{16}$$

$$N_l = (n_r^2 + (l+1)^2 + 2\rho_l n_r)^{1/2} \tag{17}$$

$$W = mc^2 \frac{n_r + \rho_l}{N_l} = mc^2\left\{1 + \frac{\alpha^2}{(n_r + ((j+\frac{1}{2})^2 - \alpha^2)^{1/2})}\right\}^{-1/2}. \tag{18}$$

$$a_s = \frac{h^2}{4\pi^2 mc^2 Z}; \quad \alpha = \frac{2\pi e^2 Z}{hc}. \tag{19}$$

CONTINUOUS SPECTRUM: $W/mc^2 > 1$

$$F_l = -i\frac{\left(\frac{W}{mc^2} - 1\right)^{1/2}}{\left(\frac{W}{mc^2} + 1\right)^{1/2}} M_r(\sigma_1 - \sigma_2) \tag{20}$$

$$
\begin{aligned}
G_l &= M_r(\sigma_1 + \sigma_2) \\
\sigma_1 &= A r^{\rho_l - 1} e^{-ik_0' r} {}_1F_1(\rho_l + iq + 1; 2\rho_l + 1; 2ik_0' r) \\
\sigma_2 &= B r^{\rho_l - 1} e^{-ik_0' r} {}_1F_1(\rho_l + iq; 2\rho_l + 1; 2ik_0' r)
\end{aligned} \tag{21}
$$

$$\frac{A}{B} = \frac{l+1+iQ}{\rho_l - iq} = \frac{\rho_l + iq}{l+1-iQ} \tag{22}$$

$$q = \frac{\frac{\alpha W}{mc^2}}{\left(\left(\frac{W}{mc^2}\right)^2 - 1\right)^{1/2}} = (Q^2 + \alpha^2)^{1/2} \tag{23}$$

$$k_0' = \frac{2\pi mc}{h}\left(\left(\frac{W}{mc^2}\right)^2 - 1\right)^{1/2}. \tag{24}$$

The discrete states of the Dirac electron are specified by the quantum numbers n_r, l, j, and u. These may have the following values:

$$
\begin{aligned}
n_r &= 0, 1, 2, \cdots \\
l &= 0, 1, 2, \cdots \\
j &= l \pm \tfrac{1}{2}, \geq 0
\end{aligned}
$$

(When $n_r=0$ the state $j=l-\frac{1}{2}$ is to be excluded.)

$$[-j] \leq u \leq [j],$$

where $[j]$ is the greatest integer contained in j.

The states of the continuous spectrum are specified by W, l, j, and u, with W arbitrary but $\geq mc^2$ and l, j, and u the same as for the discrete spectrum.

Normalization of the Wave Functions
Discrete Spectrum

We require to normalize our solutions in such a way that

$$\int_0^\infty \int_0^\pi \int_0^{2\pi} \psi\psi^* r^2 dr \cdot \sin\theta d\theta d\varphi = 1,$$

where

$$\psi\psi^* = \psi_1\psi_1^* + \psi_2\psi_2^* + \psi_3\psi_3^* + \psi_4\psi_4^*.$$

Suppose first that $j=l+\frac{1}{2}$. Then we find from Eq. (9a) that

$$\psi\psi^* = M_\theta^2[F_lF_l^*\{P_{l+1}^u P_{l+1}^{*u} + P_{l+1}^{u+1}P_{l+1}^{*u+1}\} + G_lG_l^*\{(l+u+1)^2 P_l^u P_l^{*u} + (l-u)^2 P_l^{u+1}P_l^{*u+1}\}] \tag{25}$$

or

$$\psi\psi^* = M_\theta^2[F_lF_l^* + G_lG_l^*][P_{l+1}^u P_{l+1}^{*u} + P_{l+1}^{u+1}P_{l+1}^{*u+1}],$$

as may be readily demonstrated.[17]

From the known relation

$$\int_0^\pi \int_0^{2\pi} P_l^u P_l^{*u} \sin\theta d\theta d\phi = \frac{4\pi}{2l+1}(l+u)!(l-u)! \tag{26}$$

we find

$$M_\theta^2\left(l, l+\frac{1}{2}, u\right) = \frac{1}{4\pi(l+u+1)!(l-u)!}. \tag{27}$$

The integral

$$I = \int_0^\infty [F_lF_l^* + G_lG_l^*]r^2 dr$$

can be evaluated as follows: one can easily show, by use of the generating function for the Laguerre polynomials,[18] that

$$\sum_{s=0}^\infty \binom{s+l}{s} {}_1F_1(-s; l+1; x)t^s = \frac{e^{-\frac{xt}{1-t}}}{(1-t)^{l+1}};\ l \text{ arbitrary}. \tag{28}$$

[17] Cf. e.g., D. R. Hartree, Proc. Camb. Phil. Soc. 25, 225 (1929).

[18] Courant and Hilbert, "Methoden der math. Physik," p. 78.

Hence

$$\sum_{r,s=0}^{\infty}\binom{r+2\rho}{r}\binom{s+2\rho}{s}\int_0^\infty x^{2\rho}e^{-x}{}_1F_1(-r;\,2\rho+1;\,x)\,{}_1F_1(-s;\,2\rho+1;\,x)dx\cdot t^s\tau^r$$

$$=\int_0^\infty x^{2\rho}e^{-x}\frac{e^{-xt/(1-t)-x\tau/(1-\tau)}}{(1-t)^{2\rho+1}(1-\tau)^{2\rho+1}}dx$$

$$=\frac{\Gamma(2\rho+1)}{(1-t\tau)^{2\rho+1}}=\Gamma(2\rho+1)\sum_{s=0}^{\infty}\binom{s+2\rho}{s}(t\tau)^s.$$

Therefore

$$\int_0^\infty x^{2\rho}e^{-x}{}_1F_1(-r;\,2\rho+1;\,x)\,{}_1F_1(-s;\,2\rho+1;\,x)dx=\frac{\Gamma(2\rho+1)}{\binom{s+2\rho}{s}}\delta_{rs}. \quad (29)$$

Thus from Eq. (13)

$$\int_0^\infty \sigma_1{}^2r^2dr=\frac{\Gamma(2\rho_l+1)(N_l+l+1)^2}{(2k_0)^{2\rho_l+1}\binom{n_r+2\rho_l}{n_r}}\cdot$$

$$\int_0^\infty \sigma_2{}^2r^2dr=\frac{\Gamma(2\rho_l+1)n_r{}^2}{(2k_0)^{2\rho_l+1}\binom{n_r-1+2\rho_l}{n_r-1}}\cdot$$

$$\int_0^\infty \sigma_1\sigma_2r^2dr=0.$$

Since from Eq. (12)

$$I=\frac{2M_r{}^2}{N_l+\rho_l+n_r}\int_0^\infty[N_l(\sigma_1{}^2+\sigma_2{}^2)+2\sigma_1\sigma_2(\rho_l+n_r)]r^2dr,$$

we obtain

$$M_r{}^2\left(n_r,l,l+\frac{1}{2}\right)=\frac{(N_l+\rho_l+n_r)(2k_0)^{2\rho_l+1}\Gamma(2\rho_l+n_r+1)}{n_r!2N_l[\Gamma(2\rho_l+1)]^2[(N_l+l+1)^2+n_r(n_r+2\rho_l)]}. \quad (30)$$

Now let $j=l-\frac{1}{2}$. Then from (9b) we find

$$\psi\psi^*=M_\theta{}^2[F_{-l-1}F^*_{-l-1}+G_{-l-1}G^*_{-l-1}][P_l{}^uP_l{}^{*u}+P_l{}^{u+1}P_l{}^{*u+1}], \quad (31)$$

and obtain in an exactly similar manner

$$M_\theta{}^2\left(l,l-\frac{1}{2},u\right)=\frac{1}{4\pi(l+u)!(l-u-1)!} \quad (32)$$

and

$$M_r{}^2\left(n_r,l,l-\frac{1}{2}\right)=\frac{(N+\rho+n_r)(2k_0)^{2\rho+1}\Gamma(2\rho+n_r+1)}{n_r!2N[\Gamma(2\rho+1)]^2[(N-l)^2+n_r(n_r+2\rho)]} \quad (33)$$

where in Eq. (33) the argument of N and ρ is not l, but $-l-1$. This change of argument occurs whenever $j=l-\frac{1}{2}$.

Continuous Spectrum

The angular normalizing factors are the same as for the discrete spectrum.

We first obtain an asymptotic expansion for the radial solutions, since we must here use a special normalizing method because the solutions are not quadratically integrable.

The asymptotic expansion of ${}_1F_1(\alpha;\beta;x)$ is given by[19]

$$ {}_1F_1(\alpha;\beta;x) \sim \frac{\Gamma(\beta)}{\Gamma(\alpha)} e^z x^{\alpha-\beta} + \frac{\Gamma(\beta)}{\Gamma(\beta-\alpha)}(-x)^{-\alpha}. \tag{34} $$

Using Eqs. (34) and (21), we find, omitting the prime on k_0,

$$ \begin{aligned} \sigma_1 &\sim \frac{A\Gamma(2\rho_l+1)(i)^{iq-\rho_l}}{\Gamma(\rho_l+iq+1)(2k_0)^{\rho}} \cdot \frac{e^{i(k_0 r + q\log 2k_0 r)}}{r} \\ \sigma_2 &\sim \frac{B\Gamma(2\rho_l+1)(-i)^{-iq-\rho_l}}{\Gamma(\rho_l-iq+1)(2k_0)^{\rho}} \frac{e^{-i(k_0 r + q\log 2k_0 r)}}{r}. \end{aligned} \tag{35} $$

Therefore, from Eq. (20)

$$ \begin{aligned} G_l &\sim M_r C \frac{\cos(k_0 r + q\log k_0 r - \delta_l)}{r} \\ F_l &\sim M_r C D \frac{\sin(k_0 r + q\log k_0 r - \delta_l)}{r} \end{aligned} \tag{36} $$

in which

$$ \delta_l = \rho_l \frac{\pi}{2} + \arg\Gamma(\rho_l + iq + 1) - \beta_0 - q\log 2. \tag{37} $$

$$ e^{2i\beta_0} = A/B \tag{37'} $$

$$ C = \frac{2\Gamma(2\rho_l+1)e^{-q\pi/2}\,|A|}{(2k_0)^{\rho}\,|\Gamma(\rho_l+iq+1)|} \cdot \left(\frac{A}{B^*}\right)^{1/2}. \tag{38} $$

$$ D = \left(\frac{\frac{W}{mc^2}-1}{\frac{W}{mc^2}+1}\right)^{1/2} = \left(\frac{q-Q}{q+Q}\right)^{1/2}. \tag{38'} $$

We shall use the Weyl normalization method.[20]

Call the radial normalization factor $M_r(W,l,j) = M(W)$. Then with proper choice of $M(W)$

$$ \begin{aligned} I &= \int_0^{\infty} M^*(W')r^2 dr \int_{W_1}^{W_2} M(W)\left[F_l(W)F_l^*(W') + G_l(W)G_l^*(W')\right]dW \\ &= \begin{cases} 1 & \text{when } W_1 < W' < W_2, \\ 0 & \text{when } W' \text{ lies outside the interval } (W_1, W_2). \end{cases} \end{aligned} \tag{39} $$

[19] E. W. Barnes, Trans. Camb. Phil. Soc. **20**, 253 (1906).

[20] H. Weyl, Math. Ann. **68**, 220 (1910).

If we write down Eqs. (11) for the energy value W, and their complex conjugates for the energy value W', multiply each of the resulting equations by r^2, then multiply the first equation for W by $F^*(W')$, the second by $-G^*(W')$, the first for W' by $-F(W)$, and the second by $G(W)$, and finally add, we obtain the equation

$$\frac{2\pi}{hc}\cdot(W - W')r^2[F(W)F^*(W') + G(W)G^*(W')] = \frac{\partial}{\partial r}r^2[G^*(W')F(W) - G(W)F^*(W')]. \quad (40)$$

Substituting Eq. (40) in Eq. (39), we get

$$I = \int_0^\infty M^*(W')dr \int_{W_1}^{W_2} \frac{hc}{2\pi}\frac{M(W)}{W' - W}\frac{\partial}{\partial r}[r^2G(W)F^*(W') - G^*(W')F(W)]dW$$

$$= \lim_{R\to\infty}\frac{hc}{2\pi}M^*(W')\int_{W_1}^{W_2}\frac{M(W)}{W'-W}R^2[G(W, R)F^*(W', R) - G^*(W', R)F(W, R)]dW$$

since $r^2GF = 0$ when $r = 0$.

We may therefore use our asymptotic expansions for F and G. From Eq. (36) we can write

$$I = \lim_{R\to\infty}\frac{hc}{2\pi}M^*(W')C^*(W')\int_{W_1}^{W_2}\frac{M(W)}{W' - W}[C(W)D(W')\cos Ru.\sin Ru' - C(W)D(W)\sin Ru\cdot\cos Ru']dW,$$

where

$$Ru = k_0R + q\log k_0R - \delta_l,$$

or

$$n(W) = \frac{2\pi mc}{h}\cdot\left(\left(\frac{W}{mc^2}\right)^2 - 1\right)^{1/2} + \frac{\alpha}{\left(1 - \left(\frac{mc^2}{W}\right)^2\right)^{1/2}}\frac{1}{R}\log\frac{2\pi mc}{h}R\left(\left(\frac{W}{mc^2}\right)^2 - 1\right)^{1/2} - \frac{\delta_l}{R}. \quad (41)$$

We can choose R large enough so that $u(W)$ for $W_1 \leqq W \leqq W_2$ is an increasing function of W, and so can find the inverse function $W = f(u)$, which is continuous and possesses a continuous derivative for $W > mc^2$. We make a simple rearrangement in I and change variables from W to u, obtaining

$$I = \lim_{R\to\infty}\frac{hc}{2\pi}M^*(W')C^*(W')\int_{u_1}^{u_2}\frac{M[f(u)]C[f(u)]}{f(u') - f(u)}[D[f(u')]\sin R(u' - u) + \{D[f(u')] - D[f(u)]\}\sin Ru\cdot\cos Ru']f'(u)du,$$

$$= \lim_{R\to\infty}\frac{hc}{2\pi}M^*(W')C^*(W')(I_R' + I_R'').$$

Consider

$$\lim_{R\to\infty} I_R'' = \lim_{R\to\infty} \cos Ru' \int_{u_1}^{u_2} M[f(u)]C[f(u)]f'(u)\frac{D[f(u')]-D[f(u)]}{f(u')-f(u)}\sin Ru.\, du.$$

Now $D'(W)$ exists for $W>mc^2$, and the remaining functions in the integrand are continuous, so that we can apply the well-known result[21] that

$$\lim_{n\to\infty} \int_a^b \psi(t)\sin nt\, dt = 0$$

when $\psi(t)$ is integrable in (a, b). This gives us

$$\lim_{R\to\infty} I_R'' = 0.$$

By the same argument we can show that $\lim_{R\to\infty} I_R' = 0$ when W' is not in the interval (W_1, W_2). When $W_1 < W' < W_2$, we can write, putting $u'-u = y$,

$$I_R' = D(W')\int_{u'-u_1}^{u'-u_2} M[f(u'-y)]C[f(u'-y)]f'(u'-y)\frac{\sin Ry}{f(u'-y)-f(u')}dy$$

$$= D(W')\int_{u'-u_2}^{u'-u_1} M[f(u'-y)]C[f(u'-y)]\frac{\sin Ry}{y}dy\frac{f'(u'-y)}{f'(u')}$$

$$+ D(W')\int_{u'-u_1}^{u'-u_2} M[f(u'-y)]C[f(u'-y)]f'(u'-y)\left[\frac{1}{f(u'-y)-f(u')}\right.$$

$$\left. - \frac{1}{f'(u')y}\right]\sin Ry\cdot dy = I_R''' + I_R^{IV}.$$

Since the function in the square brackets in I_R^{IV} is finite at $y=0$, the same argument as above shows that $\lim_{R\to\infty} I_R^{IV} = 0$. Further,

$$\lim_{R\to\infty} I_R''' = D(W')M(W')C(W')\pi$$

by the Dirichlet integral.[22]

Finally, therefore,

$$I = \tfrac{1}{2}hc\,|\,M(W')\,|^2\,|\,C(W')\,|^2\,D(W'),$$

and we must take

$$M_r^2(W, l, l+\tfrac{1}{2}) = 2/hcD\,|\,C\,|^2. \tag{42}$$

Since the above calculation has not made use of a particular value for j, we have also

$$M_r^2(W, l, l-\tfrac{1}{2}) = 2/hcD\,|\,C\,|^2, \tag{43}$$

where in Eq. (43) the argument of ρ and A is $-l-1$, not l.

[21] See K. Knopp, Unendliche Reihen, p. 363.

[22] Knopp, reference 21, p. 366.

Selection Rules

The selection rules for the matrix elements B^s in Eq. (4′), when retardation is neglected, have been shown by Darwin[14] to be

$$\begin{aligned} \Delta l &= 1, \\ \Delta j &= 0, \pm 1, \\ \Delta u &= 0, \pm 1. \end{aligned} \tag{44}$$

The table below gives the possible transitions:

Initial State				Initial State			
n_r	l	$l+\frac{1}{2}$	u	n_r	l	$l-\frac{1}{2}$	u
Final State				Final State			
n_r'	$l+1$	$l+3/2$	u'	n_r'	$l+1$	$l+\frac{1}{2}$	u'
n_r'	$l+1$	$l+\frac{1}{2}$	u'	n_r'	$l-1$	$l-\frac{1}{2}$	u'
n_r'	$l-1$	$l-\frac{1}{2}$	u'	n_r'	$l-1$	$l-3/2$	u'

(45)

with $u'=u$, $u\pm1$, and arbitrary n_r'. The only degeneracy of the possible final states of the discrete spectrum is that with respect to u'. If n_r' stands for the energy W of a state in the continuous spectrum, all possible final states having this value W fall together.

The Mass Absorption Coefficient of the K Shell

The atomic absorption coefficient τ_ν for a given energy jump is defined as follows:

$$\tau_\nu I(\nu)d\nu = \text{energy absorbed per second} = h\nu \cdot w'dW \tag{46}$$

where $w'dW$ ($=w'd\epsilon''$ of Eq. (8)) is the transition probability for the energy jump under consideration, and $I(\nu)d\nu$ is the intensity of the incident radiation in the range $d\nu$. Thus

$$(\tau_\nu)_K I(\nu)d\nu = h\nu \cdot w'(W; 0, 0, \tfrac{1}{2})dW,$$

since in the K shell $n_r=l=0$, and $j=\frac{1}{2}$.

The formula for the mass absorption coefficient $(\tau_\nu/\rho)_K$[23] becomes, since $dW=h\,d\nu$,

$$\left(\frac{\tau_\nu}{\rho}\right)_K = \frac{Nh^2\nu}{AI(\nu)}w'\left(W; 0, 0, \frac{1}{2}\right) = \frac{Nh^2\nu}{A8\pi c\rho(\nu)}w'\left(W; 0, 0, \frac{1}{2}\right), \tag{47}$$

where N is Avogadro's number, A is the atomic weight, and $\rho(\nu)$ is defined in connection with Eq. (5).

[23] The ρ in τ_ν/ρ is not to be confused with $\rho(\nu)$. The former is the mass of an atom, while the latter is energy density.

Consulting the table (45) of possible transitions, we see that the sum over the degenerate states in Eq. (8) extends over the initial values of u, the final values u', and $j=\frac{1}{2}, 3/2$, the only possible final l being 1. We thus obtain

$$\left(\frac{\tau_\nu}{\rho}\right)_K = \frac{2\pi e^2 cN}{3A\nu}\left[\sum_{u,u'}\left| P\left(W, 1, \frac{3}{2}, u'; 0, 0, \frac{1}{2}, u\right)\right|^2 + \sum_{u,u'}\left| P\left(W, 1, \frac{1}{2}, u'; 0, 0, \frac{1}{2}, u\right)\right|^2\right]. \quad (48)$$

Carrying out the angular integrations indicated by the definitions (8′) and (4′) of the P's, and using the angular normalizing factors given by Eqs. (27) and (32), and finally summing over u and u', we easily obtain

$$\left(\frac{\tau_\nu}{\rho}\right)_K = \frac{4\pi e^2 cN}{3A\nu}\left[\frac{8}{3}\left|\int_0^\infty F_0 G_1 r^2 dr\right|^2 + 3\left|\int_0^\infty F_{-2}G_0 r^2 dr + \frac{1}{3}\int_0^\infty F_0 G_{-2} r^2 dr\right|^2\right]. \quad (49)$$

Writing $\rho=(1-\alpha^2)^{1/2}$, $\rho'=(4-\alpha^2)^{1/2}$, $a=k_0'/k_0$, and taking

$$A = \frac{((l+1)^2+Q^2)^{1/2}}{Q} e^{i\tan^{-1}Q/(l+1)}$$
$$B = \frac{((l+1)^2+Q^2)^{1/2}}{Q} e^{-i\tan^{-1}q/\rho'} \quad (50)$$

we find for the functions F_0, G_0, G_1, G_{-2}, and F_{-2}, using Eqs. (12), (13), (20), (21), (30), (42), (43), (38), and (38′),

$$F_0 = (2k_0)^\rho \left(\frac{(1-\rho)k_0}{\Gamma(2\rho+1)}\right)^{1/2} r^{\rho-1}e^{-k_0 r}. \quad (51)$$

$$G_0 = (2k_0)^\rho \left(\frac{(1+\rho)k_0}{\Gamma(2\rho+1)}\right)^{1/2} r^{\rho-1}e^{-k_0 r} \quad (52)$$

$$G_1 = \frac{(2ak_0)^{\rho'}\,|\,\Gamma(\rho'+iq+1)\,|\,e^{q\pi/2}}{2\Gamma(2\rho'+1)}\left(\frac{2}{hc}\right)^{1/2}\left(\frac{q-Q}{q+Q}\right)^{-1/4} \cdot \left[e^{i[\tan^{-1}Q/2-ak_0 r]} r^{\rho'-1}{}_1F_1(\rho'+iq+1; 2\rho'+1; 2iak_0 r) + e^{-i[\tan^{-1}q/\rho'+ak_0 r]} r^{\rho'-1}{}_1F_1(\rho'+iq; 2\rho'+1; 2iak_0 r)\right]. \quad (53)$$

$$G_{-2} = \frac{(2ak_0)^{\rho}\,|\,\Gamma(\rho+iq+1)\,|\,e^{q\pi/2}}{2\Gamma(2\rho+1)}\left(\frac{2}{hc}\right)^{1/2}\left(\frac{q-Q}{q+Q}\right)^{-1/4} \cdot \left[e^{i[\tan^{-1}Q/-1-ak_0 r]} r^{\rho-1}{}_1F_1(\rho+iq+1; 2\rho+1; 2iak_0 r) + e^{-i[\tan^{-1}q/\rho+ak_0 r]} r^{\rho-1}{}_1F_1(\rho+iq; 2\rho+1; 2iak_0 r)\right]. \quad (54)$$

$$F_{-2} = \frac{(2ak_0)^{\rho}\,|\,\Gamma(\rho+iq+1)\,|\,e^{q\pi/2}}{i2\Gamma(2\rho+1)}\left(\frac{2}{hc}\right)^{1/2}\left(\frac{q-Q}{q+Q}\right)^{1/4}.$$

$$\cdot \left[e^{i[\tan^{-1}Q/-1-ak_0r]}r^{\rho-1}{}_1F_1(\rho+iq+1;2\rho+1;2iak_0r)\right. \tag{55}$$

$$\left. - e^{-i[\tan^{-1}q/\rho+ak_0r]}r^{\rho-1}{}_1F_1(\rho+iq;2\rho+1;2iak_0r)\right].$$

Integrating and rearranging, we obtain

$$\int_0^\infty F_0G_1r^2dr = 2^{\rho'+\rho}a^{\rho'}\cdot\left(\frac{1-\rho}{2hck_0\Gamma(2\rho+1)}\right)^{1/2}\frac{|\Gamma(\rho'+iq+1)|e^{q\pi/2}}{(1-ia)^{\rho'+\rho+1}}\left(\frac{q-Q}{q+Q}\right)^{-1/4}\cdot$$

$$\cdot\frac{\Gamma(\rho'+\rho+1)}{\Gamma(2\rho'+1)}\cdot\left[e^{-i\tan^{-1}Q/2}{}_2F_1\left(\rho'+\rho+1,\rho'-iq+1;2\rho'+1;-\frac{2ia}{1-ia}\right)\right. \tag{56}$$

$$\left.+e^{i\tan^{-1}q/\rho'}{}_2F_1\left(\rho'+\rho+1,\rho'-iq;2\rho'+1;-\frac{2ia}{1-ia}\right)\right].$$

$$\int_0^\infty F_0G_{-2}r^2dr = 2^{2\rho}a^{\rho}\cdot\left(\frac{1-\rho}{2hck_0\Gamma(2\rho+1)}\right)^{1/2}\frac{|\Gamma(\rho+iq+1)|e^{q\pi/2}}{(1-ia)^{2\rho+1}}\left(\frac{q-Q}{q+Q}\right)^{-1/4}\cdot$$

$$\cdot\left[e^{i\tan^{-1}Q/-1}\cdot{}_2F_1\left(2\rho+1,\rho-iq+1;2\rho+1;-\frac{2ia}{1-ia}\right)\right. \tag{57}$$

$$\left.+e^{i\tan^{-1}q/\rho}\cdot{}_2F_1\left(2\rho+1,\rho-iq;2\rho+1;-\frac{2ia}{1-ia}\right)\right].$$

$$\int_0^\infty F_{-2}G_0r^2dr = i2^{2\rho}a^{\rho}\cdot\left(\frac{1+\rho}{2hck_0\Gamma(2\rho+1)}\right)^{1/2}\frac{|\Gamma(\rho+iq+1)|e^{q\pi/2}}{(1-ia)^{2\rho+1}}\left(\frac{q-Q}{q+Q}\right)^{1/4}\cdot$$

$$\cdot\left[e^{-i\tan^{-1}Q/-1}\cdot{}_2F_1\left(2\rho+1,\rho-iq+1;2\rho+1;-\frac{2ia}{1-ia}\right)\right. \tag{58}$$

$$\left.-e^{i\tan^{-1}q/\rho}\cdot{}_2F_1\left(2\rho+1,\rho-iq;2\rho+1;-\frac{2ia}{1-ia}\right)\right].$$

The two hypergeometric functions in (56) cannot be readily evaluated in their present form because of very slow convergence or non-convergence of the usual series. There are two possible methods of evaluating them numerically. One method is to express them as definite integrals and then to integrate numerically. Because $\rho'-\rho-1$ is so small, the numerical integration will be inaccurate or laborious if no further transformation of the resulting integrals is made. A convenient transformation which is satisfactory over the range of values of a and q which corresponds to $\frac{1}{2}\lambda_k \leqq \lambda \leqq \lambda_k$, is that which results in the integral J defined by Eq. (62) below.

Using the relationship

$${}_2F_1(\alpha,\beta;\gamma;x) = \frac{\Gamma(\gamma)}{\Gamma(\alpha)\Gamma(\gamma-\alpha)}\int_0^1 u^{\alpha-1}(1-u)^{\gamma-\alpha-1}(1-ux)^{-\beta}du, \tag{59}$$

and making some simple transformations, we can write

$$ {}_2F_1\left(\rho' + \rho + 1, \rho' - iq + 1; 2\rho' + 1; -\frac{2ia}{1 - ia}\right) $$

$$ = \left(\frac{1 + ia}{1 - ia}\right)^{iq-\rho-1} \left\{1 + \frac{J^*}{B(\rho' - \rho, \rho' + \rho + 1)}\right\} \quad (60) $$

$$ {}_2F_1\left(\rho' + \rho + 1, \rho' - iq; 2\rho' + 1; -\frac{2ia}{1 - ia}\right) $$

$$ = \left(\frac{1 + ia}{1 - ia}\right)^{iq-\rho'} \left\{1 + \frac{J}{B(\rho' - \rho, \rho' + \rho + 1)}\right\} \quad (61) $$

where

$$ J = \int_{-1/2}^{+1/2} \left(\frac{1}{2} - t\right)^{\rho'+\rho} \left(\frac{1}{2} + t\right)^{\rho'-\rho-1} dt \left[\left(\frac{1 + ia}{1 - 2iat}\right)^{\rho'-iq} - 1\right] \quad . (62) $$

and

$$ B(\alpha, \beta) = \frac{\Gamma(\alpha)\Gamma(\beta)}{\Gamma(\alpha + \beta)} . \quad (63) $$

The other method of evaluating the hypergeometric functions in Eq. (56) is to transform them to another combination of hypergeometric functions which do converge fairly rapidly. By use of the transformation[24] connecting Y_1 with Y_3 and Y_4 one finds readily from Eq. (60) that

$$ B(\rho' - \rho, \rho' + \rho + 1) + J = \frac{(1 + a^2)^{\rho'}}{(2a)^{2\rho'}} e^{i\rho'\pi} \left[B(\rho - iq, \rho' - \rho) \left(\frac{1 - ia}{1 + ia}\right)^{\rho} \cdot \right. $$

$$ \cdot {}_2F_1\left(-\rho' - \rho, 1 + iq - \rho'; 1 + iq - \rho; \frac{1 + ia}{1 - ia}\right) \quad (64) $$

$$ + B(-\rho + iq, \rho' + \rho + 1) \left(\frac{1 - ia}{1 + ia}\right)^{iq} \cdot $$

$$ \left. \cdot {}_2F_1\left(1 + \rho - \rho', -\rho' - iq; \rho - iq + 1; \frac{1 + ia}{1 - ia}\right)\right]. $$

The series for the hypergeometric functions in Eq. (64) converge fairly rapidly for any range of wave-length. The chief difficulty in the use of this formula is the calculation of the gamma functions. High accuracy can be obtained from this formula with less work than from numerical integration, but for three-figure accuracy the latter is much quicker. All the calculations in this paper were performed by numerical integration.

The hypergeometric functions occurring in Eqs. (57) and (58) can be reduced to elementary functions by the use of the relation

$$ {}_2F_1(\alpha, \beta; \alpha; x) = (1 - x)^{-\beta} \quad (65) $$

[24] E. W. Barnes, Proc. Lond. Math. Soc. (2), **6**, 141 (1908).

Making these transformations and noting that $Q=1/a$, we obtain for the three integrals

$$\int_0^\infty F_0 G_1 r^2 dr = 2^{\rho'+\rho} a^{\rho'} \left(\frac{1-\rho}{2hck_0\Gamma(2\rho+1)}\right)^{1/2} \frac{|\Gamma(\rho'+iq+1)|\, e^{q(\pi/2-2\tan^{-1}a)}}{\Gamma(\rho'-\rho)(1+a^2)^{(\rho'+\rho+1)/2}} \left(\frac{q-Q}{q+Q}\right)^{-1/4} \cdot$$

$$\cdot \left[e^{-i[\tan^{-1}q/2-(\rho'-\rho-1)\tan^{-1}a]} \cdot \{B(\rho'-\rho,\rho'+\rho+1)+J^*\}\right. \tag{66}$$

$$\left. + e^{i[\tan^{-1}q/\rho'-(\rho'-\rho-1)\tan^{-1}a]} \cdot \{B(\rho'-\rho,\rho'+\rho+1)+J\}\right].$$

$$\int_0^\infty F_0 G_{-2} r^2 dr = 2^{2\rho} a^{\rho} \cdot \left(\frac{1-\rho}{2hck_0\Gamma(2\rho+1)}\right)^{1/2} \frac{|\Gamma(\rho+iq+1)|\, e^{q(\pi/2-2\tan^{-1}a)}}{(1+a^2)^{\rho+1/2}} \left(\frac{q-Q}{q+Q}\right)^{-1/4} \cdot$$

$$\cdot \left[ie^{-2i\tan^{-1}a} + e^{i[\tan^{-1}q/\rho+\tan^{-1}a]}\right] \tag{67}$$

$$\int_0^\infty F_{-2} G_0 r^2 dr = 2^{2\rho} a^{\rho} \cdot \left(\frac{1+\rho}{2hck_0\Gamma(2\rho+1)}\right)^{1/2} \frac{|\Gamma(\rho+iq+1)|\, e^{q(\pi/2-2\tan^{-1}a)}}{(1+a^2)^{\rho+1/2}} \left(\frac{q-Q}{q+Q}\right)^{1/4} \cdot$$

$$\cdot \left[e^{-2i\tan^{-1}a} - ie^{i[\tan^{-1}q/\rho+\tan^{-1}a]}\right]. \tag{68}$$

Substituting in Eq. (49) we obtain finally for the mass absorption coefficient for the K shell

$$\left(\frac{\tau_\nu}{\rho}\right)_K = \frac{N}{AZ} \frac{h\lambda}{3\pi mc} \frac{2^{2\rho} e^{q(\pi-4\tan^{-1}a)}}{\Gamma(2\rho+1)(1+a^2)^{\rho+1}} \left[\frac{8}{3} \frac{(2a)^{2\rho'}(1-\rho)}{(1+a^2)^{\rho'}} \cdot \right.$$

$$\cdot \frac{|\Gamma(\rho'+iq+1)|^2}{[\Gamma(\rho'-\rho)]^2} \left(\frac{q-Q}{q+Q}\right)^{-1/2} |B(\rho'-\rho,\rho'+\rho+1)+J|^2(1+\cos\phi) \tag{69}$$

$$+ 3\frac{(2a)^{2\rho}|\Gamma(\rho+iq+1)|^2}{(1+a^2)^{\rho}} \left\{(1+\rho)\left(\frac{q-Q}{q+Q}\right)^{1/2}(1+\sin\delta)\right.$$

$$\left. \left. + \frac{1-\rho}{9}\left(\frac{q-Q}{q+Q}\right)^{-1/2}(1-\sin\delta) + \frac{2}{3}(1-\rho^2)^{1/2}\cdot\cos\delta\right\}\right].$$

in which

$$\phi = \tan^{-1}\tfrac{1}{2}Q + \tan^{-1}q/\rho' - 2(\rho'-\rho-1)\tan^{-1}a + 2\tan^{-1}\chi.$$

$$\chi = \arg\left[B(\rho'-\rho,\rho'+\rho+1)+J\right]$$

$$\delta = 3\tan^{-1}a + \tan^{-1}q/\rho$$

$$a^2 = x\frac{2+xy}{2-y};\ Q = \frac{1}{a};\ q^2 = Q^2+\alpha^2;\ \alpha^2 = y(2-y);$$

$$x = \lambda_k/\lambda - 1;\ \text{and}\ y = h/mc\lambda_k.$$

The two expressions in Eq. (69) which are most difficult to calculate are the absolute value of the gamma function of complex argument, and the

integral J. The gamma function can be most conveniently calculated from the asymptotic expansion

$$\log|\Gamma(x+iy)| \sim \tfrac{1}{2}(x-\tfrac{1}{2})\log(x^2+y^2) - y\tan^{-1}y/x - x + \tfrac{1}{2}\log 2\pi + \sum_{n=1}^{\infty}\frac{B_{2n}}{2n(2n-1)}\frac{\cos[(2n-1)\tan^{-1}y/x]}{(x^2+y^2)^{n-1/2}}. \quad (70)$$

where the B_{2n} are the well-known Bernoulli numbers. By taking x large and using the difference equation satisfied by the gamma function, Eq. (70) forms a relatively easy method of calculation.

Under adverse circumstances, the calculation of the integral J could be very laborious. Fortunately, when the wave-length is confined to the range $\frac{1}{2}\lambda_k$ to λ_k, the integrand of Eq. (62) does not change rapidly and has no important oscillations, so that an approximate formula of integration may be expected to give sufficient accuracy. The formula used is one given by Woolhouse,[25] namely,

$$\int_0^1 f(x)dx = \frac{7}{390}[f(0)+f(1)] + \frac{16,807}{133,380}[f(1/14)+f(13/14)] + \frac{128}{570}[f(1/4)+f(3/4)] + \frac{71}{270}f(\tfrac{1}{2}). \quad (71)$$

It would be very difficult to obtain a numerical value for the error involved in using this formula when evaluating an integral as complicated as J. However, the writer has tried the formula in evaluating known integrals of functions which have closely the same shape as the actual integrand in J, and from these trials he is convinced that in the wave-length range mentioned above at least three- and very probably four-figure accuracy can be expected. This is further supported by the close agreement of the results for Al ($Z=13$) with those calculated from the Nishina-Rabi formula, an entirely independent procedure. The effect on the absorption coefficient of an error in calculating J depends of course upon the relative magnitude of the two parts of Eq. (69). In the range under consideration the term containing J is from 2 to 3 times as large as the other term.

Mass Absorption Coefficient at the Absorption Edge

At the absorption edge, where $\lambda=\lambda_k$, Eq. (69) cannot be used to calculate the absorption coefficient because there $a=0$ and $q=Q=\infty$. A limiting process is necessary, and it is most convenient to pass to the limit for the individual proper functions and then to integrate, instead of passing to the limit directly in Eq. (69). Another more simple method if only the form of the proper functions is necessary, is to solve the radial differential Eqs. (11) when $W=mc^2$, but this has the disadvantage for our purpose of requiring another normalization using Weyl's method.

[25] Woolhouse, Journ. Inst. Act. **27**, 122, (1888). Cf. Whittaker and Robinson, "Calculus of Observations," p. 158.

We want to find $\lim_{a\to 0} F_l$ and $\lim_{a\to 0} G_l$. To do this we consider separately the radial normalizing factor and the functions σ_1 and σ_2 (see Eq. 21)). From the well-known Stirling formula, we can write[25]

$$|\Gamma(\rho' + iq + 1)| \sim (2\pi)^{1/2} a^{-\rho'-1/2} e^{-q\pi/2},$$

also

$$|A| \sim 1, \quad \text{and} \quad (2k_0')^{\rho'} = (2k_0)^{\rho'} a^{\rho'},$$

so that from Eq. (38)

$$|C| \sim 2\Gamma(2\rho' + 1)(2k_0)^{-\rho'}(a/2\pi.)^{1/2} \tag{72}$$

Also, from Eq. (38′),

$$D = \left(\frac{q - Q}{q + Q}\right)^{1/2} = \left(\frac{(1 + a^2\alpha^2)^{1/2} - 1}{(1 + a^2\alpha^2)^{1/2} + 1}\right)^{1/2} \sim \tfrac{1}{2}a\alpha \tag{73}$$

since $q^2 = Q^2 + \alpha^2 = 1/a^2 + \alpha^2$. Therefore, from Eq. (42),

$$M_r = \frac{1}{|C|}\left(\frac{2}{hcD}\right)^{1/2} \sim \left(\frac{2\pi}{hc\alpha}\right)^{1/2} \frac{(2k_0)^{\rho'}}{\Gamma(2\rho' + 1)} \frac{1}{a} = \frac{(2k_0)^{\rho'}}{e(Z)^{1/2}\Gamma(2\rho' + 1)} \frac{1}{a}, \tag{74}$$

using Eq. (19).

It is a known property[27] of the degenerate hypergeometric function that

$$\lim_{\epsilon\to\infty} \frac{(\frac{1}{2}z)^{\alpha}}{\Gamma(\alpha + 1)} {}_1F_1\left(\frac{1}{\epsilon}; \alpha + 1; -\epsilon z^2/4\right) = J_{\alpha}(z), \tag{75}$$

where $J_{\alpha}(z)$ is the ordinary Bessel function. It is evident, therefore, that

$$\begin{aligned} \lim_{a\to 0} \sigma_2 &= \lim_{a\to 0} Br^{\rho'-1} e^{-iak_0 r} {}_1F_1(\rho' + iq; 2\rho' + 1; 2iak_0 r) \\ &= -i\Gamma(2\rho' + 1)(2k_0)^{-\rho'} r^{-1} J_{2\rho'}((8k_0 r)^{1/2}). \end{aligned} \tag{76}$$

It can easily be shown that

$$\begin{aligned} {}_1F_1(\rho' + iq + 1; 2\rho' + 1; 2i\kappa_0' r) &= \frac{2\rho'}{\rho' + iq} {}_1F_1(\rho' + iq; 2\rho'; 2ik_0' r) \\ &\quad - \frac{\rho' - iq}{\rho' + iq} {}_1F_1(\rho' + iq; 2\rho' + 1; 2ik_0' r). \end{aligned} \tag{77}$$

With Eqs. (77) and (21), we find

$$\begin{aligned} \sigma_1 \pm \sigma_2 = r^{\rho'-1} e^{-ik_0' r} &\left[A \frac{2\rho'}{\rho' + iq} {}_1F_1(\rho' + iq; 2\rho'; 2ik_0' r) \right. \\ &\left. + \left[\pm B - A\frac{\rho' - iq}{\rho' + iq} \right] {}_1F_1(\rho' + iq; 2\rho' + 1; 2ik_0' r) \right]. \end{aligned} \tag{78}$$

[26] The symbol $\backsim$, as used in this section, has the following significance. if $f(a) \backsim g(a)$ then $\lim_{a\to 0} f(a)/g(a) = 1$.

[27] G. N. Watson, "Bessel Functions," p. 154.

From Eqs. (78), (76), and (50), we find after some calculation

$$(\sigma_1 + \sigma_2) \sim a \cdot r^{-1}\Gamma(2\rho' + 1)(2k_0)^{-\rho'}\left[J_{2\rho'-1}((8k_0r)^{1/2}) \cdot (2k_0r)^{1/2} + (l + 1 - \rho')J_{2\rho'}((8k_0r)^{1/2})\right],$$

$$\lim_{a\to 0} (\sigma_1 - \sigma_2) = 2ir^{-1}\Gamma(2\rho' + 1)(2k_0)^{-\rho'}J_{2\rho'}((8k_0r)^{1/2}),$$

so that finally, with Eqs. (20) and (74),

$$\lim_{a\to 0} F_l = \alpha/e(Z)^{1/2}r \cdot J_{2\rho'}((8k_0r)^{1/2}) \tag{79}$$

$$\lim_{a\to 0} G_l = 1/e(Z)^{1/2}r \cdot \left[(2k_0r)^{1/2}J_{2\rho'-1}((8k_0r)^{1/2}) + (l+1 - \rho')J_{2\rho'}((8k_0r)^{1/2})\right]. \tag{80}$$

After some simple calculations, using the formula[28]

$$\int_0^\infty J_\nu(at)\exp(-p^2t^2)t^{\mu-1}dt = \frac{\Gamma\left(\frac{\nu+\mu}{2}\right)\left(\frac{a}{2p}\right)^\nu}{2p^\mu\Gamma(\nu+1)}\exp(-a^2/4p^2)\,{}_1F_1\left(\frac{\nu-\mu}{2}+1;\nu+1;a^2/4p^2\right),$$

we find for the mass absorption coefficient at the absorption edge

$$\left(\frac{\tau_\nu}{\rho}\right)_{K\text{edge}} = \frac{h^2N\lambda_k}{3\pi mc^2A}\frac{2^{2\rho}\exp(-4)}{Z^2\Gamma(2\rho+1)}\left[\frac{8}{3}2^{2\rho'}(1-\rho)\left[\frac{\Gamma(\rho'+\rho+1)}{\Gamma(2\rho'+1)}\right]^2 \cdot\left[2\rho'\,{}_1F_1(\rho'-\rho-1;2\rho';2) + (2-\rho')\,{}_1F_1(\rho'-\rho;2\rho'+1;2)\right]^2 + 3\cdot 2^{2\rho}\left[\alpha(1+\rho)^{1/2} - \frac{3-\rho}{3}(1-\rho)^{1/2}\right]^2\right]. \tag{81}$$

Eqs. (69) and (81) for the mass absorption coefficient have been derived for a one-electron atom. Actually, of course, the K shell contains two electrons, so that one might expect, in the absence of interaction between the electrons, merely to multiply the values for the one-electron atom by two. This is incorrect. In the one-electron atom the lowest energy level is doubly degenerate since there are two possible directions for the "spin" magnetic moment of the electron, represented analytically by $u=0$ or -1. In the two-electron atom, however, the lowest state is non-degenerate. If the Pauli exclusion principle were not in force, the degeneracy of the lowest state would be four, since in the absence of interaction each electron may have the values $u=0$ or -1. Since, however, no two electrons may have the same quantum numbers, and because of the identity of the electrons,[29] three of the degener-

[28] Watson, reference 27, p. 394.

[29] W. Heisenberg, Zeits. f. Physik **38**, 411 (1926).

ate states are ruled out, so that multiplying by two for the two K electrons and dividing by two because there is no degeneracy leaves Eqs. (69) and (81) unchanged.

Since the completion of this paper an article by Stobbe[30] has appeared in which the mass absorption coefficient is calculated by means of the non-relativistic quantum mechanics. Stobbe uses a screening constant for the K electrons which is considerably smaller than that necessary to make the energy of the model agree with that experimentally determined from the K edge. He justifies this procedure by pointing out that in the final state with one K electron ejected, the energy of the remaining electrons is different from that in the initial state, so that the absorbed frequency does not correspond exactly to the change in energy of the ejected K electron alone.

The present calculations can easily be adapted to a model with a smaller screening constant by lowering Z to compensate for the decrease in s; the results then apply to different atoms, for instance to gold (79) instead of lead (82) if s is changed from 4.512 to 1.512. With the smaller screening constant, however, the λ_k' of the model will no longer agree with the experimental value. We want the abscissas of the computed and observed curves to coincide at the experimental λ_k. Now the absorption coefficient depends on a matrix element which is a function of λ_k' and W, the energy of the ejected electron. In the present calculations W was connected with a wave-length λ' of the incident x-rays given by $W=mc^2+h(\nu'-\nu_k')=mc^2+hc(1/\lambda'-1/\lambda_k')$. In the adapted calculations ν_k' is replaced by ν_k corresponding to the actual absorption edge and so W must be connected with a wave-length λ given by $W=mc^2+hc(1/\lambda-1/\lambda_k)$. We must now use λ and not λ' in Eq. (47) since the factor multiplying the matrix element in this equation arose originally from the change in energy of the atom as a whole. The new absorption coefficient is therefore

$$\frac{\tau}{\rho}(\lambda) = \frac{\lambda}{\lambda'}\cdot\frac{\tau}{\rho}(\lambda'),$$

where

$$\frac{1}{\lambda}-\frac{1}{\lambda_k}=\frac{1}{\lambda'}-\frac{1}{\lambda_k'}.$$

When one calculates this new absorption it turns out, however, that the agreement with experiment is worse. This does not mean that if one calculated the absorption coefficient for gold using a larger screening constant that one would find better agreement with experiment, but merely that the use of a large screening constant for lead agrees better with experiment than the use of a small one with gold, and is probably to be attributed to the rapid loss of accuracy of the model as Z is decreased.

That the agreement with experiment is worse can be seen roughly from the following considerations. At the absorption edge $\lambda/\lambda'=(Z'/Z)^2$ by Moseley's law, where Z' is the atomic number used in the calculation and Z

[30] M. Stobbe, Ann. d. Physik (5), **7**, 661 (1930).

that of the atom to which it is now applied. But the observed absorption coefficients are closely in the ratio $(Z'/Z)^3$ at the edge; and the theoretical values are already too low. It is therefore not thought worth while to publish the modified values.

The writer wishes to thank Dr. I. I. Rabi for suggesting this problem, and also to express his appreciation to Professor E. H. Kennard for his constant interest and for the many stimulating discussions throughout the writer's graduate study.

INTERCHANGE OF TRANSLATIONAL, ROTATIONAL AND VIBRATIONAL ENERGY IN MOLECULAR COLLISIONS

By Clarence Zener*
Jefferson Physical Laboratory
Harvard University

(Received January 5, 1931)

Abstract

The change in internal energy of molecules upon collisions has been analysed. Formulae, (26) to (27-C), for the effective cross section of inelastic collisions have been obtained as functions of known properties of the molecules, subject to certain conditions. These conditions are: the atoms which come into contact during collision must belong to the first row of the periodic table; the vibrational quantum numbers which suffer a change must be small.

Vibrational quantum numbers have a marked reluctance to change during collisions at room temperature. The probability that a N_2 molecule in its first excited vibrational state transfer its energy to He in a head on collision is 0.0^76. The probability that another N_2 molecule absorb this energy is 0.0^44. A lack of resonance of 0.01 volt can decrease the effective cross section by a factor of 0.02.

Rotational quantum numbers change readily except in unusual cases.

I. Introduction

IN A gaseous system we often wish to know the effective cross section of a collision between two systems in which one or both suffer a change of quantum numbers. If this change involves electron jumps, as in the quenching of resonance radiation, it is not limited to collisions in which the systems would be said classically to come into contact. Such transitions have been observed to take place when the closest distance of approach is many times the classical diameter of the systems.[1] In this type of collision the changes in the motion of the two systems as a whole may be relatively unimportant in comparison to the change of quantum numbers.

In another interesting type of collision the electronic states remain unaltered, and the vibrational and rotational states are changed. The experimental data have been discussed by Oldenberg.[2] In many cases the probability of a transfer is very small even in head-on collisions. In such collisions changes in the internal molecular quantum numbers are unimportant in comparison to changes in the motion of the two systems as a whole. A study of the latter change must thus precede a study of the former. Such a procedure is adopted in this paper. The exact motion of the centers of gravity of the two colliding systems is found when the internal coordinates are replaced

* National Research Fellow.

[1] Baxter, J.A.C.S. **52**, 3920 (1930); Boeckner, Bureau Stand. **5**, 13 (1930).

[2] Oldenberg, Phys. Rev. **37**, 194 (1931).

by their averaged values. This motion corresponds to an elastic collision. The internal motions of the systems are then treated as perturbations that give rise to changes in the internal quantum numbers during collision.

The discussion of collision phenomena is preceded by an examination of inter-molecular forces (II). The principles of energy interchange may be most clearly analyzed in systems so idealized that all irrelevent difficulties are absent. Thus the interchange of vibrational and translational energy is investigated in the simplified collision of an atom and a diatomic molecule where all motion is confined to a line (III). Similarly the interchange of rotational and translational energy is examined first for the collision of an atom with a rigid symmetrical molecule, all motion being limited to a plane (IV). The results of the investigation of these idealized collisions are then combined in such a way as to give definite numerical information about collisions in an actual gaseous system (V).

II. Inter-Molecular Forces

In ordinary collisions the inter-molecular forces need be known only for those inter-molecular distances in which the overlapping of electrons is slight. At these collision distances the mutual energy may be split to a good approximation into three parts: that due to van der Waal's attraction, the negative coulomb energy arising from interpenetration of electrons, and the repulsive resonance energy. The mutual energy between two molecules is approximately the sum of the mutual energies between the constituent atoms, provided the resonance forces are taken to be repulsive.

London and Eisenschitz[3] have shown that the repulsive resonance energy between two H atoms dominates the attractive energies. This may safely be considered to be true for all atoms in the first row of the periodic table. However, this resonance energy becomes smaller both with an increase of the total quantum number n[4] and of the azimuthal quantum number l[5]. Hence the following considerations will be confined to atoms in the first row.

In the outer region of an atom, i.e., the region that overlaps in ordinary thermal collisions, the electronic density varies approximately[6] as $r^{n^*}\exp(-2\alpha s)$. Here s is the distance from the nucleus, and α is the square root of the ionization potential.[7] The asymptotic expansion of the resonance energy[8] between two atoms will contain the factor $\exp-(\alpha_1+\alpha_2)R$, where α_1 and α_2 refer

[3] E. Eisenschitz and F. London, Zeits. f. Physik **60**, 491 (1930).

[4] W. Heisenberg, Zeits. f. Physik **49**, 619 (1928).

[5] M. Delbruck, Proc. Roy. Soc. **129**, 686 (1930).

[6] D. R. Hartree, Proc. Camb. Phil. Soc. **24**, 89 (1928).

[7] Energy, length, mass will in this paper be expressed in the atomic units 13.53 volts, 0.528×10^{-8} cm, m_e, unless otherwise specified.

[8] This may be verified by examining the general type of integral that arises in calculating the resonance energy. See Zener and Guillemin, Phys. **34**, 999 (1929), Eqs. (28) and (29). When the integral logarithms are replaced by their asymptotic expansions all terms will have the factor $\exp-(\alpha_1+\alpha_2)r$. This opportunity is taken for pointing out that $m-v+1$ should replace $m-v$ in Eq. (25), and $m!/(m-v)!\cdot v+1$ should replace $e^{-\alpha}A_v(1,\alpha)$ in (26) and (30) of this reference.

to the two atoms, and R is their nuclear separation. The mutual potential between atoms or symmetrical diatomic molecules, averaged over all internal molecular coordinates, will contain the factor $\exp-(\alpha_1+\alpha_2)r$, where r is the distance between the centers of gravity of the two systems. An approximation to the actual potential may thus be written as

$$V(r) = E'' e^{(\alpha_1+\alpha_2)(r_{E''}-r)}. \tag{1}$$

The constants E'', $r_{E''}$ are to be experimentally determined. They have the relation $V(r_{E''}) = E''$. If $E'' = E_{300}$ denotes the average energy of a gas molecule at room temperature, then r_{300} will be the classical average closest distance of approach.

It is desirable to compare the theoretical formula (1) with experimental data. The data on inter-molecular forces have been thoroughly reviewed by Lennard-Jones.[9] If the constants c, α are determined to make $c\exp(-\alpha r)$ join smoothly to the repulsive energy formulae of Lennard-Jones at r_{300}, then α should be considered as the experimental value of $\alpha_1+\alpha_2$. A comparison of these constants is given in Table I.

TABLE I. *Energy constants.*

	Lennard-Jones	Spectroscopic
H_2	2.08	2.12
He	3.50	2.68
Ne	2.2	2.5

III. VIBRATION-TRANSLATION

The interchange of vibrational and translational energy will be investigated in the collision of atom A with the molecule $B-C$, the atoms A, B, C being confined to a line.

$$A \quad B \quad C$$

This interchange will be a function of the various physical parameters, such as the force beinding B and C, the repulsive force begween A and B, the initial translational and vibrational energies, and the relative masses.

If the atoms were sufficiently massive, and if the translational and vibrational energies were sufficiently great, only an investigation by classical mechanics would be necessary. But these conditions are not satisfied in the interesting cases where only the first vibrational states are excited. Nevertheless, it is profitable to consider the classical picture, as in general the same qualitative dependence upon the physical parameters will be present in the mechanics of the classical and quantum theory.

The classical picture will now be used in finding the conditions of maximum transfer of energy from vibration to translation with the optimum phase relation between the vibrational and translational motion. The system is first simplified by assuming the impact between A and B to be instantane-

[9] R. H. Fowler, Statistical Mechanics, Chap. X (1929).

ous. Then if the mean vibration velocity of B is comparable to the relative velocity of A and the molecule $B-C$, with an optimum phase relation, the impact between A and B will occur when the molecule has all its internal energy in the form of kinetic energy. The energy transfer will then be a maximum when the masses of A and B are nearly equal. However, the vibrational energy of light molecules is much larger than the mean translational energy at room temperatures. Hence in order that A strike B while the latter has a maximum velocity, A must be lighter than B.

The effect of the finite time of impact between A and B is now examined. If this time is small in comparison to the period of oscillation of the molecule B-C, the impact may be regarded as instantaneous. As it becomes large in comparison to the period of oscillation, the atom will tend to act only upon the center of gravity of the molecule. The interchange of vibrational and translational energy then becomes small. With a fixed initial translational energy, a decrease in the mass of A will lessen this time of impact, and thus increase this interchange irrespective of the mass of B.

It is of interest to compare this time of impact with the period of oscillation in collisions between actual molecules. If r is the distance between A and B, their mutual energy may be taken to be

$$V(r) = E''e^{-\alpha(r-r_E'')} \tag{1'}$$

as was seen in II. If E'' is set equal to the mutual energy E, then a reasonable value for the time of impact is the time τ_i during which $r<r_0$. Here, r_0, together with F, is determined to make the parabola

$$U(r) = F(r - r_0)^2 \tag{2}$$

join smoothly to $V(r)$ at $r=r_E$. Thus (1') has been replaced by the potential

$$W(r) = \begin{cases} F(r - r_0)^2, & r < r_0. \\ 0 \qquad\quad , & r > r_0. \end{cases} \tag{3}$$

The ratio of τ_i to the period of vibration of B-C, τ_v, is one half the ratio of the frequency of vibration of the molecule to the frequency of vibration of a particle of mass

$$\mu = \frac{M_A(M_B + M_C)}{M_A + M_B + M_C} \tag{4}$$

in the potential (2). This ratio is

$$\beta = \frac{40}{\alpha}\,\frac{\omega_0}{8106}\left(\frac{\mu}{E}\right)^{1/2}$$

where ω_0 is the wave number of the molecule, μ is expressed in units of atomic hydrogen, and E is in units of the mean energy of a gas molecule at room temperature, E_{300}. A numerical example shows this ratio to be relatively large. For instance, in the collision of He with N_2 at room temperature, $\alpha=2.4$, $\omega_0=2345$, $\mu=3.5$ $E\backsimeq 1$, giving $\beta=9$.

The above considerations lead to the following classical conclusions for light molecules. Since the intra-molecular binding forces are large in comparison to the inter-molecular repulsive forces at collision distances, and since the internal energy of these molecules is large in comparison to their temperature equilibrium translational energy, the interchange of vibrational and translational energy will be small. H_2 will absorb more readily than any other molecule translational energy not only from a C-H bond but from any light molecule.

A precise quantitative theory for the one dimensional collision is developed by the following quantum mechanical analysis.

The coordinates will be taken to be: the center of gravity of the complete system, X; the nuclear separation of molecule B-C, x; and the distance between the atom A and the center of gravity of the molecule, r. This choice has been made in order that the kinetic energy may be written as

$$T = T_X + T_x + T_r.$$

The wave equation, after eliminating the center of gravity of the complete system, then becomes[7]

$$\left\{\frac{1}{\mu_m}\frac{d^2}{dx^2} + \frac{1}{\mu}\frac{d^2}{dr^2} - V(x) - V(x, r) + E\right\}\Psi = 0 \tag{5}$$

Here

$$\mu_m = \frac{M_B M_C}{M_B + M_C}$$

and μ is given by (4). The energy $V(x)$ is the potential energy of the isolated molecule B-C, and $V(x, r)$ is the mutual energy of atom A and the molecule. The energy E has a continuous range of values. If E_i is the energy of the isolated molecule, then $p_i = \mu^{1/2}(E - E_i)^{1/2}$ is proportional to the momentum associated with the translational motion.

Let the normalized function $\psi_i(x)$ be a solution of the wave equation for the isolated molecule, namely

$$\left\{\frac{1}{\mu_m}\frac{d^2}{dx^2} - V(x) + E_i\right\}\Psi_i(x) = 0.$$

Corresponding to the physical requirement that before collision the molecule be in the vibrational state v_0, a solution of (5) is to be found of the form

$$\Psi \overset{r\to\infty}{=} \frac{(e^{ip_{v_0}r} + e^{-ip_{v_0}r})}{(p_{v_0})^{1/2}} + \sum_v \gamma_{v_0}{}^v \frac{e^{-ip_v r}}{(p_v)^{1/2}}\Psi_v(x) \tag{6}$$

The summation is over all indices for which p_v is real. The probability that the molecule has changed its vibrational quantum number from v_0 to v will be $|\gamma_{v_0}{}^v|^2$.

In order to obtain the coefficients $\gamma_{v_0}{}^v$, ψ is expanded as follows:

$$\Psi = \sum_v Q_v(r)\Psi_v(x). \tag{7}$$

The Q_v's are undetermined functions. Substitution of this expansion into (5) gives

$$\sum_v \left\{ \frac{d^2}{dr^2} - \mu V(x, r) + p_v^2 \right\} Q_v(r) \Psi_v(x) = 0.$$

Multiply by $\Psi_v(x)$ and integrate with respect to x.

$$\left\{ \frac{d^2}{dr^2} - \mu V_v^v(r) + p_v^2 \right\} Q_v(r) = \mu \sum_{v' \neq v} Q_{v'}(r) V_v^{v'}(r) \tag{8}$$

where

$$V_v^{v'}(r) = \int \Psi_v(x) V(x, r) \Psi_{v'}(x) dx.$$

By neglecting the right member an equation for the zeroth approximation, $Q_v^0(r)$, is obtained.

$$\left\{ \frac{d^2}{dr^2} - \mu V_v^v(r) + p_v^2 \right\} Q_v^0(r) = 0.$$

Since $V_v^v(\infty) \to 0$, $Q_v^0(r)$ becomes sinusoidal for large r. Denote that particular solution that vanishes at $r=0$ by $U(p_v/r)$. Let this solution be so normalised that

$$U(p_v/r) \overset{r \to \infty}{=} \frac{\sin(p_v r + \theta_v)}{p_v^{1/2}}. \tag{9}$$

Choose another particular solution by its asymptotic behavior

$$X(p_v/r) \overset{r \to \infty}{=} \frac{e^{-i(p_v r + \theta_v)}}{p_v^{1/2}}. \tag{9'}$$

The zeroth approximation to $Q_v(r)$ corresponds to an elastic collision in which the molecule has the quantum number v. Hence

$$Q_v^0(r) = \begin{cases} U(p_v/r), & v = v_0. \\ 0, & v \neq v_0. \end{cases} \tag{10}$$

The first approximation to $Q_v(r)$ is obtained by substituting this zeroth approximation into the right member of (8).

$$\left\{ \frac{d^2}{dr^2} - \mu V_v^v(r) + p_v^2 \right\} Q_v^1(r) = \begin{cases} \mu U(p_{v_0}/r) V_{v/0}^v, & v \neq v_0 \\ 0, & v = v_0. \end{cases} \tag{11}$$

The solution of these equations that satisfies the boundary condition (6) is

$$\begin{aligned} -Q_v^1(r) &= \mu X(p_v/r) \int_0^r U(p_v/r') V_{v_0}^v(r') U(p_{v_0}/r') dr' \\ &+ \mu U(p_v/r) \int_r^\infty X(p_v/r') V_{v_0}^v(r') U(p_{v_0}/r') dr' \end{aligned} \tag{12}$$

$$Q_{v_0}^1(r) = C_1 X(p_{v_0}/r). \tag{12'}$$

The validity of (12) may be verified by direct substitution into (11). The left member vaishes identically except for the term

$$-\mu U(p_{v_0}/r)V_{v_0}^{v}\{X'(p_v/r)U(p_v/r) - X(p_v/r)U'(p_v/r)\}.$$

Now the subtraction of

$$X\left(\frac{d^2}{dr^2} - \mu V_{v}^{v} + p_v^2\right)U = 0$$

from

$$U\left(\frac{d^2}{dr^2} - \mu V_{v}^{v} + p_v^2\right)X = 0$$

gives

$$\frac{d}{dr}(X'U - XU') = 0.$$

Hence

$$X'U - XU' = C.$$

But from (9), (9′), $C = -1$. Hence (12) satisfies (11) identically.

C_1 is to be determined from the equation of continuity,—

$$\int\left(\Psi\frac{d}{dr}\overset{*}{\Psi} - \overset{*}{\Psi}\frac{d}{dr}\Psi\right)dx = 0.$$

Since the second integral in (12) vanishes as r becomes infinitely large, the first two approximations to the coefficients in the expansion (7) gives a ψ of the form (6) with

$$\begin{gathered}\gamma_{v_0}^{v} = \mu\int_0^\infty dr\int_{-\infty}^{\infty} dx U(p_v/r)\Psi_v(x)V(x, r)\\ \cdot U(p_{v_0}/r)\Psi_{v_0}(x),\quad v \neq v_0.\\ \gamma_{v_0}^{v_0} = C_1.\end{gathered} \tag{13}$$

The conditions under which this first approximation is valid will now be investigated. In general the successive approximations of the Born collision method do not converge. However, if the first terms become smaller, they may form a semi-convergent series that has a physical meaning. The relative magnitude of successive approximations will depend upon the physical parameters of the system. The application of (13) is thus limited to those systems with parameters such that the first successive approximations to the solutions of (8) which vanish at $r=0$ become smaller. It will be found that all systems examined in this study satisfy this condition.

An approximation to the probability is obtained by assuming a simplified potential of the form

$$V(x, r) = E''e^{-\alpha(r-r_{E''})}(1 + qz)$$

where z is the displacement of x from its equilibrium value. A reasonable value for q is the coefficient in the first term of the expansion of $e^{-\lambda\alpha z}$, where

$$\lambda = \frac{M_C}{M_B + M_C} \cdot \tag{14}$$

Neglecting the higher powers of z limits this analysis to molecules in which the amplitudes of vibration are relatively small. With this potential $\gamma_{v_0}^{v}$ may be factored as

$$\gamma^{v}_{0} = \xi_{v_0}^{v}\eta_{pv_0}^{pv}$$

where

$$\xi_{v_0} = q\int_{-\infty}^{\infty}\Psi_{v}(z)z\Psi_{v_0}(z)dz \tag{15}$$

and

$$\eta_{pv_0}^{pv} = \mu E''\int_{0}^{\infty}U(p_v/r)e^{-\alpha(r-r_E'')}U(p_{v_0}/r)dr. \tag{15'}$$

The U's are solutions of

$$\left(\frac{d^2}{dr^2} - \mu E''e^{-\alpha(r-r_E'')} + p^2\right)U(p/r) = 0 \tag{16}$$

and are normalised to satisfy (9).

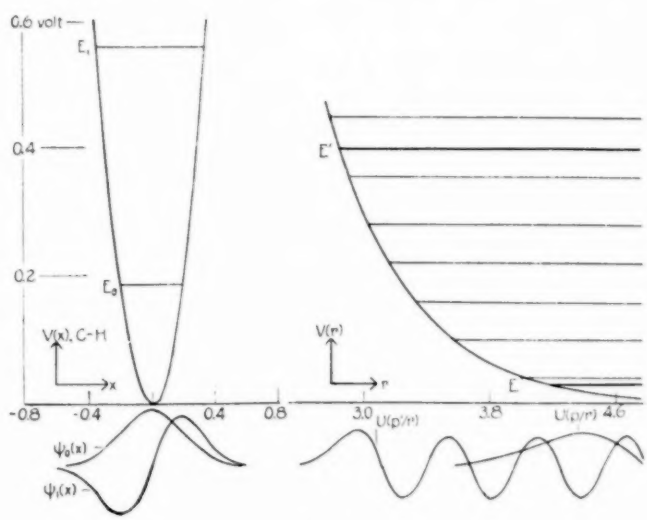

Fig. 1.

Since only a very rough approximation to $\eta_{p'}^{p}$ can be obtained without great analytical difficulties, it is profitable to consider first the qualitative dependence of $\eta_{p'}^{p}$ upon the physical parameters.

In Fig. 1 are drawn the potentials and pertinent wave functions. The energy levels to $V(r)$ are drawn for energy values whose $U(p/r)$ have nodes at

$r=r_0$, where r_0 is chosen arbitrarily at a point where $V(r)$ first becomes appreciable. Here E, E' refer to the initial and final translational energies, with $E<E'$, and p, p' to the corresponding momenta.

An increase of the molecular binding force $-dV(z)/dz$ relative to the repulsive force $-dV(r)/dr$ will increase the number of energy levels between E' and E, thus increasing the fluctuations in sign of the integrand of (17), and thus decreasing $\eta_{p'^p}$. An increase in the reduced mass μ will have a similar effect.

An increase of E and E' by similar amounts will increase $\eta_{p'^p}$ by lessening the number of energy levels between E and E'.

An examination shows that in ordinary thermal collisions between molecules whose atoms belong to the first row of the periodic table, the first maximum of $g(p/r)$ lies in the region $r<r_0$, and that several "energy levels" always lie between E and E'. The qualitative results of the classical and the quantum mechanical treatment are thus similar in such collisions. In the language of the former a decrease in the slope of $V(r)$ or an increase of the reduced mass μ results in an increase of the time of collision. In the language of the latter, similar changes result in an increased fluctuation of sign in the integrand of (17).

An analytical approximation to $\eta_{p'}^{p}$ is obtained by replacing the exponential potential by a potential which renders Eq. (16) soluble in known functions. Such a potential is

$$V_a = \frac{A}{(r-B)^2}, \quad r > B$$

$$V_a = \infty, \quad r < B.$$

The constants A, B are adjusted to make V_a as similar as possible to the potential (1′) in the important range of r. With the choice

$$V_a = \frac{4E''/\alpha^2}{(r - r_{E''} + 2/\alpha)^2} \tag{17}$$

the two potentials join smoothly at $r=r_{E''}$. A reasonable value of E'' is $(E\,E')^{1/2}$.

The differential equation (16) now becomes

$$\left\{\frac{d^2}{dx^2} - \frac{4\mu E''/\alpha^2}{x^2} + p^2\right\} U(p/x) = 0$$

where $x=r-r_{E''}+2/\alpha$. Its solution is the Bessel function

$$U(p/x) = \left(\frac{\pi}{2}\right)^{1/2} x^{1/2} J_v(px) \tag{18}$$

with

$$v = (4\mu E''/\alpha^2 + 1/4)^{1/2} \backsimeq 2(\mu E'')^{1/2}/\alpha.$$

This solution is normalized to satisfy (9).

The expression (15′) for $\eta^{p}_{p'}$ now becomes

$$\eta^{p}_{p'} = 2\pi\frac{\mu E''}{\alpha^2}\int_0^\infty \frac{J_v(px)J_v(p'x)dx}{x}.$$

The substitution of

$$\int_0^\infty \frac{J_v(px)J_v(p'x)}{x}dx = (p/p')^v/2v, \quad p < p'$$

(Watson, Theory of Bessel Functions, p. 401) reduces this to

$$\eta^{p}_{p'} = \frac{\pi(\mu E'')^{1/2}}{2\alpha}(E/E')^{(\mu E'')^{1/2}/\alpha}. \tag{19}$$

If the molecule is assumed to be vibrating as a linear oscillator, then (15) reduces to

$$\xi^{v}_{v-1} = \frac{\alpha}{2}\left(\frac{v}{\mu_m(E_v - E_{v-1})}\right)^{1/2}, \tag{20}$$

all the other integrals vanishing.

As a numerical example, consider the one dimensional collision at room temperature of He with N_2, in which N_2 is deactivated from the first excited vibrational state to the normal state. Here $\alpha = 2.14$, $E/E' = 1/8$, $\mu E'' = 58$, $\mu_m(E_1 - E_0) = 274$. The probability for this deactivation is thus given by

$$(\gamma_0^1)^2 = (\xi_0^1)^2(\eta_{p'}^{p})^2 = 0.004 \times 0.0^4 15 = 0.0^7 6. \tag{21}$$

IV. Rotation-Translation

The principles involved in the interchange of rotational and translational energy are most readily studied in the collision of a rigid diatomic molecule and an atom, all motion being confined to a plane. This collision will first be discussed from the classical standpoint.

The symmetry of the molecule limits the energy transfer in a single impact. If an electron is excited to such a state that its time average distribution is nearly spherical, then the energy interchange in a collision will become small. Hence the energy transferred during a collision will be very dependent upon the electronic state of the molecule. This has been empirically observed.[10] Comparison of the time of collision with periods of rotation is not important, since the latter is usually the larger.

In order to treat this collision problem by quantum mechanics, a suitable mutual potential must be found. If the analysis is limited to symmetrical diatomic molecules, a simple potential having the necessary properties is

$$V(r, \epsilon) = V(r)\{1 + h(\cos^2\epsilon - \tfrac{1}{2})\}. \tag{22}$$

Here r has the same meaning as in the previous section, and ϵ is the angle between the molecular axis and the line joining the atom with the center of the molecule. The potential $V(r)$ is taken to be (1′). A reasonable value for h

[10] R. Rompe, Zeit. f. Physik **65**, 428 (1930).

is obtained by requiring that the ratio $V(r, 0)/V(r, \pi/2)$ equal the ratio $V(r+x_0/2)+V(r-x_0/2)/2V([r^2+x_0^2/4]^{1/2})$, where x_0 is the nuclear separation in the molecule, and where r is set equal to r_{300}. This condition gives

$$h = \frac{2\left[e^{\alpha x_0/2} + e^{-\alpha x_0/2} - 2e^{-\alpha([r_{300}^2+x_0^2/4]^{1/2}-r_{300})}\right]}{\left[e^{\alpha x_0/2} + e^{-\alpha x_0/2} + 2e^{-\alpha([r_{300}^2+x_0^2/4]^{1/2}-r_{300})}\right]}. \tag{23}$$

By considerations similar to those leading to (5), the following wave equation of our two dimension system of a rotator and an atom may be obtained:

$$\left\{\frac{1}{I}\frac{d^2}{d\phi_1^2} + \frac{1}{\mu}\frac{1}{r}\frac{d}{dr}r\frac{d}{dr} + \frac{1}{\mu}\frac{1}{r^2}\frac{d^2}{d\phi^2} - V(r,\epsilon) + E\right\}\Psi = 0.$$

Here ϕ_1, ϕ are the azimuthal angles associated with the molecule and the line joining the atom to the center of the molecule.

A solution of this equation corresponding to the molecule being in a definite rotational state before collision, and having a probability of being in several after the collision, is obtained by a method closely analogous to that of the previous section. The zeroth approximation is of the form

$$\Psi = e^{im_1\phi_1}\sum_{m=-\infty}^{\infty} e^{i\delta_m} e^{im\phi} U_m(p_{m_1}/r).$$

The phase factor δ_m[11] is arbitrary. The function $U_m(p_{m_1}/r)$ is the solution of

$$\left\{\frac{1}{\mu}\frac{1}{r}\frac{d}{dr}r\frac{d}{dr} - \frac{1}{\mu}\frac{m^2}{r^2} - V(r) + E - \frac{m_1^2}{I}\right\}U_m(p_{m1}/r) = 0$$

that vanishes[12] at $r=0$ and is normalised to satisfy

$$U_m(p_{m_1}/r)^{r\to\infty} = \frac{\sin(p_{m1}r + \beta_{m1})}{(p_{m1}r)^{1/2}}.$$

The only allowable transitions are $m = \pm 2$. The probability that the quantum numbers change from m_1, m to $m_1-2, m+2$ is

$$\left(\gamma\begin{matrix} m_1-2, & m+2 \\ m_1, & m\end{matrix}\right)^2 = \frac{h^2}{16}\left\{\int_0^\infty U_m(p_{m_1}/r)V(r)U_{m+2}(p_{m_1-2}/r)rdr\right\}^2$$

or

$$\left(\gamma\begin{matrix} m_1-2, & m+2 \\ m_1 & m\end{matrix}\right)^2 \leqq \frac{h^2}{16}\left\{\int_0^\infty U_0(p_{m_1}/r)V(r)U_0(p_{m_1-2}/r)rdr\right\}^2. \tag{24}$$

However, these individual probabilities are not of primary interest, but only the effective cross section of such a collision. If

$$\gamma\begin{matrix} m_1-2 & m+2 \\ m_1 & m\end{matrix} = \begin{matrix} 1, & m < m_0 \\ 0, & m > m_0\end{matrix}$$

[11] W. Pauli, Probleme der Modernen Physik p. 42. (Hirzel, Leipzig, 1928.)

[12] The formulation of this boundary condition is rather arbitrary, as an equally justifiable condition would be to require that $U(p/r)$ have a zero slope at $r=0$. However, as long as the probability remains negligibly small that the atom pass through the molecule, both boundary conditions will give the same result.

this effective cross section would be equal to the kinetic theory cross section, σ_{KT}. Here, m_0 is the largest m for which the molecule and atom would classically come into contact. An upper limit to the effective cross section σ_{eff} is obtained by using the equality sign in (24) when $m < m_0$, and setting the left member equal to zero when $m > m_0$. This gives

$$\sigma_{eff} < \frac{h^2}{16}\left\{\int U_0(p/r)V(r)U_0(p'/r)rdr\right\}^2 \sigma_{KT},$$

in which p_{m_1}, p_{m_1-2} have been replaced by p, p'.

An approximation to this integral is obtained in a manner identical to that used in the previous section. The only difference is that here the relation $v = 2(\mu E'')^{1/2}/\alpha$ is exact. An upper limit to the cross section is then

$$\sigma_{eff} < \frac{h^2}{16}(\eta_{p'}^{p})^2 \sigma_{KT}$$

in which $\eta_{p'}{}^{p}$ is given by (19).

As a numerical example, consider the probability that a N_2 molecule, considered as non-vibrating, give two quanta of rotational energy to a He atom in a two dimensional collision at room temperature. In this example $h = 1.3$, $(\eta_{p'}{}^{p})^2 = 11$, resulting in

$$\sigma_{eff} < 1.2\,\sigma_{KT}.$$

V. General Collisions

In the previous sections discussion has been restricted to a one-dimensional collision of an atom and a vibrating molecule, and to a two-dimensional collision of an atom and a rotating molecule. The analysis is now extended to three-dimensional collisions between two molecules both of which vibrate and rotate.

The quantum mechanical treatment of such a collision in three dimensions is difficult, since the equation whose solution corresponds to an elastic collision is not in general separable in the mutual coordinates. However, in the classical theory collisions of the second kind are most probable between an atom and vibrator when all motion is confined to a line, and between an atom and rotator when all motion is confined to a plane. We may expect a similar relation in quantum mechanics, so the previous inequalities obtained for one and two dimensional collisions may be taken to be valid for three-dimensional collisions.

Provided the amplitude of vibrations are relatively small, the mutual potential may be approximated by the product of functions of individual coordinates. Thus when both molecules are diatomic, a simple potential is

$$V = V(r)(1 + a_1z_1)(1 + a_2z_2)(1 + f_1(\epsilon_1)(1 + f_2(\epsilon_2)) \qquad (25)$$

where $V(r)$ is taken to be $(1')$; z_1 and z_2 are the displacements of the internuclear separations of the two molecules from their equilibrium values; ϵ_1 and ϵ_2 are the mutual angles between the line joining the centers of gravity of the

two molecules and the axes of the two molecules; and f_1, f_2 are arbitrary functions.

When the mutual potential is so factorable, the probability of an inelastic collision will also be expressible as a product. One factor of this product will be a function of the constants of translational motion. Denote this factor by $P_{E,E'}$. Each of the other factors will be associated with a change of one quantum number. These factors will be independent of one another. For example, in a collision in which the vibrational quantum number v changes to $v-1$, the associated probability factor $P_{v,v-1}$ will not be influenced by changes of other quantum numbers.

Hence if σ_{KT} is the kinetic theory cross section of a collision, the effective cross section of a collision in which the quantum numbers $v_1, l_1, \cdots$ change to $v_1', l_1', \cdots$ will be

$$\sigma_{\text{eff}} < \sigma_{KT} P_{E,E'} P_{v_1,v_1'} P_{l_1,l_1'} \cdots . \tag{26}$$

In the following description of these factors, atomic units[7] are used.

When μ refers to the reduced mass of the two systems, α to the sum of the square roots of the ionization energies (in units of 13.53 volts) of the two atoms which become adjacent during collision, $E(E')$ to the smaller (greater) of the initial and final mutual energies of translation, and $E'' = (E\,E')^{1/2}$, reference to (19) shows that for sub-elastic collisions

$$P_{E,E'} = \frac{\mu E''\pi^2}{4\alpha^2} \cdot (E/E')^{2(\mu E'')^{1/2}/\alpha}. \tag{27a}$$

In super-elastic collisions[13] $P_{E,E'}$ is to be multiplied by the factor $(E/E')^{1/2}$.

When the mutual potential contains only the first power of the displacement of a vibrator from its equilibrium position, the vibrational quantum number can change only by unity. Reference to (20) shows that the factor $P_{v,v-1}$ associated with a change of vibrational quantum number $v \rightarrow v-1$ or $v-1 \rightarrow v$ is

$$P_{v,v-1} = \frac{\lambda^2\alpha^2 v}{4\mu_m(E_v - E_{v-1})} \tag{27-b}$$

where the difference in energy between the two states is $E_v - E_{v-1}$, where λ is given by (14), and μ_m is the reduced mass of the vibrator.

If one of the colliding systems is a symmetrical diatomic molecule, the dependence of the interaction energy upon the mutual angle ϵ is approximately expressed by the factor $1+h(\cos^2\epsilon - \frac{1}{2})$, corresponding to (22). The constant h, determined from (23), varies from 1 to 1.5 for diatomic symmetrical molecules whose electronic states are normal. If the electronic states are highly excited, h may approach zero. Insofar as this approximation is valid, the molecule can change its rotational quantum number l by only ± 2. The corresponding probability factor is

$$P_{l,l\pm 2} = h^2/16. \tag{27-c}$$

The statistical factor[13] relating the probability of the transition $l \rightarrow l+2$ to that of $l+2 \rightarrow l$ is neglected.

A few general observations will be drawn from the above formulae.

The molecules to which this analysis applies change a few rotational quantum numbers freely.

The transfer of vibrational energy may be difficult even in cases of exact resonance,[14] e.g. the cross section for the transfer of vibrational energy from a N_2 molecule in its first excited state to a normal N_2 at room temperature is $0.0^{4}4 \times$kinetic theory cross section. This resonance cross section increases both with the reduced mass of the two molecules, and with temperature. However, the effects of a lack of resonance are most marked in heavy molecules. If the reduced mass is 30 m_H, the effective cross section is reduced by a factor of 0.025 if the translational energy must change by 0.01 volt at room temperature.

The efficiency of H_2 as contrasted to He in deactivating molecules[15] cannot be explained as due to their difference in mass. It is to be ascribed to the much greater facility with which H_2 can absorb a considerable amount of energy by a change of a few rotational quantum numbers, than by a change of translational energy.

The writer wishes to express his gratitude to Professor Kemble for frequent discussions, and to Harvard University for enabling him to commence this study in Bristol, England.

[13] Ruark and Urey, Atoms, Molecules and Quanta p. 491, McGraw-Hill (1930).

[14] O. K. Rice, Zeits. f. physik. Chem. **7**, 226 (1930).

[15] C. N. Hinshelwood, The Kinetics of Chemical Change in Gaseous Systems, Oxford, 1929, p. 151.

THE ABSORPTION COEFFICIENT FOR SLOW ELECTRONS IN THALLIUM VAPOR

By Robert B. Brode
Department of Physics, University of California

(Received January 19, 1931)

Abstract

The absorption coefficient α has been observed by sending a beam of electrons through thallium vapor and measuring the decrease in intensity of the beam as a function of the pressure of the vapor. α, plotted as a function of the velocity of the electrons, decreases rapidly to a minimum of 15 at 1.4 volts, rises less rapidly to a maximum of 51 at 4.5 volts, and then slopes off gradually to 20 at 100 volts.

IN THE study of the absorption coefficients of the monatomic elements of the periodic system, all of the noble gases,[1,2] four of the alkali metals[3] and three of the elements of the second column, i.e., Hg,[4] Cd and Zn,[5] have been investigated. Thallium has been chosen for the extension of these observations to the third column of the periodic table. In the vapor state thallium is monatomic but it differs from all of the elements previously investigated in the nature of its normal spectroscopic state. The thallium normal state is of a P type while all of the other elements mentioned above have normal states of the S type.

For the range of pressure (5×10^{-3} to 5×10^{-2} mm of Hg) necessary for satisfactory measurements, thallium requires temperatures from 550 to 630° C. The apparatus was therefore enclosed in a quartz tube. The electric connections to the apparatus were made by fusing molybdenum wires into quartz capillaries. This was not a vacuum tight seal but it was sufficient to prevent the rapid diffusion of the metal vapor out of the quartz tube. The molybdenum wires were continued in quartz tubes to the outside of the furnace. Quartz to Pyrex graded seals enabled vacuum tight connections to be made by tungsten seals through the Pyrex.

The metal parts of the apparatus were made of tantalum as shown in the cross-sectional view of the apparatus in Fig. 1. The tungsten filament, F, was the source of electrons which were bent in a circle through the slit S and into the collecting box B at the end of the path. The mean radius of the path was 7.0 mm and the widths of the slits at F, S, and B were 0.5, 1.0, and 0.5 mm respectively.

In the preparation of the tube the spaces on both sides of the quartz capillaries were connected to the vacuum pumps. The apparatus was baked

[1] C. Ramsauer, Ann. d. Physik **72,** 345 (1923).
[2] C. E. Normand, Phys. Rev. **35,** 1217 (1930).
[3] R. B. Brode, Phys. Rev. **34,** 673 (1929).
[4] R. B. Brode, Roy. Soc. Proc. **A125,** 134 (1929).
[5] R. B. Brode, Phys. Rev. **35,** 504 (1930).

out to 800°C and the metal parts glowed to a bright yellow by an induction furnace. A small amount of thallium metal was then slowly distilled into the lower end of the apparatus. The vacuum connections to the quartz tube and to the Pyrex seals were sealed off.

The main portion of the tube was enclosed in a non-inductively wound electric furnace. The small tube containing the metal was enclosed in a heavy copper tube in a separate furnace directly below the main furnace. The temperatures in the two furnaces were measured by chromel-alumel thermocouples. From the vapor pressure equation and the temperature of the lower furnace the pressure of the thallium vapor could be calculated. This pressure was corrected for the difference in pressure caused by the difference in temperatures of the upper and lower furnaces.

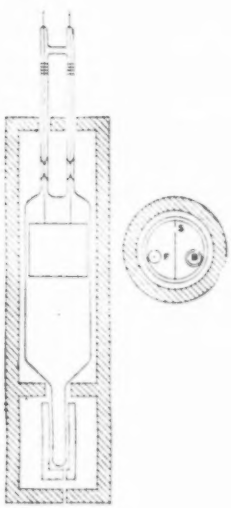

Fig. 1. Diagram of apparatus and furnaces.

The measurements of the absorption coefficient were made in the same way as those previously described for mercury.[4] The total emission from the filament was assumed to be proportional to the initial current I_0 that would have reached the end of the path if there had been no collisions. The current I at the end of the path was measured by a galvanometer connected to the box B. The currents I and I_0 are related by the equation, $I = I_0 e^{-\alpha x p}$, where α is the absorption coefficient, x the path length and p the pressure of the absorbing vapor. From this equation the logarithm of the ratio of I/I_0 should be a linear function of the pressure. Measurements were made at from 3 to 5 pressures for every velocity studied and the value of α computed from this linear relation.

The results of the measurements are shown in Fig. 2, where the absorption coefficients in cm^2 per cm^3 of the thallium vapor at 1 mm pressure at 0°C are plotted as a function of the velocity of the electrons which is expressed in square root of volts. The first two resonance potentials, 3.3 and 4.5 volts, and

the ionization potential, 6.1 volts, are indicated by the letters *R*, *R*, and *I*. The curve is characterized by a sharp minimum at 1.4 volts and a maximum at 4.5 volts.

The magnitude of the absorption coefficient depends on the constants chosen for the equation relating the vapor pressure and the temperature. Measurements of the vapor pressure of thallium have been made by Gibson[6] and von Wartenberg.[7] Professor Gibson has advised me to use the data of von Wartenberg instead of his own. He suggested that his own data for thallium vapor pressures might be somewhat uncertain because of the effect of the high temperatures, 1000 to 1600°C, on the elastic properties of the quartz of which his manometer was constructed. The vapor pressure of thallium measured by Gibson at 970°C, his lowest temperature, agrees well with the value from von Wartenberg's data for the same temperature. For the vapor pressure equation, $\log p_{\text{mm}} = B - A/T$, the International Critical Tables[8] give the values $A = 6{,}280.$ and $B = 6.14$, based on Gibson's high temperature data.

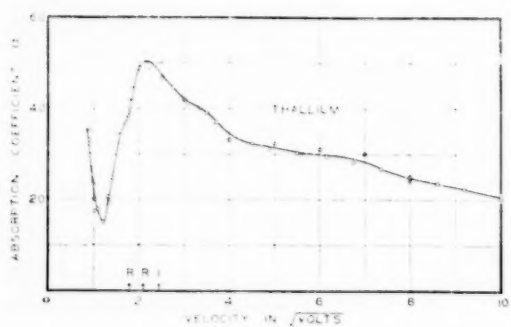

Fig. 2. The absorption coefficient α for electrons in thallium vapor as a function of the velocity of the electrons.

The data of von Wartenberg give for the constants the values $A = 8{,}890.$ and $B = 8.55$, which are the values used in this experiment to calculate the vapor pressure. At the temperatures used in this experiment, the I. C. T. values of the pressure are about five times those of von Wartenberg for the same temperature. If the I. C. T. values of the constants were used, the values of α shown in Fig. 2 should be reduced to about 1/5 of their value or at 4.5 volts, the maximum, $\alpha = 10$ and at 100 volts $\alpha = 4$. These values seem improbably small as helium has a value of $\alpha = 15$ at 4.5 volts and $\alpha = 3.5$ at 100 volts.

In the curves for thallium vapor, the alkali metal vapors and the heavier noble gases, the maximums are at about the resonance potentials while the minimums are at definitely lower velocities. This means that the probability of an elastic collision between an electron and an atom increases as the energy of the electron approaches the critical potential of the atom.

[6] G. E. Gibson, Dissertation, Breslau (1911).
[7] H. von Wartenberg, Zeit. f. Electrochemie **19**, 482 (1913).
[8] International Critical Tables, Vol *III*, 205.

Because of the maxima and minima in the absorption coefficient curves, the relative magnitude of the curves of different elements is somewhat uncertain. By taking the value of the absorption coefficient for a velocity well beyond the region of maxima and minima, a definite order of arrangement for the elements can be obtained. Choosing arbitrarily 100 volts as the velocity for comparison of the curves, the order of arrangement of the absorption coefficients for the 13 monatomic elements that have been measured is, with the exception of thallium, inversely proportional to the ionization potential. To fit into this arrangement, thallium with an ionization potential of 6.1 volts should have an absorption coefficient at 100 volts of about 100 instead of 20. Further experimental observations will be necessary to determine whether this deviation of thallium from the general order is really a property of the thallium atom or is due to the inaccuracies in the vapor pressure. Since the normal state of the thallium atom is a P state as compared with S states for the other atoms, it would not be unexpected to find a real difference.

OSCILLATIONS AND TRAVELLING STRIATIONS IN AN ARGON DISCHARGE TUBE

By T. C. Chow
Palmer Physical Laboratory, Princeton University

(Received January 15, 1931)

Abstract

The effects of current and external circuit conditions on the frequency of travelling striations were observed. Some information concerning the voltage fluctuations at different parts of the tube was obtained. Electron temperatures in the positive column were determined at different pressures. A set of wave-lengths bearing simple relations with the length of the tube were calculated by means of Tonks' and Langmuir's theory of electric sound waves and the experimental values of the flash frequency.

Introduction

IN THE course of an experiment to determine certain quantities in the positive column of a discharge tube, the author encountered the difficulty that the voltage across the tube was not constant. After an unsuccessful attempt to eliminate this fluctuation, it was thought desirable to investigate the phenomenon in more detail.

Oscillations in a discharge tube were observed and studied quite long ago. Recent work has been done by Penning,[1] Tonks, and Langmuir,[2] Webb and Pardue,[3] Fox[4] and others. Webb, Pardue, and Fox found that the phenomenon of travelling striations studied by Aston and Kikuchi,[5] Whiddington,[6] and others was accompanied by oscillations. In this paper a few more points are reported concerning travelling striations and oscillations in an argon discharge tube with a positive column.

Apparatus and Method

The discharge tube is shown in Fig. 1. The length of the tube was 72.5 cm. The inner diameter was 7.2 cm. An oxide coated cylindrical nickel cathode C and a hollow cylindrical nickel anode A were used. The shortest distance between cathode and anode was 60 cm. The tube was baked out at about 350°C for several hours. The cathode and anode were degassed by means of an induction coil. Between the tube and the pumping system there were two liquid air traps with a stopcock between them. During a run this stopcock was closed. Liquid air was continually kept on the trap which was on the tube side of the stopcock. For the study of voltage fluctuation a cath-

[1] Penning, Phys. Zeits. **27,** 187 (1926).
[2] Tonks and Langmuir, Phys. Rev. **33,** 195 (1929).
[3] Webb and Pardue, Phys. Rev. **32,** 946 (1928).
[4] Fox, Phys. Rev. **35,** 1066 (1930).
[5] Aston and Kikuchi, Roy. Soc. Proc. London **98,** 50 (1921).
[6] Whiddington, Proc. Leeds Phil. Soc. **1,** 467 (1929).

ode-ray oscillograph was used. For the observation of instantaneous pictures of the discharge tube and the measurement of flash frequency, a stroboscope, which is essentially a rotating toothed-wheel together with a fixed slit put right behind it, was used.

Results

1. *An instantaneous picture of the discharge.* (*Fig. 1*). The negative glow and the head of positive column remain stationary. Flashes travelling from anode to cathode run into the head of the positive column but do not run across the Faraday dark space. There are cases in which the Faraday dark space is not present. In these cases, it is observed that the flashes run into the negative glow which is stationary. The distance between successive flashes is of the order of 10 cm.

2. *Fluctuation of space potential in the tube.* In a non-oscillating tube we know that there is a definite potential distribution. When oscillations are present and the potential difference between cathode and anode fluctuates it is quite natural to expect that the space potential distribution should fluc-

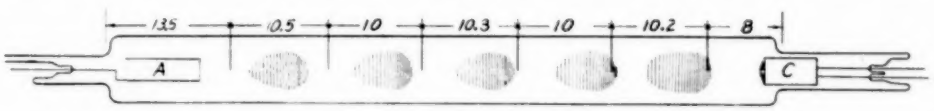

Fig. 1. Diagram of tube. The shaded regions are luminous parts. The numbers represent the distances in cm between the different probe wires.

tuate too. In order to get exact information one has to take Langmuir probe wire measurements at particular phases of the cycle of voltage fluctuation at different parts in the tube. Wishing to continue with his original problem, the author has not gone into this work. He reports here such information as he has been able to obtain otherwise. There are a number of probe wires situated at different parts of the tube. When they are left floating in the tube each of them charges up to a certain potential negative with respect to the surrounding space such that electrons and positive ions reach the wire at equal rates. If the surrounding space potential is fluctuating the potential of the floating wire must also fluctuate. The fluctuation of the probe wire potential would be just equal to that of the space potential provided the ratio of the concentration of positive ions and that of electrons and the ratio of the velocities remain unchanged. What was done, therefore, was to connect anode or cathode and each one of the probe wires successively to a pair of deflecting plates of the cathode ray oscillograph. The amplitudes of voltage fluctuation at different parts with respect to cathode and anode were observed. The results are shown in Table I. Each vertical line shows the position of a probe wire and the numbers in the column under it give the corresponding voltage fluctuations. The pressures are given in the first column. The upper row corresponding to a particular pressure gives the amplitudes of the voltage fluctuation in volts between the probe wires and the anode. The lower row gives the amplitudes with respect to the cathode.

TABLE I. *Amplitudes of the voltage fluctuations in different parts of the tube with respect to the anode and cathode. Pressures are all measured when the gas is at room temperature. After two hours of running the pressure does not change very much.*

Pressure (mm Hg)	Anode	Position of probe wires					Cathode
4.2		24	24	24	24	24	22
	22		5			1	
3.9		24	24	24	24	24	22
	22	7	5	3	3	1	
3.2							24
	24					1	
2.8			24				24
	24					1	
2.3				24			24
	24					1	
1.7				24			24
	24			1		0	
1.45				24			24
	24			0		1	
1.25		24	24	24	24	24	24
	24	3	2	0	11	0	
1.06		24					24
	24				11	0	
0.915							24
	24				3	0	
0.775		28	28	28	24	24	24
	24	5	5	2	13	0	
0.67		32	29	29	24	24	24
	24	7	7	5	14	1	
0.58		32	29	29	25	24	24
	24	8	8	6	3	0	
0.50		32	32	32	24	24	24
	24	10	9	8	15	1	
0.43		33	33	32	25	25	25
	25	10	10	9	25	1	
0.36		32	32	32	25	25	25
	25	11	10	10	29	1	
0.31		32	32	29	29	25	25
	25	11	11	11	29	0	
0.265		32	32	32	25	25	25
	25	11	13	11	4	0	
0.22		23	36	32	27	26	29
	29	11	15	11	3	0	
0.16		24	39	29	29	29	29
	29	15	16	10	5	0	
0.113		31	36	27	29	31	31
	31	18	18	8	2	0	
0.096		29	38	25	32	32	32
	32	18	18	9	2	1	
0.085		29	38	24	27	29	29
	29	18	14	10	2	3	
0.071		31	44	25	28	30	28
	28	16	23	14	10	2	

Travelling striations do not appear distinctly until the gas pressure is reduced to about 0.775 mm. However, fluctuations of luminosity are still present at high pressures. The frequency of luminosity fluctuation can still be measured. The probe wire nearest the cathode is on the cathode side of the negative glow, except in a few cases at high pressures when the positive column extends very close to the cathode. The position of the second probe wire with respect to the positive column goes from inside the head to just outside in the pressure range from 0.775 mm to 0.071 mm. Very little can be concluded from these values because we do not know the phase differences between the voltage fluctuations at different parts. However, we can say that the disturbance is very small in the cathode region compared with that in the anode region. This seems to agree with the fact that the travelling striations are present in the positive column. It has also been observed that when the second probe wire is situated in a rather distinct Faraday dark space, there is no voltage fluctuation between this probe wire and the cathode and also no voltage fluctuation between the first probe wire and cathode.

3. *Variation of flash frequency with current through the tube.* Whiddington observed that this phenomenon of travelling striations covers quite a large range of current. He divided the moving striations into five types according to their velocities as the current is increased. Since it is observed that the distance between successive striations does not change appreciably with current the relation between flash frequency and current is therefore similar to that between velocity and current. By flash frequency we mean the number of striations moving across a certain cross-section of the tube per second. The result is summarized in Table II. There are two modes of frequency change,

TABLE II. *Variation of flash frequency with current through the tube. Battery voltage $E=62$ volts.*

Current (amp.)	Flash frequency	Voltage across tube (volts)	Remarks
0.27	1.71×10^3	53.0	Current unsteady
0.6	1.89 "	47.9	light fluctuation
1.0		44.0	visually observed.
2.6	0.97×10^3	37.3	Steady, instantaneous picture clear.
3.0	1.14 "	34.5	
3.4	1.19 "	33.5	"
3.8	1.21 "	33.0	"
4.4	1.23 "	32.3	"
5.0	1.26 "	32.0	"
5.4	1.26 "	32.0	"
6.0	4.71 "	31.5	"
3.5	1.18 "	34.0	"

one is a continuous variation and the other is a discontinuous jump. In the continuous region the frequency increases with the current. The relation is indeed not simple. One would suspect that the current is not the only thing responsible for the change of frequency because in order to change the current other quantities in the circuit have been changed too; for instance, the external resistance in the circuit. Other observations are therefore made to test the effect of the external circuit.

4. *For a given current the frequency changes with the external resistance (noninductive).* An interesting fact was observed. When a large battery voltage (E) is used, thus with large external resistance, the Faraday dark space ex-

TABLE III. *Variation of flash frequency with external resistance.*

Current	Battery voltage	Voltage across tube	Flash frequency	External series resistance
0.4 amp.	60 volts	53.1	9.88×10^2	118 ohms approx.
0.4 "	118 "	51.7	1.92×10^3	166 " "
0.4 "	345 "	51.7	2.09×10^3	733 " "

ists. When E is small the Faraday dark space disappears. On one occasion I was able to observe a Faraday dark space, although not so distinct, by using E equal to about 60 volts. The frequency measured was 1.61×10^3. Suddenly the Faraday dark space disappeared and the frequency became 9.8×10^2. This change seems to correspond to a change-over from a "fast-type" to a "slow-type" in the previous current-frequency relation.

5. *Inductance increases the frequency, capacity decreases it.* The frequency decreases rapidly with increase in the capacity put in parallel with the tube.

TABLE IV. *Variation of flash frequency with inductance and capacity.*

Flash frequency	Condition in external circuit
2.22×10^3	Only noninductive resistance about 300 ohms
1.92×10^3	With a condenser of 2 mf connected parallel to tube
2.40×10^3	An inductance in series with series resistance
E equal about 120 volts $V=58.8$ volts $i=0.2$ amp. kept same in three cases	

When the capacity in parallel with the tube was large, the Faraday dark space disappeared. Under this condition, although no distinct striation can be seen, there are bright and less bright regions. These regions fluctuate violently in position.

6. *The filament current has an effect on the frequency. An increase in the filament current decreases the frequency.*

TABLE V. *Variation of flash frequency with filament current.*

Filament current	Current in tube	Voltage across tube	Flash frequency	External resistance
6.2 amp.	0.3 amp.	87.5 volts	2.21×10^2	842 ohms
8.7 "	0.3 "	51.7 "	2.08×10^2	961 "
$E=340$ volts				

7. *A search for electric sound waves: variation of flash frequency with pressure.* That the flash frequency is the same as the sound frequency heard in a telephone receiver connected to the circuit suggests that there might be present a kind of electric sound wave such as Tonks and Langmuir derived in

their theory of plasma ion oscillation. Their expression for the velocity of electric sound waves is this

$$v = 3.9 \times 10^5 \left(\frac{T_e m_e}{m} \right)^{1/2}$$

where T_e is the electron temperature in degrees m_e and m are the masses of the electron and the argon atom, respectively. The frequency of the electric sound wave is indeterminate from their theory. The only condition is that λ is very much greater than $(\pi k T_e/ne^2)^{1/2}$. Experimental values of T_e and calculated values of v at different pressures are given in Table VI. They are not in agreement with the flash velocities. If the flash frequency were the

TABLE VI. *Experimental values of electron temperature and calculated values of velocity of electric sound waves. Current is kept at 2 amperes for all readings.*

Pressure (mm Hg)	Flash frequency ν	Flash velocity (cm/sec.)		Electron temperature (volts)	Calculated velocity of electric sound wave v_s	$\lambda_s = v_s/\nu$	$\lambda_s/72$
0.071	1772	2.52×10^4		2.22	2.30×10^5	130	1.81
.085	1500	2.18 "	(i)	1.78	2.07 "	138	1.92
.096	1286	1.86 "		1.67	2.01 "	156	2.17
.113	1106	1.60 "		1.59	1.96 "	177	2.46
.16	940	1.50 "		1.71	2.03 "	216	3.00
.22	701	1.12 "		1.73	2.04 "	291	4.04
.265	667	1.07 "		1.68	2.01 "	302	4.19
.31	561	8.98×10^3	(ii)	1.71	2.03 "	362	5.02
.36	494	7.89 "		1.59	1.95 "	395	5.48
.43	453	7.25 "		1.55	1.93 "	427	5.93
.5	359	3.95 "		1.36	1.81 "	502	6.97
.58	332	3.48 "	(iii)	1.18	1.68 "	504	7.00
.67	311	4.36 "	(i)	1.35	1.80 "	579	8.04

Another set of electron temperature measurements taken at a different time and using another probe wire in the positive column are given below.

0.068	2404			1.27	1.75×10^5	72.7	1.01
	1220	1.41×10^4		1.96	2.18 "	178	1.47
	980 (ii)	1.14 "		1.44	1.86 "	190	2.64
	758	8.8×10^3		1.47	1.88 "	247	3.43

(i) Distance between successive striations = 14.5 cm. approx.
(ii) Distance between successive striations = 16 cm. approx.
(iii) Distance between successive striations = 10.5 cm. approx.

same as that of electric sound waves, the wave-length would be very long compared with the distance between flashes. However, there is a very peculiar relation between all these calculated λ's. Most of them are integral or half-integral multiples of a certain length which is rather closely the length of the whole tube. (A few deviate from integers or half-integers but most of them are within experimental errors. Flash frequency is subject to 1 percent error. Electron temperature may have a maximum deviation of 5 percent.) This would mean that if we take the frequency of electric sound waves (suppose there is such a kind of wave in the tube) equal to some higher harmonics

of the flash frequency the wave-length of the electric sound waves turns out to be a fraction of the tube length like a standing wave in that distance. The author does not attempt to interpret this phenomenon but believes that the fact is a real one, and may be very significant. The relation between flash frequency and pressure is plotted in Fig. 2.

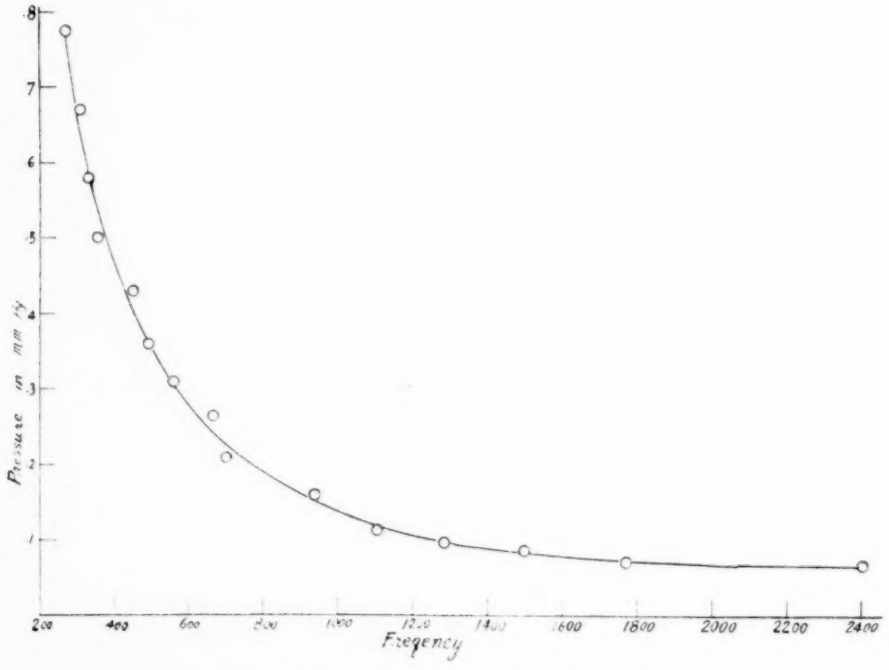

Fig. 2. The relation between flash frequency and pressure.

8. *Miscellaneous note.* There is often found a ring of glow light surrounding the anode. As the pressure is reduced this ring of velvet glow moves down towards the end of the anode. Sometimes the discharge is so unsteady that the needles of the voltmeter and the ammeter vibrate. In the range of pressure in which travelling striations are observed it is often possible to restore the discharge to steady condition by putting a magnet somewhere near the tube. Then distinct travelling striation patterns can be seen. There are a certain number of definite regions in which the magnet must be put in order to be effective. Right above the head of the positive column, and above the negative glow are favorable places but by no means the only places. Once the magnet had to be put a little behind the cathode. In some previous observations, some places near the anode are also effective.

In this laboratory, Dr. Cravath found oscillations too in his mercury discharge tube. His tube had about the same length as mine; the diameter was even larger. It was suggested that the large diameter of the tube is responsible for oscillations because the larger the diameter the smaller will be the area of the wall surface per unit volume of the tube. Loss of ions and electrons

due to recombination at the wall will be less, so that the concentrations of ions and electrons in the tube are large. Therefore the process of cumulative ionization is favorable for the production of ions and electrons. The rate of production of ions and electrons by cumulative ionization processes is proportional to the square of the electron concentration. A small change of electron concentration will cause a large change in the rate of production of ions and electrons. This is a state of instability. A tube of about one inch diameter was built. However, oscillations existed as badly as in the tube with large diameter. This would mean that the above theory is certainly incomplete, if not wrong.

The author wishes to thank Professor K. T. Compton and Professor H. D. Smyth for their deep interest and encouragement.

COLD EMISSION FROM UNCONDITIONED SURFACES

By Willard H. Bennett*
Norman Bridge Laboratory of Physics, Pasadena, California

(Received January 26, 1931)

Abstract

The greatest difficulty in obtaining higher potentials in tubes is due to auto-electronic emission from the electrode surfaces. A study of emission from unconditioned metals is described leading to the result that either loose fine particles in a tube, or else the targets of emission will probably have more to do with the quantity of emission than will the kind and "conditioning" of the cathode itself.

NUMEROUS measurements have been made of the emission in high electric fields, from fine wires and fine points of metals, which have been heated nearly to melting, in vacuum, and thus thoroughly conditioned.[1] Since metal parts in high voltage tubes are so restricted in size and shape by the necessity of such heating, it has been considered of importance to investigate cold emission with a view to finding what else can be done to a metal surface to decrease the emission, besides heating to high temperatures. This problem is of particular interest in connection with the development of a design for a tube to give higher order potentials than those now obtainable with unconditioned or partially conditioned electrodes.[2]

1. Apparatus

The experimental apparatus was designed by Julius Pearson in accordance with plans outlined by R. A. Millikan, to measure the current passing between electrodes in high vacuum at known fields. Spherical electrodes were used at distances small compared with the radius of either electrode.

The cathode was mounted on a fixed steel post extending down into the evacuated bulb, as shown in Fig. 1. The anode was mounted on a steel post which could either be moved towards or away from the cathode by means of the micrometer screw, and also which could be rotated about the cathode by turning the movable part of the base, as shown in Fig. 2. When the latter rotation was made, the anode retained its orientation so that fresh surfaces both of the anode and of the cathode were brought together at each setting of the base. Several sets of readings were thus possible at each mounting of the electrodes.

* National Research Fellow.

[1] Rother, Ann. d. Physik **81,** 317 (1926) G. E. Co. of London, Phil. Mag. (7) **1,** 609 (1926); Eyring, MacKeown and Millikan, Phys. Rev. **31,** 900 (1928); Stern, Gossling and Fowler, Proc. Roy. Soc. **124,** 699 (1929).

[2] Lauritsen and Cassen, Phys. Rev. **36,** 988 (1930); Coolidge, J. Franklin Inst., **202,** 639 (1926); Tuve, Hafstad and Dahl, Phys. Rev. **35,** 1407 (1930); Brasche and Lange, Naturwiss. **18,** 765 (1930).

The anode post was sealed vacuum-tightly to the fixed part of the base by means of a copper syphon. Both the cathode post and the anode base were sealed to the glass bulb with red sealing wax. The bulb was connected to the pumps at all time. An ionization gauge was used for measuring pressures.

The source of potential was a Thordarson transformer and kenetron rectifier, the potential being smoothed out with a 0.25 microfarad condenser. This generator, which gave up to 20 kv steady potential, was connected through a 10,000,000 ohm xylene-alcohol resistance to the cathode post. The

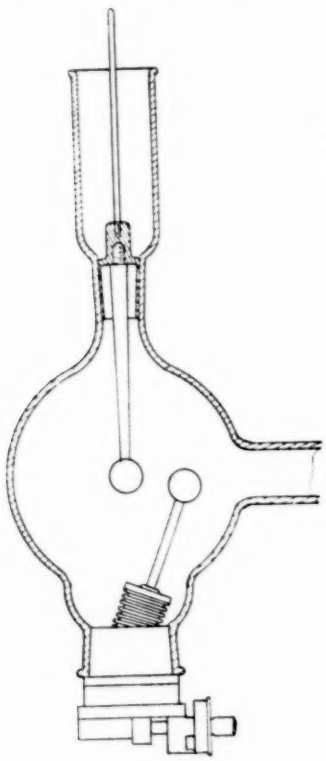

Fig. 1. Diagram of tube.

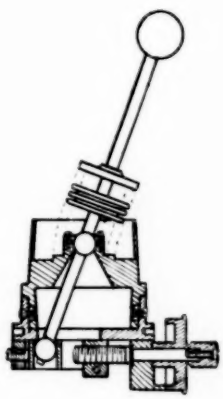

Fig. 2. Diagram of anode.

potential difference applied between the electrodes was measured by the electrostatic voltmeter which was calibrated with a sphere-gap. The anode base was connected to the current measuring circuit. The entire high-potential generator was enclosed in a grounded screen cage, since it was found that without it, leakage currents in the air would get to the galvanometer giving large deflections.

2. Method of Observation

Immediately before mounting, the electrodes were polished with 600 mesh carborundum powder held on the heel of the hand. They were washed in alcohol, dried without touching, and mounted.

The field between the electrodes could be varied by varying either the

distance between the electrodes or the applied potential. Numerous measurements showed that the two methods gave the same result.

After the first complete field-current curve had been measured, the potential was cut off and the electrodes touched to measure the setting of the micrometer for zero distance between electrodes. The e.m.f's in the rectifying tube (not more than 5 volts) were sufficient to give dependable deflections on the galvanometer upon contact. The largest emission previously drawn was again drawn at the corresponding field, and it was assumed that the intermediate determination of the zero had not effectively changed the surfaces for further study. When mixed electrodes were used (see section 6), zero distance was always measured after all measurements of emission were completed.

The data collected were plotted with the inverse field times 10^6 and the logarithm of the current, as coordinates. The points on the curves represent the lower limits of the current at each sitting. This was done because a study showed that in those comparatively few cases the current varied over a material range, the lowest value was quite near the final value if allowed to become steady. Most of the first emission curves are curled back at currents above 10^{-4} amperes because the drop in applied potential caused by the drop through the external resistance becomes appreciable at this value. No attempt has been made to draw straight lines to represent characteristics because it is believed to be more important to keep clearly in mind the probable uncertainty of the measurements. It is believed that reliable conclusions can be drawn only when the zone on a figure enclosing all of the emission from one kind of electrode surface is entirely separate from the zone enclosing all of the emission from another kind of an electrode surface.

3. General Observations

The behavior of surfaces which have not been "conditioned"is exceedingly erratic and unsystematic. In spite of this fact, a very considerable amount of data was taken in an attempt to determine statistically what relations (1) degree of polish, (2) purity, (3) electroplating, (4) hardness and (5) work function, have to emission. Measurements were made on cast iron, steel, armco iron, vacuum fused electrolytic iron, magnesium (two grades of purity), aluminum, copper, brass, zinc, gold-plated copper, nickel-plated brass, chromium-plated brass, and "Plymite" (an extremely hard compound of tungsten and carbon). This quite extensive study did not lead to any conclusive results.

It was established, however, that with fair polish and fair purity, or better, the first emission always began at a much higher field, and suffered a sudden spontaneous increase of a large order of magnitude at a still higher field, i.e., a "breakdown," than the fields at which emission was drawn from the same emitting surface subsequently.

4. Effect of Space Charge Due to Positives

The possibility suggested itself that positives liberated from the anode by the electron stream from the cathode, might follow the electron stream,

which is known to be well focussed, and set up a space charge which in turn increased the emission. This possibility was tested by measuring the emission in an apparatus as shown in Fig. 3. *P* is a needle-point of the metal to be studied. It was mounted on a screw-in-vacuum which could be moved by a magnet, in the direction of the point. *A* and *B* are polished copper bars, six inches long, 3/4 inch wide, and 1/8 inch thick, with edges rounded. There was a hole in *A* as shown, through which the point was extended toward *B*. *A* and *P* were at ground potential and *B* was at any desired potential up to 20,000 volts. Currents were measured from *P*. Any desired magnetic field up to 7,000 gauss could be applied perpendicularly to the figure by an electromagnet with pole-pieces as shown. The apparatus was always baked out before

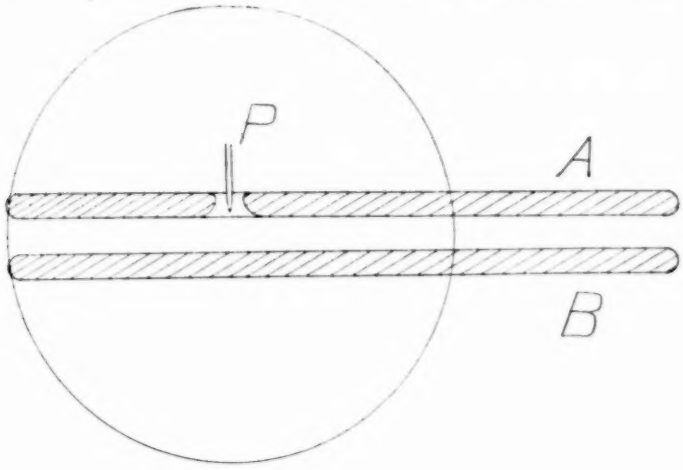

Fig. 3. Diagram of apparatus for measuring emission in magnetic field.

measurements were begun, and the pressure between the bars was, in all experiments, less than 1×10^{-5} mm, as shown by an ionization gauge at the opposite end of the tube from the pumping outlet.

Both a tungsten and a copper needle-point were tried. Emission began from the points at a comparatively low potential, and decreased (fatigued) even with increased potentials. There were times, however, during this fatigue, when the emission would remain steady within five percent for several minutes.

If the tip of the point, *P* is above the plane of the lower face of the upper plate, and a magnetic field of 7,000 guass is applied to apparatus of the dimensions used in this experiment, it can be shown that electrons emitted from *P* cannot arrive at the plate *B* directly below *P*, but will be displaced along *B* to some place beyond the region of this magnetic field.

The cycloidal path predicted by the theory was actually seen outlined on the glass walls opposite the space between the plates, and displaced down the tube to the edge of the region of high magnetic field.

Emission was drawn from *P* in the above position and the current measured while putting the magnetic field on and off. The magnetic field was

found to have no effect on the magnitude of the current, to within five percent, which was the degree of steadiness of the emission from the points.

The conclusion may be drawn that if the positives which are known to go from the anode to the cathode, produce a space charge near the emitting surface, the effect of this space charge on the field at the surface is *not* of importance in determining the magnitude of emission after breakdown.

5. Effect of Discharges through Hydrogen on Emitting Surfaces

Four filaments were mounted on the tube shown in Fig. 1 at the four quadrants about the center electrode. They were sealed in glass plugs which could be sealed with wax into the ground glass joints on the tube as shown in Fig. 4. At the side of one of these joints, the pumping tube V was attached.

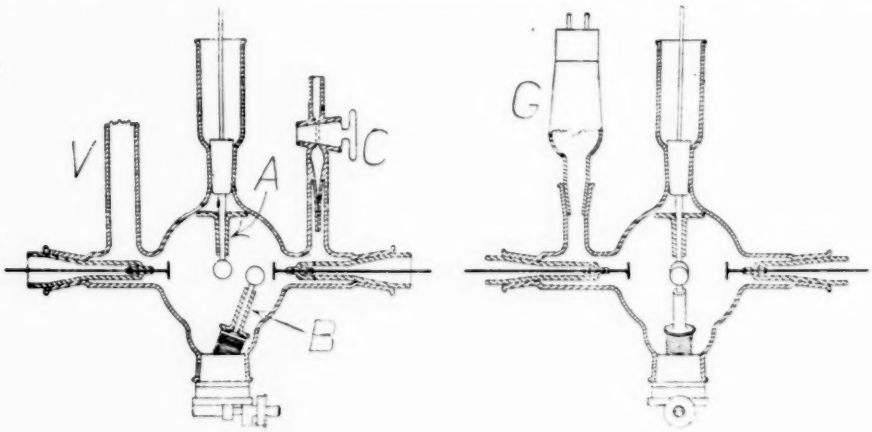

Fig. 4. Diagram of tube showing arrangement of four filaments.

At the side of another, the ionization gauge G was attached. At the side of a third, a slow gas inlet C consisting of a fine capillary and a stopcock was attached. Glass shields for both steel electrode posts, A and B, were mounted to eliminate emission from the posts and also to protect them from sputtering.

Copper electrodes were used throughout this work on the effect of discharge through hydrogen.

In order to differentiate sharply between the true effect of discharges upon the emitting surfaces and any auxiliary phenomena in the tube, tests were made of the effect of lighting the filaments introducing hydrogen to atmospheric pressure and pumping out, introducing air similarly, letting stand for up to sixteen hours, and bombarding with electrons (20 m.a., bringing the electrode to about 75°C temperature). The changes due to none of these treatments was materially greater than the changes observed between repeated measurements of the characteristic of a particular surface.

Fig. 5 is submitted as a basis of comparison for the following figures. Curves 1, 2, 3, and 4 are the first emission observed at each of four independent emitting areas. Curves 5, 6, 7 and 8 are the subsequent emissions for the same areas in order.

Each group of three curves in Fig. 6 represents the history of an independent emitting area. In each group, curve 1 represents the first emission, which emission followed bombardment with positives at the current and for

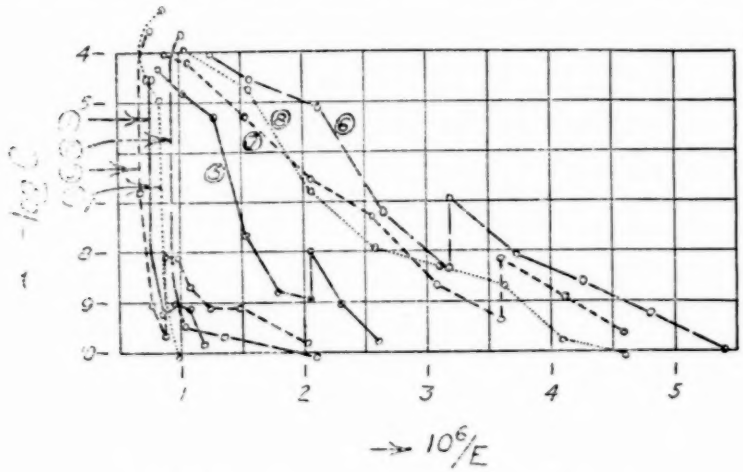

Fig. 5. Emission from untreated copper electrodes.

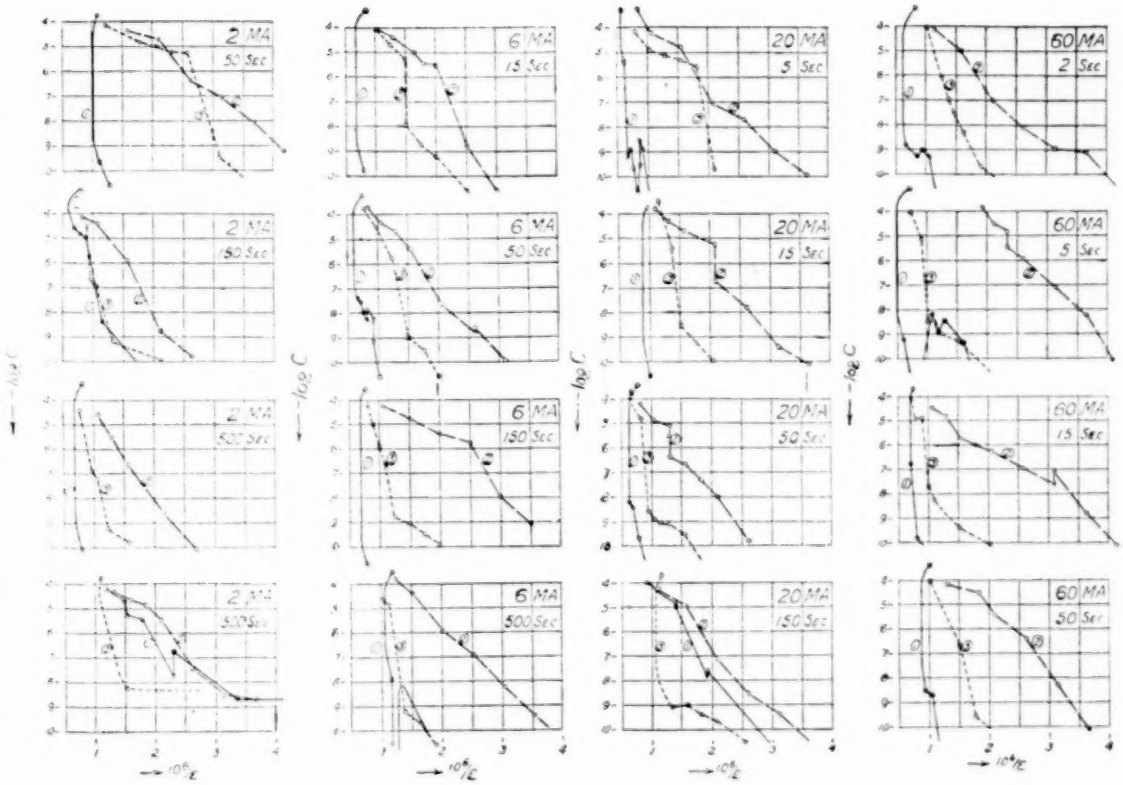

Fig. 6. Effect of discharge through hydrogen.

the time indicated. Curve 2 represents the subsequent emission, which was measured immediately following the first emission. Curve 3 represents the emission which followed another bombardment with positives at the same current and for the same time as before. These bombardments were made through hydrogen at the highest pressure (between 1 mm and 12 mm pressure) which would permit the negative glow completely to surround the bombarded electrode, which was the cathode in both the glow discharge and the measurement of the emission.

A study of the curves will show that up to a certain point, bombardment with positives does not seem to affect the field at which breakdown first occurs, but that there is a current and time for which a bombardment with positives restores the emitting surface after breakdown to the condition it had before breakdown occurred.

6. Effect of the Anode

Measurements were made of the emission from a copper cathode but with various anodes. Anodes used were of copper, iron, magnesium, zinc, plymite,

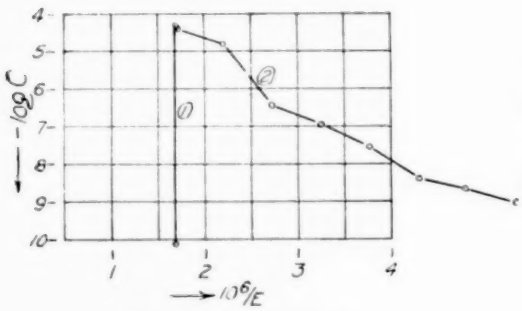

Fig. 7. Plymite anode.

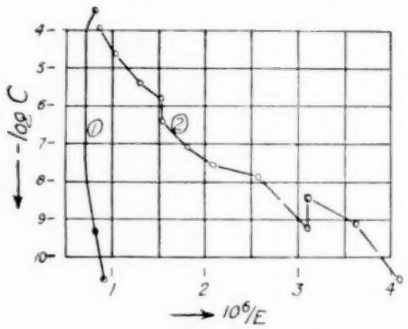

Fig. 8. Copper anode.

aluminum, chromium-plate, and molybdenum. Complete sets of measurements were made for at least four independent emitting areas for each combination of electrodes, and the set which appeared to be most typical for each kind of anode is shown with the corresponding label in Figs. 7 to 14. The curves are numbered in the order taken.

Repeated attempts to fatigue the emitting surfaces on copper cathodes, using copper, plymite, or iron anodes, giving emission like that shown in curve 2 of Figs. 7, 8 or 10, respectively, failed to give any significant change in slope. The change was uncertain with a zinc anode.

On the other hand, using either a molybdenum, aluminum, chromium, or magnesium anode, the emitting surface quickly fatigued to a new group of curves occupying a zone on the figure definitely removed from that occupied by subsequent emission curves for copper anodes, and corresponding to much lower currents from the same fields.

7. Temporary Breakdown

Frequently, with various electrodes, throughout the entire investigation, there have occurred very sudden large order increases in current (up to 10^6)

which behaved like premature breakdowns. These presently just as suddenly completely disappeared, accompanied by a distinct click of the glass, sounding as though a metal particle had hit the glass. On pushing the field up, the breakdown occurred at the usual field and all subsequent currents behaved the same as though the premature breakdown had not occurred.

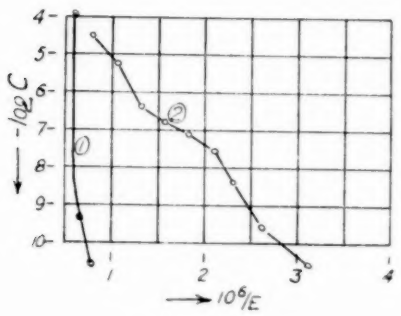

Fig. 9. Iron anode.

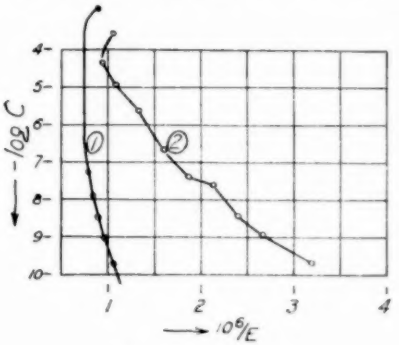

Fig. 10. Zinc anode.

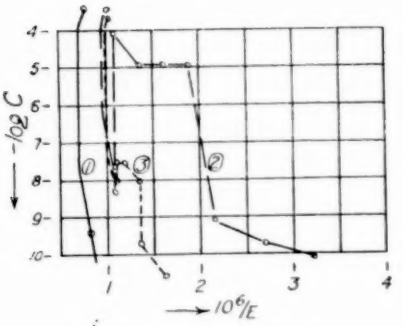

Fig. 11. Magnesium anode.

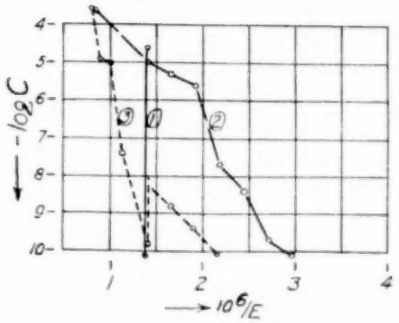

Fig. 12. Aluminum anode.

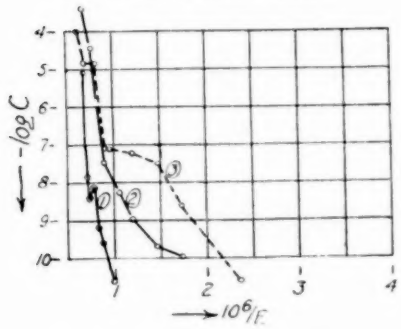

Fig. 13. Chromium plate anode.

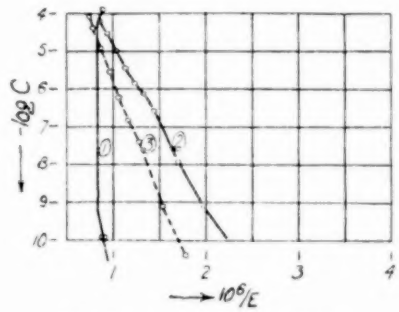

Fig. 14. Molybdenum anode.

8. Discussion

The idea that the first breakdown is simply due to a rupturing of the surface of the cathode and that the emission is determined by the composition and conditioning of the cathode, has appeared to be open to question from early in this investigation.

The phenomenon of premature breakdown seems to leave no doubt that foreign particles either from the anode or from parts of the tube other than the cathode, *can* fly through the tube to the cathode, adhere, give emission, and be torn from the cathode leaving no scar on the cathode of sufficient irregularity to give measurable emission.

Following excessive discharge through hydrogen (which was observed to give sputtering), the first emission was seen to behave either as though a complete breakdown has been produced during the discharge through hydrogen, or else as though no sensible effect had been produced on the cathode surface at all (see curves 1, each of the lower four groups in Fig. 6). It was never observed after sputtering had been produced in the tube either during these measurements or with any other electrodes under different conditions, that immediately subsequent field-current curves lay in the region between the two zones belonging to emission leading up to the usual breakdown, or the emission following the usual breakdown, respectively. This fact would seem to indicate that the adhesion of a loose particle to the cathode gives emission indistinguishable from that following the usual breakdown.

Following breakdown, when molybdenum, aluminum, chromium, or magnesium were used as anode, the lowest subsequent currents measurable occurred at fields much higher than those at which the lowest currents occurred when copper was used as the anode. The most plausible explanation of this seems to be that auto-electronic emission is from a particle torn from the anode and which is adhering to the cathode.

If, on the other hand, the breakdown is due to a rupturing of the copper cathode surface, it would be necessary to suppose that the steeper slopes, when one of the above four metals was used as anode, are due to beating down the ragged edges by positives coming from the anode at emission currents of less than 10^{-11} amperes, and that the emitting point is bombarded with positives of the same order of density as occur in a discharge through hydrogen of several milliamperes spread over the entire cathode surface. In view of the small size of the emitting points, this is a possible supposition. It is further supported by the fact that after prolonged auto-electronic discharge, the white color of the anode metal becomes distinguishable as a small spot at the emitting point on the copper cathode. This explanation, however, forces us to the conclusion that the emission measured is from a surface of metal originally composing the anode, and hence the emission is determined by the metal used as anode, anyhow.

In conclusion, the author wishes to thank Drs. Millikan, MacKeown, and Lauritsen for advice borne of their longer experience in this field, and also Dr. Millikan for making available the necessary facilities for this investigation.

SCATTERING OF HIGH VELOCITY ELECTRONS IN HYDROGEN AS A TEST OF THE INTERACTION ENERGY OF TWO ELECTRONS

By Hugh C. Wolfe*
California Institute of Technology, Pasadena

(Received January 26, 1931)

Abstract

1. The electronic scattering of high velocity electrons is considered as a test of the formulas for the interaction energy of two electrons. Three formulas for the interaction energy of two Dirac electrons are considered: I, the simple electrostatic interaction, II, the Gaunt formula, III, the Breit formula.

2. The Dirac transition probability method is reviewed briefly.

3. The cross-section of free electrons at rest for scattering high velocity electrons is calculated by the Dirac transition probability method, using each of the three formulas for interaction energy. Random distribution of spins is assumed. Relativistic variation of mass with velocity is taken into account, removing the symmetry about 45° of the classical scattering formula. Expanded to terms in β^2 the formulas obtained are compared with the classical Darwin formula and the recent formula of Mott. They differ from Mott's formula and from each other by terms of order β^2.

4. For high-velocity electrons, the scattering by hydrogen may be considered as the sum of nuclear and electronic scattering. A criterion for the validity of this procedure is obtained. The advantage of using hydrogen as the scatterer in experiments to test these formulas is discussed.

I. THE scattering of electrons by hydrogen may be considered as the sum of the scattering by free protons and the scattering by free electrons, provided the incident velocity is high and the scattering angle is not too near 0 or $\pi/2$. A criterion for the validity of this approximation is developed in section 4.

The cross-section for scattering depends upon the energy of interaction of the scatterer and the scattered particle and there is no completely justified theoretical formula for the interaction of two electrons or of an electron and a proton. Three formulas have been used,

$$\begin{aligned} &\text{I} \quad V = e^{\text{I}}e^{\text{II}}/r \\ &\text{II} \quad V = e^{\text{I}}e^{\text{II}}/r\left[1 - (\alpha^{\text{I}}\cdot\alpha^{\text{II}})\right] \\ &\text{III} \quad V = e^{\text{I}}e^{\text{II}}/r\left[1 - \frac{(\alpha^{\text{I}}\cdot\alpha^{\text{II}})}{2} - \frac{(\alpha^{\text{I}}\cdot r)(\alpha^{\text{II}}\cdot r)}{2r^2}\right]. \end{aligned} \tag{1}$$

The α's, written here as vectors, have components which are the matrices of four rows and columns appearing as coefficients in the Dirac linear Hamiltonian for one particle. r is the distance between the particles. I is just the electrostatic interection. II includes "spin" terms. III includes also the effect of

* National Research Fellow.

retardation of the potentials. III, which was first derived by Breit,[1] on the analogy $v/c \to \alpha$, and which is obtained in first approximation from the Heisenberg-Pauli field theory by systematic neglect of the infinite proper energy terms, has the most theoretical justification. However, Breit[2] has calculated the fine structure of helium with it and his results are no better than those of Gaunt,[3] who derived and used II. This failure may be due to the inadequacy of the approximate wave functions used. It is, therefore, of interest to find another place to use these formulas, where it may be possible to determine which gives results in better agreement with experiment.

For scattering of electrons by protons, a calculation similar to that given here for scattering by electrons has been carried out. The result is that the extra terms in II or III have a negligible influence. Massey[4] concurs in this result. Thus Mott's calculation using I, gives the best formula for nuclear (proton) scattering.[5]

2. The cross-section of an electron for scattering electrons is calculated here in first approximation by the transition probability method of Dirac.[6] The Hamiltonian for the system, incident electron plus scatterer, is to be written in the form $H = H^\circ + V$, where H° represents the system as it is observed experimentally. The eigenstates $\Psi(\alpha')$ of the unperturbed system whose Hamiltonian is H°, are known and are specified by giving the values, here assumed continuous in range, of a set of observables, $\alpha_1 \cdots \alpha_u$, which are constants of the motion. We shall frequently use α to represent $\alpha_1 \cdots \alpha_u$. The state Ψ of the system whose Hamiltonian is H is to be expanded in the eigen Ψ's of the unperturbed system,

$$\Psi = \int \Psi(\alpha') d\alpha' a(\alpha'),$$

where $a(\alpha')$ is a function of the time, i.e., the method of variation of constants. Substituting in the equation

$$H\Psi = \frac{ih}{2\pi} \frac{\partial}{\partial t} \Psi,$$

we obtain an integral equation for the time variation of $a(\alpha')$. Assuming that at some initial time our system would certainly be observed in the state α°, i.e., initially $a(\alpha') = a^\circ \delta(\alpha' - \alpha^\circ)$, this equation reduces to a simple differential equation which can be integrated. The normalization of the $a(\alpha')$ is such that we are concerned not with one system but with an ensemble of similar

[1] Breit, Phys. Rev. **34,** 553 (1929).

[2] Breit, Phys. Rev. **36,** 383 (1930).

[3] Gaunt, Proc. Roy. Soc. **A122,** 513 (1929).

[4] Massey, Proc. Roy. Soc. **A127,** 666 (1930).

[5] Mott, Proc. Roy. Soc. **A124,** 425 (1929). He formulates the problem rigorously, using Gordon's solutions of the Dirac equation, and approximates by expanding in powers of $\alpha = Z(2\pi e^2/hc)$, neglecting terms in α^2.

[6] Dirac, Proc. Roy. Soc. **A114,** 243 (1927) or Dirac, Principles of Quantum Mechanics, Oxford, 1930, section 54.

systems. The number of systems in our ensemble is $|a^\circ|^2 \int dx |\psi_{\alpha 0}(x)|^2$, where x stands for the whole set of coordinates and $\psi_{\alpha 0}(x)$ is a solution of the wave-equation for the unperturbed system in the initial state. Then $|a(\alpha')|^2 d\alpha'$ is the number of systems at time t such that α lies between α' and $\alpha'+d\alpha'$. The expression for $|a(\alpha')|^2$ shows that essentially only those transitions occur in which energy is conserved. If we transform to a new set of parameters, $W, \gamma_1 \cdots \gamma_{u-1}$, which are arbitrary independent functions of the α's, the number of transitions per second from the initial state to states in which the γ's have values between γ' and $\gamma'+d\gamma'$ is found, by integration with respect to W', to be

$$4\pi^2/h^2 |a^0|^2 |(W^0, \gamma'|V|W^0, \gamma^0)|^2 J(W^0, \gamma') d\gamma_1' \cdots d\gamma'_{u-1}. \tag{2}$$

$J(W^\circ, \gamma')$ is the Jacobian, $\partial(\alpha_1' \cdots \alpha_u')/\partial(W', \gamma_1' \cdots \gamma_{u-1}')$, with the values $W^\circ, \gamma_1' \cdots \gamma'_{u-1}$ for the variables. $(W^\circ, \gamma'|V|W^\circ, \gamma^\circ)$ is the matrix element $(\alpha'|V|\alpha^\circ)$, where the α's are so determined that the parameters, $W, \gamma_1 \cdots \gamma_{u-1}$, have the values $W^\circ, \gamma_1^\circ \cdots \gamma_{u-1}^\circ$ in the initial state and $W^\circ, \gamma_1' \cdots \gamma_{u-1}'$ in the final state. If $V = V(x,p)$ is a function of the coordinates and conjugate momenta, then

$$(\alpha'|V|\alpha^0) = \int N_{\alpha'} \psi_{\alpha'}(x) dx V\left(x, \frac{h}{2\pi i}\frac{\partial}{\partial x}\right) \psi_{\alpha 0}(x). \tag{3}$$

All of our expressions assume that the wave functions have the continuous spectrum normalization, equivalent to the Dirac δ normalization. $N_{\alpha'}$ is the normalizing factor for the final state wave functions and is given[7] by

$$N_{\alpha'}^2 \int dx \bar{\psi}_{\alpha'}(x) \int_{\alpha'-\Delta\alpha'}^{\alpha'+\Delta\alpha'} d\alpha'' \psi_{\alpha''}(x) = 1. \tag{4}$$

For our purposes, the normalization of the initial state wave functions is quite arbitrary. This is because we are interested in the cross-section for scattering, σ_s, which is defined from the classical treatment of collision scattering by

$$\sigma_s = \frac{\text{Number of transitions per sec. of the specified type, i.e. (2)}}{(\text{Flux of incident particles}) \cdot (\text{number of scatterers})}. \tag{5}$$

Both $|a^\circ|^2$ and the initial state normalizing factors occur in both numerator and denominator and cancel out.

3. In our problem the Hamiltonian H° is the sum of the Dirac linear Hamiltonians for two free electrons. The wave equation for the unperturbed system is

$$\left[W - \frac{hc}{2\pi i}\{(\alpha^{\mathrm{I}} \cdot \mathrm{grad}^{\mathrm{I}}) + (\alpha^{\mathrm{II}} \cdot \mathrm{grad}^{\mathrm{II}})\} - mc^2(\alpha_0^{\mathrm{I}} + \alpha_0^{\mathrm{II}})\right] \psi = 0.$$

This equation has solutions of the form $\psi = \psi^I \psi^{II}$ with $W = W_1 + W_2$, where ψ^I is a solution of

[7] Oppenheimer, Phys. Rev. **31**, 66 (1928).

$$\left[W_1 - \frac{hc}{2\pi i}(\alpha^{\mathrm{I}} \cdot \mathrm{grad}^{\mathrm{I}}) - mc^2\alpha_0{}^{\mathrm{I}}\right]\psi^{\mathrm{I}} = 0$$

and similarly ψ^{II}. The solution in the form of plane waves has been given by Darwin.[8] The four components of ψ^I are

$$\begin{aligned}
\psi_3 &= AS_1{}^{\mathrm{I}} \quad \psi_1 = \frac{-Ap_{1z} - B(p_{1x} - ip_{1y})}{mc + W_1/c} S^{\mathrm{I}}, \\
\psi_4 &= BS_1{}^{\mathrm{I}} \quad \psi_2 = \frac{-A(p_{1x} + ip_{1y}) + Bp_{1z}}{mc + W_1/c} S_1{}^{\mathrm{I}}
\end{aligned} \tag{6}$$

where

$$W_1 = c(m^2c^2 + p_{1x}{}^2 + p_{1y}{}^2 + p_{1z}{}^2)^{1/2}$$

$$S_1{}^{\mathrm{I}} = \exp\left[\frac{2\pi i}{h}(p_{1x}x_1 + p_{1y}y_1 + p_{1z}z_1 - W_1t)\right].$$

Darwin shows that the orientation of the spin axis, as given by its colatitude f, measured from the z axis, and longitude ω, is given by the relation $-B/A = \cot f/2e^{i\omega}$. Accordingly, $A=0$, $B=1$, means that the spin is "parallel" to the z axis, and the corresponding four components of the wave function may be represented by the one symbol Ψ_α. Likewise, $B=0$, $A=1$, means that the spin is "antiparallel" to the z axis and for this case we may write ψ_β. The constants of the motion, whose values designate the eigenstates of the unperturbed system (the α's of section 2), are the components of momentum of the two particles p_{1x}, p_{1y}, p_{1z}, p_{2x}, p_{2y}, p_{2z}. We shall use a lower index 1 or 2 to indicate that the corresponding momentum is (p_{1x}, p_{1y}, p_{1z}) or (p_{2x}, p_{2y}, p_{2z}). Thus the symbol $\psi_{2\alpha}{}^I$ means the four component wave function in the coordinates (x_1, y_1, z_1) for momentum (p_{2x}, p_{2y}, p_{2z}) with $A=0$, $B=1$.

To take account of the random distribution of spins of the two electrons before the collision, we use wave functions for the initial state which represent equal probabilities for each electron to have its spin parallel or antiparallel to the z axis. As pointed out by Oppenheimer,[9] our wave functions must be antisymmetric to conform to the Pauli principle, since we are dealing with identical particles with spin. Accordingly, our initial state wave functions may have the form

$$\begin{aligned}
\psi_a &= 1/(2)^{1/2}(\psi_{1\alpha}{}^{\mathrm{I}}\psi_{2\alpha}{}^{\mathrm{II}} - \psi_{2\alpha}{}^{\mathrm{I}}\psi_{1\alpha}{}^{\mathrm{II}}) \\
\psi_b &= 1/(2)^{1/2}(\psi_{1\beta}{}^{\mathrm{I}}\psi_{2\beta}{}^{\mathrm{II}} - \psi_{2\beta}{}^{\mathrm{I}}\psi_{1\beta}{}^{\mathrm{II}}) \\
\psi_c &= \tfrac{1}{2}(\psi_{1\alpha}{}^{\mathrm{I}}\psi_{2\beta}{}^{\mathrm{II}} - \psi_{2\beta}{}^{\mathrm{I}}\psi_{1\alpha}{}^{\mathrm{II}} + \psi_{1\beta}{}^{\mathrm{I}}\psi_{2\alpha}{}^{\mathrm{II}} - \psi_{2\alpha}{}^{\mathrm{I}}\psi_{1\beta}{}^{\mathrm{II}}) \\
\psi_d &= \tfrac{1}{2}(\psi_{1\alpha}{}^{\mathrm{I}}\psi_{2\beta}{}^{\mathrm{II}} - \psi_{2\beta}{}^{\mathrm{I}}\psi_{1\alpha}{}^{\mathrm{II}} - \psi_{1\beta}{}^{\mathrm{I}}\psi_{2\alpha}{}^{\mathrm{II}} + \psi_{2\alpha}{}^{\mathrm{I}}\psi_{1\beta}{}^{\mathrm{II}}).
\end{aligned} \tag{7}$$

where the first three of these are symmetric in the spins and the fourth is antisymmetric in the spins.

The spin distribution in the final state is not to be measured and is deter-

[8] Darwin, Proc. Roy. Soc. **A120**, 621 (1928).
[9] Oppenheimer, Phys. Rev. **32**, 361 (1928).

mined only by the transition probabilities. Wave functions representing any spin orientations can be built up by superposition of four wave functions of the type (7). We shall use a ϕ to represent the complex conjugate of a final state wave function, only the complex conjugates occurring in our formulas. The final state momenta will be designated by p_{1x}', p_{1y}', p_{1z}', p_{2x}', p_{2y}', p_{2z}'. The total transition probability out of any one of the four initial spin states is the sum of the transition probabilities to four final spin states of type (7). We shall have taken account of the initial random spin orientations if we take the unweighted average of the total probabilities of transition out of the four initial spin states. Specifically, this means to calculate sixteen cross-sections for scattering, using the matrix elements obtained from all combinations of $\phi_a, \phi_b, \phi_c, \phi_d$ with $\psi_a, \psi_b, \psi_c, \psi_d$, and to take one fourth of the sum.

We shall transform from $p_{1x}, p_{1y}, p_{1z}, p_{2x}, p_{2y}, p_{2z}$ to a new set of parameters $W, P_x, P_y, P_z, \theta, \phi$ (the $W, \gamma_1 \cdots \gamma_{u-1}$ of section 2), where (P_x, P_y, P_z) is the momentum of the center of gravity and θ, ϕ are the polar angles of the momentum (p_{1x}, p_{1y}, p_{1z}), the z axis being taken as pole. The equations of transformation are

$$W = c(m^2c^2 + p_1^2)^{1/2} + c(m^2c^2 + p_2^2)^{1/2} \qquad P_x = p_{1x} + p_{2x}$$
$$\cos\theta = p_{1z}/p_1 \qquad P_y = p_{1y} + p_{2y}.$$
$$\tan\phi = p_{1y}/p_{1x} \qquad P_z = p_{1z} + p_{2z}$$

It is convenient also to use center of gravity coordinates X, Y, Z, relative coordinates x, y, z and relative momenta p_x, p_y, p_z, the equations of transformation being

$$X = \tfrac{1}{2}(x_1 + x_2) \quad x = x_1 - x_2 \quad p_x = \tfrac{1}{2}(p_{1x} - p_{2x})$$
$$Y = \tfrac{1}{2}(y_1 + y_2) \quad y = y_1 - y_2 \quad p_y = \tfrac{1}{2}(p_{1y} - p_{2y})$$
$$Z = \tfrac{1}{2}(z_1 + z_2) \quad z = z_1 - z_2 \quad p_z = \tfrac{1}{2}(p_{1z} - p_{2z}).$$

Note that

$$\frac{\partial(x_1, y_1, z_1, x_2, y_2, z_2)}{\partial(X, Y, Z, x, y, z)} = 1.$$

Let us now consider the matrix elements $(\alpha'|\, V|\alpha^\circ)$. They are of the form

$$\int \cdots \int dx_1 \cdots dz_2 \phi_i V \psi_j$$

where i and j take on the values a, b, c, d. V is considered as an operator on ψ_j. The integrand will consist of a sum of terms of the form

$$\phi_{l's'}{}^{\mathrm{I}}\phi_{n't'}{}^{\mathrm{II}} V \psi_{ls}{}^{\mathrm{I}}\psi_{nt}{}^{\mathrm{II}}$$

where l, n, may be 1, 2 or 2, 1; l', n' may be 1, 2 or 2, 1; s, t, s', t' may be α or β. The only operators contained in V are the Dirac α's and the result of their operation is just to permute the four components of a ψ function and to introduce some factors -1 or i. Also α^I operates[10] only on ψ^I and α^{II} on ψ^{II} so that, for example,

[10] The two electrons are independent in the unperturbed system and all matrices associated with one commute with all matrices associated with the other.

$$\phi^{\mathrm{I}}\phi^{\mathrm{II}}\alpha_1{}^{\mathrm{I}}\alpha_3{}^{\mathrm{II}}\psi^{\mathrm{I}}\psi^{\mathrm{II}} = (\phi^{\mathrm{I}}\alpha_1{}^{\mathrm{I}}\psi^{\mathrm{I}})(\phi^{\mathrm{II}}\alpha_3{}^{\mathrm{II}}\psi^{\mathrm{II}}).$$

We write the expressions (6) for the four components of $\phi_{l'}{}^{I}$ in the form $(\phi_{l'}{}^{I})_\lambda = a_\lambda' S_{l'}{}^{I}$, and for the four components of $\psi_l{}^{I}$ in the form $(\psi_l{}^{I})_\lambda = a_\lambda S_l{}^{II}$, where $\lambda = 1, 2, 3, 4$, and define

$$\begin{aligned}
\Omega_4 &= a_1'a_1 + a_2'a_2 + a_3'a_3 + a_4'a_4 \\
\Omega_1 &= a_1'a_4 + a_2'a_3 + a_3'a_2 + a_4'a_1 \\
\Omega_2 &= a_1'a_4 - a_2'a_3 + a_3'a_2 - a_4'a_1 \\
\Omega_3 &= a_1'a_3 - a_2'a_4 + a_3'a_1 - a_4'a_2.
\end{aligned} \tag{8}$$

We define Ω''s similarly in terms of the components of $\phi_{n'}{}^{II}$ and $\psi_n{}^{II}$. Further we write

$$S = \exp\left[2\pi i/h\left\{(p_l{}^0\cdot r_1) + (p_n{}^0\cdot r_2) - (p_{l'}'\cdot r_1) - (p_{n'}'\cdot r_2)\right\}\right].$$

Then with our three V's of (1), we have for our typical term in the integrand

$$\phi_{l's'}{}^{\mathrm{I}}\phi_{n't'}{}^{\mathrm{II}}V\psi^{\mathrm{I}}{}_{ls}{}^{\mathrm{I}}\psi_{nt}{}^{\mathrm{II}} =$$

$$\begin{aligned}
\mathrm{I}\quad & e^2/r\left[\Omega_4\Omega_4'\right]S \\
\mathrm{II}\quad & e^2/r\left[\Omega_4\Omega_4' - \Omega_1\Omega_1' + \Omega_2\Omega_2' - \Omega_3\Omega_3'\right]S \\
\mathrm{III}\quad & e^2/r\left[\Omega_4\Omega_4' - \tfrac{1}{2}\left\{\Omega_1\Omega_1' - \Omega_2\Omega_2' + \Omega_3\Omega_3'\right\}\right. \\
& \left. - 1/2r^2\left\{x\Omega_1 - iy\Omega_2 + z\Omega_3\right\}\left\{x\Omega_1' - iy\Omega_2' + z\Omega_3'\right\}\right]S.
\end{aligned} \tag{9}$$

Since

$$\begin{aligned}
(p_1\cdot r_1) + (p_2\cdot r_2) &= (P\cdot R) + (p\cdot r) \\
(p_1\cdot r_2) + (p_2\cdot r_1) &= (P\cdot R) - (p\cdot r),
\end{aligned} \tag{10}$$

it follows that in every case our integrand contains a factor

$$\exp\left[\frac{2\pi i}{h}\left\{(P^0\cdot R) - (P'\cdot R)\right\}\right].$$

Consequently, if we carry out the integration in the variables X, Y, Z, x, y, z instead of x_1, y_1, z_1, x_2, y_2, z_2, every matrix element has the factor

$$\int\int\int dXdYdZ \exp\left[\frac{2\pi i}{h}\left\{(P^0\cdot R) - (P'\cdot R)\right\}\right].$$

This integral is of the nature of a δ function of $(P^\circ - P')$ so that we have a transition probability only between initial and final states such that the momentum of the system is conserved, as well as the energy. Consequently, we shall be interested only in the number of transitions from the initial state to final states in which θ lies between θ and $\theta+d\theta$ and ϕ lies between ϕ and $\phi+d\phi$. This means going back to (2), the γ''s being P_x', P_y', P_z', θ, ϕ, and integrating with respect to P_x', P_y', P_z' as we had previously integrated with respect to W'. Although P' occurs in other factors, e.g., in J, besides

$$\left|\int\int\int dXdYdZ \exp\left[\frac{2\pi i}{h}\left\{(P^0\cdot R) - (P'\cdot R)\right\}\right]\right|^2,$$

this factor predominates and assures us that we shall have contributions to the integral only for $P' = P^\circ$. Accordingly, we insert $P' = P^\circ$ in all other factors and take them outside the integration. We note that the remaining integral is just the cube of

$$\int_{-\infty}^{\infty} dP_x' \left| \int_{-\infty}^{\infty} dX \exp\left[\frac{2\pi i}{h}(P_x^0 - P_x')X\right] \right|^2.$$

We replace $\int_{-\infty}^{\infty} dX$ by $\lim_{X=\infty} \int_{X}^{X} dX$ and carry out the limiting process after integrating with respect to P_x', obtaining $\lim_{X=\infty} 2hX$. Thus the factor obtained from integration over P_x', P_y', P_z' is just h^3V, where V is the infinite volume of space.

For the remainder of our considerations, we may note that instead of using the parameters $W, P_x, P_y, P_z, \theta, \phi$ and inserting $W' = W^\circ$ and $P' = P^\circ$, it is more convenient to use $p_{1x}, p_{1y}, p_{1z}, p_{2x}, p_{2y}, p_{2z}$, where the values assigned are to be determined by the principles of conservation of energy and momentum, together with the requirement that p_1' shall have the direction $\theta\phi$. For the initial state, we shall take

$$p_{1x}^0 = p_1^0 = \frac{mv}{(1-\beta^2)^{1/2}}; \; p_{1x}^0 = p_{1y}^0 = p_{2x}^0 = p_{2y}^0 = p_{2z}^0 = 0 \qquad (11)$$

which means that we consider a plane wave of electrons of velocity $v = \beta c$, incident in the z direction on electrons at rest. For the final state, since we have symmetry about the z axis, we are independent of ϕ and may most conveniently use $\phi = 0$. We shall also introduce the notation

$$\gamma = 1/(1-\beta^2)^{1/2}, \; \sigma = \sin\theta, \; \rho = \cos\theta.$$

Then we have

$$\begin{aligned} p_{1x}' &= p_1^0 \frac{2\sigma\rho}{2+(\gamma-1)\sigma^2} & p_{2z}' &= -p_1^0 \frac{2\sigma\rho}{2+(\gamma-1)\sigma^2} \\ p_{1y}' &= 0 & p_{2y}' &= 0 \\ p_{1z}' &= p_1^0 \frac{2\rho^2}{2+(\gamma-1)\sigma^2} & p_{2z}' &= p_1^0 \frac{(\gamma+1)\sigma^2}{2+(\gamma-1)\sigma^2}. \end{aligned} \qquad (12)$$

The density of particles being $\sum_{\lambda=1}^{4} |\psi_\lambda|^2$, we have by (6) a density $2\gamma/\gamma+1$ electrons per cc in our incident beam and a density of one electron per cc of scatterers. Accordingly, the incident flux is $2\gamma v/\gamma+1$ and the number of scatterers is V, the infinite volume of space. The Jacobian, J, of (2) has the value

$$J = \frac{4m^2v\gamma\rho\sigma[2\gamma-(\gamma-1)\sigma^2][\gamma(\gamma+1)\sigma^2+2\rho^2]}{[2+(\gamma-1)\sigma^2]^4}.$$

From the normalization of the final state wave functions by (4), we find for the factor $N_{\alpha'}$.

$$N^2 = \frac{(\gamma+1)[(\gamma+1)^2\sigma^2 + 4\rho^2]}{2h^6[2\gamma - (\gamma-1)\sigma^2][\gamma(\gamma+1)\sigma^2 + 2\rho^2]}.$$

With this value of J in (2) and of N in (3), we insert in (5) and obtain

$$\sigma_s = \frac{4\pi^2 m^2 \rho\sigma(\gamma+1)^2[(\gamma+1)^2\sigma^2 + 4\rho^2]d\theta d\phi}{h^4[2+(\gamma-1)\sigma^2]^4} F^2,$$

where F^2 is one fourth of the sum of the squares of the factors obtained by integration over the relative coordinates in the sixteen matrix elements of the interaction energy, V.

To evaluate F^2, we must go back to (9), which is the typical term of our integrand if we write S_r instead of S and understand by S_r the remainder of the exponential factor, S, after taking out

$$\exp\left[\frac{2\pi i}{h}\{(P^0\cdot R) - (P'\cdot R)\}\right].$$

As a consequence of (10) and using the values of p° and p' given by (11) and (12), this remaining factor has the following form, determined by values of l and l',

$$\begin{aligned}
l=1,\quad l'=1 \quad & S_r = \exp\left[\frac{2\pi i}{h}(p_2'\cdot r)\right] \\
l=2,\quad l'=2 \quad & S_r = \exp\left[-\frac{2\pi i}{h}(p_2'\cdot r)\right] \\
l=2,\quad l'=1 \quad & S_r = \exp\left[\frac{2\pi i}{h}(p_1'\cdot r)\right] \\
l=1,\quad l'=2 \quad & S_r = \exp\left[-\frac{2\pi i}{h}(p_1'\cdot r)\right].
\end{aligned} \tag{14}$$

The integration of (9) with respect to the relative coordinates x, y, z, may be carried out in cylindrical coordinates[11] or in polar coordinates, the pole being taken in the direction of the momentum p_k' which occurs in S_r. In the latter case, convergence is obtained by taking account of screening at infinite distance. The integrals occurring are

$$\begin{aligned}
&\int\int\int dx\,dy\,dz\; 1/r \exp\left[2\pi i/hp_k'^2\right] = h^2/(\pi p_k'^2) \\
&\int\int\int dx\,dy\,dz\; z^2/r^3 \exp\left[2\pi i/hp_k'^2\right] = -h^2/(\pi p_k'^2).
\end{aligned} \tag{15}$$

[11] Oppenheimer, Zeits. f. Physik **43**, 413 (1927).

Then the integration of (9) over the relative coordinates gives

$$\begin{aligned}
&\text{I} \quad \frac{e^2h^2}{\pi p_k'^2}[\Omega_4\Omega_4'] \\
&\text{II} \quad \frac{e^2h^2}{\pi p_k'^2}[\Omega_4\Omega_1' - \Omega_1\Omega_1' + \Omega_2\Omega_2' - \Omega_3\Omega_3'] \qquad (16) \\
&\text{III} \quad \frac{e^2h^2}{\pi p_k'^2}[\Omega_4\Omega_4' + \Omega_2\Omega_2' - (\Omega_1\rho_k - \Omega_3\sigma_k)(\Omega_1'\rho_k - \Omega_3'\sigma_k)].
\end{aligned}$$

Here ρ_k and σ_k are the cosine and sine of the angle between $+p_k'$ and the z axis.

The remainder of the task is the evaluation of the Ω's and Ω''s, the summing of the various terms of the type (16) that occur in each matrix element, the squaring of the resulting expressions and taking one fourth of their sum. Only the results are given here.

For purposes of comparison with previous formulas, it is useful to expand all our expressions in powers of β^2, neglecting higher powers than β^2. The resulting formulas for the cross-section of a free election at rest for scattering electrons into a solid angle $\sin\theta d\theta d\phi$ are

$$\sigma_s = \frac{e^4}{m^2v^4}\sin 2\theta\, 2d\theta\, d\phi\left[\frac{1}{\sigma^4} + \frac{1}{\rho^4} - \frac{1}{\sigma^2\rho^2} - \frac{\beta^2}{4}f(\theta)\right] \qquad (17)$$

where $f(\theta)$ is given by

$$\begin{aligned}
&\text{I} \quad f(\theta) = \frac{4}{\sigma^4} + \frac{2}{\rho^4} - \frac{1}{\sigma^2\rho^2} \\
&\text{II} \quad f(\theta) = \frac{4}{\sigma^4} + \frac{2}{\rho^4} - \frac{2}{\sigma^2\rho^2} \qquad (18) \\
&\text{III} \quad f(\theta) = \frac{4}{\sigma^4} + \frac{2}{\rho^4} - \frac{3}{\sigma^3\rho^2}.
\end{aligned}$$

The purely classical formula of Darwin[12] gives the first two terms in the bracket,

$$\frac{1}{\sigma^4} + \frac{1}{\rho^4} = \operatorname{cosec}^4\theta + \operatorname{cosec}^4(\pi/2 - \theta).$$

Mott[13] has calculated the scattering of electrons by electrons, using interaction formula I, rigorously on the wave mechanics, taking account of interchange phenomena but not of the relativistic variation of mass with velocity. For low velocities, his formula is better than ours. In the region in which our formulas apply, we may neglect the square and higher powers of $1/137\beta$, in

[12] Darwin, Phil. Mag. **27**, 499 (1914).
[13] Mott, Proc. Roy. Soc. **A126**, 259 (1930).

which case Mott's formulas gives just the first three terms in the bracket of (17). It may be noted that $f(\theta)$ is not symmetric about the angle $\theta=\pi/4$, whereas the classical formulas had this symmetry. This was to be expected because, when we take account of the relativistic variation of mass with velocity in setting up the equations for the conservation of energy and momentum, the angle between the two scattered electrons is not $\pi/2$ but is $\arccos\{(\gamma-1)\sigma\rho/(\gamma+1)^2\sigma^2+4\rho^2)^{1/2}\}$ or, in the same approximation as the above, $\arccos\{\beta^2/8[1+\beta^2/4(2+\rho^2)]\sin 2\theta\}$.

For comparison with experimental data, we should use the complete formula, rather than the expansion in powers of β^2. Our F^2 can be written in the form

$$F^2=\frac{c^4h^4[2+(\gamma-1)\sigma^2]^4}{\pi^2m^4c^4(\gamma^2-1)^2[4+(\gamma-1)(\gamma+3)\sigma^2]^2}F(\theta). \tag{19}$$

Substituting (19) in (13), we have

$$\sigma_s=\frac{c^4(\gamma+1)^2\sin 2\theta\, 2d\theta\, d\phi}{m^2v^4\gamma^4[4+(\gamma-1)(\gamma+3)\sigma^2]}F(\theta) \tag{20}$$

where the complete expression for $F(\theta)$ is

$$\begin{aligned}
\text{II}\quad F(\theta)=&\frac{1}{\sigma^4}+\frac{1}{\rho^4}-\frac{1}{\sigma^2\rho^2}+\frac{(\gamma-1)}{\sigma^4\rho^4}\left[3\sigma^6+\sigma^4\rho^6-\sigma^6\rho^2+\frac{2\rho^6(1+\sigma^2\rho^2)}{\gamma+1}\right.\\
&\left.-\frac{2(\gamma+1)\sigma^2\rho^4}{4+(\gamma-1)(\gamma+3)\sigma^2}\right]\\
&+\frac{(\gamma-1)^2}{8\sigma^4\rho^4}\left[\sigma^6\{12-(\gamma+1)(\gamma-3)\sigma^2+2\gamma(\gamma+2)\sigma^4\}\right.\\
&+\frac{8\sigma^4\rho^4(3+\sigma^2)}{\gamma+1}+\frac{24\sigma^4\rho^4}{4+(\gamma-1)(\gamma+3)\sigma^2}-\frac{16(\gamma-1)\sigma^2\rho^6}{(\gamma+1)[4+(\gamma-1)(\gamma+3)\sigma^2]}\\
&\left.+\frac{8\rho^6(1+3\sigma^2+3\sigma^4)}{(\gamma+1)^2}-\frac{32\gamma\sigma^2\rho^6}{[4+(\gamma-1)(\gamma+3)\sigma^2]^2}\right].
\end{aligned} \tag{21}$$

$$\begin{aligned}
\text{III}\quad F(\theta)=&\frac{1}{\sigma^4}+\frac{1}{\rho^4}-\frac{1}{\sigma^2\rho^2}+\frac{(\gamma-1)}{2\sigma^4\rho^4}\left[5\sigma^6+\sigma^8+\frac{4\rho^6}{\gamma+1}+\frac{4\sigma^2\rho^6}{(\gamma+1)^2}\right]\\
&+\frac{(\gamma-1)^2}{4\sigma^4\rho^4}\left[\sigma^4\{-4+23\sigma^2+(\gamma^2+6\gamma-13)\sigma^4+(\gamma^2-2\gamma-3)\sigma^6-(\gamma^2-5)\sigma^8\}\right.\\
&+\frac{2\sigma^4\rho^4(5-4\sigma^4)}{\gamma+1}+\frac{8\sigma^2\rho^4(2+2\sigma^2+(2\gamma-3)\sigma^4-(\gamma-1)\sigma^6)}{4+(\gamma-1)(\gamma+3)\sigma^2}\\
&\left.+\frac{4\rho^6(1+3\sigma^2+2\sigma^4)}{(\gamma+1)^2}-\frac{16(\gamma^2-1)\sigma^4\rho^4}{[4+(\gamma-1)(\gamma+3)\sigma^2]^2}\right].
\end{aligned}$$

4. *Criterion for neglect of orbital motion of electron in hydrogen.* The scattering of elections in hydrogen may be considered as the sum of the scattering by free protons and the scattering by free electrons, both at rest, provided the error in the scattering by the electrons, due to their orbital motion, is negligible. This error is of the order

$$\epsilon = \Delta\sigma_s/\sigma_s$$

where $\Delta\sigma_s$ is the change in σ_s if the square of the momentum of the incident electron is changed by the square of the orbital momentum of the electron in the atom or molecule. Using our formulas for σ_s, we obtain a value for ϵ which, for fast electrons and small angles may be written

$$\epsilon \sim \frac{1 - 3/2\beta^2}{10^4\beta^2 \sin\theta}$$

and for angles near $\pi/2$ may be written

$$\epsilon \sim \frac{1 - \frac{1}{2}\beta^2}{10^4\beta^2 \cos^2\theta}.$$

This is just equivalent to considering the error in the nuclear scattering formula of Wentzel when we drop the $1/k^2a^2$ term[14] and obtain $1/\sin^4\theta/2$ instead of $1/[\sin^2\theta/2+(1/ka)^2]^2$. For a 140,000 volt electron, the error is 1 percent at 7° angle of scattering.

5. Since scattering at angles greater than $\pi/2$ is purely nuclear and should be given by Mott's formula,[15] while scattering at angles less than $\pi/2$ is both nuclear and electronic, it is hoped that the part of the scattering due to the electrons may be separated off experimentally and compared with the formulas derived here. Hydrogen is suggested as the scatterer for this test, in spite of the experimental difficulties of working with gases, first because there, only, is the electronic scattering, which increases with the atomic number Z, comparable with the nuclear scattering, which increases with Z^2, and second because the separation of nuclear and electronic scattering is possible at lower voltages with hydrogen than with any other element, the necessary voltage going up roughly with Z. Mr. H. V. Neher, at this institute, is hoping to carry out experiments in the scattering of high velocity electrons in hydrogen in the near future.

The writer wishes to thank Professor J. R. Oppenheimer for many helpful suggestions.

[14] Sommerfeld, Wave Mechanics, Dutton, 1930, p. 197.
[15] Reference 5.

ON THE GRAVITATIONAL FIELD PRODUCED BY LIGHT

By Richard C. Tolman, Paul Ehrenfest and Boris Podolsky
Norman Bridge Laboratory of Physics, Pasadena, California

(Received January 19, 1931)

Abstract

Expressions are obtained, in accordance with Einstein's approximate solution of the equations of general relativity valid in weak fields, for the effect of steady pencils and passing pulses of light on the line element in their neighborhood. The gravitational fields implied by these line elements are then studied by examining the velocity of test rays of light and the acceleration of test particles in such fields. Test rays moving parallel to the pencil or pulse do so with uniform unit velocity the same as that in the pencil or pulse itself. Test rays moving in other directions experience a gravitational action. A test particle placed at a point equally distant from the two ends of a pencil experiences no acceleration parallel to the pencil, but is accelerated towards the pencil by *twice* the amount which would be calculated from a simple application of the Newtonian theory. The result is satisfactory from the point of view of the conservation of momentum. A test particle placed at a point equally distant from the two ends of the track of a pulse experiences no net integrated acceleration parallel to the track, but experiences a net acceleration towards the track which is satisfactory from the point of view of the conservation of momentum.

§1. *Introduction.* The purpose of this article is to investigate, from the standpoint of the general theory of relativity, the gravitational field in the neighborhood of steady beams and isolated pulses of light.[1]

In Part I of the article we shall obtain a general expression for the line element in the presence of a flow of electromagnetic radiation, which will be taken for simplicity as travelling in the X-direction. The calculation will be made on the assumption that the effect of the radiation is small enough so that Einstein's approximate solution of the gravitational equations valid in weak fields can be employed.

In Part II we shall then examine the special form assumed by the line element in the neighborhood of a thin pencil of radiation travelling along the X-axis. We shall find that the pencil must be taken as having only a finite length in order to keep the field weak enough to justify the use of Einstein's approximate method of solution, and hence shall consider the pencil of radiation as travelling between an emitting and an absorbing body which are a finite distance apart.

Abstracting from the gravitational effect of the absorbing and emitting bodies, we shall then investigate the gravitational action of the radiation by determining the effect of its field on the velocity of test rays of light and on the acceleration of test particles in the neighborhood of the pencil. As to the

[1] An investigation of the gravitational field of radiation has also recently been carried out by Rosenfeld, Zeits. f. Physik **65**, 589 (1930). The article deals, however, with questions relating to quantization rather than with the problems which we shall treat in the present paper.

behavior of the test rays, we shall find that a ray of light moving parallel to the pencil and in the same direction would have unit velocity, the same as that in the pencil itself; but in the case of rays moving in other directions we shall find that they would suffer a gravitational disturbance when in the field of the pencil. As to the behavior of test particles, we shall find that a stationary test particle located at a point equally distant from the two ends of the pencil would experience no acceleration parallel to the track of the pencil, but would be accelerated towards the pencil by *twice* the amount, which would be calculated from the Newtonian theory of gravitation by taking the gravitational mass of the radiation as equal to its energy divided by the square of the velocity of light.

The fact that the acceleration of the particle is twice that which would be calculated from a simple application of the Newtonian theory does not seem surprising, when we recall that the bending of a ray of light in passing through a given gravitational field, say that of the sun, is found theoretically and experimentally in the case of weak enough fields to permit the Newtonian approximation, also to be *twice* that which would be calculated from the Newtonian theory taking the gravitational mass of the light as equal to its inertial mass. The occurrence of the factor 2 in both places permits us to retain our familiar ideas as to the conservation of momentum as a first approximation.

In Part III we shall turn to a consideration of the gravitational field in the neighborhood of a passing pulse of radiation, and shall find that this would vary with the time in a manner to be calculated by the method of retarded potentials, the gravitational influence spreading out from the pulse with the velocity of light. As in the case of the pencil of radiation, we shall find also here that we must limit the track of the pulse so as to lie between an emitting and an absorbing body a finite distance apart, since Einstein's approximate method of solving the gravitational equations would fail at the time when the pulse passes abreast of the point of interest, if we should assume an infinite length for the track.

With regard to the behavior of test rays of light in the neighborhood of the track, we shall again find that a ray of light moving parallel and in the same direction as the pulse would have unit velocity, the same as that of the pulse itself, and that rays of light moving in other directions would be subject to a gravitational effect when in the field of the passing pulse. To investigate the behavior of particles in the field of the pulse, we shall consider a stationary test particle, located at a point equally distant from the two ends of the track lying between the source and absorber, and then determine in accordance with the method of retarded potentials what acceleration the particle would receive as a result of the gravitational influences emitted from this portion of the track. Parallel to the track we shall find that the particle would first be accelerated in the direction of motion of the pulse and later in the opposite direction, but that the time integral of this component of the acceleration corresponding to the total influence emitted from the portion of the track considered would be zero. Perpendicular to the motion of the pulse we shall find as a *net* result that the particle would act as though attracted to-

wards the track, and that the time integral of the perpendicular acceleration, corresponding to the total influence emitted from the portion of the track considered, would be just sufficient so that here also as in the case of the pencil of radiation we could maintain in first approximation our older ideas as to the conservation of momentum for the gravitational interaction of a particle with light.

Part I. General Treatment of the Gravitational Field of Radition

§2. *Einstein's approximate solution of the field equations.* We may now proceed to a general treatment of the gravitational field due to radiation. We shall assume the total amount, density and distribution of the radiation to be such that the gravitational potentials $g_{\mu\nu}$ occurring in the general theory of relativity will differ but slightly from the values which they have in empty space. Such an assumption would presumably be justified in the case of any ordinary beam or pulse of light that we might encounter in nature or the laboratory, and introduces a great simplification by permitting the use of Einstein's approximate solution of the gravitational equations, valid in the case of weak fields.

In accordance with this approximate treatment we may write the line element in the form

$$ds^2 = g_{\mu\nu}dx_\mu dx_\nu = (\delta_{\mu\nu} + h_{\mu\nu})dx_\mu dx_\nu \tag{1}$$

where the symbols $\delta_{\mu\nu}$ denote the Galilean values of $g_{\mu\nu}$, namely -1, $+1$ and 0, and the $h_{\mu\nu}$ are small quantities of the first order whose square can be neglected. We may also use the symbols $\delta^{\mu\nu}$ and $\delta^\nu{}_\mu$ to denote the Galilean values of $g^{\mu\nu}$ and $g^\nu{}_\mu$ and define the quantities $h^\nu{}_\mu$ and h by the equations

$$h_\mu{}^\nu = \delta^{\nu\alpha}h_{\mu\alpha} \text{ and } h = h_\alpha{}^\alpha. \tag{2}$$

It can then be shown that an approximate solution of the equations of general relativity which connect the metric with the distribution of matter and energy is given by the equation[2]

$$\left[h_\mu{}^\nu - \tfrac{1}{2}\delta_\mu{}^\nu h\right](x, y, z, t) = -4\iiint \frac{[T_\mu{}^\nu](\bar{x}, \bar{y}, \bar{z}, t-r)}{r}d\bar{x}d\bar{y}d\bar{z} \tag{3}$$

where the integration is to be taken over all elements of spatial volume $d\bar{x}$ $d\bar{y}d\bar{z}$, the quantity r is the coordinate distance from the element of volume at $\bar{x}$, $\bar{y}$, $\bar{z}$ to the point of interest at x, y, z, and $[T_\mu{}^\nu]$ is the value of the energy-momentum tensor in the element of volume at such a time $t-r$, that an influence travelling from $\bar{x}$, $\bar{y}$, $\bar{z}$ with unit velocity would reach the point of interest x, y, z at the time of interest t.

§3. *The energy-momentum tensor for radiation.* To use the above solution in our problem, we must have an expression for the energy-momentum tensor for radiation. In any purely electromagnetic field, however, is it known that

[2] See Eddington, "The Mathematical Theory of Relativity," Cambridge 1923, Eq. (57.6)

the components of the energy-momentum tensor using natural coordinates have the values illustrated by the following typical examples.[3]

$$T_1^1 = \tfrac{1}{2}(X^2 - Y^2 - Z^2) + \tfrac{1}{2}(\alpha^2 - \beta^2 - \gamma^2) \tag{4}$$

$$T_1^2 = XY + \alpha\beta \tag{5}$$

$$T_1^4 = \beta Z - \gamma Y \tag{6}$$

$$T_4^4 = \tfrac{1}{2}(X^2 + Y^2 + Z^2) + \tfrac{1}{2}(\alpha^2 + \beta^2 + \gamma^2) \tag{7}$$

where X, Y, Z are the components of the electric field strength and α, β, γ are the components of the magnetic field strength at the point of interest.

Applying these equations now to the case of radiation which we take for simplicity to be moving parallel to the X-axis in the positive direction, and noting the relations of (4) and (5) to the Maxwellian stresses in the field, of (6) to the Poynting vector, and of (7) to the energy density, it can be shown that the only surviving components of the energy-momentum tensor for the case of polarized or unpolarized incoherent radiation will be

$$T_1^1 = -\rho \qquad T_4^4 = \rho \qquad T_1^4 = -\rho \qquad T_4^1 = \rho \tag{8}$$

where ρ is the density of energy, and, since the velocity of light is unity, also the density of energy flow at the point of interest. The results assume the justifiability of neglecting diffraction phenomena, such as would occur at the boundary of a beam of radiation where the hypothesis of a flow of energy solely in the X-direction could not be strictly valid.

§4. *The general form of line element due to radiation.* The above equations give the components of the energy-momentum tensor in coordinates which are Galilean at the point of measurement, but to the order of approximation of the solution we are to use, they may also be taken as the components of that tensor in our general system of coordinates which differs from the Galilean form only by quantities of the first order, and hence may be substituted into equation (3) to determine the form of the line element.

Doing so we obtain

$$\begin{aligned}
h_1^1 - \tfrac{1}{2}h &= 4\int \frac{[\rho]dV}{r} \\
h_2^2 - \tfrac{1}{2}h &= 0 \\
h_3^3 - \tfrac{1}{2}h &= 0 \\
h_4^4 - \frac{1}{2}h &= -4\int \frac{[\rho]dV}{r} \\
h_1^4 &= -h_4^1 = 4\int \frac{[\rho]dV}{r}
\end{aligned} \tag{9}$$

with all other components of h_μ^ν equal to zero. And remembering the value of h and the method of raising suffixes given by equations (2) we can easily solve these equations for the $h_{\mu\nu}$. We then obtain as the only surviving components

[3] See Eddington, reference 2, Eqs. (77.41–4).

$$h_{11} = h_{44} = -h_{14} = -h_{41} = -4\int \frac{[\rho]dV}{r} \tag{10}$$

and these values of the $h_{\mu\nu}$ can be substituted into Eq. (1) to give the general form of the line element due to radiation travelling in the X-direction.

Part II. The Gravitational Action of a Pencil of Light

§5. *The line element in the neighborhood of a limited pencil of radiation.* As a first application of the expression for the line element due to radiation travelling in the X-direction, it would be natural to try to treat the gravitational field in the neighborhood of a thin pencil of radiation of uniform density, stretching in the X-direction from minus to plus infinity. But this proves to be impossible by the method adopted, since the values of the $h_{\mu\nu}$ come out infinite when the integration indicated in Eq. (10) is performed, which would invalidate the approximate solution of the gravitational equations that has been used.

If we consider, however, a thin pencil of radiation of limited length l and constant linear density ρ, passing steadily along the X-axis between a source at $x=0$ and an absorber at $x=l$, this difficulty does not arise, since we can then evidently write in accordance with Eq. (10) for the contribution of the radiation to the gravitational field at any point of interest x, y, z in the neighborhood of the pencil,

$$\begin{aligned} 4\int \frac{[\rho]dV}{r} &= -h_{11} = -h_{44} = h_{14} = h_{41} \\ &= \int_{u=0}^{u=l} \frac{4\rho du}{[(x-u)^2 + y^2 + z]^{21/2}} \\ &= 4\rho \log \frac{[(l-x)^2 + y^2 + z^2]^{1/2} + l - x}{[x^2 + y^2 + z^2]^{1/2} - x} \end{aligned} \tag{11}$$

which remains finite for finite values of the density ρ and length of pencil l.

It should be noted that Eq. (11) has been derived on the assumption of a *steady* pencil of radiation between the source and absorber, so that no explicit introduction of retarded potentials into the calculation was necessary. Hence of course the expression obtained would not be applicable in the neighborhood of times when the pencil is being started or stopped. It should also be noted that Eq. (11) gives only the contribution of the radiation in the pencil to the gravitational field and neglects the contribution of the bodies which act as source and absorber. This includes a neglect of any effects resulting from changes in the motion or internal condition of these bodies which might themselves be thought of as connected with the flow of radiation.

With these restrictions, however, the values of the surviving components of $h_{\mu\nu}$ given by Eq. (11) may be substituted into Eq. (1) to give the form of the line element in the neighborhood of the pencil of radiation.

§6. *Velocity of a test ray of light in the neighborhood of the pencil.* Having obtained Eq. (11) which gives the effect of the radiation on the form of the line element, we may now investigate the motion of test rays of light and test particles as affected by the presence of the pencil. In accordance with the theory of general relativity, the velocity of light will be given by setting the expression for the line element ds equal to zero. Substituting the values for the components of $h_{\mu\nu}$ given by (11) into the general expression for the line element (1) setting the result equal to zero, and writing

$$h = 4\rho \log \frac{[(l-x)^2 + y^2 + z^2]^{1/2} + l - x}{[x^2 + y^2 + z^2]^{1/2} - x} \tag{12}$$

as an abbreviation, (not the h of §2) we then easily obtain for the velocity of a test ray in the X-direction parallel to the pencil, the two cases

$$\frac{dx}{dt} = +1 \quad \text{and} \quad -\frac{1-h}{1+h} \tag{13}$$

and for the velocity say in the Y-direction in a plane perpendicular to the pencil, the two cases

$$\frac{dy}{dt} = \pm (1-h)^{1/2}. \tag{14}$$

In accordance with these expressions, we note that a test ray of light moving parallel to the pencil and in the same direction would have unit velocity the same as that in the pencil itself, but that rays moving in other directions would have a variable velocity depending as might be expected on their position in the gravitational field of the pencil. Furthermore, it can easily be shown for the case of a test ray moving parallel to the pencil and in the same direction that we should have, not only $dx/dt=1$, but also $d^2x/dt^2=d^2y/dt^2=d^2z/dt^2=0$, which is a satisfactory result from the point of view of the stability of the light pencil itself.

§7. *Acceleration of a test particle in the neighborhood of the pencil.* We may also use our knowledge of the line element to investigate the gravitational acceleration which would be experienced by a test particle placed in the neighborhood of the pencil.

In accordance with the theory of general relativity, the acceleration of a particle is determined by the equation for a geodesic

$$\frac{d^2x_\alpha}{ds^2} + \left\{\mu\nu, \alpha\right\} \frac{dx_\mu}{ds} \frac{dx_\nu}{ds} = 0 \tag{15}$$

and if we apply this equation to a particle which is at rest in our system of coordinates, we can substitute

$$\frac{dx_\mu}{ds} = 0 \text{ for the cases } \mu = 1, 2, 3 \tag{16a}$$

and to our order of approximation

$$\frac{dx_\mu}{ds} = \frac{dt}{ds} = 1 \text{ for the case } \mu = 4 \tag{16b}$$

so that equation (15) will then assume the simple form

$$\frac{d^2x}{dt^2} = -\left\{44, 1\right\}, \quad \frac{d^2y}{dt^2} = -\left\{44, 2\right\}, \quad \frac{d^2z}{dt^2} = -\left\{44, 3\right\} \tag{17}$$

for the cases $\alpha = 1, 2, 3$.

To calculate the values of the Christoffel symbols occurring in equations (17), we have the general equation of definition

$$\left\{\mu\nu, \sigma\right\} = \frac{1}{2}g^{\sigma\lambda}\left(\frac{\partial g_{\mu\lambda}}{\partial x_\nu} + \frac{\partial g_{\nu\lambda}}{\partial x_\mu} - \frac{\partial g_{\mu\nu}}{\partial x_\lambda}\right) \tag{18}$$

and noting the values of the $g_{\mu\nu}$ which correspond to Eqs. (11), we shall evidently obtain to our order of approximation the simple expressions

$$\frac{d^2x}{dt^2} = -\frac{1}{2}\frac{\partial h_{44}}{\partial x}, \quad \frac{d^2y}{dt^2} = -\frac{1}{2}\frac{\partial h_{44}}{\partial y}, \quad \frac{d^2z}{dt^2} = -\frac{1}{2}\frac{\partial h_{44}}{\partial z}. \tag{19}$$

Substituting then for h_{44} the value given by (11), and performing the indicated differentiations, we can finally obtain, after some simplifications, for the acceleration of a stationary test particle parallel to the line of the pencil the expression

$$\frac{d^2x}{dt^2} = 2\rho\left\{\frac{1}{\left[x^2 + y^2 + z^2\right]^{1/2}} - \frac{1}{\left[(l-x)^2 + y^2 + z^2\right]^{1/2}}\right\} \tag{20}$$

and for the acceleration in a plane perpendicular to the pencil expressions of the form

$$\frac{d^2y}{dt^2} = -\frac{2\rho y}{y^2 + z^2}\left\{\frac{x}{\left[x^2 + y^2 + z^2\right]^{1/2}} + \frac{l-x}{\left[(l-x)^2 + y^2 + z^2\right]^{1/2}}\right\}. \tag{21}$$

The first thing of importance to be noted from these rather complicated expressions for the acceleration is the fact, in accordance with Eq. (20), that the acceleration parallel to the pencil becomes zero for a particle placed at a point $x = l/2$ midway between the two ends of the pencil. Furthermore for a particle midway between the two ends of the pencil, with $x = l/2$ and $z = 0$, Eq. (21) gives for the acceleration towards the pencil the simple result

$$-\frac{d^2y}{dt^2} = \frac{2\rho l}{y\left[(l/2)^2 + y^2\right]^{1/2}}. \tag{22}$$

The most important characteristic of these expressions for the acceleration, however, is the fact that they can easily be shown to be exactly *twice* as great as would be calculated from the simple Newtonian theory by taking

the gravitational mass of the radiation equal to its inertial mass. This is due to the fact that the quantity $h_{44}/2$ occurring in Eqs. (19) is twice the simple Newtonian expression for the gravitational potential of the pencil. As noted in the introduction this is a very satisfactory result, since in the case of weak fields we now see that the factor 2 occurs not only as is known in the expression for the action of a particle on light, but also in the expression for the action of light on a particle, and we are hence able to retain in first approximation our familiar ideas as to the conservation of momentum.

Part III. The Gravitational Action of a Pulse of Light

§8. *The line element in the neighborhood of a pulse of radiation.* As already noted, the considerations of Part II were only applicable to the gravitational field surrounding a steady pencil of light and we shall now turn to a consideration of the gravitational field of a passing pulse of radiation. This will be more complicated to treat since the field will obviously be non-static and we shall have to make specific use of the method of retarded potentials to determine the way in which the gravitational effect spreads out from the moving pulse.

Let us consider a pulse of radiation, of length λ, linear density ρ, and small cross-section, travelling along the X-axis from $x=0$ to $x=l$, which may be taken as the points at which the radiation emerges from the source and enters the absorber, or as giving an arbitrary portion of the track selected for investigation. Furthermore, let us for convenience choose our time scale to make $t=0$ when the front end of the pulse crosses the point $x=0$, so that at any later time t the front end of the pulse will be located at $x=t$ and the rear end at $x=t-\lambda$.

Let us now take some point of interest x, y, z in the neighborhood of the track, and calculate with the help of Eq. (10) the gravitational field produced by the pulse at this point at the time t. Since Eq. (10) has to be applied in accordance with the method of retarded potentials, let us denote by $x=a$ the position of the front end of the pulse and by $x=b$ the position of the rear end of the pulse when they "emit" the gravitational influence which is received at the point x, y, z at the time t. Then we may evidently write in accordance with Eq. (10) for the gravitational potentials at x, y, z and t

$$\begin{aligned} 4\int \frac{[\rho]dV}{r} &= -h_{11} = -h_{44} = h_{14} = h_{41} \\ &= \int_{u=b}^{u=a} \frac{4\rho du}{\left[(x-u)^2+y^2+z\right]^{21/2}} \\ &= 4\rho \log \frac{\left[(x-a)^2+y^2+z^2\right]^{1/2}-x+a}{\left[(x-b)^2+y^2+z^2\right]^{1/2}-x+b} \end{aligned} \tag{23}$$

provided we take the YZ-dimensions of the pulse as small compared with $(y^2+z^2)^{1/2}$.

To evaluate this result, however, we must determine a and b as functions of the time. To do this we note that $t-a$ is the distance through which the

gravitational influence "travels" in going from the front end of the pulse to reach the point x, y, z at the time t, and hence we can evidently write

$$(t-a)^2 = (x-a)^2 + y^2 + z^2 \tag{24}$$

and solving obtain for a the expression

$$a = \frac{t^2 - x^2 - y^2 - z^2}{2(t-x)}. \tag{25}$$

Similarly we obtain for b the expression

$$b = \frac{(t-\lambda)^2 - x^2 - y^2 - z^2}{2(t-\lambda-x)}. \tag{26}$$

In using these expressions in connection with Eq. (23), however, we shall take the position of the rear end of the pulse to be $b=0$ until the pulse has completely emerged from the source at $x=0$, and take the position of the front end as $a=l$ after the pulse has started to enter the absorber at $x=l$. We do this since our interest lies in the gravitational influences correlated with the track of the pulse between $x=0$ and $x=l$.

Substituting the above values of a and b into Eq. (23), we then easily obtain the three following cases for the time intervals indicated

$$\begin{aligned}
4\int\frac{[\rho]dV}{r} &= -h_{11} = -h_{44} = h_{14} = h_{41} \\
&= 4\rho\log\frac{t-x}{[x^2+y^2+z^2]^{1/2}-x} \quad \begin{cases}\text{from } t = [x^2+y^2+z^2]^{1/2} \\ \text{to} \quad t = [x^2+y^2+z^2]^{1/2}+\lambda\end{cases} \\
&= 4\rho\log\frac{t-x}{t-\lambda-x} \quad \begin{cases}\text{from } t = [x^2+y^2+z^2]^{1/2}+\lambda \\ \text{to} \quad t = l+[(l-x)^2+y^2+z^2]^{1/2}\end{cases} \\
&= 4\rho\log\frac{[(l-x)^2+y^2+z^2]^{1/2}-x+l}{t-\lambda-x} \quad \begin{cases}\text{from } t = l+[(l-x)^2+y^2+z^2]^{1/2} \\ \text{to} \quad t = l+[(l-x)^2+y^2+z^2]^{1/2}+\lambda\end{cases}
\end{aligned} \tag{27}$$

and the form of the line element in the different time intervals indicated will be given by substituting these values for the surviving components of $h_{\mu\nu}$ in the general expression for the line element (1). The results show that here also as in the case of the pencil it is necessary to take a limited track for the light pulse, since if the pulse were regarded as coming from an infinitely remote position on the X-axis the field would become infinite at the time $t=x$ when the pulse comes abreast of the point of interest. With our treatment, however, there is no effect from the track of the pulse before the time $t=[x^2+y^2+z^2]^{1/2}$, nor after the time $t=l+[(l-x)^2+y^2+z^2]^{1/2}+\lambda$.

§9. *Velocity of a test ray of light in the neighborhood of the pulse.* Substituting these values for the components of $h_{\mu\nu}$ into the expression for the line element (1) and setting the result equal to zero, we can now obtain information as to the velocity of test rays as affected by the pulse. Writing for simplicity

$$h = 4\int\frac{[\rho]dV}{r} \tag{28}$$

as a general abbreviation for the different expressions given by Eqs. (27), we then easily obtain for the velocity of a test ray in the X-direction parallel to the track, the two cases

$$\frac{dx}{dt} = +1 \text{ and } -\frac{1-h}{1+h} \tag{29}$$

and for the velocity in a plane perpendicular to the track, say in the Y-direction, the two cases

$$\frac{dy}{dt} = \pm (1-h)^{1/2}. \tag{30}$$

As in the case of the pencil, we note that a test ray of light moving parallel to the motion of the pulse and in the same direction would have unit velocity the same as that for the pulse itself, but that rays moving in other directions would have a variable velocity depending on time and position. Here too, it can easily be shown for the case of a test ray moving parallel to the motion of the pulse and in the same direction that we should have, not only $dx/dt=1$, but also $d^2x/dt^2=d^2y/dt^2=d^2z/dt^2=0$, which is a satisfactory result from the point of view of the stability of the pulse itself.

§10. *Acceleration of a test particle due to the pulse.* We must now investigate the gravitational acceleration which would be experienced by a test particle as a result of the passage of the pulse of light. If we take the particle as stationary the accelerations will evidently be determined by the same Eqs. (17)

$$\frac{d^2x}{dt^2} = -\{44, 1\}, \quad \frac{d^2y}{dt^2} = -\{44, 2\}, \quad \frac{d^2z}{dt^2} = -\{44, 3\} \tag{31}$$

as were applicable in the case of the pencil, but the values of the Christoffel symbols will of course be different. To calculate these we may again start with the general equation of definition

$$\{\mu\nu, \sigma\} = \frac{1}{2}g^{\sigma\lambda}\left(\frac{\partial g_{\mu\lambda}}{\partial x_\nu} + \frac{\partial g_{\nu\lambda}}{\partial x_\mu} - \frac{\partial g_{\mu\nu}}{\partial x_\lambda}\right) \tag{32}$$

and noting the values of the $g_{\mu\nu}$ which correspond to Eqs. (27), we can evidently write to our order of approximation

$$\begin{aligned} \{44, 1\} &= -\frac{1}{2}\left(\frac{\partial h_{41}}{\partial t} + \frac{\partial h_{41}}{\partial t} - \frac{\partial h_{44}}{\partial x}\right) \\ \{44, 2\} &= \frac{1}{2}\frac{\partial h_{44}}{\partial y} \\ \{44, 3\} &= \frac{1}{2}\frac{\partial h_{44}}{\partial z}. \end{aligned} \tag{33}$$

Substituting the values of h_{44} and h_{41} given by Eqs. (27), and for simplicity considering the particle to be placed at point for which $z=0$, we can obtain for the acceleration parallel to the track of the pulse during the time intervals indicated

$$\begin{aligned}
\frac{d^2x}{dt^2} &= 2\rho\left(\frac{1}{t-x}+\frac{1}{(x^2+y^2)^{1/2}}\right) && \begin{cases}\text{from } t=(x^2+y^2)^{1/2}\\ \text{to } \ t=(x^2+y^2)^{1/2}+\lambda\end{cases}\\
&= 2\rho\left(\frac{1}{t-x}-\frac{1}{t-\lambda-x}\right) && \begin{cases}\text{from } t=(x^2+y^2)^{1/2}+\lambda\\ \text{to } \ t=l+\left[(l-x)^2+y^2\right]^{1/2}\end{cases} \qquad (34)\\
&= -2\rho\left(\frac{1}{t-\lambda-x}+\frac{1}{\left[(l-x)^2+y^2\right]^{1/2}}\right) && \begin{cases}\text{from } t=l+\left[(l-x)^2+y^2\right]^{1/2}\\ \text{to } \ t=l+\left[(l-x)^2+y^2\right]^{1/2}+\lambda\end{cases}
\end{aligned}$$

And for the acceleration perpendicular to the track we obtain for the same time intervals

$$\begin{aligned}
\frac{d^2y}{dt^2} &= \frac{-2\rho y}{(x^2+y^2)^{1/2}\left[(x^2+y^2)^{1/2}-x\right]} && \begin{cases}\text{from } t=(x^2+y^2)^{1/2}\\ \text{to } \ t=(x^2+y^2)^{1/2}+\lambda\end{cases}\\
&= 0 && \begin{cases}\text{from } t=(x^2+y^2)^{1/2}+\lambda\\ \text{to } \ t=l+\left[(l-x)^2+y^2\right]^{1/2}\end{cases} \qquad (35)\\
&= \frac{2\rho y}{\left[(l-x)^2+y^2\right]^{1/2}}\,\frac{1}{\left[(l-x)^2+y^2\right]^{1/2}+l-x} && \begin{cases}\text{from } t=l+\left[(l-x)^2+y^2\right]^{1/2}\\ \text{to } \ t=l+\left[(l-x)^2+y^2\right]^{1/2}+\lambda.\end{cases}
\end{aligned}$$

In accordance with these expressions, we see that parallel to the track the particle would first be accelerated in the same direction as the motion of the pulse, and then in the opposite direction. On the other hand perpendicular to the motion of the pulse, the particle would first be accelerated towards the track and later away from it. And we must now investigate the total integrated acceleration corresponding to the whole track of the pulse, and compare the results with those which might be expected in first approximation from our older ideas as to the conservation of momentum.

§11. *Time integral of acceleration of test particle due to the pulse.* Making use of the expressions for the acceleration of the test particle parallel to the track of the pulse given by Eqs. (34), we may now obtain the time integral of the acceleration over the three intervals given, and adding together obtain an expression for the total time integral corresponding to the track of the pulse. Doing so and cancelling out a considerable number of balancing terms, it can easily be shown that we finally obtain for the total integral

$$\int \frac{d^2x}{dt^2}dt = 2\rho\lambda\left\{\frac{1}{(x^2+y^2)^{1/2}}-\frac{1}{\left[(l-x)^2+y^2\right]^{1/2}}\right\}. \qquad (36)$$

As might be expected the net acceleration of the test particle parallel to the track depends on the relative magnitudes of the total length of the track l and

the distance along the track x at which the particle is placed. When the test particle is midway between the two ends of the track at $x=l/2$, there is no net acceleration parallel to the track. Otherwise the net parallel acceleration is in the direction towards which the longer segment of the track lies.

Turning now to the acceleration perpendicular to the track it can easily be shown from Eqs. (35) that we obtain for the net integrated acceleration

$$\int \frac{d^2y}{dt^2}dt = -\frac{2\rho\lambda}{y}\left\{\frac{x}{(x^2+y^2)^{1/2}} + \frac{l-x}{[(l-x)^2+y^2]^{1/2}}\right\}. \tag{37}$$

And considering the particle to be located midway between the two ends of the track at $x=l/2$ this reduces to

$$\int \frac{d^2y}{dt^2}dt = -\frac{2\rho\lambda l}{y[(l/2)^2+y^2]^{1/2}}. \tag{38}$$

This result may now be compared with what would be expected from a simple application of ideas as to the conservation of momentum for the combined interaction of particle and light pulse. If we write

$$m = \rho\lambda \tag{39}$$

as an abbreviation for the mass of the light pulse, i.e., its energy divided by the square of the velocity of light, and write M for the mass of the particle, Eq. (38) will then give us for the total momentum acquired by the (stationary) test particle towards the track

$$\int M\frac{d^2y}{dt^2}dt = -\frac{2mMl}{y[(l/2)^2+y^2]^{1/2}}. \tag{40}$$

On the other hand it is well known that the deflection of light in passing through the gravitational field of a particle can be taken in first approximation as twice that which would be calculated from a simple application of the Newtonian theory of gravitation, so that we can evidently write for the momentum acquired by the light pulse in passing over the track

$$\int_0^l \frac{2mMy}{[(l/2-t)^2+y^2]^{3/2}}dt = +\frac{2mMl}{y[(l/2)^2+y^2]^{1/2}} \tag{41}$$

which is equal and opposite to the expression for the momentum acquired by the particle. And since a similar correspondence can be shown for the more general case when the particle is not located midway between the ends of the track, it is evident that we can retain in considerable measure our simple ideas as to the conservation of momentum as a first approximation even in so complicated a process as that of the interaction between a particle and a pulse of light.

Part IV. Conclusion

§12. *Some remarks on the problem.* This completes the material which we desired to present in this article. It is particularly hoped that the treatment

has clarified the problem of the mutual gravitational interaction of radiation and a particle, since we have given special attention to the behavior of a particle in the gravitational field of light, while the treatment of the converse problem of the behavior of light in the gravitational field of a particle is well known.

This converse problem is of course the one of usual importance in connection with astronomical observations when we are interested in the effect of the gravitational fields of stars or other particles on the behavior of a ray of light coming from a distant object. Its treatment can usually be carried through with less difficulty and higher approximation than was feasible for the problems which we have considered in the present paper. This arises partly from the fact that we have the exact Schwarzschild solution for the gravitational field surrounding a stationary point particle, and partly from the fact that disturbances in the motions of neighboring particles which are produced by the passage of a pulse of light cannot in general communicate their effects back in time to affect the gravitational field through which the pulse itself has to pass.

One of the main results of the present article has been to show that in the case of weak fields the gravitational action of light on a particle can in considerable measure be correctly calculated from the Newtonian theory of gravitation provided we take the gravitational mass of the radiation as twice its inertial mass. And since it was already known in the case of weak fields that the gravitational action of a particle on light could in considerable measure also be correctly calculated from the Newtonian theory by taking the gravitational mass of the radiation as twice its inertial mass, we have thus shown the possibility of extending the domain in which we can use our simple ideas as to the conservation of momentum. Of course in general we should expect to be able to use the more complicated ideas as to the conservation of momentum which can be obtained by the device of introducing the *pseudo* energy-momentum tensor t_μ^ν, but the extent to which the simple ideas would be applicable does not appear to have been certain prior to this investigation.

§*13. Other examples of the gravitational field due to radiation.* The effects of radiation on the gravitational field, studied in this article, may also be compared with two other cases in which radiation has been found to produce a different (greater) effect than ordinary matter on the gravitational field.

The first example is furnished by the case of the static Einstein universe where it has been found[4] that the radius R of a universe *filled with stationary incoherent matter* would be connected with the proper density of matter ρ by the expression

$$\frac{1}{R^2} = 4\pi\rho \tag{42}$$

while for a universe *filled solely with radiation* of density ρ the relation would be given by the expression

[4] See for example, Tolman, Proc. Nat. Acad. **15**, 297 (1929), Eqs. (35) and (37).

$$\frac{1}{R^2} = \frac{16}{3}\pi\rho. \tag{43}$$

The second example is furnished by the case of the gravitational field of a sphere of perfect fluid of proper macroscopic density ρ_{00} and pressure p_0. Writing the line element for such a sphere in the form

$$ds^2 = -e^{\mu}(dx^2 + dy^2 + dz^2) + e^{\nu}dt^2 \tag{44}$$

where μ and ν are functions of $r=(x^2+y^2+z^2)^{1/2}$, it is found[5] that the line element degenerates at great distances from the sphere into the approximate Schwarzschild form

$$ds^2 = -\left(1+\frac{2m}{r}\right)(dx^2 + dy^2 + dz^2) + \left(1-\frac{2m}{r}\right)dt^2 \tag{45}$$

where the constant m has the value, obtained by integration over the material in the sphere,

$$m = \int (\rho_{00} + 3p_0)e^{\nu/2}dV_0 \tag{46}$$

dV_0 being the element of proper volume. Since for radiation we have $3p_0 = \rho_{00}$ and for incoherent matter at ordinary temperatures have $p_0 \ll \rho_{00}$, it is evident here too that the radiation in the sphere can be regarded as having a greater effect on the gravitational field than matter of the same density.

[5] Tolman, Phys. Rev. **35**, 875 (1930).

RAMAN LINES OF CYCLOPROPANE AND VALENCE PROPERTIES OF SOME ORGANIC COMPOUNDS

By Robert C. Yates
Mathematics Department, Johns Hopkins University

(Received January 19, 1931)

Abstract

Three fundamental wave-numbers for C_3H_6 are calculated from the equations of motion of a system of three particles vibrating in a plane. The character of a single bond acting adjacent to a double bond in CH_3CHO and again to a triple bond in CH_3CN is studied.

Introduction

IN SEVERAL recent papers appearing in the Physical Review[1,2,3,4] the dynamic properties of molecules were studied with the purpose of correlating the lines of the Raman spectra with different motions of the system. It was assumed that the restoring force arises from a change in the bond length and from a change in the angle between adjacent bonds. It was further assumed that the non-polar chemical bond exhibits the same characteristics throughout the range of organic compounds. For the single bond structure the force constants, k_1 for linear displacement and k_2 for angular displacement, were found to be 5×10^5 and 0.6×10^5 dynes per cm, respectively. These assumptions are adhered to in the present paper but many of the mathematical steps in the calculations are omitted because of the similarity to previous work.[3]

Cyclopropane

We consider here the small vibrations in a plane of three particles of the same mass m, lying at the vertices of an equilateral triangle. The unstrained bond is of length $2a$, each bond forming a side of the triangle. Let (x_iy_i), θ_i be the components of displacement of the particles and the angular changes, respectively. (Note: This problem is particularly interesting from the chemical standpoint because it offers a means of testing the validity of the Bayer strain theory.)

In an inertial system the center of gravity remains at rest and if this point be taken as the origin of coordinates

$$\sum x_i = 0, \quad \sum y_i = 0. \tag{1}$$

[1] C. F. Kettering, L. W. Shutts, and D. H. Andrews, Phys. Rev. **36,** 531 (1930).
[2] D. H. Andrews, Phys. Rev. **36,** 544 (1930).
[3] R. C. Yates, Phys. Rev. **36,** 555 (1930).
[4] A. B. Lewis, Phys. Rev. **36,** 568 (1930).

Since the sum of the forces is zero angular momentum about the origin is constant. This we assume to be zero, giving

$$y_2 = y_1 + 3^{1/2}(x_1 + x_2). \tag{2}$$

The changes in the bond lengths after displacement are found to be [by Eqs. (1) and (2)]

$$\left.\begin{aligned} \Delta_1 &= x_1 - x_2 \\ \Delta_2 &= -\tfrac{1}{2}\left[7x_1 + 8x_2 + 3(3)^{1/2}y_1\right] \\ \Delta_3 &= -\tfrac{1}{2}\left[x_1 + 2x_2 + 3(3)^{1/2}y_1\right] \end{aligned}\right\}. \tag{3}$$

If θ_i be small, we find by taking only two terms in a Taylor expansion

$$\left.\begin{aligned} 4a\theta_1 &= -3y_1 - 3^{1/2}(5x_1 + 4x_2) \\ 4a\theta_2 &= -3y_1 + 3^{1/2}(x_1 + 2x_2) \\ 4a\theta_3 &= 6y_1 + 2(3)^{1/2}(2x_1 + x_2) \end{aligned}\right\}. \tag{4}$$

The energy functions are set up in the usual manner[3]

$$\left.\begin{aligned} T &= (m/2)\sum_1^3(\dot{x}_i^2 + \dot{y}_i^2) \\ &= m\left[4\dot{x}_1^2 + 4\dot{x}_2^2 + 3\dot{y}_1^2 + 7\dot{x}_1\dot{x}_2 + 3(3)^{1/2}(\dot{x}_1 + \dot{x}_2)\dot{y}_1\right] \\ V &= -(k_1/2)\sum_1^3\Delta_i^2 - 2a^2k_2\sum_1^3\theta_i^2 \\ &= -(3k_1/4)\left[9x_1^2 + 12x_2^2 + 9y_1^2 + 18x_1x_2 + 8(3)^{1/2}x_1y_1 + 10(3)^{1/2}x_2y_1\right] \\ &\quad -(9k_2/8)\left[14x_1^2 + 8x_2^2 + 6y_1^2 + 20x_1x_2 + 8(3)^{1/2}x_1y_1 + 4(3)^{1/2}x_2y_1\right] \end{aligned}\right\} \tag{5}$$

giving the equations of motion

$$\left.\begin{aligned} 2m\ddot{x}_1 &= -(3k_1/2)\left[x_1 - 2x_2 - (3)^{1/2}y_1\right] - (9k_2/2)\left[3x_1 + 2x_2 + (3)^{1/2}y_1\right] \\ 2m\ddot{x}_2 &= -(3k_1/2)\left[x_1 + 4x_2 + (3)^{1/2}y_1\right] + (9k_2/2)\left[x_1 + (3)^{1/2}y_1\right] \\ 2m\ddot{y}_1 &= -\left[(3)^{1/2}k_1/2\right]\left[x_1+2x_2+3(3)^{1/2}y_1\right]+\left[3(3)^{1/2}k_2/2\right]\left[x_1+2x_2-(3)^{1/2}y_1\right] \end{aligned}\right\} \tag{6}$$

These yield frequencies:

$$\nu_1 = (1/2\pi)\left[3(k_1 + 3k_2)/2m\right]^{1/2};\quad \nu_2 = (1/2\pi)\left[3(k_1 + 3k_2)/2m\right]^{1/2};$$

$$\nu_3 = (1/2\pi)(3k_1/m)^{1/2}.$$

The molecule C_3H_6 is analogous to the system studied if we assume the mass of the hydrogens concentrated at the nuclei of the carbon atoms. Using $k_1 = 5\times10^5$, $k_2 = 0.6\times10^5$, $m = 13/6.06\times10^{23}$ we find the wave-numbers

$$\bar{\nu}_1 = \bar{\nu}_2 = 400\ \text{cm}^{-1};\quad \bar{\nu}_3 = 1350\ \text{cm}^{-1}$$

where $\bar{\nu} = \nu/3\times10^{10}$.

Character of Multiple Bonds

Two particles of the same mass m are joined to a central particle M by bonds with force constants k_1 and k_2. Let k_3 be the proportionality constant dependent on the change in the angle between the bonds. The particles lie along a straight line in the position of equilibrium and motion is assumed to be in a given plane. The equations of motion are

$$\left.\begin{aligned} mM\ddot{x}_1 &= -k_2[(m+M)x_1 + mx_2] \\ mM\ddot{x}_2 &= -k_1[mx_1 + (m+M)x_2] \\ mM\ddot{y}_1 &= -2k_3[2m+M]y_1 \end{aligned}\right\} \tag{7}$$

with frequencies given by the characteristic:

$$\begin{vmatrix} mM\mu^2 + k_2(m+M) & k_2 m & 0 \\ k_1 m & mM\mu^2 + k_1(m+M) & 0 \\ 0 & 0 & mM\mu^2 + 2k_3(2m+M) \end{vmatrix} = 0. \tag{8}$$

We assume that the groups of atoms in acetaldehyde and methylcyanide lie along a line in the state of rest and take the masses of the end groups as 15.5 and 14.5, respectively. In the former molecule k_1 and k_2 are assigned the values 5×10^5 and 10×10^5 (for single and double bond); in the latter 5×10^5 and 15×10^5 (single and triple bond).

We find for CH_3CHO $\tilde{\nu}_1 = 1695$, $\tilde{\nu}_2 = 844$ as compared with observed Raman data 1716 and 932 which is in good agreement.

The motion of the system that alters the angle between the bonds gives rise to a wave-number in the neighborhood of 440 cm^{-1}. Using this in $mM\mu_2 + 2k_3(2m+M) = 0$ [see Eq. (8)] we evaluate k_3 as 0.26×10^5 dynes per cm.

For CH_3CN we find $\tilde{\nu}_1 = 2095$, $\tilde{\nu}_2 = 905$ compared with the observed values 2240 and 860. The third Raman line occurs at 350 cm^{-1}. This gives $k_3 = 0.15 \times 10^5$ for the bending constant between the single and triple bond.

In these two molecules the assumption on the position of the groups in equilibrium is somewhat dubious. However, the evidence points strongly to a decided weakening of the bending force when multiple bonds lie adjacent to single bonds.

DUST FIGURE IN LIQUID INSULATOR

By Y. Toriyama
Hokkaido Imperial University, Japan

(Received October 9,1930)

Abstract

A dust figure is obtained on the surface of an ebonite plate immersed in a liquid insulator, by dusting it after the application of voltage with a fine powder containing mixture of red lead and resin.

There is a relation between the size of the dust figure and the break down voltage of the liquid insulator.

I. Introduction

As THERE is a certain relation between a sparkover in gases and Lichtenberg's figure or the dust figure in the gases, some connection may exist between the break down phenomena of the liquid insulator and Lichtenberg's figure or the dust figure in the liquid insulator. The dust figure in the liquid insulator, mainly ordinary transformer oil, is here studied to throw light on the break down phenomena of the transformer oil.

II. Dust Figure in Transformer Oil by Impulse Voltage

In order to dry the transformer oil, it is heated to 105°C−110°C for two or three hours, and then filtrated with a paper filter.

Electrodes and an ebonite plate are then immersed in the oil as shown in Fig. 1. (In Fig. 1, N is a needle electrode, P is a plate electrode, E is the ebonite plate, and M_1 C C W denotes the impulse generator). When an impulse

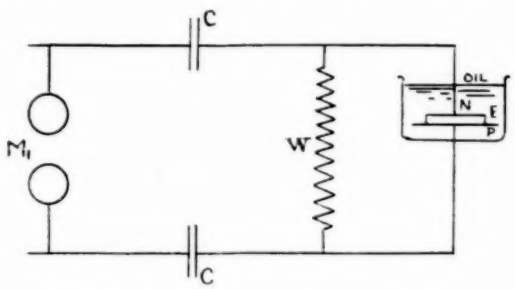

Fig. 1. Diagram of apparatus.

voltage is applied between N and P, and the ebonite plate is then pulled out of the oil, an electric charge will remain on its surface. By sprinkling a fine powder containing a mixture of red lead and resin on the plate, and then washing it gently in gasoline a clear dust figure is produced.

Since the particles of the powder will become electrified by mixing, the positively electrified red lead will stick to the negatively electrified surface,

and the negatively electrified resin will stick to the positively electrified parts. If the dusted surface is then washed in gasoline, the negatively charged part will look reddish because of red lead, and the positively charged part will look yellowish white because of the resin.

An example of a positive dust figure in the oil is shown in Fig. 2, and that of a negative figure in Fig. 3. The crest value of the applied impulse voltage in both cases is 35 k.v. By applying an impulse voltage of 35 k.v., the mean value of the radii of 15 positive figures was 7.13 mm, and that of the negative figures was 4.62 mm. The ratio $R+/R-$ ($R+$ and $R-$ denoting the radius of positive and negative figure respectively) was 1.54.

As mentioned above, the diameter of the positive figure is larger than that of the negative figure. The reason for this fact may be explained somewhat in the following manner. When the impulse voltage is applied between N and P, the needle being the positive pole, the negative ions (including electrons) produced in the ionization by collision will move towards the needle, while the positive ions move radially outwards. Owing to the fact that the velocity

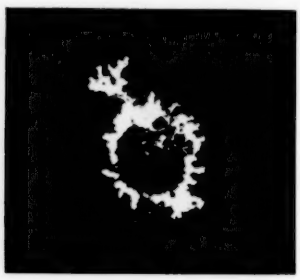

Fig. 2. Positive dust figure in oil. $M_1=8$ mm. Impulse voltage, maximum value, 35.0 k.v. Magnification 1.5.

Fig. 3. Negative dust figure in oil. $M_1=8$ mm. Impulse voltage, maximum value, 35.0 k.v. Magnification 1.5.

of negative ions is greater than that of positive ions, the positive ions will remain near the needle N, so that the high potential gradient at the end of the needle will be weakened by the positive space charge. And the region of high potential gradient will move in time from the needle outwards, and the front of ionization by collision will proceed radially outwards along the ebonite surface. In other words, the potential gradient at the front of the ionization wave, spreading along the surface, will be much larger at a certain moment than the gradient electrostatically calculated.

In the case of a negative needle, the positive ions will remain at the end of the needle, so the ionization by collision may not proceed as in the former case. Accordingly, the radius of the positive figure is greater than that of the negative figure for the impulse voltage of the same intensity.

The radii of the positive and negative dust figures decrease with increasing temperature of the transformer oil, and the ratio $R+/R-$ also decreases with increasing temperature. But the form of the figure does not change. The experimental result is shown in Fig. 4.

The size of the positive and negative figures increases with decreasing atmospheric pressure. The case of a positive figure is shown in Fig. 5.

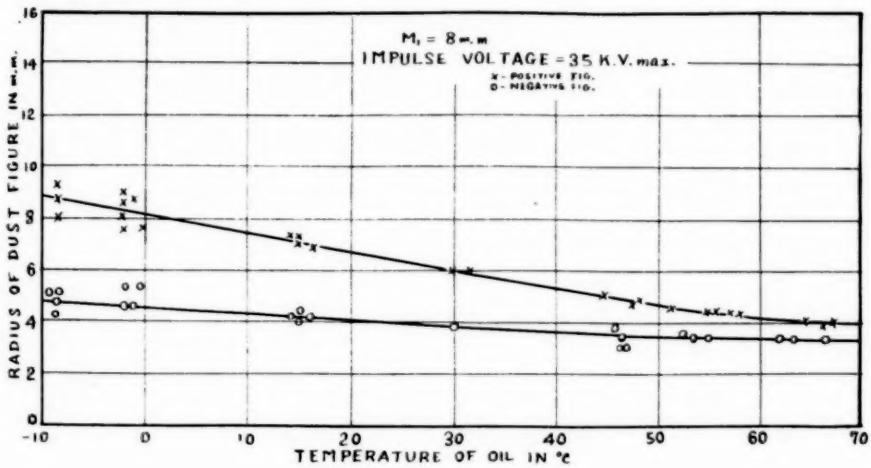

Fig. 4.

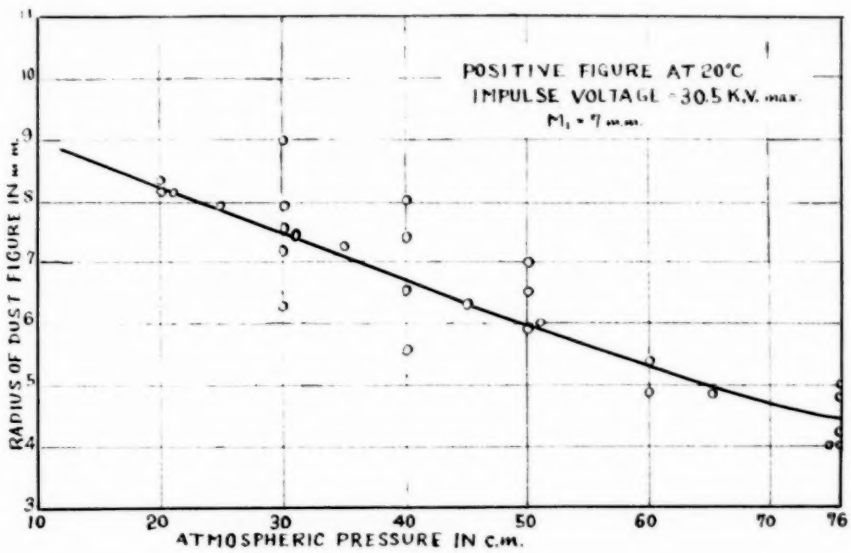

Fig. 5.

A comparison, between the size of the dust figure in the oil and the break down voltage of the oil is as follows:—

(1). In the range of the temperature from $-10°C$ to $70°C$, the break down voltage of the oil increases with increasing temperature.

The size of the dust figure decreases with increasing temperature in the same range of temperature.

(2). The break down voltage of oil decreases with decreasing atmospheric pressure,[1] and the size of the dust figure increases with decreasing atmospheric

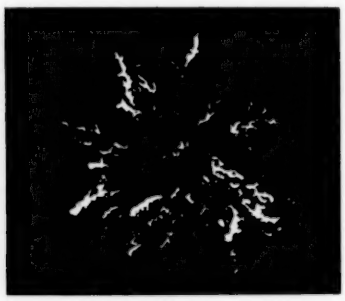

Fig. 6. Dust figure by A. C. voltage. Voltage, effective value 20.0 k.v.

pressure. Briefly, in the case of increasing break down voltage of the oil, the size of the dust figure in the oil decreases, and vice versa. Since the dust figure in the oil may be produced by the partial electric break down of the

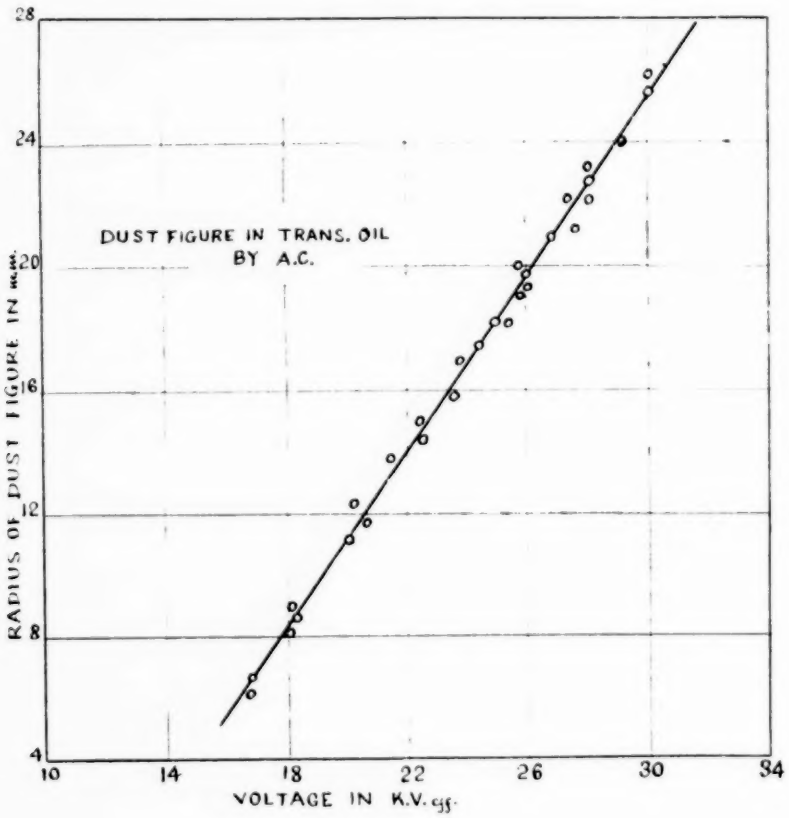

Fig. 7.

[1] J. Sorge, Archiv f. Elekt. **13,** (1924).

oil, the theory that there is a relation between the break down voltage and the dust figure is reasonable.

The conduction through the oil may be ionic or electrolytic. The break down voltage of the oil does not depend on the conductivity of the oil,[2] and neither does the size of the dust figure. The conductivity of the oil does not depend upon the atmospheric pressure.[3] However, the size of the dust figure changes with the atmospheric pressure. From the above two facts, it may be certain that the dust figure is not due to the ionic phenomena, but to the electronic phenomena. From the study of the dust figure it may be concluded that the break down of the transformer oil is a pure electric phenomena.

III. Dust Figure in Transformer Oil by A. C. Voltage

The dust figure in the oil, applying A. C. voltage, can be obtained in the same process as in the case of an impulse voltage. An example of the figure when applying 20 k. v. eff. is shown in Fig. 6.

The radius of the dust figure increases almost linearly with the applied A. C. voltage.

The relation between the radius of the figure and the applied voltage is shown in Fig. 7.

The size of the dust figure by A. C. voltage increases with decrease of the atmospheric pressure.

[2] Y. Toriyama, Archiv f. Elekt. **19**, (1927).
[3] Nikuradse, Zeits. f. techn. Physik. No. 12, (1929).

THE RESISTANCE OF BISMUTH IN ALTERNATING MAGNETIC FIELDS

By William W. Macalpine
The Marcellus Hartley Research Laboratory,
Columbia University, New York, New York

(Received January 22, 1931)

Abstract

Apparatus for producing a field of 100 gauss r.m.s. at 10^6 cycles with a 50 watt tube is described. Also a method of measuring the behavior of bismuth wire in such a field at liquid air temperature. For this purpose a potentiometer has been developed for the measurement of the amplitude and phase of voltages at frequencies up to at least 10^6 cycles per second. It was found that the resistance of the bismuth follows the instantaneous values of the field, having a magnitude at any instant equal to what it would have if the field at that instant were maintained constant. The precision of the magnitude calculated from the various factors involved is ± 3.5 percent and the experimental value is normal within this precision. At 55 kilocyles and room temperature the resistance of the bismuth was also found to be normal in magnitude and phase.

I. Introduction

A GREAT deal of work has been done on the various galvanomagnetic and thermomagnetic effects since the discovery of the Hall effect in 1879 by E. H. Hall. This work is abstracted in L. L. Campbell, "Galvanomagnetic and Thermomagnetic Effects.[1]" It is to be noted that these investigations were carried out without the aid of the three electrode tube and auxiliary apparatus and experimental technique developed in conjunction with the tube, the investigations having been made for the most part before the tube came into general use. The results of the experiments on the resistance of bismuth in alternating magnetic fields varied widely and it was that state of affairs which seemed to make it desirable to investigate its behavior with modern equipment.

Most of the earlier experiments were limited to low audio frequencies (25 to 100 cycles usually) or to magnetic fields which were made to change rapidly, as from zero field to some steady value. Results showed that the magnitude of the change in resistance often was not as great with a.c. as with d.c. fields and frequently a lag was found. However, it is evident that some of these results were erroneous because of the inadequacy of the apparatus available.

In the present experiments bismuth wire 0.06 mm diameter was mounted bifilarly and immersed in liquid air in a combined d.c. and a.c. field, the latter having a frequency of about 10^6 cycles per second. A direct current which was maintained constant by a r.f. choke was passed through the wire and so an a.c. voltage proportional to its resistance appeared across the wire. This

[1] Previous work done in connection with the subject of the present paper is summarized on pp. 166, 191–194.

voltage was measured in amplitude and phase by a potentiometer constructed for the purpose. Measurements had been made previously at 55 kilocycles and room temperature.

It has been shown by various investigators that the Ettingshausen and Nernst effects cause the appearance of a voltage opposing that due to the resistance drop in the bismuth. This effect is illustrated by Kapitza[2] in his work at high magnetic fields. However, with alternating fields this effect would diminish rapidly as the frequency is increased and its voltage would approach a 90° lead with respect to the field. The effect must be entirely negligible at the frequencies used in the present case due to the "thermal inertia" of the metal, which is caused by its heat capacity. Even with constant fields it would be almost zero with a round wire due to the thermal conductivity of the wire.

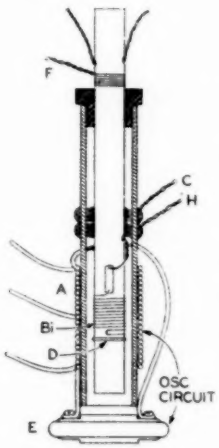

Fig. 1.

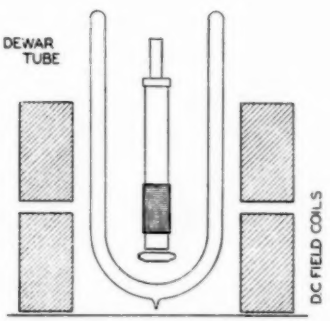

Fig. 2.

Fig. 1. (left) Oscillating circuit, mounting of bismuth wire, etc.
Fig. 2. (right) Location of oscillating circuit within Dewar tube and d.c. field coils.

II. Apparatus

The mounting of the bismuth wire, the coil for obtaining the a.c. field and various other necessary coils are shown in Fig. 1. Coil *A* and condenser *E* form an oscillating circuit which is driven by a power tube, the coil producing the required a.c. field. This coil is wound on a Pyrex tube 3/4 in. diameter and has 36 turns No. 17 wire, the length of the coil being about 2 in. The condenser is 0.003 mfd. Inside the Pyrex tube a 3/8 in. diameter bakelite tube is supported by a bakelite plug. The bismuth wire is wound bifilarly on the bakelite tube, being laid in threads cut in the tube, as it is found that if wound on the surface with even the lightest tension necessary to wind the wire properly, the cooling in liquid air causes it to break. When wound in the threads the tension can be made sufficiently light to prevent breaking, but it is not necessary to have it so light that the wire appears loose. In order to

[2] P. Kapitza, Roy. Soc., Proc. **A119**, 402, 430 ff. (1928).

make it a bifilar winding, two screws are cut, the threads of one screw lying midway between adjacent threads of the other. There are twelve double turns and the axial length of the winding on the tube is 1/2 in. Two thin phosphor bronze strips are used as terminals for the bismuth wire, which is fastened to them with Wood's metal. The strips are secured to the bakelite tube by wrappings of ordinary thread, and a pair of twisted leads of No. 28 wire is connected to their upper ends. Below the bismuth wire is a single turn *D* of No. 28 wire with twisted leads. This is used to measure the a.c. field and to give its vector as a reference for measurements of phase. Two other coils, *H* and *C*, are shown. The first has 5 turns and is used to supply the potentiometer. The other has 19 turns and is used to neutralize undesired voltages appearing in the bismuth wire in a way to be described below. The above apparatus is put in an unsilvered Dewar tube and the whole then placed inside a pair of large coils as shown in Fig. 2. These two coils have an inside diameter of 24 cm outside 38 cm and total height of 24 1/2 cm. Each coil has 375 turns of coarse litz. When the oscillating circuit is placed at the center of these coils they have no appreciable effect on the efficiency of the circuit. They are energized from the d.c. power supply and give ample field for the experiment without undue heating.

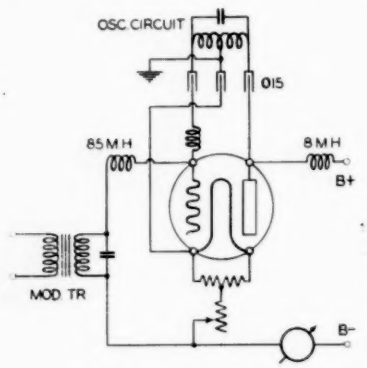

Fig. 3. The oscillator.

The oscillator is shown in Fig. 3, and is of the Hartley type. With the UV 211, a 50 watt tube, fields of 100 gauss r.m.s. could be obtained without overloading the tube. A small choke is inserted in the grid lead to the oscillating circuit to suppress parasitic oscillations. Grid modulation is used by means of the transformer shown. The particular connection of the modulator with r.f. choke is used to prevent audio frequency from getting into the oscillating coil and thence to the detector of the potentiometer. A slight amount of the modulating frequency getting directly to the detector causes either a poorly defined or a double minimum.

The connections to the bismuth wire are shown in Fig. 4. Direct current from a battery may be passed through the wire in either direction, being held constant by an 85 mh radio frequency choke. A 1/2 mfd mica condenser isolates the d.c. from the potentiometer. All condensers and batteries are at ground potential for the high frequency. Although the bismuth wire is bifilarly wound there is some net induced e.m.f., principally at the end connections. Also there is some capacity between the oscillating coil and the phosphor bronze strips used as terminals for the wire, and since the voltages obtained in the former may be several hundred volts, the resulting voltages in the bismuth wire are appreciable compared to the voltages in which we are interested, which are only a few millivolts. In order to compensate for these voltages coil *C* is used. One side of this coil is grounded and the other side is passed through a variable resistance and variable condenser in parallel, to the

ungrounded side of the lead to the bismuth wire, as shown in Fig. 4. The resistance is a non-inductive 25,000 ohm variable unit. The variable condenser is of the midget type with maximum capacity of 50×10^{-12} farads. It may be noted that if the stray voltages induced in the bismuth wire should require it, coil *C* could have a tap and suitable number of turns, the tap being grounded and the variable resistance connected to one side and variable condenser to the other.

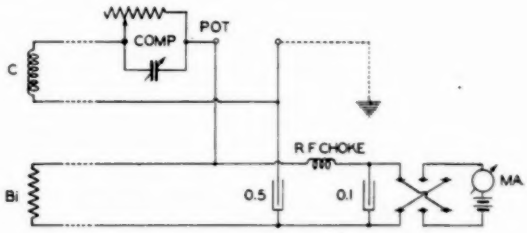

Fig. 4. Circuit connections to bismuth wire.

Fig. 5 is a diagram of the potentiometer and its associated circuits. There are two circular slide wires called the *R* dial and the *C* dial through which flow currents approximately equal in amplitude and approximately 90° apart in phase. These currents are supplied by coil *H* of Figs. 1 and 5 through a shielded transformer *Tr* and the resistances *R* and condensers *C*, which latter determine the amplitude and phase of the currents in the slide wires. A center tapped wire in parallel with each slide wire serves to connect them together at their electrical mid-points.

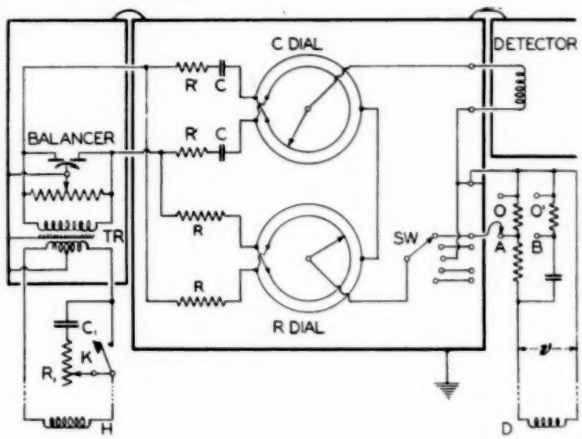

Fig. 5. The potentiometer circuits.

The two sliders are connected in series with the potential to be measured, by a selector switch *Sw*, and a detector. The latter is a grid leak detector with a tuned input transformer whose primary impedance approximately matches that of the potentiometer. Signals are audible because the oscillator, Fig. 3, is modulated.

At the lower right corner of Fig. 5 is shown a calibration circuit which con-

sists of two voltage dividers across the voltage v from a coil such as D of Fig. 1. Voltage v is measured by a thermovoltmeter. The potentiometer dials are calibrated by obtaining the settings for silence in the detector for points O and A, and O' and B' thus determining the number of millivolts per division for each dial. Then the unknown potential, which has been connected to another point of the selector switch, is measured.

Due to distributed inductance and capacity and to skin effect, the constants of the calibration and potentiometer circuits are uncertain, and a more accurate system is desirable. The potentiometer is shielded so the only driving force is through the transformer Tr. A phase shifting circuit C_1R_1 is included in the primary circuit of the transformer, which may rotate the phases of the currents in the two slide wires without altering their relative phase or amplitude. The settings for the calibration circuit are obtained and then the phases of the potentiometer currents rotated through approximately 90° and the new settings for the calibration circuit obtained. A simple calculation then gives the ratios of the currents in the two slide wires and their relative phases. At one million cycles this ratio may be determined to within 1 percent and the phases to 1/2°.

The details of this system and other features of the potentiometer have been described more fully by the author.[3]

III. Experimental Procedure

The d.c. field of the large coils was measured by the usual ballistic galvanometer method, using a fixed search coil and obtaining the galvanometer throw when the magnetizing current was switched on or off. Since it was not practical to have coils which would give a uniform field care was taken to have the test coil and later the bismuth wire close to the center of the large coil where the field is fairly uniform. The variation of the resistance of the bismuth wire with d.c. field was determined by ordinary d.c. bridge measurement and gave the usual curve, parabolic at first and then becoming straight. The a.c. measurements should be made with the d.c. field current at such a value that the curve of resistance vs. field strength is practically a straight line.

In taking a set of measurements, the potentiometer is first calibrated. Then setting the selector switch for the bismuth measurements the compensating circuit is adjusted to bring the dial readings to about their midpoint. This should be done with the continuous field at the value to be used in the measurements immediately following, since the setting of the compensator depends on the resistance of the bismuth wire. Then readings may be taken in succession with various values of d.c. flowing through the wire beginning and ending with zero to make sure that no change has occurred in the compensating circuit or any other circuit during the readings. With no continuous field, no change in voltage was observable for various values of d.c. flowing through the bismuth wire. The vector voltage due to the varying resistance of the bismuth wire is then represented by the difference in dial

[3] W. W. Macalpine, Proc. I.R.E. **18**, 1144 (1930).

readings between those with no d.c. flowing through the wire and those with the value of d.c. in question, the continuous field being the same in both cases. The effect of the leads from the bismuth wire to the potentiometer may be tested by making some measurements with the ordinary leads and then repeating them with considerably longer leads added. The actual leads used were twisted only where they pass up through the 3/8 in. bakelite tube on which the bismuth wire was mounted, a length of 4 in.

In order to measure the field it is necessary to know the diameter of turn D, which may be found at room temperature but not easily in liquid air. For this purpose coil F of 18 turns was wound on the bakelite tube well above the level reached by the liquid air. The voltages induced in D and F were then measured before and after adding the liquid air. The relative voltages induced in F and D were found to be about the same in and out of the liquid air, within experimental error and therefore the area of D changed little in liquid air, due probably to its being on bakelite. The magnetic and electrical properties of the liquid air are of such magnitude that they have little effect on the circuits, and so need not be taken into consideration.

IV. Data and Results

Table I gives the arrangement of the various test circuits used to calibrate the potentiometer. These were supplied by coil D of Fig. 1. Circuits a, b, c, d are those illustrated in the lower right hand corner of Fig. 5. Vectors a, b, f, g, p are those with normal phase, switch K in Fig. 5 closed, while c, d, h, k, q are with the phase of the potentiometer currents rotated.

Table I. *Test circuits.*

Vectors a,c	$DA=929$ ohms	$OA=17.4$ ohms
b,d	$DB=153\times10^{-12}$ farads	$OB=16.1$ "
f,h	193×10^{-12} "	11.5×10^{-9} farads
g,k	929 ohms	9.9×10^{-9} "
p,q	bismuth vectors	

In Table II each of the values of the coordinates *as read* are the average of several readings made at various times during the experimental run and include both positive and negative readings. The leads to coil D were reversed for the negative readings. In the cases of p and q readings were taken with various values of i, the current in the bismuth wire, but all are reduced to the equivalent readings for $i=17.8$ ma. The rectangular coordinates are calculated with the use of α and m as determined by Eqs. (1) and (2) of the article on the potentiometer.[4] v is the voltage induced in turn D and is given in dial divisions, being calculated from the column of *lengths* by the ratios *v/length*, which are calculated from the above data on the test circuits. It should be noted that the value of v in dial divisions for the $a\ b\ f\ g$ system is not necessarily equal to its value for the $c\ d\ h\ k$ system. The phase angle of each vector with respect to the positive R axis is given under θ_R.

[4] Reference 3, $(90°-\alpha)$ is the phase angle between the currents in the two slide wires, while m is the ratio of the current in the C dial to that in the R dial.

TABLE II. *Experimental data.*

Vector	Coordinates: As Read R'	Coordinates: As Read C'	Coordinates: Rectangular R	Coordinates: Rectangular C	Length	$\frac{v}{\text{Length}}$	v	θ_R
a	75.0	29.6	72.6	28.1	77.8	54.5	4240	21.2°
b	−21.7	69.6	−27.3	66.1	71.5	59.4	4247	112.4
f	67.8	26.8	65.7	25.5	70.5	60.5	4265	21.2
g	17.3	−64.8	22.5	−61.6	65.6	62.7	4115	290.0
p	−21.1 ±0.8	86.0 ±0.5	−28.0	81.7	86.4 ±0.9			108.9 ±0.5
					Average		4217	±25
c	31.3	−75.9	37.4	−72.1	81.2		4426	297.3
d	68.3	37.2	65.3	35.3	74.2		4408	28.4
h	27.8	−67.6	33.2	−64.2	72.3		4375	297.3
k	−64.0	−31.1	−61.5	−29.5	68.2		4276	205.7
q	83.8 ±0.4	38.3 ±0.7	80.7	36.4	88.5 ±0.8			24.3 ±0.4
					Average		4371 ±24	

$f = 1.09 \times 10^6 \pm 0.5\%$ cycles per second.
$H/I = 25.0 \pm 1.5\%$ gauss per ampere in d-c field coils.
$dR/dI = 1.55 \pm 0.5\%$ ohms/amp. at $I = 16.1$ amp.
R = d-c resistance of bismuth wire.
$i = 0.0178 \pm 1\%$ d-c amp. flowing in bismuth wire.
$A = 0.810 \pm 2.5\%$ sq. cm, area of turn D, Fig. 1.
Temperature = that of liquid air (about −185°C).
$H_{a-c} = 400$ gauss, approximately.
$v = 1.5$ volts r.m.s., approximately.
$H = 27$ gauss r.m.s., "

The experimental precision of the length of the test vectors a, b, c, d, etc. was about ±0.5 percent and of the angles θ_R, ±0.25°, making the precision of the average values of v ±1 percent. The estimated precision of A is large because of its uncertainty due to immersing the turn in liquid air. Any contraction occurring would increase the calculated value in Table III, which will bring the ratio of measured to calculated values nearer unity.

The calculated high frequency field is

$$H = \frac{v}{2\pi f A} \times 10^8 \text{ gauss}$$

and the high frequency voltage appearing across the bismuth should be

$$e = ir = iH\frac{dR}{dH} = i\frac{dR}{dH}\frac{v}{2\pi f A} \times 10^8.$$

Substituting the above figures: $e = 0.0199 \times v$ volts. The precision of e as calculated from those of its various factors is ±3.5 percent.

The measured value of the length of the vectors p and q must be corrected for the drop due to the compensator, which in this set of measurements had a resistance of 5700 ohms and a capacity of about 45×10^{-12} farads, including capacity of leads. Since the resistance of the bismuth was about 100 ohms, the compensator reduced the a.c. voltage across it by 1/58 and rotated its

phase $-1.6°$. Also, calculation shows that the average field of the oscillating coil on the surface occupied by the bismuth wire was 1.2 percent higher than the average linking turn D which was used to measure the field (see Appendix). Making these corrections to the lengths of the vectors p and q for the compensator and field we have the following results: $p=86.9$, $q=89.0$.

From the value of the *coordinates—as Read* of Table II, the values of α and m may be calculated[3], using both the a, b, c, d set of vectors and the f, g, h, k set. The former gives $\alpha=-0.086$ and $m=0.944$, and the latter $\alpha=-0.099$, and $m=0.950$, the average being $\alpha=-0.092$ and $m=0.947$. Using these values of α and m to find the correction for the α^2m^2 terms, it is found that for both sets of vectors the correction to α is $+0.008$ and that to m is $+0.004$. Thus the true values are $m=0.95$, the correction to m being almost negligible; and $\alpha=-0.092+0.008$, or $-4.8°$. It may be noted that no phase correcting resistances R' of Fig. 5 were used in series with the C dial of the potentiometer in this instance. In regard to the $\phi\beta$ corrections, they may be shown to be negligible. The angles θ, β and ϕ may be found from Table II, and are: $\theta=21°$, $\beta=6°$, $\phi=-1°$ in the a, b, c, d case and $\phi=+1°$ in the f, g, h, k case.

The phase of the magnetic field is determined from that of vectors f and h since these are the vectors for a test circuit of two mica condensers in series. Such circuits introduce very little phase shift due to the small phase angle of the condensers. The phase of vector p with respect to the field is then $108.9° - (90+21.2) = -2.3°$ and similarly that of q is $-3.0°$. Taking into account the phase shift of $-1.6°$ produced by the compensator as noted above, these angles become $-0.7°$ and $-1.4°$, respectively.

The following table gives the above two results as *III* and *IV* and two others obtained similarly on a different date as *I* and *II*. In the latter case it was found that the calculated $e=0.0200\times v$. The columns marked *equivalent e*—Bi give the values of the lengths of the calculated and measured vectors multiplied by the proper ratio to make the calculated length 100.0.

TABLE III. *Results.*

Result	v	e − Bi		Equivalent e − Bi		Phase respt. to field
		Calc.	Meas.	Calc.	Meas.	
I	4300	86.0	88.9 ± 1.5	100.0 ± 3.5	103.4 ± 1.7	0.3° ± 0.9°
II	4400	88.0	91.1 ± 1.0	100.0 ± 3.5	103.5 ± 1.1	−0.6° ± 0.6
III	4217	83.9	86.9 ± 0.9	100.0 ± 3.5	103.6 ± 1.1	−0.7 ± 0.6
IV	4371	87.0	89.0 ± 0.8	100.0 ± 3.5	102.3 ± 0.9	−1.4 ± 0.5
Average				100.0 ± 3.5	103.2 ± 0.6	−0.6° ± 0.5°

$$\frac{Measured}{Calculated} = 1.032 \pm 3.5 \text{ percent}$$

$$Phase = -0.6 \pm 0.5°.$$

It is thus seen that the change in resistance of bismuth at 10^6 cycles per second is normal in magnitude and phase.

V. Measurements at 55 kilocycles, Room Temperature

The above method was first developed at 55 kilocycles, but this work will be described only briefly here. In place of the arrangement of Figs. 1 and 2 a magnet was made from four rings of Western Electric dust core cemented together. This core was cut into two parts to facilitate winding and an air gap formed by cutting away three rings to make the area of the gap that of a single ring, or approximately 1 sq. cm. The oscillating circuit consisted of a mica condenser and two coils in series, one on each side of the air gap, driven by a 50 watt tube in a suitable circuit. Fields up to 700 gauss r.m.s. were easily obtained but those used ranged from 100 to 300 gauss since no cooling system was employed at the bismuth wire. Two coils as close to the air gap as the oscillating coils would allow supplied the d.c. field. These were supplied from the 110 volt d.c. lines with series resistance, a wave trap being employed in series to prevent them from short circuiting the high frequency circuit. The bismuth wire was wound on a mica form which slipped into the air gap. A single turn corresponding to D of Fig. 1 was shellacked to one of two sheets of mica covering the bismuth wire. The connections to the potentiometer were similar to those at the higher frequency except that instead of using the compensator a small coil in series with the leads to the bismuth wire was coupled loosely to the coil of the wave trap. The result obtained was that the resistance of the bismuth wire behaved normally both in phase and magnitude in 55 kilocycle fields, at room temperature.

In conclusion I wish to express my thanks to Professor M. I. Pupin for allowing me the use of The Marcellus Hartley Research Laboratory and for his interest in the work.

Appendix

Note on the field in the solenoid

The ideal condition would be that the a.c. field within the oscillating coil in Fig. 1 is uniform, which would be strictly true only for a very long solenoid. Considerations of efficiency of the coil require that its length be not too long with respect to its diameter. In order to determine what correction would be required due to non-uniformity of the field, its average values over the bismuth wire and turn D were calculated. Briefly the calculation is as follows: The increment of field at p due to an element of circular turn perpendicular to the X axis and with center on that axis is

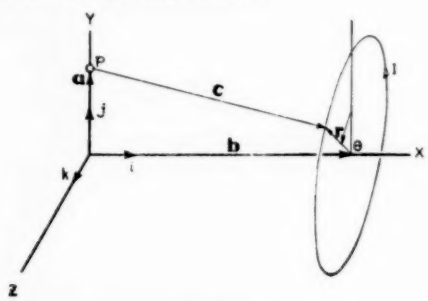

Fig. 6.

$$d\boldsymbol{h} = \frac{I}{C^3}\mathbf{c} \times (i \times \boldsymbol{r})d\theta$$

$$= \frac{Ird\theta}{C^3}[i(r - a\cos\theta) - jb\cos\theta - kb\sin\theta]$$

where $c^2 = b^2 + r^2 + a^2 - 2ra\cos\theta = A - B\cos\theta$. Integrating around the complete turn, the Z component vanishes and

$$\frac{h_i}{I} = \frac{2}{\sqrt{(A+B)}}\left[F\left(k, \frac{\pi}{2}\right) + \frac{2r^2 - A}{A - B}E\left(k, \frac{\pi}{2}\right)\right] \tag{1}$$

$$\frac{h_j}{I} = \frac{2b}{a\sqrt{(A+B)}}\left[F\left(k, \frac{\pi}{2}\right) - \frac{A}{A - B}E\left(k, \frac{\pi}{2}\right)\right] \tag{2}$$

where

$$k = \sqrt{(2B/(A+B))}$$

$$F\left(k, \frac{\pi}{2}\right) = \int_0^{\pi/2} \frac{dZ}{(1 - k^2\sin^2 Z)^{1/2}}$$

the complete elliptic integral of the first order,

$$E\left(k, \frac{\pi}{2}\right) = \int_0^{\pi/2} (1 - k^2\sin^2 Z)^{1/2}dZ$$

the complete elliptic integral of the second order.

In obtaining the above expressions for the components of h, the following integrals are used:

$$\int_0^{\pi} \frac{d\theta}{(A - B\cos\theta)^{1/2}} = \frac{2}{\sqrt{(A+B)}}F\left(k, \frac{\pi}{2}\right)$$

$$\int_0^{\pi} \frac{d\theta}{(A - B\cos\theta)^{3/2}} = \frac{2\sqrt{(A+B)}}{A^2 - B^2}E\left(k, \frac{\pi}{2}\right).$$

The latter is found by writing for $A - B\cos\theta$

$$(A - B)\cos^2\theta/2 + (A + B)\sin^2\theta/2.$$

Eqs. (1) and (2) were plotted for various values of b, with a = radius of turns of bismuth wire and were integrated by planimeter for three points on the wire, the average field on the wire being found from these values. Similarly the average field in turn D was found.

The result was that the average value of the field on the bismuth wire is 1.2 percent higher than the average field linking turn D.

STRAIN AND DIAMAGNETIC SUSCEPTIBILITY

By H. E. Banta
Rice Institute, Houston, Texas

(Received January 20, 1931)

Abstract

The magnetic susceptibility of copper and silver wires has been measured by the Gouy method before and after various annealing processes. Also, the susceptibility has been measured before and after straining specimens beyond the elastic limit, the strains being either twists or stretches. The susceptibilities are found to be increased by as much as 20 percent for copper and 3 percent for silver by annealing at red heat for 15 minutes in an atmosphere of CO_2. This increase is probably due to release of occluded gases or to oxidation or recombination of impurities. Straining the specimens beyond the elastic limit is found to produce no measurable change of susceptibility. Francis Bitter has observed a large effect due to straining these metals beyond the elastic limit. The reason for Bitter's results is not clear, but it is pointed out that no effect is to be expected in copper, at least, because crystals of this metal are isotropic magnetically and have no observable magnetostriction.

RECENTLY Francis Bitter[1] has made the surprising and important observation that annealed copper (impure, paramagnetic) and silver wires suffer a very appreciable change of magnetic susceptibility when strained beyond the elastic limit. This result is surprising for the following reasons. Straining a wire beyond the elastic limit may have the effect of breaking up large crystals into smaller ones. Slipping occurs along cleavage planes, crystal boundary planes are distorted, segregated impurities are redistributed, and new orientations may result for the axes of the tiny crystals. In addition to these effects certain parts of the wire will be left elastically extended, other parts elastically compressed as a result of the unequal slipping of various sections of the wire. These residual strains in a wire have for years been a source of annoyance to users of the Eötvös torsion balance.

It appears, therefore, that the change of susceptibility of a wire when stretched might be explained by two factors: (1) the orienting effect on the small crystals, and (2) the setting up of a strained condition in the wire. In the case of copper the first factor must be ruled out because Montgomery[2] has shown that copper crystals are isotropic magnetically. The second factor is also inadequate for the following reason: the reciprocal relations between strain and magnetization may be expressed by the equation $\partial I/\partial p = \partial e/\partial H$, where I, H, p, and e are, respectively, intensity of magnetization, magnetic field, applied stress, and strain $\partial l/l$. The last two quantities are along the H direction. This equation is based on thermodynamical principles and according to Honda[3] has been verified experimentally even in the case of iron

[1] Francis Bitter, Phys. Rev. **36**, 978 (1930).
[2] Carol G. Montgomery, Phys. Rev. **36**, 498 (1930).
[3] Honda, Magnetic Properties of Matter, p. 46.

and nickel, where hysteresis would tend to make the equation inapplicable. It should hold accurately where hysteresis is negligible, as in copper. In copper, however, magnetostriction is so small that it has never been detected; thus $\partial e/\partial H$ is negligible and therefore $\partial I/\partial p$, or $H\partial K/\partial p$ must be very small. The absence of magnetostriction in copper thus shows that the susceptibility K is unaffected by applied pressures. Hence the second factor given above must be ruled out as an explanation. Accepting Bitter's experimental results, the only conclusion appears to be that the above description of the processes involved in stretching a wire is incomplete.

Accordingly, a series of tests on the effect of strain on the susceptibility of copper and silver was made. As in Bitter's experiments, the Gouy method was used. An analytical balance was mounted about half a meter above an electromagnetic with pole-pieces (truncated cones) 1 cm in diameter and 4 mm apart. The specimen, in the form of a wire about 15 cm long and 2 or 3 mm in diameter, was suspended from one arm of the balance by a silk thread. the lower end of the wire being centered with respect to the pole-pieces. The force on the wire is given by the equation $F=KH^2a/2$ where K, H, and a are the volume susceptibility, magnetic field intensity at the lower end of the wire, and cross-sectional area of the sample, respectively.

When the specimen was suspended 15 cm above the poles of the magnet the balance was not deflected by a measurable amount. Therefore the above equation requires no correction for the field at the top of the specimen. All samples were diamagnetic.

The first set of results was obtained for commercial copper wire about 2.6 mm in diameter. Forces on the samples were measured; they were then twisted beyond the elastic limit by various amounts and the forces again measured. A representative part of these results is shown in Table I. These

TABLE I. *Effect of twist on susceptibility.*

Sample	F_1 dynes	Angle of twist	F_2 dynes	ΔF
1	7.44	0	7.53	+.09
2	7.15	$\pi/2$	7.26	+.11
3	7.20	π	6.95	−.25
4	7.08	2π	7.11	+.03
4	7.11	30π	7.00	−.11

wires did not all have the same diameter, so the forces are different for the different samples. The samples had been well annealed, first in a flame, then in an electric furnace in air. The oxide coating consequent to annealing was removed by sand-papering the surface. It appears that the values of ΔF are within the limits of experimental error. The average value of ΔF is −0.03 dyne and there are both positive and negative values. Furthermore in this experiment it is doubtful whether F could be determined accurately to more than 0.2 dyne. We conclude therefore that K is unaffected by twisting the copper wire greatly beyond the elastic limit. The average specific susceptibility cal-

culated for these samples is 0.5×10^{-7}. For pure copper Montgomery gives 0.85×10^{-7}.

A series of experiments on stretched copper wire was then made. The order of magnitude of F (corrected for changes in diameter) was about the same as in the set of observations shown in Table I. This degree of accuracy was at first considered sufficient, since Bitter got ΔF as large as $\frac{1}{2}F$; but later, pole pieces with larger areas (in order to minimize errors of adjusting the specimen between the pole-pieces) were put on the electro-magnet, and crossed telescopes fastened to its frame to provide accurate control over the position of the specimen. The measurement of the force on a specimen which had been removed and replaced could then be repeated to 0.1 dyne.

The preliminary work showed that annealing a copper wire affected its susceptibility. For example, the force on a specimen was measured, it was heated to redness in CO_2 for about three minutes, cooled slowly, and the force again measured. Successive forces, each determined after a three minute heat treatment, were -6.0, -6.5, -7.0, -7.3, and -7.3 dynes. Similar effects due to annealing have been obtained by Davies and Keeping[4] for copper-antimony alloys. They attribute the phenomenon to changing of the nature of the compounds of copper and antimony. Some samples in the present experiments were heated to a bright red heat in a vacuum, and gave off a gas which, at ordinary pressure, had about half the volume of the copper. The nature of this gas is not known. Therefore it was possibly the presence of impurities or freeing of adsorbed gas which produced the increase of F noted above. The foregoing results indicate that an annealing at red heat for about fifteen minutes is necessary in order to secure the final stable value of the susceptibility. Therefore all further annealings were done in CO_2, holding the specimen above red heat for fifteen minutes and allowing it to cool slowly. All further cleanings are by immersion in boiling HCl for about two minutes, unless otherwise stated.

A second specimen of copper which was slightly paramagnetic when uncleaned was obtained. With its surface sand-papered $F=0.0$ dyne. Annealed, $F=-3.04$ dynes. This is sample A in Table II. Another sample was not annealed, but was cleaned with acid and a value $F=-5.1$ dynes found; some of the surface was then removed with sand-paper and F found to be -5.4 dynes. Thus it appears that paramagnetic impurities were removed from the surface by sand-papering. It is therefore possible that some of the increase of F at annealing is due to the removal (possibly by oxidation) of impurities at or near the surface. When thoroughly annealed this specimen had a value of $F=-6.4$ dynes.

Chemically pure samples of copper and silver were obtained from Baker and Company. These are shown as C and D, respectively, in Table II. The procedure with each sample of Table II was as follows: the force F was measured (except sample B); the wire was annealed and cleaned, and its force F_1 again measured. It was then stretched till its length changed permanently

[4] G. W. Davies and E. S. Keeping, Phil. Mag. **7**, 145 (1929).

by the fraction $\Delta l/l$, cleaned, and the force F_2 again measured. Again it was annealed and cleaned, and the force F_3 again measured. The forces in this table are shown in mg, the units in which they were measured. The d's are diameters of the samples. Multiplying by $(d_1/d_2)^2$ corrects F_2 for the change in cross-sectional area consequent to stretching; so $F_1 - F_2(d_1/d_2)^2$, shown in the table as ΔF, is a measure of the change of K when the sample is stretched.

TABLE II. *Effect of stretching on susceptibility.*

Sample	F mg	F_1 mg	d_1 mm	$\Delta l/l$	F_2 mg	d_2 mm	F_3 mg	$F_2(d_1/d_2)^2$ mg	ΔF mg	$K\times10^6$
A	0.0	3.1	2.61	.10	2.9	2.48	—	3.2	+0.1	−0.22
B*	5.4	—	2.58	.12	4.7	2.43	5.7	5.3	−0.1	−0.48
C	8.0	9.2	3.00	.10	8.6	2.85	8.5	9.4	+0.2	−0.51
C′	—	8.6	2.85	.195	7.2	2.61	7.2	8.6	0.0	−0.51
D	28.7	30.0	3.00	.235	24.3	2.70	24.3	29.9	−0.1	−1.62

* Note: This specimen was annealed in a flame for about one minute at less than red heat before F was obtained. It was given no further annealing before being stretched. Specimen C' is the specimen C after all the data following C were obtained. (F_1 for C' should be the same as F_3 for C except for experimental error.)

Since ΔF is within the limit of experimental error it seems reasonable to conclude that K is unaffected by the stretch. Also, since F_3 is the same as F_2 (except for B), we conclude that annealing a wire of copper or silver which has been hardened by severe stretching does not affect its magnetic susceptibility, provided proper heat treatment has stabilized the wire magnetically before it is strained.

The data on B show that straining a wire which has been imperfectly annealed does not affect its susceptbility. In these experiments the specimens were given permanent strains as large as were used in Bitter's experiments, and the accuracy of measurement was sufficient to detect an effect at least 1/10 as large as Bitter observed. In no case has Bitter's effect been detected. Furthermore, as pointed out in the introduction, there is reason for disbelieving in the reality of the effect because of the absence of magnetostriction in copper and silver.

The conclusion may therefore be drawn that the magnetic susceptibility of copper and silver is not appreciably affected by straining wires of copper and silver beyond the elastic limit. The reason for Bitter's results is not evident.

It is indeed a pleasure to thank Dr. C. W. Heaps for many helpful suggestions and criticisms throughout the investigation.

SOME PHYSICAL PROPERTIES OF COMPRESSED GASES I. NITROGEN*

By W. Edwards Deming and Lola E. Shupe
Fertilizer and Fixed Nitrogen Investigations Bureau of Chemistry and Soils, Washington, D.C.

(Received January 11, 1931)

Abstract

The writers have adjusted and extrapolated the *compressibility data* obtained by Bartlett and his collaborators on nitrogen, so that very accurate *p-v-T data from −70 to 600° and up to 1200 atm.* are available. A suitable graphical scheme has been devised for obtaining the derivatives $(dv/dp)_T$, $(dv/dT)_p$, $(d^2v/dT^2)_p$ at any point in order that some of the physical properties of the gas can be calculated. This graphical scheme depends on the relation of $\alpha \equiv RT/p - v$ and $\Delta \equiv v(pv/RT - 1)$ to p,v,T, and on the relations of the derivatives of α and Δ to the derivatives of v. Errors in the estimation of the slope of an α or Δ curve at any point introduce much smaller errors into the derivatives of v, since the derivatives of α and Δ enter as correction terms to the derivatives of v just as α and Δ are corrections to v itself.

A *graphical process is used as originally in MS for adjusting the p-v-T* data and all the physical properties derived from it. This process is based on the assumption that surfaces such as p-v-T; α-v-T; or Δ-v-T are smooth and hence that the curves in any family of isotherms or isobars show related characteristics. It throws most of the adjustment on v, where it belongs, since the measurements of p and T are much more accurate than those of v. Such an adjustment enhances the precision of the compressibility data and of the calculations made from it.

The *specific volume, density, coefficients* $(-p/v)(dv/dp)_T$ *and* $(T/v)(dv/dT)_p$, *fugacity*, C_p, $C_p - C_v$, C_v, and μ are calculated and shown in curves and a table for the fourteen pressures and twelve temperatures in the range studied. *Inversion pressures and temperatures* are read from the μ vs. p isotherms and the μ vs. T isobars.

The calculations of C_p agree well with the experimental values of Krase and Mackey, who worked at 30, 100, 125, 150° up to 700 atm. and at 50° to 800 atm. The agreement is probably within the experimental error, but the trends of the two sets suggest that a real difference may exist. At 30° the calculated C_p drift below the experimental values at pressures above 400 atm., becoming 0.13 cal/mole · deg low at 700 atm. At 50° the agreement is good to 800 atm. At 100, 125, 150° the calculated C_p drift above the experimental values, but the disagreement reaches only 0.2 cal/mole · deg at 600 and 700 atm.

As one might expect, $C_p - C_v$ approaches R at all temperatures as the pressure approaches zero. In general, $C_p - C_v$ increases at any particular pressure as the temperature decreases. $C_p - C_v$ shows a strong maximum at about 200 atm. at the lowest temperatures. With increasing temperature this maximum comes at higher and higher pressures, and gradually disappears. The C_v vs. T isobars show some curious tendencies. C_v along the 20 atm. isobar stays constant and equal to 2.50 R from −70 to 100°C, then it rises slowly to 5.15 cal/mole · deg at 600°. Along the 40, 60, 80, and 100 atm. isobars, C_v drops a few hundredths of a cal/mole · deg below 2.50 R at −70°, the drop being greater the greater the pressure. Along the 200 atm and higher pressure isobars, C_v rises as the temperature falls below 50°, and the rise is steeper the greater the pressure. At 600° C_v is about 5.18 cal/mole deg or 2.61 R for all pressures.

* An abstract of this paper appeared in the program for the Chicago meeting of the American Physical Society, November 28 and 29, 1930.

RECENT extensions of compressibility data on several gases to 1000 atm. from -70 to 300° and 400° published by Bartlett[1] and his collaborators at this laboratory have made possible the calculation of such physical properties as pressure and temperature coefficients of volume expansion, fugacity, change in heat capacity with pressure, difference between the heat capacity at constant pressure and that at constant volume, Joule-Thomson coefficient, and inversion temperatures and pressures, all at the various temperatures and pressures throughout the range of experimentation and as much further as extrapolations can safely be made.

With extrapolations made by a method to be described, we have reliable compressibility data on nitrogen from -70 to 600° up to 1200 atm. The physical properties of this gas might be expected to show some interesting properties over such a wide range, and we have endeavored to investigate them.

In order to calculate these physical properties from compressibility data it is necessary to evaluate the derivatives $(dv/dp)_T$, $(dv/dT)_p$, $(d^2v/dT^2)_p$ wherever desired. Analytical or graphical methods can be devised for this purpose. Perhaps the best analytical method of getting $(dv/dp)_T$ over a limited pressure range is to write pv as a power series in p along an isotherm. However, no set of coefficients can be found that will satisfactorily follow the trend of pv for nitrogen through the whole range of pressures along any isotherm; one set of constant seems to hold fairly well to some intermediate pressure, depending on the temperature, and another set is necessary from this pressure on up to 1000 atm. This introduces a discontinuity, and the intermediate pressure is thus at the ends of the two ranges. End points are the least trustworthy and we usually get two values for $(dv/dp)_T$ at the discontinuity, and it is then necessary to resort to graphical methods to smooth out the disagreement. The same difficulty exists in getting $(dv/dT)_p$; v^2 expressed as a power series in T seems to fit at low pressures, v as a power series in T seems to fit at high pressures; so there is a break at the intermediate pressure again. These empirical formulas are satisfactory for first derivatives but not for second derivatives except over a limited range. Jakob[2] used them to get the change in heat capacity of air up to 200 atm. from -80 to 250.° He recognized that at the highest temperatures his calculation of $(d^2v/dT^2)_p$ showed evidence of being untrustworthy. Drs. E. P. Bartlett and H. L. Cupples of this laboratory used Jakob's scheme with nitrogen up to 1000 atm. and the difficulties mentioned above were encountered, but by calling on graphical determinations at certain points they obtained results that were valuable, though probably not as reliable as those gotten by the method to be described. We have made free use of some of the ideas in their unpublished manuscript.

The ideal way to obtain these physical properties would be through an

[1] Bartlett, J. Amer. Chem. Soc. **49,** 687 (1927); **49,** 1955 (1927); Bartlett, Cupples, Tremearne, ibid. **50,** 1275 (1928); Bartlett, Cupples, Tremearne, Hetherington, ibid. **52,** 1363 (1930); Bartlett, Hetherington, Kvalnes, Tremearne, ibid. **52,** 1374 (1930); Kvalnes and Gaddy, ibid. **53,** 394 (1931).

[2] Max Jakob, Zeits. f. Techn. Physik, **4,** 460 (1923).

equation of state, but this should not be attempted at pressures and temperatures where it appears not to give trustworthy results. Extensive calculations have been made only with the Beattie-Bridgeman[3,4] formula, but the ranges of temperature and pressure covered in the present paper probably far exceed the limits of validity of any existing equation of state. Since the calculation of the constants in the Beattie-Bridgeman formula for high pressure data on nitrogen were made, further work by the writers[5] has shown that its constants are different above and below the critical density for hydrogen and a 3:1 mixture of hydrogen and nitrogen. The calculations with nitrogen[4] were carried only a trifle beyond the critical density and it is possible that if higher densities had been included a different set of constants would have been indicated for densities above critical. If this second set had been introduced the formula would doubtless have been found to fit better at high pressures than was concluded in our paper, but calculations of the desired physical properties at medium and high pressures are surely more reliable when made by the graphical method about to be described. By it no discontinuities are introduced and the precision can be estimated by the regularity of the graphs of the quantities evaluated.

The authors of the Beattie-Bridgeman equation of state have used it to find the heat capacities and Joule-Thomson coefficients of air and ammonia[6] at ordinary temperatures and relatively low pressures, where the increase ΔC_p in heat capacity is usually a small fraction of the heat capacity at 1 atm. C_p is computed by calculating the change ΔC_p in heat capacity with pressure and adding it to the value of C_p at 1 atm., and when $\Delta C_p/C_p$ is small, large errors in ΔC_p are overlooked when observed and calculated values of C_p are compared.

After studying the α and Δ curves for nitrogen, we decided that it is expecting too much of any formula that it should follow the trends of the p-v-T data as faithfully through the whole range as is desired for determining the physical properties sought after. The following graphical process was developed in the hope of obviating some of the difficulties with analytical methods.

The v vs. T isobars are nearly straight lines from -70 to 600° even to 1200 atm., but by plotting residuals their curvature can be measured easily. If the gas were perfect, the v vs. T isobars would be straight lines through the origin having slopes inversely proportional to the pressure. Any departure from the perfect gas law is evidenced by residuals such as

$$\Delta \equiv v(pv/RT - 1) \tag{1}$$

and

$$\alpha \equiv RT/p - v \tag{2}$$

[3] Beattie and Bridgeman, Proc. Amer. Acad. Arts Sci. **63,** 229 (1928); J. Amer. Chem. Soc. **49,** 1665 (1927), ibid. **50,** 3133 (1928); and later papers.

[4] Deming and Miss Shupe, J. Amer. Chem. Soc. **52,** 1382 (1930).

[5] Deming and Miss Shupe, J. Amer. Chem. Soc. March 1931 (two papers).

[6] Oscar C. Bridgeman, Phys. Rev. **34,** 527 (1929); James A. Beattie, Phys. Rev. **34,** 1615 (1929); James A. Beattie, Phys. Rev. **35,** 643 (1930).

being different from zero; likewise any departure of $(-p/v)\ (dv/dp)_T$ and $(T/v)\ (dv/dT)_p$ from unity is evidenced by $(d\Delta/dp)_T$, $(d\alpha/dp)_T$, $(d\Delta/dT)_p$, $(d\alpha/dT)_p$ being different from zero. Fig. 1 shows how straight the 200 atm. v vs. T isobar is, how much curvature the corresponding Δ and α curves have, and that their shapes are different. There are relations between the slopes

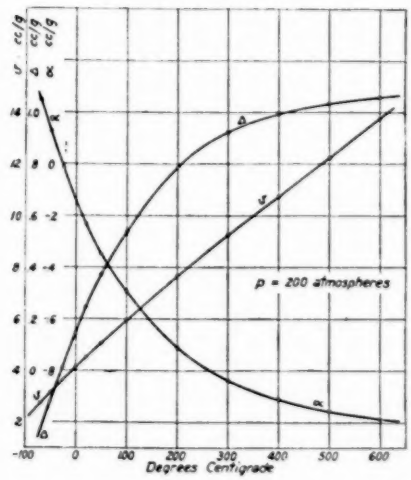

Fig. 1. Graphs of v, Δ, and α vs. T with p constant. This shows that the Δ and α curves have great curvature compared with the v vs. T curve, and that the Δ and α curves are of very different shape.

of the v vs. T, Δ vs. T, and α vs. T isobars; likewise there are relations between the slopes of v vs. p, pv vs. p, Δ vs. p, α vs. p, Δ vs. ρ (density) isotherms. The relations between these are as follows:

$$(T/v)(dv/dT)_p = \frac{pv/RT + (T/v)(d\Delta/dT)_p}{1 + 2\Delta/v} \tag{3}$$

$$(T/v)(dv/dT)_p = RT/pv - (T/v)(d\alpha/dT)_p \tag{4}$$

$$(-p/v)(dv/dp)_T = 1 - \rho(dpv/dp)_T \tag{5}$$

$$(-p/v)(dv/dp)_T = RT/pv + (p/v)(d\alpha/dp)_T \tag{6}$$

$$(-p/v)(dv/dp)_T = \frac{pv/RT - (p/v)(d\Delta/dp)_T}{1 + 2\Delta/v} \tag{7}$$

$$(-p/v)(dv/dp)_T = -pv/RT(2\Delta/v + 1 + \rho^2(d\Delta/d\rho)_T) \tag{8}$$

$$(d^2v/dT^2)_p = -(d^2\alpha/dT^2)_p \tag{9}$$

$$(2\Delta/v + 1)(d^2v/dT^2)_p = (d^2\Delta/dT^2)_p - \frac{2p}{RT}\,\frac{(\Delta/T - (d\Delta/dT)_p)^2}{(2\Delta/v + 1)^2}. \tag{10}$$

A 1 percent error in estimating the slope of an α vs. T or a Δ vs. T isobar may mean only a few hundredths percent error in $(dv/dT)_p$, since by Eqs. (3) and (4) the slopes $(d\alpha/dT)_p$ and $(d\Delta/dT)_p$ enter as correction terms to the

slope that the v vs. T isobar would have if the gas were perfect, just as α and Δ are correction terms to v by Eqs. (1) and (2). Likewise, any error in the determination of $(-p/v)\,(dv/dp)_T$ is diminished according to Eqs. (5), (6), (7), (8). The different families of isobars and isotherms have quite different appearances, so the effect on $(-p/v)\,(dv/dp)_T$ or $(T/v)\,(dv/dT)_p$ of any personal error in estimating the slope of a curve on account of its having a particular shape may be balanced out at that point by a determination from some other curve of different shape. It was not noticeable that the determinations of these derivatives from the α curves were consistently higher or lower than those from the Δ curves or any others.

In order to determine $(d^2v/dT^2)_p$ one can plot $(dv/dT)_p$ vs. T isobars and read the slope at the desired point. Or, one can plot $(d\alpha/dT)_p$ or $(d\Delta/dT)_p$ vs. T isobars, and from the slope of these curves and the relations between $(d^2v/dT^2)_p$ and $(d^2\alpha/dT^2)_p$ or $(d^2\Delta/dT^2)_p$, one can determine $(d^2v/dT^2)_p$. Both methods were used; the results agreed well, and their averages at the various points are shown in Fig. 2.

The most probable positions of observed points lie on the most plausible graph (curve or surface) that can be drawn from them. The most probable values are not uniquely determined by a graphical method, because they depend on the weight assigned by the investigator to various essentials. An adjustment by least squares depends on the weights assigned to the observations so it, too, is subject to the taste and judgment of the computer or observer. Schemes of curve fitting or adjusting that give unique results are incapable of weighting the observations and of throwing the adjustment where it belongs. This has been discussed in two papers by the senior author.[7]

We adopted as a working principle that, in the range investigated, all surfaces such as p, v, T; Δ, p, T; α, p, T; $(d\alpha/dT)_p, p, T$; etc.; have no sharp ridges nor breaks; accordingly all families of isobars and isotherms should be smooth curves without sharp bends or cusps. All the curves in a given family should show their relationship one to another since they can be considered as sections all cut from the same surface, so that each helps to regulate the drawing of the others. The p-v-T data themselves were adjusted by first drawing smooth curves through the Δ vs. p isotherms and reading off Δ from them, then by plotting these Δ against T with p constant and smoothing these curves for the final values of Δ. The specific volumes were calculated from these final values of Δ. The precision of adjusted observations is strengthened by a wide range of temperature and pressure, such as that studied in this work.

The final values shown in the table and curves were smoothed with respect to temperature and pressure, except where they had been derived from others that had already been smoothed. The regularity of the points on the Δ and α curves attests to the high precision of the compressibility data and gave promise that thermodynamic calculations derived from them should be reliable.

[7] W. Edwards Deming, Proc. London Phys. Soc. **42**, 97 (1930); Phil. Mag. **11**, 146 (1931).

TABLE I. *Some physical properties of compressed nitrogen derived from experimental data on compressibility.*

1	2	3	4	5	6	7	8	9
t	p	v	ρ	f	$-\frac{p}{v}\left(\frac{dv}{dp}\right)_T$	$\frac{T}{v}\left(\frac{dv}{dT}\right)_p$	ΔC_p	μ
°C	atm	cc/g	g/cc	atm			cal/mole°	°/atm
−70°	20	28.50	.03508	19.22	1.053	1.162	.50	.627
	40	13.71	.07294	36.91	1.075	1.347	1.12	.592
	60	8.840	.1131	53.31	1.075	1.530	1.79	.538
	80	6.460	.1548	68.66	1.052	1.682	2.46	.470
	100	5.082	.1968	83.18	1.004	1.806	3.13	.408
	200	2.725	.3669	152.1	.717	1.564	5.17	.128
	300	2.150	.4652	227.2	.514	1.162	5.19	.029
	400	1.896	.5273	319.2	.403	.918	5.10	−.013
	500	1.743	.5738	433.0	.345	.776	5.04	−.033
	600	1.642	.6090	575.5	.309	.675	5.00	−.045
	800	1.508	.6630	976.2	.280	.551	4.97	−.057
	1000	1.421	.7035	1596	.250	.459	4.93	−.065
	1100	1.388	.7204	2021	.250	.408	4.89	−.070
	1200	1.358	.7365	2545	.250	.356	4.81	−.074
−50°	20	31.75	.03149	19.48	1.031	1.129	.45	.559
	40	15.50	.06452	37.92	1.048	1.259	.93	.511
	60	10.13	.09872	55.49	1.048	1.381	1.43	.463
	80	7.492	.1335	72.38	1.030	1.477	1.92	.405
	100	5.952	.1680	88.75	1.000	1.560	2.41	.355
	200	3.139	.3186	168.4	.775	1.462	3.76	.136
	300	2.394	.4178	255.1	.590	1.158	3.85	.035
	400	2.068	.4836	357.8	.472	.937	3.84	−.012
	500	1.878	.5325	483.4	.397	.799	3.77	−.035
	600	1.753	.5705	638.1	.360	.699	3.72	−.050
	800	1.591	.6284	1063	.313	.578	3.66	−.064
	1000	1.485	.6736	1701	.286	.491	3.61	−.072
	1100	1.443	.6928	2127	.286	.449	3.56	−.076
	1200	1.408	.7103	2645	.286	.404	3.48	−.081
−25°	20	35.75	.02798	19.70	1.018	1.094	.36	.470
	40	17.65	.05666	38.80	1.025	1.191	.75	.424
	60	11.66	.08578	57.43	1.025	1.266	1.14	.383
	80	8.694	.1150	75.69	1.008	1.328	1.53	.339
	100	6.950	.1439	93.70	.900	1.377	1.90	.298
	200	3.645	.2744	183.6	.830	1.363	2.95	.134
	300	2.704	.3698	281.4	.653	1.149	3.12	.040
	400	2.287	.4372	395.5	.540	.961	3.02	−.008
	500	2.046	.4888	532.4	.455	.831	2.91	−.035
	600	1.890	.5291	697.6	.415	.732	2.81	−.052
	800	1.695	.5901	1121	.353	.608	2.72	−.069
	1000	1.567	.6382	1784	.325	.526	2.66	−.078
	1100	1.516	.6598	2205	.325	.491	2.62	−.081
	1200	1.473	.6789	2703	.320	.457	2.53	−.085
0°	20	39.67	.02521	19.84	1.010	1.068	.29	.387
	40	19.72	.05071	39.38	1.010	1.128	.60	.344
	60	13.11	.07627	58.72	1.005	1.183	.92	.308
	80	9.828	.1018	77.91	.993	1.235	1.24	.277
	100	7.886	.1268	97.05	.978	1.265	1.53	.247
	200	4.139	.2416	194.6	.850	1.281	2.34	.125
	300	3.020	.3311	301.3	.696	1.136	2.55	.043

TABLE I. (Cont'd.) *Some physical properties of compressed nitrogen derived from experimental data on compressibility.*

1	2	3	4	5	6	7	8	9
t	p	v	ρ	f	$-\frac{p}{v}\left(\frac{dv}{dp}\right)_T$	$-\frac{T}{v}\left(\frac{dv}{dT}\right)_p$	ΔC_p	μ
°C	atm	cc/g	g/cc	atm			cal/mole°	°/atm
	400	2.510	.3984	424.2	.590	.983	2.48	−.005
	500	2.217	.4510	569.2	.510	.863	2.37	−.033
	600	2.032	.4922	741.8	.466	.765	2.30	−.052
	800	1.798	.5560	1194	.390	.639	2.20	−.071
	1000	1.650	.6060	1834	.360	.557	2.13	−.080
	1100	1.591	.6286	2246	.360	.530	2.08	−.082
	1200	1.543	.6481	2732	.350	.503	2.01	−.084
20°	20	42.74	.02340	19.92	1.003	1.055	.25	.325
	40	21.33	.04688	39.70	1.001	1.099	.50	.291
	60	14.23	.07027	59.41	.995	1.140	.75	.263
	80	10.70	.09347	79.12	.983	1.182	.99	.236
	100	8.604	.1162	99.06	.970	1.199	1.22	.211
	200	4.524	.2210	201.0	.860	1.223	2.05	.114
	300	3.271	.3058	313.1	.720	1.117	2.32	.043
	400	2.693	.3713	441.5	.628	.994	2.33	−.002
	500	2.360	.4238	591.8	.550	.880	2.27	−.031
	600	2.146	.4659	768.9	.500	.786	2.22	−.051
	800	1.880	.5318	1226	.417	.660	2.13	−.071
	1000	1.717	.5823	1861	.387	.580	2.06	−.080
	1100	1.654	.6047	2265	.387	.554	2.03	−.082
	1200	1.601	.6248	2737	.373	.534	1.98	−.083
50°	20	47.33	.02113	20.01	.998	1.037	.19	.248
	40	23.72	.04217	40.05	.992	1.070	.37	.228
	60	15.87	.06301	60.18	.984	1.099	.54	.208
	80	11.97	.08356	80.44	.975	1.125	.71	.188
	100	9.639	.1038	100.9	.961	1.138	.86	.169
	200	5.078	.1969	207.5	.845	1.151	1.46	.094
	300	3.640	.2747	325.4	.753	1.092	1.77	.038
	400	2.967	.3371	459.7	.670	.995	1.88	−.001
	500	2.572	.3888	615.4	.597	.895	1.90	−.003
	600	2.320	.4311	796.4	.540	.808	1.89	−.050
	800	2.010	.4974	1254	.456	.688	1.83	−.071
	1000	1.821	.5492	1878	.423	.611	1.78	−.080
	1100	1.748	.5720	2268	.418	.588	1.76	−.081
	1200	1.688	.5925	2719	.402	.566	1.74	−.083
100°	20	54.87	.01822	20.08	.995	1.023	.12	.162
	40	27.59	.03624	40.36	.987	1.041	.24	.149
	60	18.52	.05400	60.87	.975	1.052	.35	.138
	80	14.00	.07143	81.64	.965	1.064	.46	.126
	100	11.29	.08856	102.1	.953	1.078	.56	.114
	200	5.955	.1679	213.7	.881	1.078	1.01	.058
	300	4.243	.2357	337.0	.791	1.037	1.33	.020
	400	3.421	.2924	476.8	.716	.974	1.53	−.010
	500	2.928	.3416	636.3	.652	.896	1.63	−.035
	600	2.612	.3828	819.2	.601	.828	1.67	−.052
	800	2.225	.4494	1271	.515	.720	1.70	−.072
	1000	1.994	.5014	1867	.471	.649	1.77	−.080
	1100	1.909	.5239	2232	.463	.623	1.86	−.083
	1200	1.836	.5447	2649	.445	.597	1.98	−.085

TABLE I. (Cont'd.) *Some physical properties of compressed nitrogen derived from experimental data on compressibility.*

1	2	3	4	5	6	7	8	9
t	p	v	ρ	f	$-\frac{p}{v}\left(\frac{dv}{dp}\right)_T$	$\frac{T}{v}\left(\frac{dv}{dT}\right)_p$	ΔC_p	μ
°C	atm	cc/g	g/cc	atm			cal/mole°	°/atm
200°	20	69.82	.01432	20.15	.990	1.008	.07	.075
	40	35.21	.02840	40.62	.980	1.013	.14	.063
	60	23.68	.04223	61.45	.970	1.017	.21	.053
	80	17.93	.05578	82.63	.960	1.017	.27	.044
	100	14.48	.06905	104.2	.950	1.017	.33	.035
	200	7.637	.1309	218.8	.895	1.003	.59	.002
	300	5.389	.1856	346.3	.835	.970	.79	−.022
	400	4.287	.2333	489.0	.775	.923	.94	−.041
	500	3.622	.2761	649.4	.720	.875	1.05	−.056
	600	3.192	.3133	829.7	.675	.828	1.15	−.067
	800	2.655	.3767	1261	.601	.748	1.30	−.082
	1000	2.333	.4286	1804	.550	.672	1.41	−.092
	1100	2.217	.4511	2126	.537	.644	1.46	−.095
	1200	2.120	.4718	2485	.516	.610	1.51	−.098
300°	20	84.64	.01181	20.18	.990	1.003	.05	.010
	40	42.70	.02342	40.71	.980	1.003	.09	.002
	60	28.73	.03480	61.62	.970	.997	.14	−.006
	80	21.75	.04597	82.92	.960	.997	.18	−.012
	100	17.57	.05692	104.6	.951	.992	.22	−.018
	200	9.230	.1083	219.6	.907	.969	.39	−.042
	300	6.467	.1546	346.7	.858	.934	.53	−.058
	400	5.098	.1962	487.4	.808	.894	.64	−.071
	500	4.277	.2338	643.1	.762	.860	.73	−.077
	600	3.735	.2678	815.7	.722	.825	.81	−.084
	800	3.060	.3268	1218	.658	.751	.91	−.096
	1000	2.657	.3764	1709	.607	.694	.98	−.103
	1100	2.509	.3985	1994	.594	.665	1.00	−.105
	1200	2.387	.4190	2306	.570	.642	1.02	−.107
400°	20	99.39	.01006	20.17	.991	.976	.03	−.043
	40	50.12	.01995	40.69	.983	.996	.07	−.047
	60	33.71	.02967	61.56	.975	.990	.10	−.051
	80	25.50	.03921	82.81	.968	.983	.13	−.055
	100	20.59	.04858	104.4	.960	.983	.16	−.058
	200	10.76	.09289	218.6	.915	.949	.28	−.074
	300	7.502	.1333	343.6	.874	.916	.40	−.082
	400	5.879	.1701	480.6	.832	.889	.45	−.088
	500	4.912	.2036	630.7	.791	.855	.51	−.094
	600	4.263	.2346	795.1	.755	.828	.56	−.097
	800	3.456	.2893	1172	.700	.767	.63	−.105
	1000	2.976	.3360	1621	.650	.714	.67	−.110
	1100	2.798	.3574	1876	.635	.693	.69	−.112
	1200	2.653	.3770	2154	.612	.670	.70	−.113
500°	20	114.1	.008765	20.16	.991	.997	.02	−.068
	40	57.50	.01739	40.65	.985	.990	.04	−.072
	60	38.65	.02588	61.47	.975	.982	.06	−.076
	80	29.22	.03422	82.63	.969	.982	.08	−.080
	100	23.57	.04242	104.1	.960	.974	.09	−.082
	200	12.27	.08149	217.1	.921	.943	.17	−.093
	300	8.521	.1174	339.9	.885	.912	.24	−.098

TABLE I. *Some physical properties of compressed nitrogen derived from experimental data on compressibility.*

1	2	3	4	5	6	7	8	9
t	p	v	ρ	f	$-\frac{p}{v}\left(\frac{dv}{dp}\right)_T$	$\left(\frac{Tdv}{vdT}\right)_p$	ΔC_p	μ
°C	atm	cc/g	g/cc	atm			cal/mole°	°/atm
	400	6.651	.1504	473.3	.847	.889	.29	−.101
	500	5.530	.1808	618.2	.812	.858	.34	−.104
	600	4.783	.2091	775.6	.780	.835	.38	−.107
	800	3.848	.2599	1131	.728	.781	.44	−.112
	1000	3.290	.3039	1547	.682	.736	.48	−.115
	1100	3.084	.3242	1781	.665	.715	.49	−.116
	1200	2.916	.3429	2033	.644	.698	.50	−.116
600°	20	128.8	.007766	20.15	.992	.995	.01	−.083
	40	64.87	.01542	40.60	.985	.987	.03	−.087
	60	43.57	.02295	61.36	.976	.987	.04	−.090
	80	32.93	.03037	82.43	.969	.978	.05	−.093
	100	26.54	.03768	103.9	.961	.978	.06	−.095
	200	13.77	.07264	215.8	.926	.943	.11	−.101
	300	9.528	.1050	336.6	.891	.917	.15	−.106
	400	7.409	.1350	466.9	.860	.891	.19	−.110
	500	6.141	.1628	607.4	.829	.864	.23	−.114
	600	5.294	.1889	758.9	.800	.838	.26	−.116
	800	4.234	.2362	1097	.746	.792	.31	−.117
	1000	3.604	.2775	1488	.707	.753	.33	−.119
	1100	3.369	.2968	1705	.691	.737	.34	−.119
	1200	3.177	.3148	1938	.670	.720	.35	−.119

In most p-v-T determinations, the measurement of v is subject to greater error than those of p and T. The Δ and α curves are large scale deviation graphs of residuals of volume and they greatly magnify any error in v, so it is possible to smooth out any irregularities that may be in the original data, and put the adjustment where it belongs. Δ can probably be smoothed to within 0.005 cc/g; and since $(dv/d\Delta)_{p,T}=1/(2pv/RT-1)$, the smoothed specific volumes should be accurate to within 0.005 cc/g except in the extrapolated region and in the small range where $pv<RT$.

After considerable practice in laying a straight edge tangent at various points along a curve where the slopes are definitely known, it was found possible to estimate the slope at any point within half a percent, in trial after trial. It thus seemed that our various families of curves represented the most likely course of the p-v-T relations, and that the required derivatives could be gotten very accurately by mechanical means.

The tables published by Bartlett *et al.* show compressibility factors $pv/(pv)_s$ at the different pressures and temperatures. The denominator $(pv)_s$ is the value of pv at S.T.P. In order to find the specific volume of the gas it is required to know the volume of 1g at S.T.P. Birge gives 22414.1 cc as the volume of a mole of an ideal gas at S.T.P.

$pv/(pv)_s$ at 1 atm. is close to 1/1.00046. The gas used by Bartlett contained 0.9993 nitrogen and 0.0007 inert gas, presumably argon; the apparent molecular weight is therefore taken as 28.025. The volume adopted for 1

g at S.T.P. is accordingly $22414.1/1.00046 \times 28.025 = 799.42$ cc, and the value of RT at 0° is $22414.1/28.025 = 799.79$ cc atm./g. When one of Bartlett's compressibility factors is divided by the pressure and multiplied by 799.42 the result is the volume in cc of 1 g of the gas at the given temperature and pressure.

Some of the temperatures listed by Bartlett *et al.* were not integral; further a calibration of their thermocouple by the Bureau of Standards showed that the temperatures published[1] as −25°, −50°, −70° should have been −24.99°, −49.93°, −69.90°. We have made the slight alterations necessary to change his data to integral temperatures by a sensitive method of interpolation.[5]

At pressures below 100 atm. we used a compilation deduced by Dr. Bartlett from all the available data, chiefly from Amagat, the Reichsanstalt, and the cryogenic laboratory at Leiden, since Bartlett worked at the low pressures only to tie his results with those of previous observers. This compilation was kindly furnished us by Dr. Bartlett in a private communication. Our Δ vs. p isotherms give an easy and reliable means of interpolating to even pressures—one has only to read off Δ at any desired p and calculate v therefrom; accordingly we list results at 20, 40, 60, 80, 100 atm. rather than at the odd pressures one gets by converting meters of Hg to atm.

The Δ vs. p isotherms also give a reliable method of extrapolating to higher pressure; since the original ten isotherms constitute a family of curves, one can not go far wrong in extending them a reasonable distance. This was done and values of Δ were read at 1100 and 1200 atm. The specific volumes calculated at these pressures are probably not in error by 0.01 cc/g, judging from the regularity of the Δ vs. p isotherms and the values of $(dv/d\Delta)_{p,T}$ in this region. In the same way the Δ vs. T isobars give a means of extrapolating to temperatures higher than 400°. Values of Δ were read from the extended isobars at 500 and 600°. In order to estimate the error of the extrapolations, the Δ vs. T isobars were first plotted only to 300° and were extrapolated to 400° and the Δ read at that temperature. Later the observations at 400° were plotted and the smoothed Δ read. The two sets of specific volumes calculated from these two sets of Δ agreed closely, the probable error being 0.17 percent.

The value of these extrapolations, if they are reliable, must be considerable. To extend the experiments to 1200 atm. and 600° would entail enormous expense and labor. Calculations at 1100 atm. and 500° were included, because with them, at least, there should not be any risk. All the calculations in the extrapolated region tied on to the others satisfactorily, so it seems safe to assume that they were made successfully.

The final values of the physical properties at the twelve temperatures and fourteen pressures are shown in the table, or in the figures. Their preparation and implications will now be discussed.

Column 3 shows the specific volumes, which were calculated from the adjusted values of Δ through Eq. (1). The densities in column 4 are the reciprocals of the specific volumes.

The fugacities in column 5 were computed from the smoothed values of α by Lewis and Randall's[8] graphical method.

In columns 6 and 7 the pressure and temperature coefficients of volume expansion are shown. The reason for listing $-(p/v)\ (dv/dp)_T$ and not $-(1/v)\ (dv/dp)_T$ is that the former is dimensionless, and this fact facilitates changing units. Thus if one wishes to get the pressure coefficients at 100° for pressures in meters Hg, one has only to plot the values in column 6 for the 100° isotherm against p in atmospheres, and then graduate the scale of abscissas in the new units of pressure; one can then read $-(p/v)\ (dv/dp)_T$ for any number of meters Hg. The ordinates need not be changed in any way because they are dimensionless. Another advantage is that we can see at a glance how far this coefficient departs from unity, which is the value it would have if the gas were perfect. $(T/v)\ (dv/dT)_p$ was listed for the same reasons. The pressure coefficients of column 6 were adjusted from determinations given by the pv vs. p, α vs. p, Δ vs. p, and Δ vs. ρ isotherms through Eqs. (5), (6), (7), (8); the temperature coefficients of column 7 were adjusted from determinations given by the α vs. T and Δ vs. T isobars through Eqs. (3) and (4). The unsmoothed values at any point determined by the different methods nearly always agreed closely; when they disagreed more than 1 percent even at the highest pressures we went back and reconsidered the curves. Particular care was given to the determinations of $(T/v)\ (dv/dT)_p$, because this derivative enters to the second power in the calculation of $C_p - C_v$ and because it is used to get $(d^2v/dT^2)_p$, which enters into the calculation of ΔC_p.

Probably the most important properties that result from these calculations are C_p and C_v. For this reason extreme care was exercised to obtain the greatest possible precision for ΔC_p, which is shown in column 8. This depends on $(d^2v/dT^2)_p$ through the thermodynamic equation

$$(dC_p/dp)_T = -T(d^2v/dT^2)_p, \tag{11}$$

which when integrated along an isotherm gives

$$C_p = C_p' + \int_{p'}^{p} -T(d^2v/dT^2)_p dp. \tag{12}$$

C_p' is the heat capacity at pressures p'. The $-T(d^2v/dT^2)_p$ vs. p isotherms are shown in Fig. 2. The area under a given isotherm between any two abscissas is the change in C_p between those abscissas. The values of ΔC_p obtained by Eq. (12) from the curves in Fig. 2 were smoothed with respect to temperature and pressure before being listed in column (8).

In drawing the curves of Fig. 2 it was necessary to know something about their course in the region $0 < p < 20$, since p' was 1 atm. In an extremely rarefied condition the gas would have some characteristics of a perfect gas. The question has been raised by the writers[9] whether $(d^2v/dT^2)_p$ and $(dC_p/dp)_T \to 0$ as $p \to 0$, as they would if the heat capacity of the actual gas at very low pres-

[8] Lewis and Randall, Thermodynamics, pp. 192 to 195, McGraw-Hill (1923).

[9] Deming and Miss Shupe, Phys. Rev. **37**, 220 (1931).

sure behaves like that of a perfect gas. For the calculations in this paper we have assumed that $(dC_p/dp)_T \neq 0$ at $p=0$, and for its value we have used, wherever it seemed feasible, the one given by the Beattie-Bridgeman equation of state with constants determined[4] from these same compressibility data. In Fig. 2 are shown the graphs of $-T(d^2v/dT^2)_p$ vs. p isotherms. The points are the averages of determinations made from the α vs. T and Δ vs. T isobars through Eqs. (3), (4), (9), (10). The curves given by Beattie's formula[6] are shown dashed and they are drawn as far as the equation of state might be expected to hold, namely, as far as the critical density. At 100, 200, 300, and 400° the dashed curves seem to be the best curves that could be drawn to the points shown.

The curves in Fig. 2 for 20, 50, and 100° are not quite flat from 20 to 100 atm. This is the range of pressure considered by Hoxton[10] in discussing the

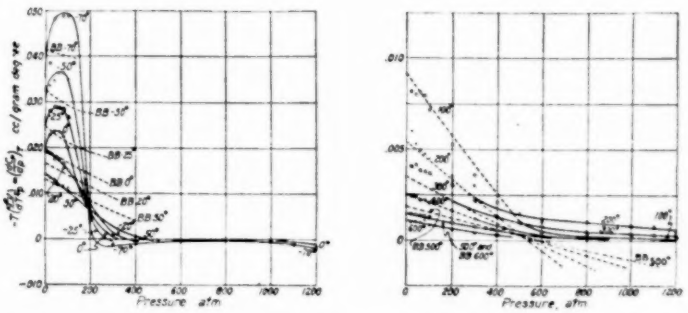

Fig. 2. $(dC_p/dp)_T$ vs. p isotherms. The full lines are drawn to the points determined from the p-v-T data. The dashed curves are given by the Beattie-Bridgeman equation of state, and are drawn as far as the critical density. Where only the dashed line is shown, the Beattie-Bridgeman values were accepted. To avoid confusion, some of the curves are not drawn at high pressures. The area under a particular curve between any two pressures is the change in heat capacity (in cc atm./g deg.) between these two pressures, at that temperature.

variation of the heat capacity of oxygen at 26° obtained in the experiments of Workman.[11] Hoxton speaks of a "change in c_p per atmosphere relative to its value at one atmosphere, the temperature being constant and taken as 26°C," and says that Workman found this quantity $\delta \equiv (dC_p/dp)_T/C_p'$ to be constant and equal to 0.00165 parts per atm. This implies that for oxygen the $(dC_p/dp)_T$ vs. p 26° isotherm is flat. There are reasons to expect C_p for nitrogen and oxygen to be similar in some ranges of temperature and pressure; e.g., their C_p values at one atmosphere for various temperatures are sometimes[12] expressed by the same formula, and Jakob's results for air are very similar to ours for nitrogen in some respects (*vide infra*). Our curves in Fig. 2 show that δ for nitrogen should decrease slightly with pressure. Taking 0.0178 and 0.0125 as the average ordinates for the 20° and 50° isotherms from

[10] L. G. Hoxton, Phys. Rev. **36,** 1091 (1930).

[11] E. J. Workman, Phys. Rev. **36,** 1183 (1930).

[12] E. D. Eastman, Specific Heats of Gases at High Temperatures, Bureau of Mines Techn. Paper 445 (1929).

20 to 100 atm. in Fig. 2, and interpolating linearly to 26°, δ turns out to be 0.00164 parts per atm. for nitrogen, very nearly what it is for oxygen.

In order to find C_p from Eq. (12) it is necessary to adopt values of C_p' at some pressure p' for the different temperatures. Several formulas have been devised to express C_p at 1 atm. as a function of T. As far as we know none of these is expected to extend to temperatures much below 20°. For C_p' at the low temperatures we finally accepted Brinkworth's[13] three values, which are 6.91, 6.92, 7.20 at 10, −78, −183°. A smooth curve through these points met Partington and Shilling's[14] formula very well at 30°, so we constructed a curve through Brinkworth's three points and points calculated from Partington and Shilling's formula above 30°, and from this curve read the values for C_p' that are listed below.

$t°C$	−70	−50	−25	0	20	50
C_p' (1 atm.)	6.92	6.91	6.91	6.91	6.91	6.92
$t°C$	100	200	300	400	500	600
C_p'	6.94	6.98	7.01	7.05	7.09	7.13

Eastman's formula would not join on to Brinkworth's points satisfactorily. At 200° Eastman's and Partington and Shilling's formulas differ by 0.1 cal/mole·deg. As the temperature increases the disparity widens even more, which shows that more precise direct calorimetric measurements of C_p at 1 atm. are needed.

It is difficult to estimate the accuracy of the ΔC_p, which are shown in column 8. The relation of the curves and points in Fig. 2 suggests that the precision of the calculations is greatest at the highest pressures. The calculated values of C_p agree well with the experimental values of Mackey and Krase.[15] They worked to 700 atm. at 30, 100, 125, 150° and to 800 atm. at 50°. Their points have been inserted in Fig. 4, so that observed and calculated values can be compared at a glance. The dashed curves represent calculated values obtained by interpolating along C_p vs. T isobars. At 50° the agreement is excellent through the entire range of experiment. At 30° the calculated values run below the experimental ones above 400 atm., and at 100, 125, 150° the calculated values lie above the experimental ones throughout the entire range. While the discrepancy is probably not greater anywhere than the experimental error of the calorimetric measurements, the trend of the calculated curves is definitely away from the experimental points above and below the 50° isotherm. An incorrect assumption for C_p at 1 atm. would result in a constant distance between an experimental and a calculated isotherm. A constant difference above, say, 100 atm. might mean that the corresponding isotherm in Fig. 2 is incorrectly drawn between 0 and 100 atm. But we are at a loss to account for the *constantly widening* gap between the calculated and experimental points at 30° above 350 atm., and for that at 100, 125, and 150.° The precision of the points in Fig. 2 does not diminish

[13] J. H. Brinkworth, Proc. Roy. Soc. **A111,** 124 (1926).
[14] Partington and Shilling, The Specific Heats of Gases, p. 145, D. van Nostrand (1924).
[15] B. H. Mackey and Norman W. Krase, J. Ind. and Eng. Chem. **22,** 1060 (1930).

with increasing pressure, and they could hardly be *consistently* in error by so great an amount as to account for the widening gaps. It thus seems impossible that the discrepancy can be laid to the calculations from the p-v-T data.

Witkowski's curves[16] for air go only to 100 atm., but it is interesting to note that the hump that appears in Fig. 3 at the lowest temperatures appears

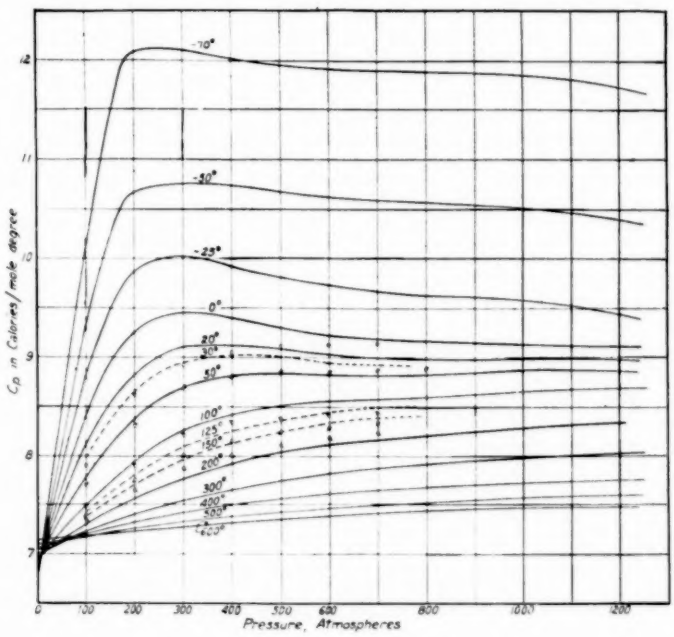

Fig. 3. Variation of C_p for nitrogen with pressure. Mackey and Krase's values ○ 30°, ♂ 50°, ↖ 100°, ↙ 125°, ↘ 150°.

in his curves for $-100°$ and lower temperatures; also that the pressure at which the hump appears decreases as the temperature decreases with both air and nitrogen.

Comparison with Jakob's[2] calculations of C_p for air show agreement within a few percent at 100 and 200° through 200 atm., and within a few percent at $-50°$ and 50 atm.

$$C_p - C_v = -T(dv/dT)_p^2/(dv/dp)_T. \tag{13}$$

Since the derivatives used in Eq. (13) have already been evaluated, $C_p - C_v$ can be calculated at each pressure and temperature. The results are shown in Fig. 4. In view of the precision claimed for the first derivatives, the error in $C_p - C_v$ should not exceed 0.3 percent, which is about as close as the graph can be read. It will be noticed that these curves all run toward the ordinate

[16] Witkowski, Phil. Mag. **42**, 1 (1896). These curves are shown in Partington and Shilling's book, p. 154.

R as p approaches zero. It was found that our values of $C_p - C_v$ for nitrogen agree closely with Jakob's for air; for example, our 100 atm. isobar almost

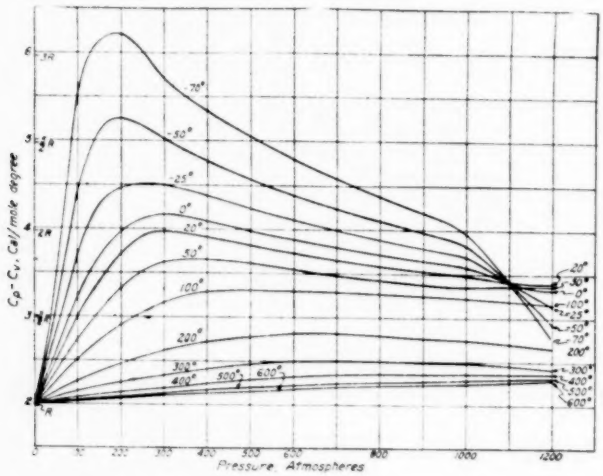

Fig. 4. The variation of $C_p - C_v$ for nitrogen with pressure at various temperatures.

coincides with his for 100 kg/cm² throughout his entire range of temperature. Our $C_p - C_v$ values were smoothed with respect to temperature and pressure.

The values of $C_p - C_v$ from which Fig. 4 was plotted were subtracted from the values of C_p in Fig. 3 to get the C_v graphed in Fig. 5. It will be seen that

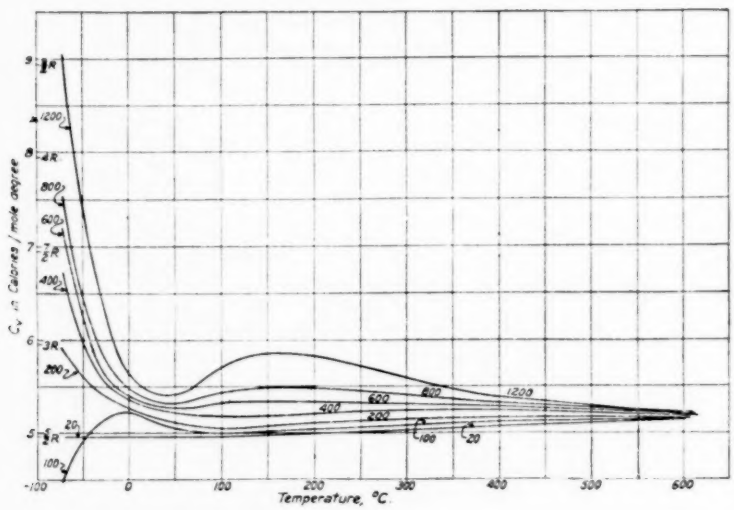

Fig. 5. Variation of C_v for nitrogen with temperature at constant pressure. The numbers on the isobars denote atmospheres.

C_v at 20 atm falls from 5.15 cal/mole·deg (2.59 R) at 600° to 2.50 R at 100°, and it stays there as the temperature is lowered to −70°. An increase in pres-

sure lowers C_v at $-70°$ until 100 atm. is reached; at 200 atm. and higher, C_v rises as the temperature falls below 20°, and the rise is steeper the higher the pressure. Above 400° it is evident that C_v is approaching the same value for all pressures; at 600° C_v is about 5.18 cal/mole·deg or 2.61 R from 20 to 1200 atm. Jakob's calculated values of c_v for air, when plotted, show the same behavior at low temperatures for his entire pressure range, which included 200 kg/cm². His 200 kg/cm² isobar would fall off faster than his 100 kg/cm², instead of rising like the 200 atm. isobar in Fig. 5; but 200 kg/cm² is at the end of his pressure range and he lays no claim for accuracy there, so it can only be conjectured how C_v for air compares with C_v for nitrogen above 100 atm. Various explanations of this behavior in Fig. 5 have been considered, but they will not be discussed here because we prefer to present results only.

The Joule-Thomson coefficient can be calculated from the equation

$$\mu C_p = T(dv/dT)_p - v \tag{14}$$

by using the values already found for C_p and $(dv/dT)_p$. They are listed in column 9. The inversion temperatures for the various pressures are where

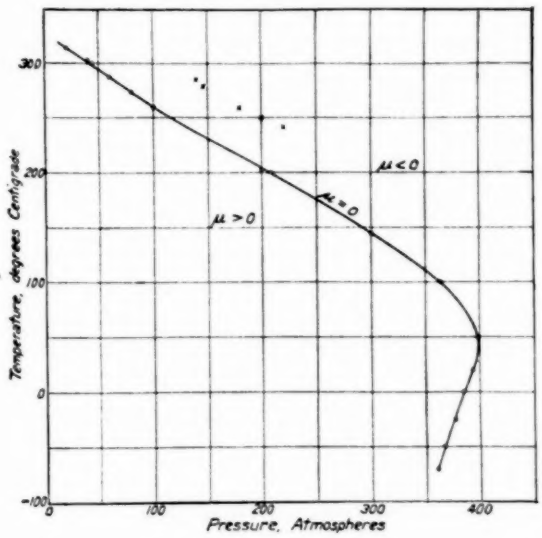

Fig. 6. Inversion curve for nitrogen. The points were read from the μ vs. T isobars and the μ vs. p isotherms. μ denotes Joule-Thomson coefficient $\mu=(dT/dp)_H$. x denotes Roebuck's inversion points for air.

the μ vs. T isobars cross the ordinate $\mu=0$, and the inversion pressures for the various temperatures are where the μ vs. p isotherms cross the ordinate $\mu=0$. The inversion curve, Fig. 6, is plotted from the inversion points so obtained. There are no existing data on the Joule-Thomson coefficient for nitrogen, so a comparison with observed values is not yet possible. Roebuck's[17] values for air give the inversion points marked x on Fig. 6.

[17] Roebuck, Proc. Amer. Acad. Arts Sci. **60**, 535 (1925); **64**, 314 (1930) International Critical Tables **5**, 144, first edition.

If the results derived in the present paper are a step toward the determination of the heat capacity and other physical properties of gases, the importance of compressibility data must be recognized. The calculations in this paper were made by two people in nine weeks time. Compressibility data on a number of gases are now available; their physical properties will be determined as rapidly as possible and will appear in subsequent papers. The method will doubtless undergo changes that will result in greater precision.

This work was undertaken at the suggestion of Dr. Edward P. Bartlett, formerly of this laboratory. We have enjoyed the encouragement and willing cooperation from him and the staff at this laboratory throughout the course of the work. We wish also to acknowledge indebtedness to Professor James A. Beattie of the Massachusetts Institute of Technology for his interest in the work, especially in the heat capacity at low pressures, and to Professor L. G. Hoxton of the University of Virginia for his encouragement and many helpful suggestions.

Note added in proof, February 16, 1931: Some results on C_p for nitrogen to be read by E. J. Workman at the New York meeting of the American Physical Society on February 26, 1931 make possible further comparison between the present calculations and experimentally obtained results. Workman has obtained $C_p : C_p'$ at 30, 60, 90, 130 kg/cm² at 26° and 60°C. C_p read from the original tracing of Fig. 3 at these points gives the following comparison. *W* denotes Workman, *D* denotes Deming and Miss Shupe. 6.916 and 6.926 cal/mole deg were adopted for C_p' at 26° and 60°.

	p kg/cm²	p atm.	26°C $C_p : C_p'$	60°C $C_p : C_p'$
W	30	31	1.0443	1.0324
D			1.05	1.04
W	60	62	1.0900	1.0665
D			1.10	1.07
W	90	93	1.1332	1.0990
D			1.15	1.11
W	130	134.5	1.1863	1.1395
D			1.21	1.15

LETTERS TO THE EDITOR

Prompt publication of brief reports of important discoveries in physics may be secured by addressing them to this department. Closing dates for this department are, for the first issue of the month, the twenty-eighth of the preceding month; for the second issue, the thirteenth of the month. The Board of Editors does not hold itself responsible for the opinions expressed by the correspondents.

The Thermodynamic Treatment of Chemical Equilibria in Systems Composed of Real Gases. II. A Relation for the Heat of Reaction Applied to the Ammonia Synthesis Reaction. The Energy and Entropy Constants of Ammonia. A Correction.

In a paper having the above title, published in the Physical Review **36,** 1008 (1930) the numerical value given for the quantity $\Sigma(\nu_i s_{0i}')$ has been found incorrect. Eq. (13) should read: $\Sigma(\nu_i s_{0i}') = -22.9850$. The entropy constant (s_{0i}') for ammonia appearing in Table III should be -22.9809. This requires several corrections in Table IV, which when revised is as follows.

TABLE IV. *Values of several thermodynamic quantities for one mole of hydrogen, nitrogen and ammonia at 0°C and 1 atmosphere; and the increase Δ of these quantities when one mole of ammonia is formed from its elements all reactants and products being at 0° and 1 atmosphere. Units: 15°-calories, degrees Centigrade, moles.*

	Hydrogen	Nitrogen	Ammonia	Δ
U	0	0	−10078.0	−10078
H	543.0	542.4	−9542.9	−10628.5
S	0	0	−23.0538	−23.054
F_{VT}	0	0	−3781.3	−3781
F_{pT}	543.0	542.4	−3246.2	−4332
pV	542.96	542.39	535.14	−550.50

No changes are necessary in part I, Phys. Rev. **36,** 743 (1930), or part III, Jour. Am. Chem. Soc. **52,** 4239 (1930), of the series of three papers.

L. J. GILLESPIE
J. A. BEATTIE
Massachusetts Institute of Technology,
Cambridge, Massachusetts,
February 10, 1931.

Reflection of High Velocity Electrons from Solid Surfaces

Bothe[1] has derived an expression for the angular distribution of electrons which are transmitted by matter and which have penetrated sufficient thickness to become completely diffused, and finds fair agreement with experimental work done with β-particles. It becomes of interest[2] to know the angular distribution of electrons emitted backwards from solid surfaces, since it is possible that the two distributions are similar. This question, together with the determination of absolute values of reflection, was studied during an investigation on scattering of high velocity electrons by thin foils.

If we call the half-angle of the solid cone about the normal to the surface, θ_1, and the half-angle subtended by the opening through which the electrons emerge, θ_2, then experimentally all electrons, due to an originally homogeneous beam, emitted between these two cones are collected in a field-free space. The ratio of this number to the total number incident on the surface will be called ρ'. A small correction (less than 2 percent) may be made to ρ' for the electrons which come back between θ_2 and 0°. The corrected value, ρ, is then plotted as a function of θ. The following elements have been tested: Pb, Sn, Cu, Al, C, Be. The curve showing the variation of ρ with angle, for the heavier elements and voltages above 100,000, agrees with the curve $\rho_0 \sin^2\theta$ to within 1 percent, where ρ_0 is the

[1] W. Bothe, Zeits. f. Physik **54,** 161 (1929).

value of ρ at $\theta=90°$. The intensity at any angle is therefore given by the simple cosine law. Small deviations from this law are found for the lighter elements such as C and Be, especially at voltages below 70,000. More investigations are being conducted. Bothe's expression for the angular distribution of transmitted electrons which are completely diffused, deviates from the distribution found experimentally for electrons emitted in a backward direction, by about 5 percent at $\theta=45°$, both curves coinciding at 0° and 90°.

For beryllium ρ_0, or the "rediffusion constant" of Webster,[2] is found to be 0.0291 for 70,000 volt electrons and decreases to 0.0248 at 130,000 volts, instead of being 0.043 which he deduces. These values include all electrons emitted. In the case of beryllium, only 2 percent of the emitted electrons have energies below 2,000 volts.

A decrease in ρ is found for all the lighter elements with increase of voltage. In the range between 45,000 and 130,000 volts, this decrease amounts to 7 percent in the case of aluminum, becomes 0.6 percent for tin and less than 0.1 percent for lead.

H. VICTOR NEHER

Department of Physics,
California Institute of Technology,
February 7, 1931.

[2] D. L. Webster, Phys. Rev. **37**, 119 (1931).

The Extrapolation of Atomic Structure Factor Curves

In a recent[1] note under the above title, D. K. Froman has derived an extrapolation formula for atomic structure factors on the basis of "electron distributions indicated by the wave equation." Although it is certainly true that quantum mechanics can be taken as the basis for deriving such formulas, it is of interest to note that Froman's result can be obtained without any appeal to a specific theory of the electron distribution causing the atomic structure factor. We have in mind simply the fact that repeated integrations-by-parts of Froman's Eq. (2) which defines the structure factor of the n^{th} order gives us at once the result that:

$$F_n = \sum_k a_{kn}\left(\frac{D}{n}\right)^{2k} = \sum_k a_{kn}\left(\frac{2\sin\theta}{\lambda}\right)^{-2k}$$

where:

$$a_{kn} = \frac{(-1)^k}{(2\pi)^{2k}}\left[\left(\frac{U(r)}{r}\right)^{(2k-2)}\cos\frac{2\pi nr}{D}\right]_{r=0}^{r=D/2},$$

the notation being that used by Froman.

The first equation is clearly identical with Froman's Eq. (8), and his Eq. (12) can be derived similarly. It is thus seen that Froman's extrapolation formula is the general consequence of the definition of the structure factor, being in fact, the asymptotic expansion for F_n, and is independent of any wave-mechanical interpretation of the electron distribution.

MORRIS MUSKAT

Gulf Research Laboratory,
Pittsburgh, Pennsylvania
February 17, 1931.

[1] D. K. Froman, Phys. Rev. **36**, 1339 (1930).

Nuclear Spin of Aluminum

The recent letter by J. H. Bartlett, Jr. on nuclear spin has been read with a great deal of interest, and in view of the importance of the subject the writers would like to point out an apparent discrepancy. After a careful survey of the work done on the hyperfine structure of the lines of various elements, the writers had reached the same general conclusions as Bartlett. It was disconcerting, however, to find that Janicki (Ann. **29**, 833, (1909)) and Wali-Mohammed (Astrophys. J. **39**, 185, (1914)) had both photographed the Al lines 3944A and 3961A using Lummer-Gehrcke plates and found them "very sharp and simple."

Recently, while studying different light sources for the purpose of finding the most suitable source for use in analyzing the hyperfine structure nitrogen lines, occasion presented itself for photographing the following Al lines in a Schüler hollow cathode discharge cooled by liquid air.

A Fabry-Perot interferometer, with fixed etalons, was used in conjunction with a Zeiss triple prism spectrograph for analyzing the lines. Several exposures, made under different conditions and with different etalons, were made on each line. Mirrors having a reflection coefficient of 90 percent or greater were used, so that the resolving power of the interferometer was about 10^6. Under these conditions all four Al lines were found to be sharp and lacking in structure.

Typical microphotometer curves of these

lines are shown in Fig. 1. From a careful study of all the curves obtained from various Al lines, and from the lines of various other elements in which structure is clearly present, it is estimated that if these Al lines have structure the average separation is not greater than 0.006A.

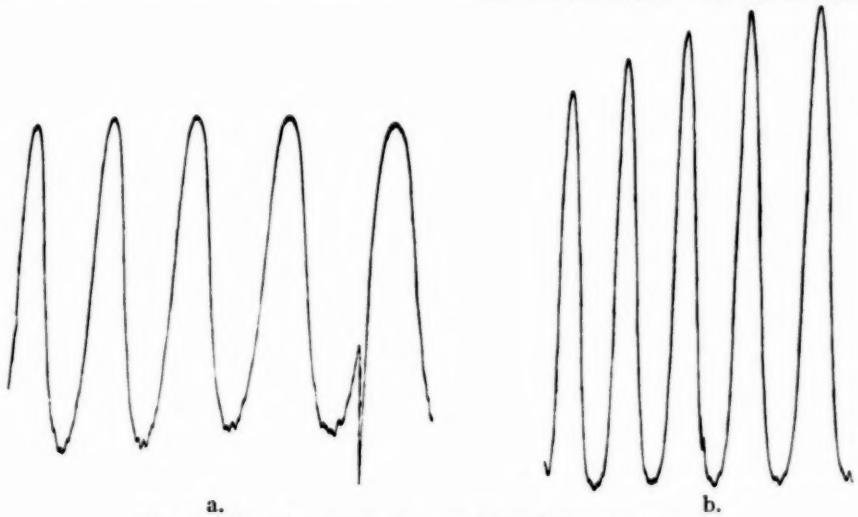

a. b.

Fig. 1. Microphotometer curves of interferometer patterns. (a) Al I λ3961. (b) Al II λ4663.

As is shown in Table I, the lines 3944A and 3961A constitute the first member of the sharp series of Al I and result from an electron transition s to p. According to other hyperfine structure data (White, Phys. Rev. **35**, 1146 (1930) *et al.*) such a transition should give wide hyperfine structure separations. The line 4663A results from a p to d electron transition and although this would probably not show as wide a hyperfine structure as the s to p transition, it should be observable if the nuclear moment of Al was different from zero.

Since Aston (Phil. Mag. **49**, 934 (1923)) reports Al to have only one isotope at 27, the present data indicate that Al in no way fits any of the proposed schemes of the building-up process in the nucleus or the theories of nuclear moments. For, if as Heitler and Herzberg (Naturwiss. **17**, 673 (1929)) assume, the electron in the nucleus loses its power to determine what the statistics of the nucleus shall be, then the 27 protons determine the nuclear moment and an odd number of $(1/2)\cdot(h/2\pi)$ units would be expected. If the electron does not lose this power, the nuclear moment would be determined by the 27 protons plus 14 electrons, and one would still expect an odd number of $(1/2)\cdot(h/2\pi)$ units for the nuclear spin. But the available data indicate that this moment is zero.

Recent data on the value of the nuclear moment for nitrogen still leave some doubt as to what the real value is. Al and N may, then, be considered as disturbing exceptions to present theories of nuclear structure.

TABLE I. *Aluminum arc and spark lines which show no hyperfine structure.*

	λ	Classification	Total line width
Al I	3944.025	$3p^2P_{\frac{1}{2}}-4s^2S_{\frac{1}{2}}$	0.032A
Al I	3961.537	$3p^2P_{1\frac{1}{2}}-4s^2S_{\frac{1}{2}}$	0.029A
Al II	4226.812	$3s4d^3D_3-3s9f^3F_4$	0.034A
Al II	4663.054	$3s3d^1D_1-3s4p^1P_1$	0.037A

We are indebted to Mr. A. Rosenblum for preparing the microphotometer curves used in this analysis.

R. C. GIBBS
P. G. KRUGER

Physical Laboratory,
Cornell University,
February 21, 1931.

What Requirements must the Schrödinger ψ-Function Satisfy?

In a recent paper with the above title, G. Jaffé[1] contends that the proper solutions of the wave equation must be everywhere finite and continuous, and that the condition of quadratic integrability is not enough. In support of the latter point he shows that a solution for the angle part of the wave function of the central field problem for the case $m=0$, may be obtained for non-integral values of 1: this solution is quadratically integrable but has a logarithmic singularity. Since this would result in a continuum of spectroscopic terms quite unknown in experiment, Jaffé concludes that the condition of finiteness and continuity is required.

The authors are presenting a paper in which this question is of central importance and therefore find it advisable to point out that Jaffé's conclusion is not at all necessary and in fact is surely too stringent for many problems in atomic structure.

The reason a solution such as that mentioned by Jaffé is possible, is that when the wave equation is expressed in polar coordinates some of the coefficients have singularities not brought in by the potential energy. If the equation is written in Cartesian coordinates there are no singularities except those of the potential energy function. We see then that the singularities are introduced into the equation by the transformation from Cartesian to polar coordinates. This is substantiated by the fact that at the singular points in question the Jacobian of the transformation from Cartesian to polar coordinates vanishes, showing that the transformation at these points is not legitimate.

Of all possible coordinate systems the Cartesian is to be preferred in the wave equation because of its simplicity, homogeneity (volume element constant), and isotropy (line element diagonal with constant coefficients). From the form of the equation we are led to expect that a proper wave function should have no singularities except at those of the potential function. Hence in the case of the hydrogen problem a quadratically integrable singularity is permissible at the origin, but not elsewhere.

Without giving up the condition of quadratic integrability as being sufficient restriction on the wave function, one can rule out Jaffé's example for the following reason: The wave equation is not the best starting point for the theory. The fundamental thing is the integral

$$J = \int \left(\frac{h^2}{4\pi^2} T\left(q, \frac{\partial \psi}{\partial q}\right) + V\psi^2 \right) d\tau$$

where $T(q, p)$ is the classical expression for kinetic energy in terms of coordinates and momenta and V is the potential energy.

The function ψ is determined by the condition that J be a minimum. Its minimal values are the energy levels. The Euler equation corresponding to this variational integral is the wave equation. However, satisfying the wave equation is necessary but not sufficient to make this integral a minimum.[2] From the wave equation $H\psi = E\psi$, we can obtain the integral form $\int \bar{\psi}_n H \psi_n d\tau = E_n$ which in Cartesian coordinates can be shown to be the equivalent of J. This comes from the fact that the condition of quadratic integrability is sufficient to insure the vanishing of the surface integral by which J differs from $\int \bar{\psi} H \psi d\tau$. In polar coordinates the two need not be equal when singularities arise at the boundaries.

In the case which Jaffé mentions, if l is not an integer, not only is J not a minimum but it is *infinite* and therefore the solutions for this case can have no physical significance.

In general if the wave function has a singularity the energy integral will be infinite except possibly if the potential function has a singularity in the same place. The ultimate criterion then for an acceptable wave function is that J be finite (and a minimum). As a rough working rule we may demand of the function that it be integrable in the square and that it be finite and continuous wherever the potential energy is finite. If we introduce singularities (physically non-existent) in the potential energy we must be prepared to put up with singularities in the wave function at those points. When, in the future, we get a deep enough insight into the nature of the physical problems so that we can replace the singular values of the potential energy by their true finite values, the singularities of the wave functions will also be removed. But until then we must be content with results which differ from the facts to the same degree as do the assumptions from which we start.

R. M. Langer
N. Rosen
Massachusetts Institute of Technology,
February 23, 1931.

[1] Jaffé, Zeits. f. Physik **66**, 770 (1931).

[2] Courant-Hilbert, Methoden der Math. Phys. I, p. 165.

BOOK REVIEWS

Magnetic Phenomena. SAMUEL ROBINSON WILLIAMS. Pp. xxii+230. 150 figures. McGraw-Hill, New York, 1931. Price $3.00.

Professor Williams has been deeply interested in magnetic phenomena for many years and has already contributed much to their study, both personally and by stimulating others to independent research. His attempt in the present monograph to enlist additional recruits for the attack upon magnetic strongholds is therefore of especial interest. He has decided that the college undergraduate should be approached and now offers him a text-book of an unusual kind in which almost undue emphasis is laid upon the unfinished and provisional character of much of the available information. His choice of audience naturally limits him somewhat both in the total content of his book and in the mode of presentation. He has cut down the mathematics required of the reader to such an extent that he often loses desirable rigor and even, in several places, falls into confusing errors. It would have been much better, in the opinion of this reviewer, to expect a good working knowledge of the calculus in all cases.

Under one or other of the chapter headings "magneto-magnetics, magneto-mechanics, magneto-acoustics, magneto-electrics, magneto-thermics, magneto-optics, cosmical magnetism, magnetic theories and experimental facts" will be found some account, however brief, of almost everything known about magnetism. The topics selected for most detailed comment are, as they should be, those with which the author is personally most familiar. The bibliography, especially in these selected parts, is unusually rich in the earlier references. In other places the treatment is much more sketchy, and some omissions from the index (e.g. crystal!), make it hard to discover how much of the most recent work has been covered. Some of the omissions are surprizing. The most careful search, after a critical reading of the entire text, fails to disclose any reference to the great electromagnet at Bellevue or to the magneto-caloric effect and related phenomena. The postponement of magneto-crystallic effects to some future treatise also seems most unfortunate.

The publisher's part of the work is well done, unless the rather numerous misprints in the text and disagreements in lettering between figures and text are attributable to his staff.

The reviewer has tried to convey the mixture of pleasure and disappointment which affected him during his review. A reader to whom more of the phenomena are wholly new would probably derive a larger proportion of pleasure and, perhaps, be incited to straighten things out for himself. This, of course, is just what the author wishes.

L. W. MCKEEHAN

Gmelin's Handbuch der Anorganischen Chemie. 8 Auflage; herausgegeben von der Deutschen Chemischen Gesellschaft; System Nummer 59. Eisen; Teil A, Lieferung 3: Pp. 313–586. Verlag Chemie G. m. b. H. Berlin, 1930, price RM 40 (subscription price RM 32).

The above volume is of a more technical character than most of the other of Gmelin's Handbooks; a complete literature review with bibliography on the passivity of pure and technical iron (written by Dr. E. Liebreich), its chemical behavior and its corrosion (by Dr. M. Rudolph, Dr. A. Eisner and Dr. A. Kotowski) and its metallurgy (Prof. R. Durrer, Dr. H. Lueb and Dr. M. W. Neufeld) are given. The material has been collected in a non-critical way, thus giving the book a compilatory character as in the other issues of the same edition. It seems to the reviewer that with the five previous volumes the present one comprises the most complete monograph we have at present on the physical, chemical and metallurgical properties of iron and it forms a worthy addition to the Gmelin series.

I. M. KOLTHOFF

The Quantum Theory. FRITZ REICHE. Translated by H. S. Hatfield and Henry L. Brose. Pp. viii+218. Figs. 15. E. P. Dutton and Company, Inc., New York, 1931. Price, $2.10.

The first English edition of this book, dated 1922, was a translation of the German original the preface of which bears the date October 1920. To the present edition the translators have

contributed a chapter of twenty-four pages which together with nine pages of notes and references covers developments since 1920. The result is that nine of the ten chapters are written from the point of view of ten or more years ago, while the tenth, covering developments since that date, must, because of its brevity, devote to any important topic an amount of space "less than ϵ" in the sense in which mathematicians often use that phrase. What constituted a clear exposition in the light of the day when it was written will, in many instances, prove misleading for the student of today, while the last chapter will surely be almost unintelligible to one whose knowledge of the subject is based upon reading the first nine.

A. ELLETT

Photoelectric Cells and Their Applications. A discussion at a joint meeting of the Physical and Optical Societies (of London), June 4 and 5, 1930. Editor, JOHN S. ANDERSON. Published by the Physical and Optical Societies, London, 1930. Price, 12 s 6 d.

Physicists and engineers in general will welcome a condensed account of some of the recent developments in the technique of manufacturing and using photoelectric cells. The present volume is a compilation of 31 papers on this subject presented at the London symposium, and includes a report of the interesting and lively discussion which followed. While such a book may lack the unity and completeness of a treatise by an individual author, it has the advantage of allowing the presentation of many specialized problems by those most familiar with them, and of bringing out many different, and sometimes conflicting, points of view.

Following an opening paper by H. S. Allen on the early history of photoelectric cells, there is a paper by N. R. Campbell discussing Fowler's recent wave-mechanical theory of the selective photoelectric effect. There are then seven papers dealing with the manufacture, characteristics, and uses of various types of modern cells. The papers by P. Selenyi on the sodium cell, by L. J. Davies and H. R. Ruff on the thin-film caesium cell, and by T. W. Case on the barium cell are of especial interest, since they give considerable data on the characteristics of these cells. The five papers on the technique of measuring and amplifying photoelectric currents will be of particular value to those interested in photoelectric sound reproduction. A number of problems connected with the distortionless amplification of rapidly varying photo-currents are discussed in detail. Many physicists will be disappointed to find no discussion of the methods of amplifying *unvarying* currents.

We find next a series of ten papers covering the fields of photoelectric photometry, microphotometry, and spectrophotometry. K. S. Gibson contributes a particularly comprehensive review of modern methods in spectrophotometry, with an excellent critical survey of the advantages and limitations of photoelectric cells in this field. Finally, there are two papers on biological applications and four on selenium cells. In one of the latter H. Thirring presents considerable data to support the contention that the "frequency response" of well-designed selenium cells is sufficiently good, contrary to common belief, to make them superior to gas-filled alkali metal cells for sound reproduction. In the discussion reported at the end of the volume one finds a heated argument over this point, with the selenium cell adherents somewhat outnumbered, but not outdone.

On the whole the volume contains a surprising amount of useful information. It has been carefully edited and printed, though one feels that it is of sufficient worth to have merited a better binding.

L. A. DUBRIDGE

The New Physics. Third English edition. ARTHUR HAAS. Pp. 172, figs. 7. E. P. Dutton and Co., New York, 1930. Price $2.15.

This small volume contains seven lectures, in which the author endeavors to "describe the picture of Nature revealed by modern physics in the most intelligible manner possible, and without the use of any mathematical formulae". The subjects treated are the electromagnetic theory of light, molecular statistics, electron theory, quantum theory, the theory of the chemical elements, relativity and gravitation, and quantum mechanics. The lecture last mentioned appears for the first time in this edition. Several others have been revised.

The style is simple and direct. The educated layman will be able to read the book with understanding. The professional physicist will find it too elementary to warrant more than a cursory scanning of its pages.

H. H. MARVIN

Laboratory Manual of Physics. C. M. KILBY. Pp. 129, figs. 75. D. Van Nostrand Co., New York, 1930. Price, $1.75.

The manual contains descriptions of sixty-five experiments which can, for the most part be performed with inexpensive apparatus. The several fields of physics all are well represented. The experiments are described in the briefest form possible, adequate for the experiment, but not calculated to lead the thoughtful student beyond the immediate result sought. A tabular form for observations and results is given, in every case. The illustrations are well drawn, with the exception of the electrical wiring diagrams. The manual is adapted fairly well to the needs of students who have not had physics in the high school.

H. H. MARVIN

Cours D'Optique. G. BRUHAT. Pp. 756, figs. 657. Masson and Cie, Paris, 1931. Price, 100 francs.

This advanced text-book in optics begins with the usual introductory survey of the fundamental principles. The following two sections give an excellent treatment of interference and diffraction with many good figures and numerical illustrations. Experimental applications receive a good deal of attention. Part four deals with polarization and the electromagnetic theory of light. Here the classical ideas on vibrations of electrons due to electromagnetic waves are repeated without apology. Part five, on the optics of anisotropic and disymmetric media, is especially complete. In particular, experimental technique is not overlooked. Part six, on spectroscopy, is merely a descriptive resumé using the language of the Bohr-Sommerfeld theory. The treatment is carried no farther than in the early editions of Sommerfeld's "Atombau." Prominent among the omissions are: the theory of optical instruments, thermal radiation, and the optics of moving media. As an advanced text, dated 1931, it is disappointing in its conservatism, although as a treatise on classical optics and its experimental application, it is one of the very best.

J. VALASEK

A Treatise on Physical Chemistry. A Cooperative Effort by a Group of Physical Chemists. Edited by HUGH S. TAYLOR. Second edition, 1931. D. Van Nostrand Company, Inc., New York. Two volumes. Vol. I, XV+852+48 pp. (indices); Vol. II, XII+865+48 pp. (indices). Price $15.00 (not sold separately).

The scope and authority of this outstanding cooperative work on physical chemistry are evident from the list of chapter headings and authors. I, The Atomic Concept of Matter, Hugh S. Taylor; II, The Energetics of Chemical Change, Hugh S. Taylor; III, The Kinetic Theory of Gases and Liquids, K. F. Herzfeld and Hugh M. Smallwood; IV, Imperfect Gases and the Liquid State, K. F. Herzfeld and Hugh M. Smallwood; V, The Solid State of Aggregation, Robert N. Pease; VI, Thermochemistry, A. L. Marshall; VII, The Laws of Dilute Solutions, J. C. W. Frazer; VIII, Homogeneous Equilibria, Graham Edgar; IX, Heterogeneous Equilibrium, Arthur E. Hill; X, The Measurement of Electrical Energy, G. A. Hulett; XI, Conductance, Ionization and Ionic Equilibria, J. R. Partington; XII, The Electrochemistry of Solutions, Herbert S. Harned; XIII, Electrometric Methods in Analytical Chemistry, N. Howell Furman; XIV, Reaction Velocity in Homogeneous Systems, Francis Owen Rice; XV, Reaction Velocity in Heterogeneous Systems, Hugh S. Taylor; XVI, Quantum Theory and Atomic Structure, Saul Dushman; XVII, The Third Law of Thermodynamics and the Calculation of Chemical Constants, Worth H. Rodebush; and in part by T. Jefferson Webb; XVIII, Photochemistry, Hugh S. Taylor; XIX, Infrared Radiation in Chemical Processes, H. Austin Taylor; XX, Colloids, Elmer O. Kraemer; XXI, Radioactivity, S. C. Lind.

Since the publication of the first edition in 1924 important advances have been made in most of the fields covered by the treatise. This has necessitated the more or less thorough re-

vision of chapters VI, XI, XII, XIII, XIV, XV, XVII, XVIII, XIX, and XXI. The important chapters II, IV, XVI, and XX have been written anew, three of them by authors other than those of the former edition. The remaining chapters, reprinted practically unchanged from the first edition, deal with topics in which little advance has been made in recent years, with one exception, discussed below.

In chapters III and IV, 175 pages, an admirable treatment of the kinetic theory of gases and liquids has been presented by Herzfeld and Smallwood. Dushman has given in the 277 pages of chapter XVI a well-balanced introduction to quantum theory and atomic structure which in my opinion has no rival for the purpose for which it was intended, to provide the student in physical chemistry, who usually has a none too extensive preparatory training in mathematics and theoretical physics, with a working knowledge of the fundamental facts of this field. The recent developments in quantum mechanics have not been grafted onto the article written in 1924; instead they have been thoroughly incorporated in the chapter, which has been completely rewritten from the new point of view provided by them.

The careful selection of mathematical methods adapted to the capacity of the readers for whom the treatise is primarily intended, physical chemists and students of physical chemistry, shown in these chapters and in most of the others is not always evident. In chapter XVII the condensed treatment of statistical mechanics and its application to entropy calculations makes difficult reading. This fault is more strikingly shown in the treatment of the Bose-Einstein and Fermi-Dirac statistics, consisting of page after page of equations, with interspersed remarks which are hardly clarifying, such as "—if it is assumed that cells, but not molecules have identity, then the number of ways in which this association can be realized is—" A modern treatment of this topic, following a sound and sufficiently extensive discussion of statistical mechanics, could be made understandable. This chapter also suffers from the emphasis laid on the unnecessary and often confusing chemical constant.

The fourth new chapter, XX, provides an excellent, thorough, and up-to-date discussion of colloids.

Structural chemistry lies within the scope of this treatise, as is recognized in the inclusion of a long chapter on atomic structure. And yet the important field of the structure of solids, in which great advances have been made in recent years, is dismissed in a chapter of 30 pages, reprinted practcally without change from the 1924 edition, and in which there are almost as many incorrect as correct statements. Thus to the sodium chloride arrangement is attributed a simple cubic lattice, and to caesium chloride a body-centered lattice. The fundamental cell of the hexagonal close-packed arrangement is said to be a prism with an equilateral triangle as its base. The very simple zinc oxide arrangement is described as "difficult to visualize or to draw." The carbon rings in naphthalene and anthracene are said to be staggered. Half a page, including a figure, is devoted to a description of the staggered-plane graphite structure, although the correct structure was discovered in 1924. Despite the fact that the structure of hexamethylenetetramine had been determined before 1924 and those of hexamethylbenzene, nonacosane, urea, and others since then, the discussion of organic compounds is restricted to Bragg's early incorrect work on naphthalene and anthracene and Astbury's inconclusive study of tartaric acid.

Band spectra and results derived from them, which are becoming more and more important to physical chemistry, are mentioned briefly in several chapters. Some of the discussion is not calculated to provide much enlightenment to the student; in chapter XIX it is stated that the molecule HI is not ionic, but instead "forces exist between the two nuclei." A unified and more extensive treatment of band spectra would be a desirable addition to the book.

The revisions and additions, which increase the treatise 36 percent in length over the first edition, change it from a valuable to a more valuable reference book for the physical chemist and student of physical chemistry. Selected chapters might be successfully used as texts for courses in physical chemistry; in any case the treatise should admirably supplement the more elementary and condensed texts customarily used, inculcating the research viewpoint and indicating the lines of work in which research is being actively carried on. The physicist should find the treatise useful when he becomes involved in work bordering on physical chemistry.

LINUS PAULING